Imperial College London

Optimising M-S-H Cement using Brucite

Mercedes Baxter Chinery

Imperial College London

Supervisors: Prof. Luc Vandeperre, Department of Materials; Dr. Hong Wong, Department of Civil and Environmental Engineering

Imperial College London

Background

- Sludges from Sellafield ponds need to be turned into a waste form
- Known to be rich in $Mg(OH)_2$
- A novel cement based on MgO and SiO_2 sets as strong as OPC
- Opportunity to use the waste as an encapsulating cement

Imperial College London

Previous Work

- M-S-H system using MgO as raw material
- Optimised by Zhang (DIAMOND, 2012)
- Compressive strength as expected
- Good dimensional stability

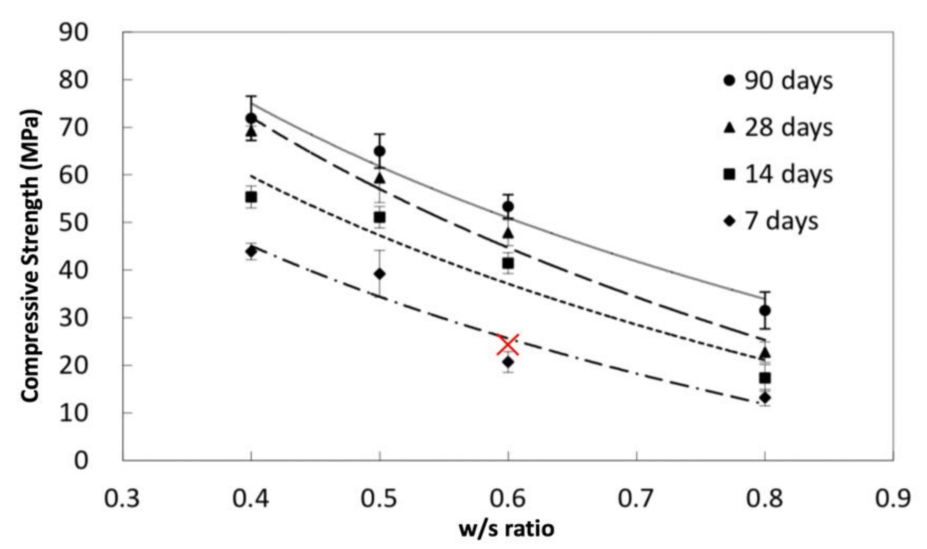

Imperial College London

Optimising Cement

- Investigating how replacing MgO with $Mg(OH)_2$ affects the properties
  - Fluidity
  - Compressive Strength
  - Composition
- Improve the properties so in line with the requirements

Imperial College London

Initial tests

- Comparison of systems
  - Mg/Si ratio maintained as 1
  - Additives
- Mix wasn't very fluid
- Didn't set within 7 days
- Very little strength development

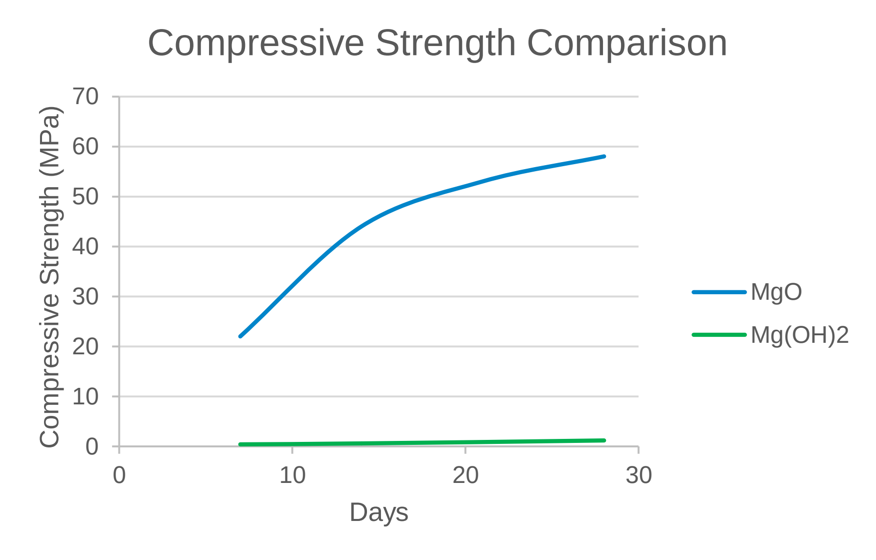

Imperial College London

Results

- $Mg(OH)_2$ does not dissociate
- Lack of strength development

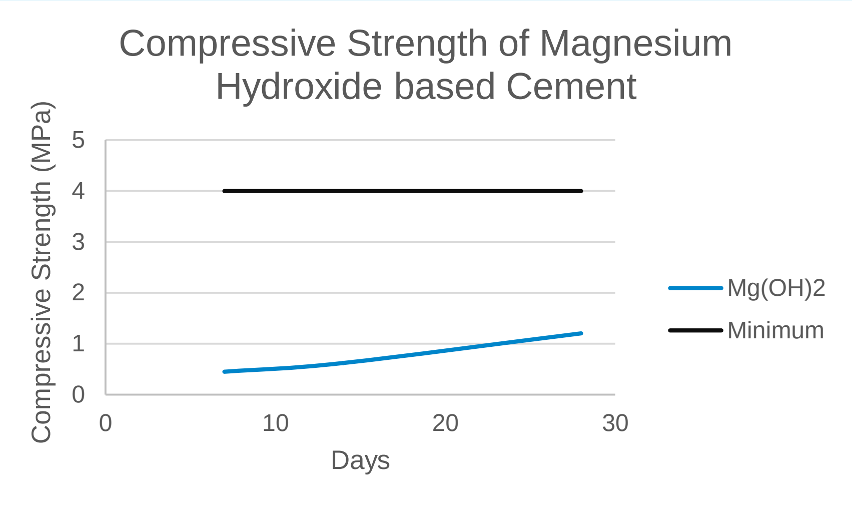

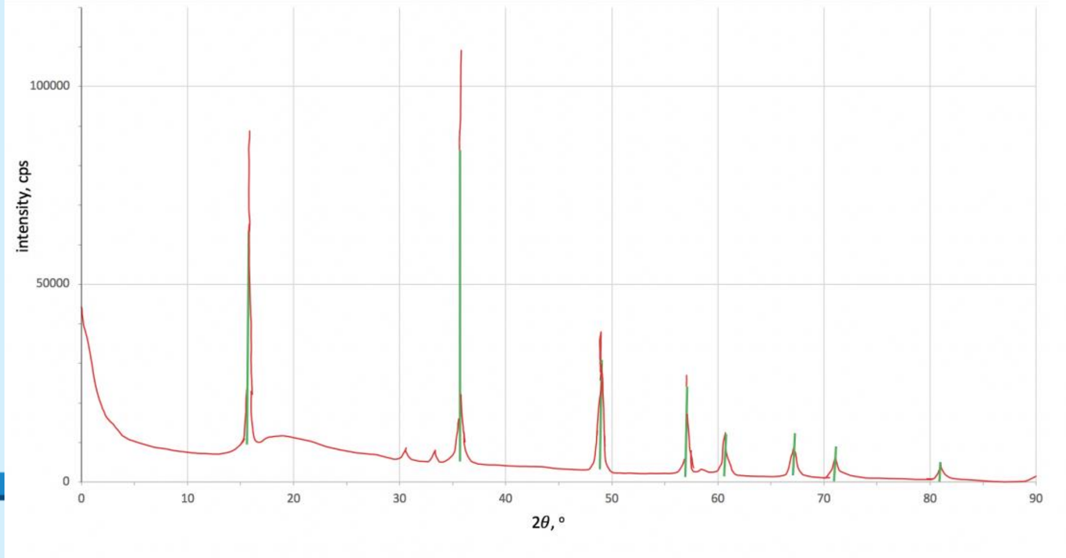

Imperial College London

Results

- Fluidity
  - NaHMP
  - Giessfix/Dolapix
- MSH development
  - $MgCO_3$ /$MgNO_3$
- Dimensional Stability
  - Addition of sand

Imperial College London

The dissolution of $Mg(OH)_2$

- $Mg(OH)_2$ most stable form
- Need to find the conditions for which $Mg(OH)_2$ wants to dissociate

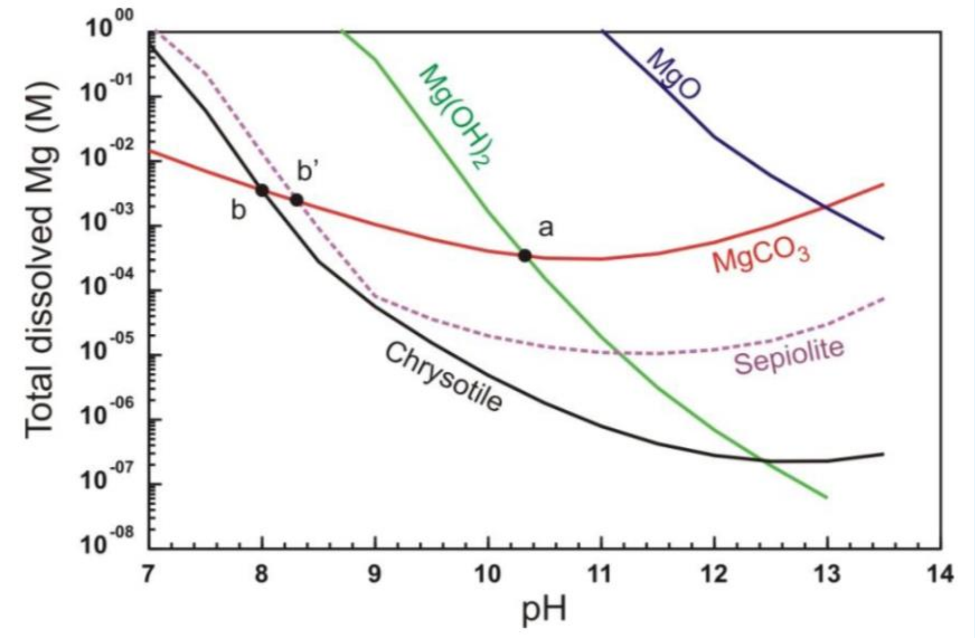

Imperial College London

Promoting $Mg(OH)_2$ dissolution

- Cure samples under a variety of pH conditions
- XRD analysis of the samples
- Recreate conditions within the MSH

Next Steps

- Testing durability, mechanical properties and understand composition
- Understand how to adapt to a sludge based cement

Imperial College London

TRANSCEND

Transformative Science and Engineering for Nuclear Decommissioning

Improving *in situ* acoustic characterisation of suspensions with machine learning methods

Joe Hartley, University of Leeds

Theme 1 – Integrated Waste Management

14/05/2021
Joint Nuclear Event Webinar

Energy
For a Low Carbon Future

Background

- Graduated from the University of Sheffield in 2019.
    - Material Science and Nuclear Engineering MEng.
    - FYP: A Dissolution Study of Thermally Treated Chabazite By Hot Isostatic Pressing.
- October 2020: Started PhD at University of Leeds:
    - Advanced Ultrasonic Characterisation of Slurry Flows

TRANSCEND

Transformative Science and Engineering for Nuclear Decommissioning

Research Challenge

- ILW legacy sludge at Sellafield needs to be pumped out of ponds to be processed.
- Characterisation data on the sludge is scarce;
  - Remote online monitoring system is needed to characterize the sludge during pipe-flow.

Figure 13: Composition of ILW by waste group

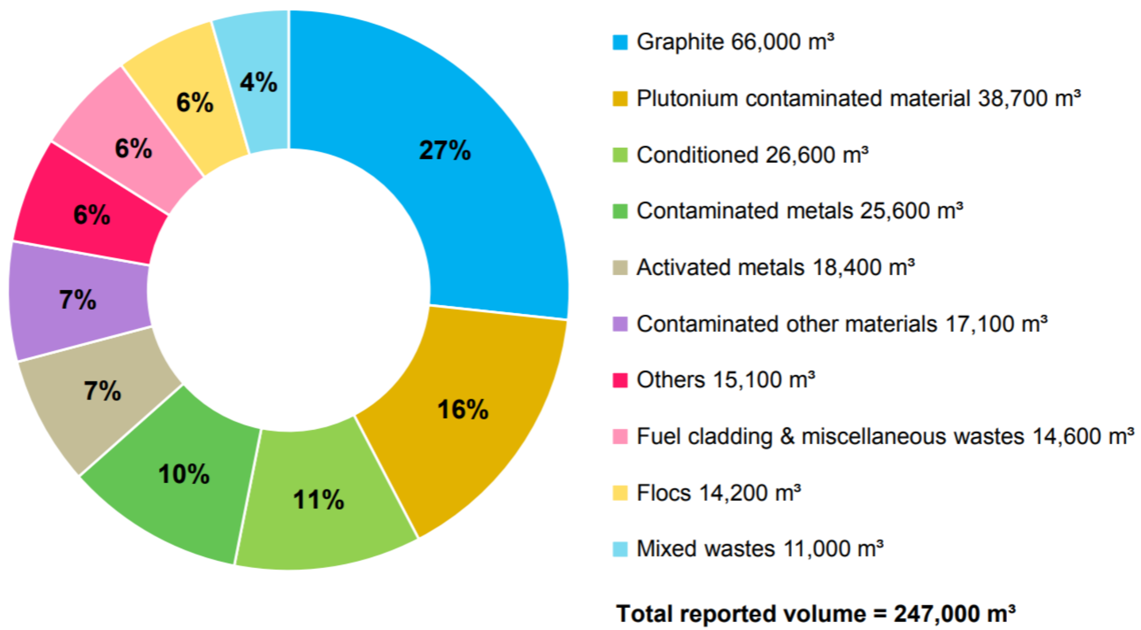

https://ukinventory.nda.gov.uk/wp-content/uploads/2020/01/2019-Waste-Report-Final.pdf https://www.youtube.com/watch?v=Yu7-D37SKOY&ab_channel=SellafieldLtd

Similar Use of Acoustics

Acoustic Backscatter System has been used industrially to characterise slurries:

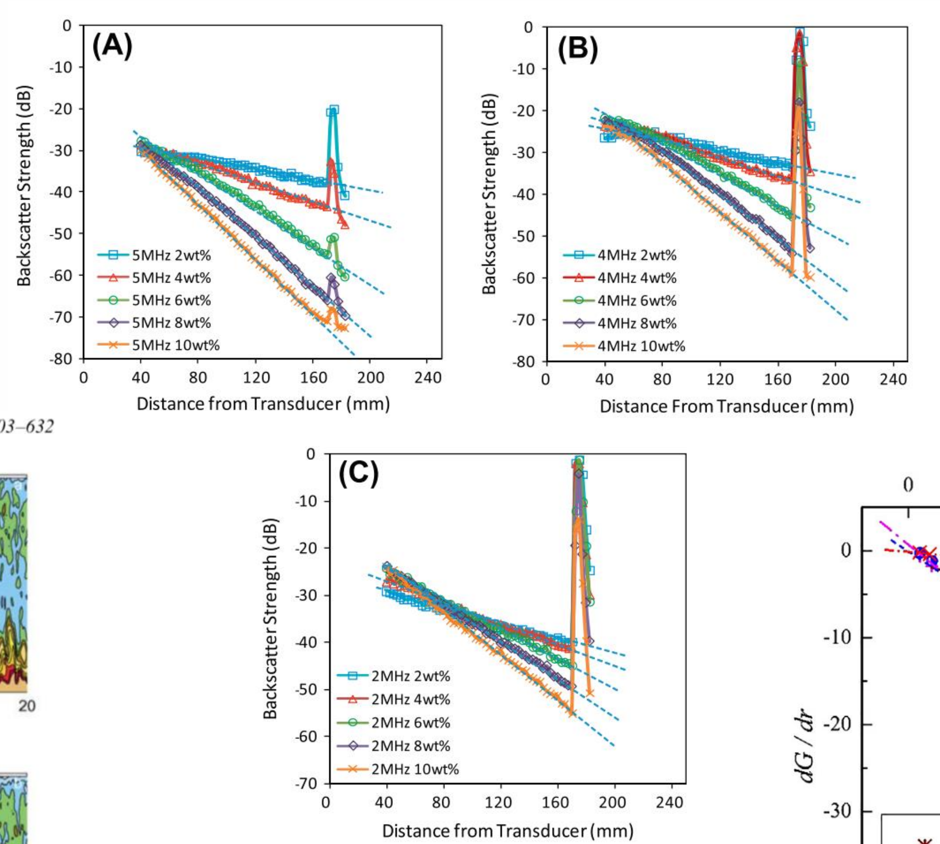

P.D. Thorne, D.M. Hanes / Continental Shelf Research 22 (2002) 603–632

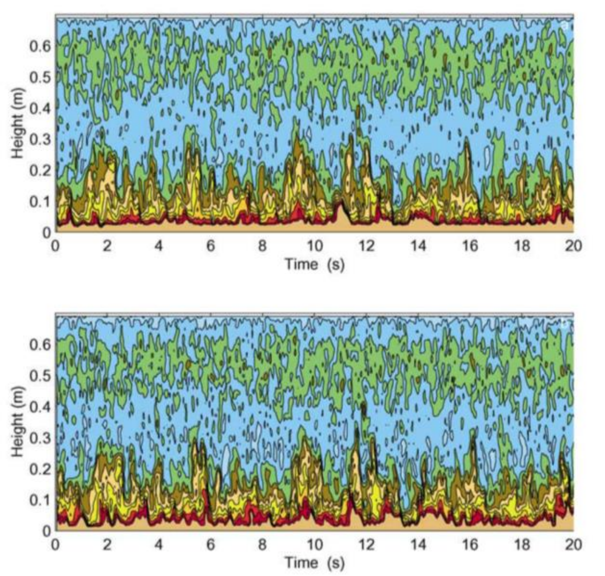

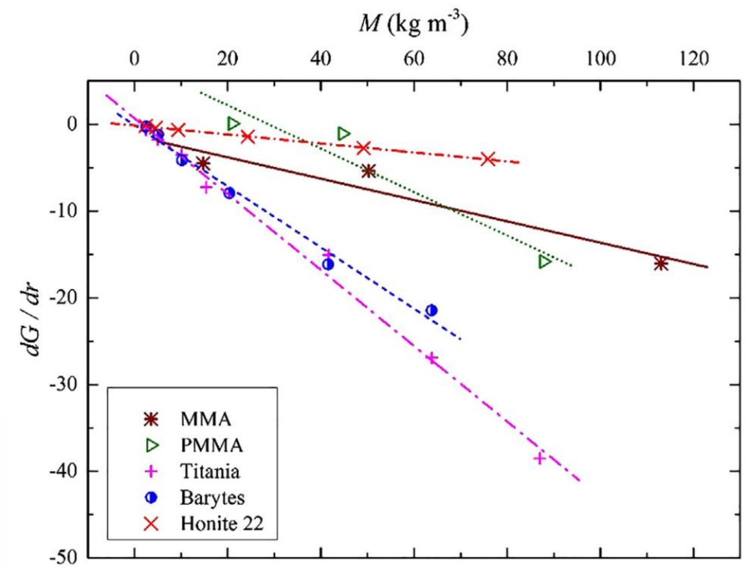

Thorne, Hanes; *A reveiw of acoustic measurement of small-scale sediment processes*

DOI:10.1016/j.mineng.2011.12.003

DOI: 10.1016/j.apacoust.2018.10.022

Acoustic Instrumentation

- UVP-DUO from Met-Flow.
- Has been used in the department for nearly a decade – good expertise.
- Frequency range from 1–8 MHz
- Active radii for the transducers are 2.5 – 10 mm; 2.5 or 5 mm is ideal for non-intrusive attachment on pipelines.

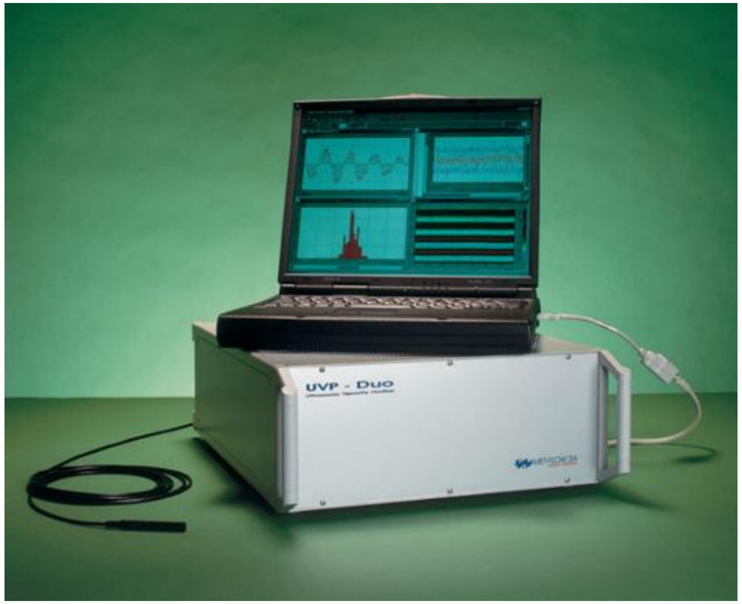

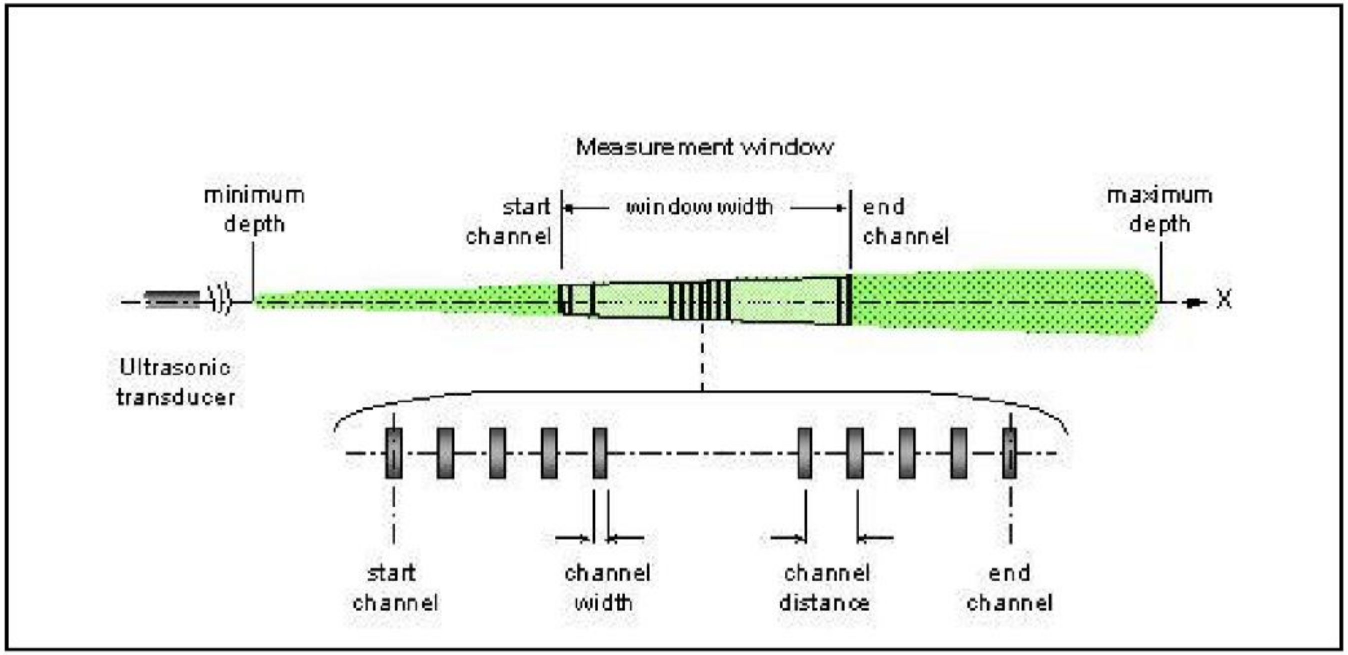

UVP Monitor Model UVP-DUO With Software Version 3, User's Guide, Draft Ed., Met-Flow, Release 5, 1/07/02.

Progress since last meeting

- Moved to Leeds
- Lab inductions
- MatLab Courses
- Python Courses
- Recorded data for analysis:
    - Spherical glass particles and irregular plastic material
- Completed data analysis in Excel
- Edited code in Matlab to find sediment attenuation coefficient
- Partially converted this to a Python script

Speherical Glass Particles

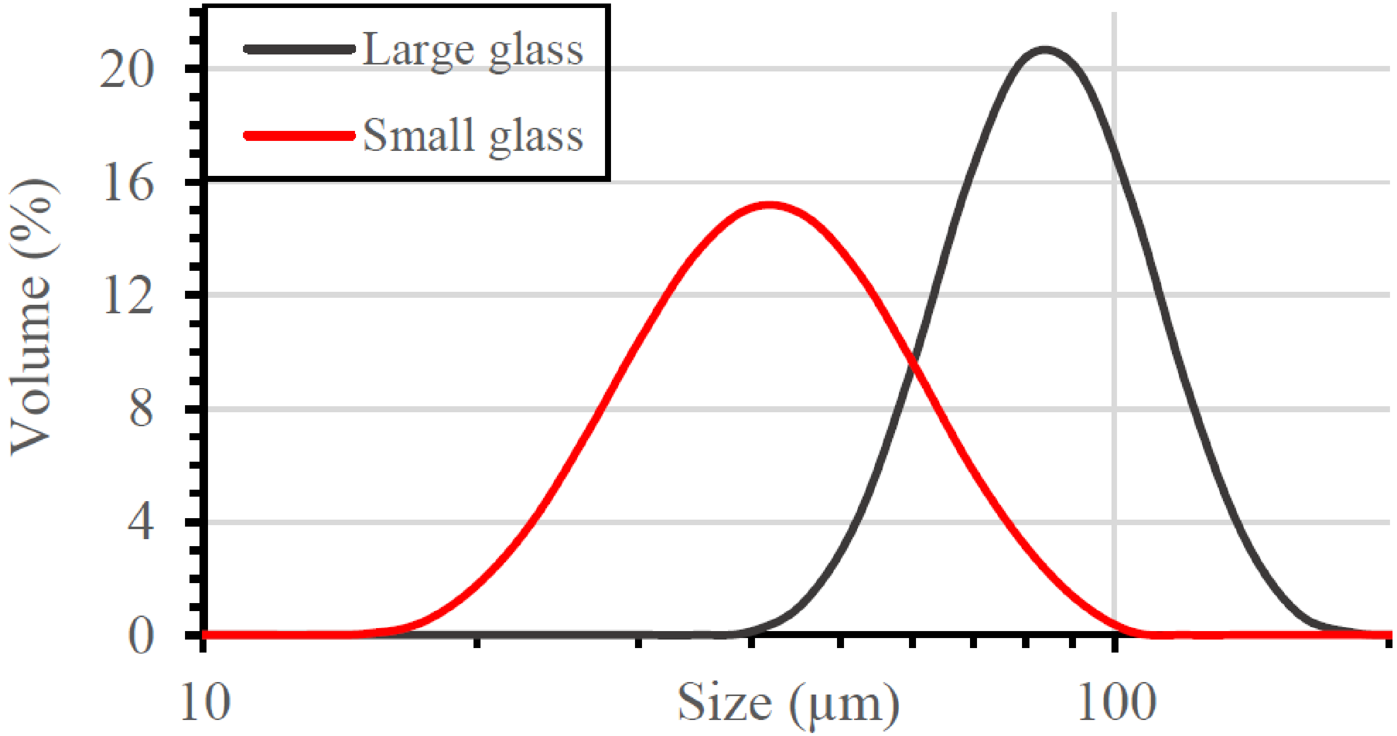

https://www.guyson.co.uk/aftersales/guyson-blast-media/glass-blast-media

Material Name	Manufacturer	Particle d_{50} (µm)
Honite-22	Guyson	45.5
Honite-16	Guyson	78.6
Honite-12	Guyson	173.4

DOI: 10.1121/2.0001303

DOI:10.1109/ULTSYM.2017.8091603

Experimental Setup

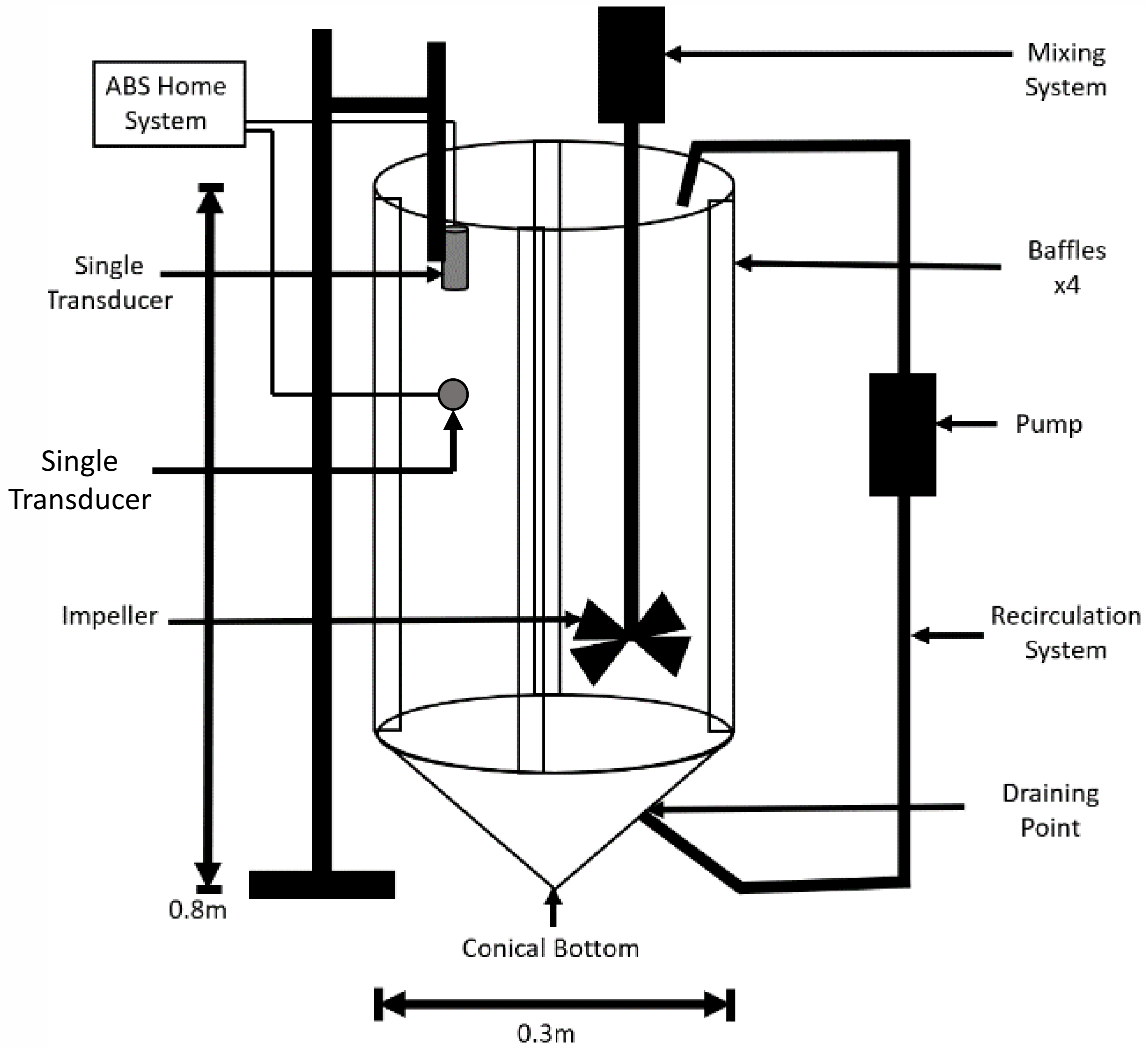

DOI: 10.1121/2.0001303

Backscatter Voltage

$$V_{RMS} = \frac{k_t k_s}{\Psi r} M^{0.5} e^{-2r(\alpha_w + \alpha_s)}$$

V_{RMS} – backscatter voltage
k_s – sediment specific backscatter constant
k_t – transducer specific backscatter constant
Ψ –near field correction factor
r – distance from transducer
M – concentration of sediment (g/l)
α_w/ α_s – attenuation due to water and sediment respectively

$$G = \ln(\Psi r V) = \ln(k_t k_s) + \frac{1}{2} lnM - 2r(\alpha_w + \alpha_s)$$

ξ^m – concentration independent attenuation coefficient

$$\alpha_s = M\xi^m$$

Determination of sediment attenuation coefficient

$$\xi^m = -\frac{1}{2}\frac{d}{dM}\left[\frac{d}{dr}[\ln(\Psi r V)]\right] = -\frac{1}{2}\frac{d^2G}{dMdr}$$

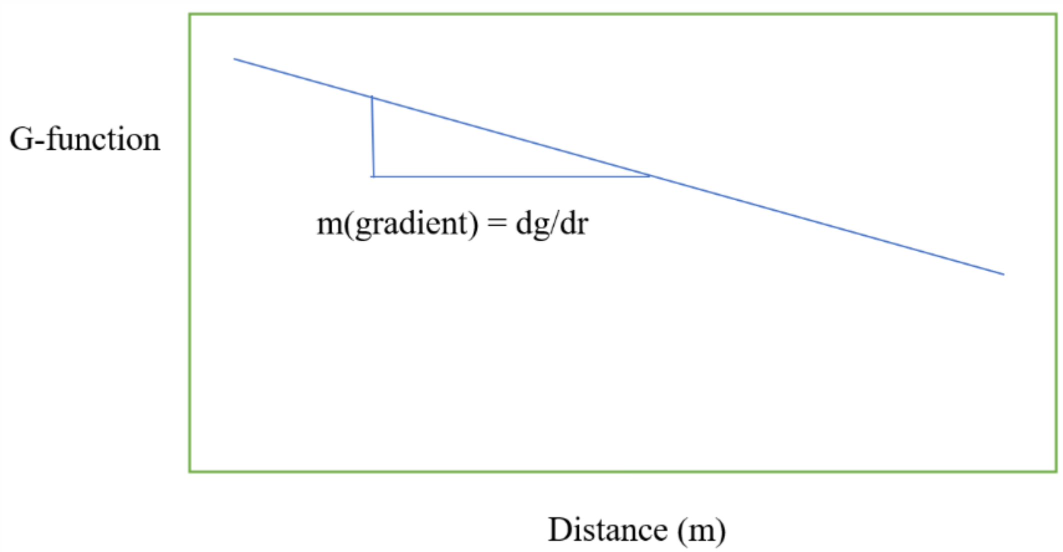

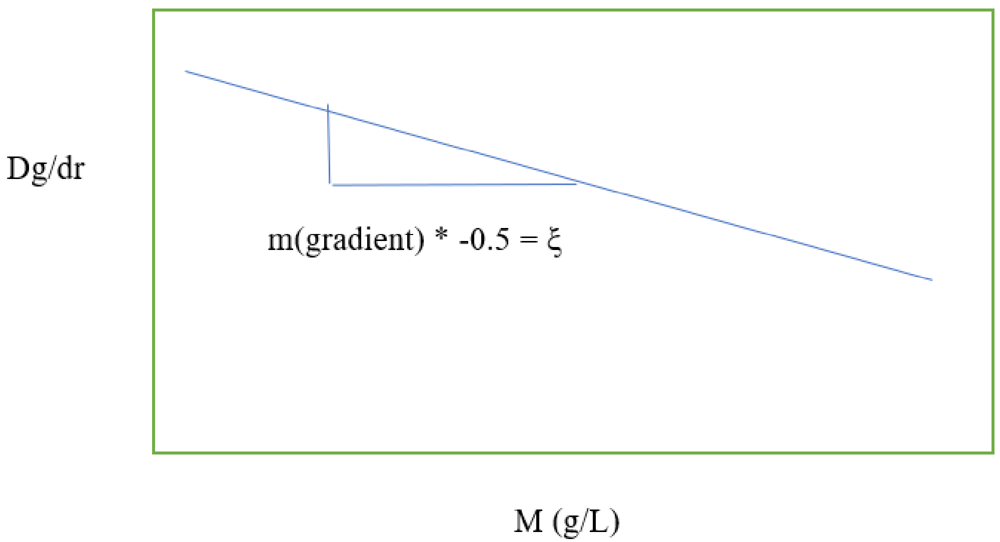

2.5mm 4MHz probe

In situ

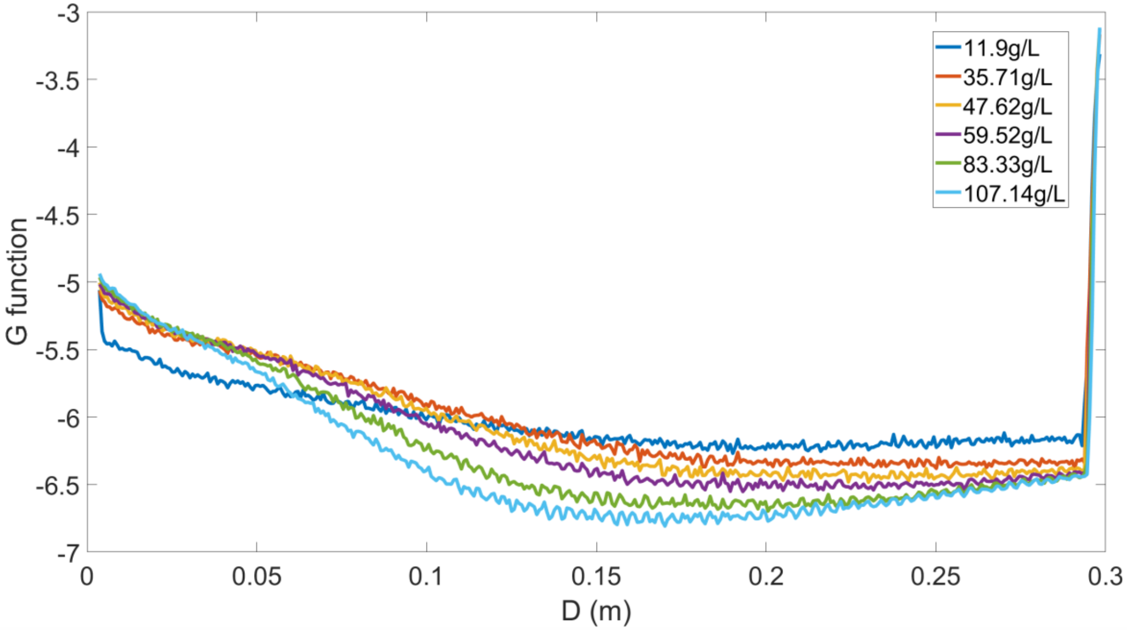

Ex situ

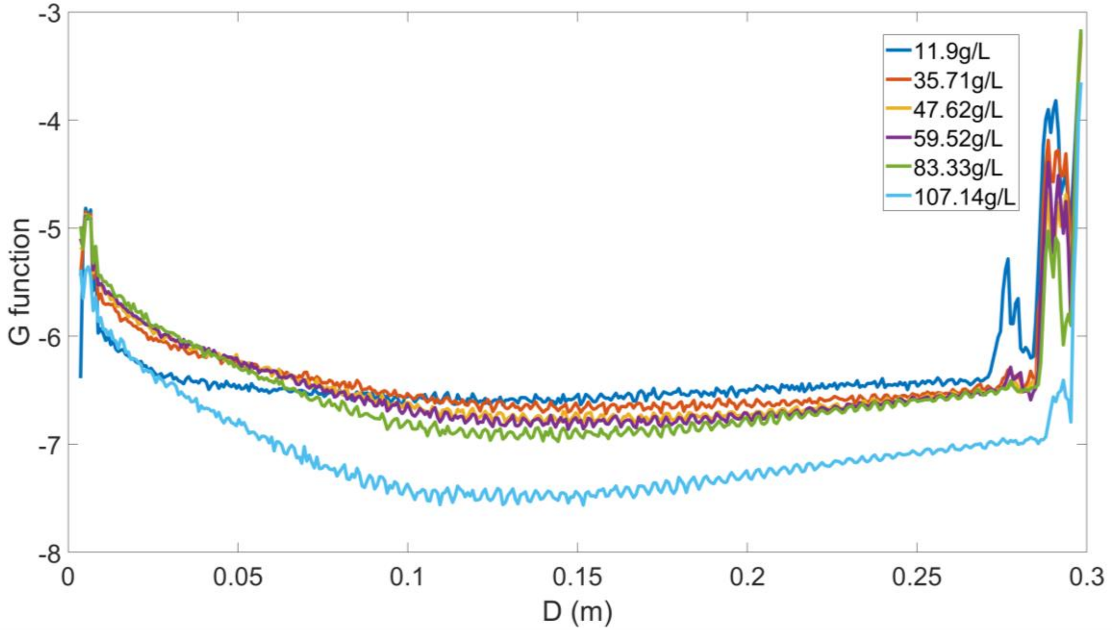

2.5mm 4MHz probe

In situ

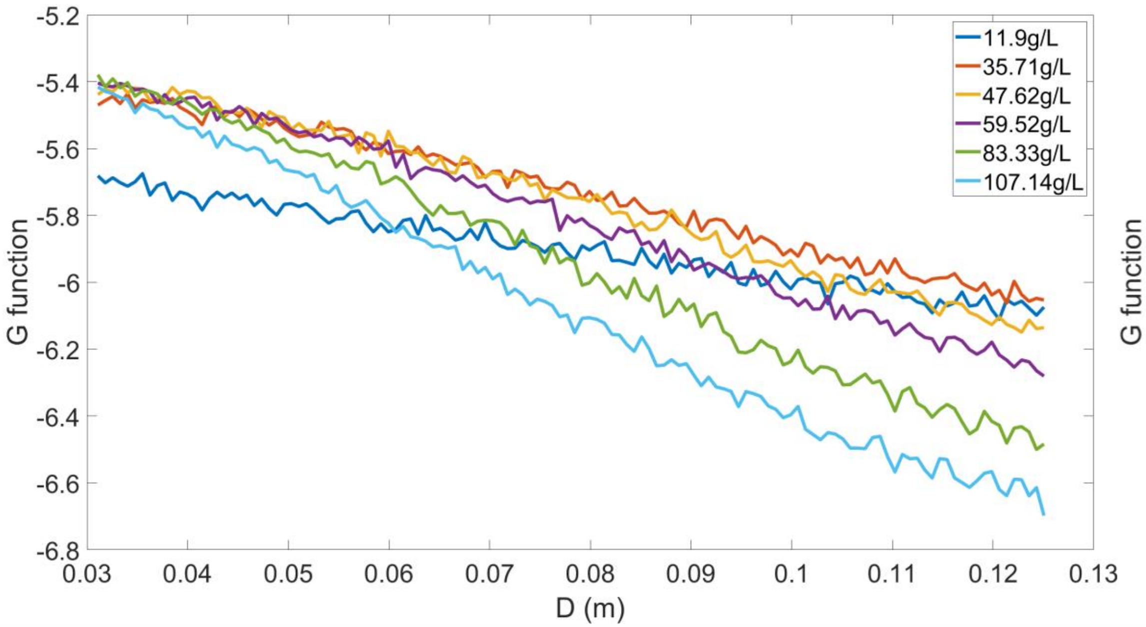

Ex situ

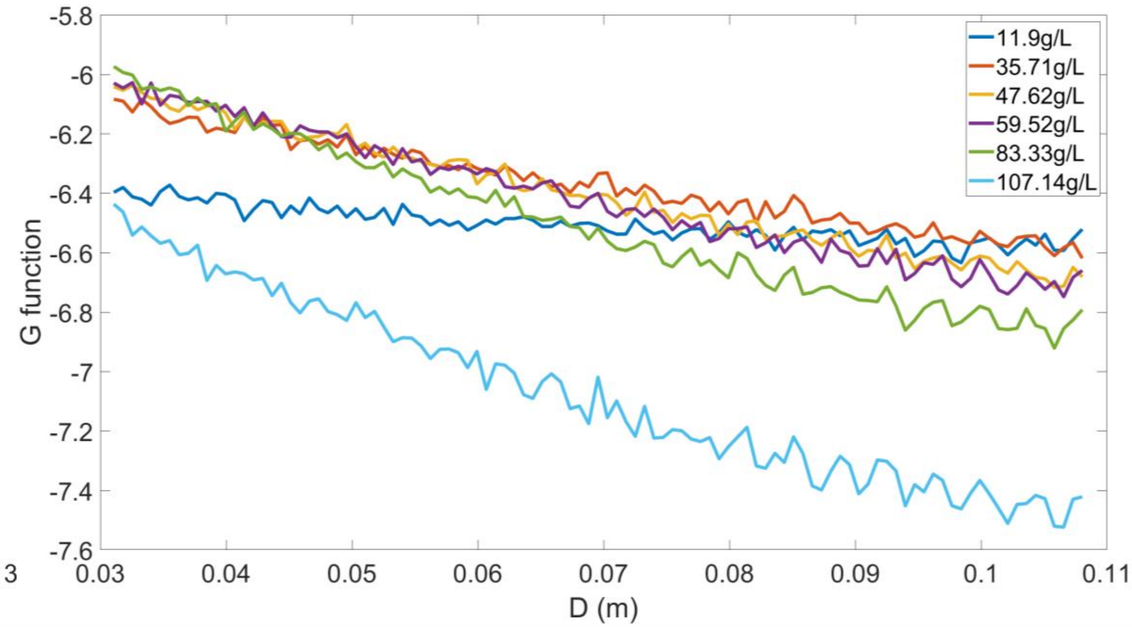

2.5mm 4MHz probe

In situ

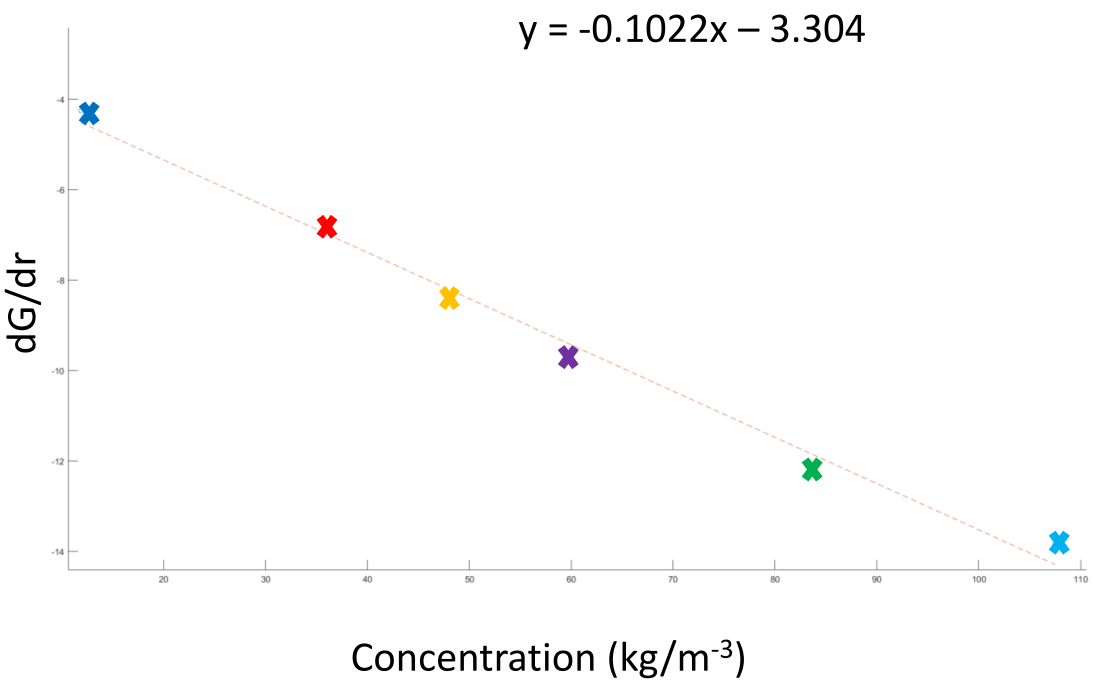

Ex situ

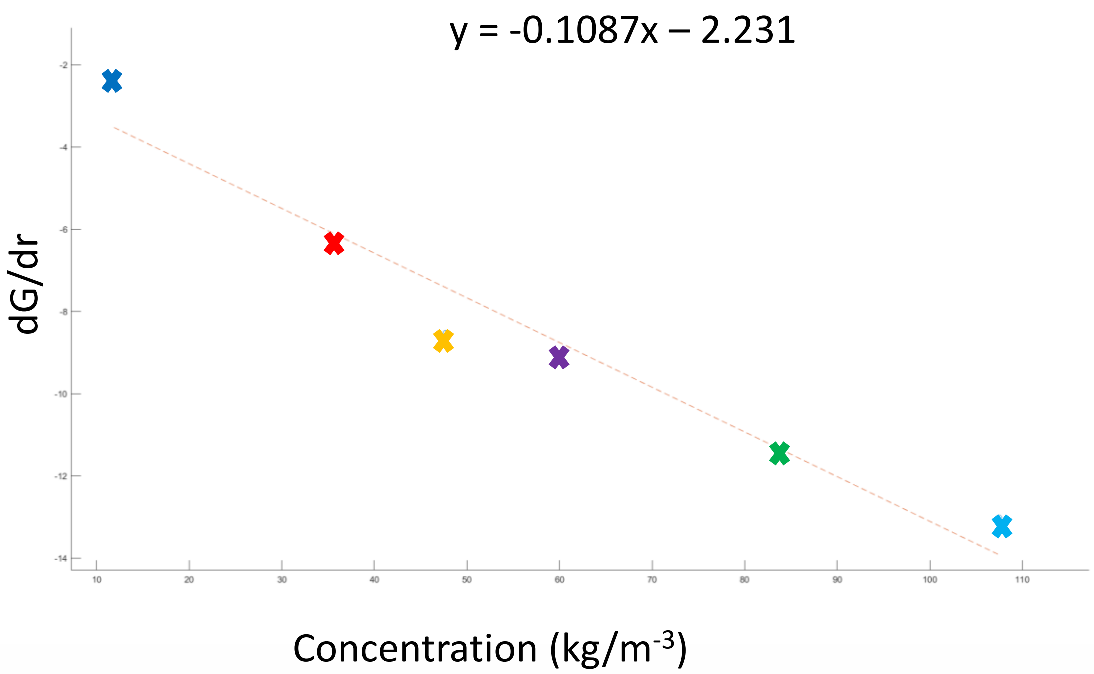

Results - ξ^m

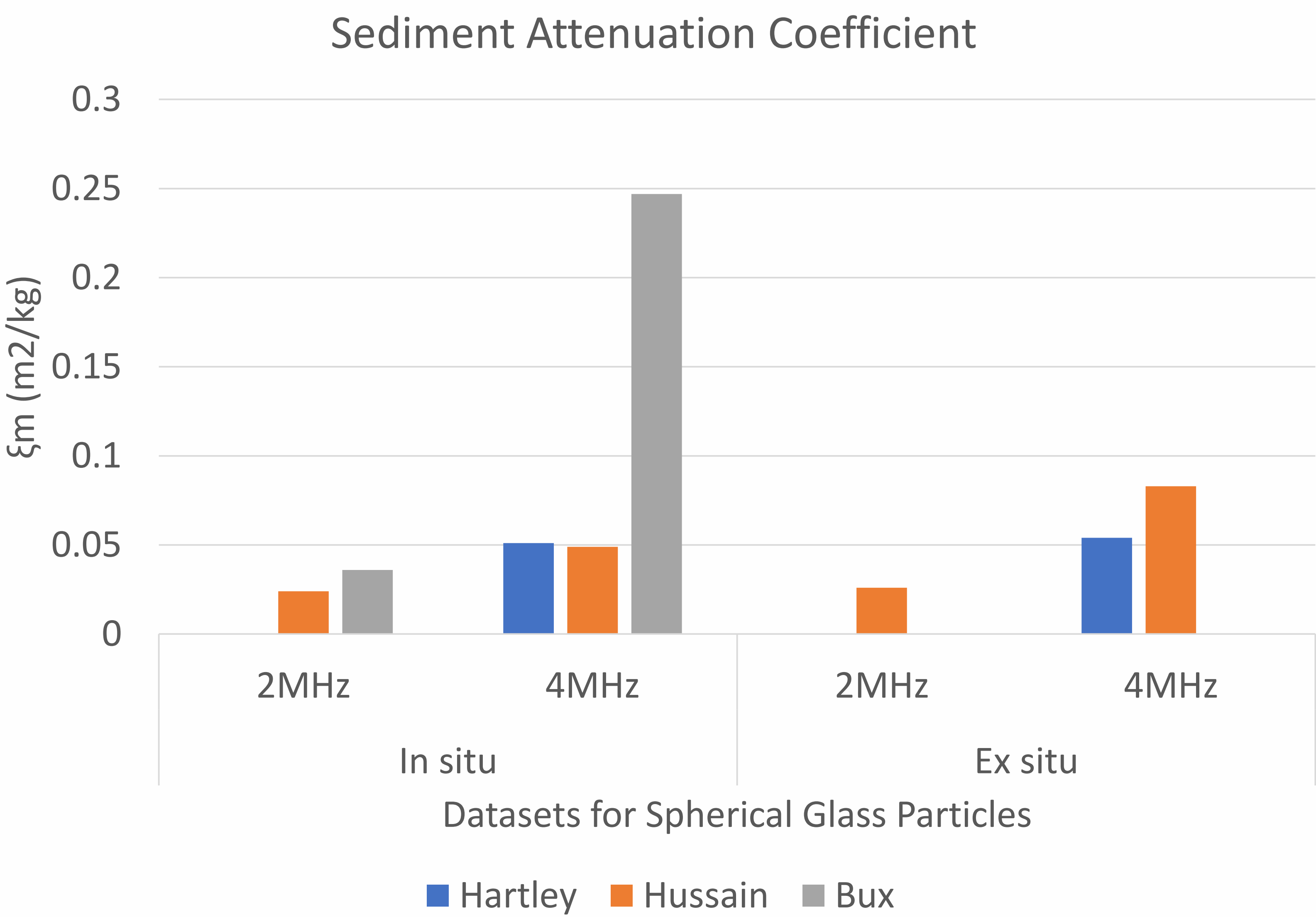

Bux et al. (2019) - 10.1016/j.apacoust.2018.10.022

Next Steps

- Transfer current data analysis method on MatLab to Python
- Determine k_s and k_t from the measured data
- Compare the measured backscatter voltage to the calculated backscatter voltage from the equations detailed within the literature
- Repeat this for different sizes of spherical glass particles
- Produce tighter size fractions of the glass particles by sieving
- Use the Mastersizer to verify particle size and distribution
- Run the same tests but with the tighter size fractions to see if there's any difference

ML and How It Will Be Applied

- Machine Learning:
  - making the computer learn from studying data and statistics.
  - a step into the direction of artificial intelligence (AI).
  - program that analyses data and learns to predict the outcome.
- Essentially pattern matching '*test*' data to the '*training*' data.

https://www.python.org/static/community_logos/python-logo-master-v3-TM.png | https://whimsical.com/machine-learning-roadmap-2020-CA7f3ykvXpnJ9Az32vYXva

Further steps

- Research more into the various methods of Machine Learning and decide which is best for this application
- Move to looking at bidisperse mixtures of the sieved fractions
- Work through code analysing these data
    - Can we see the two size fractions? Or do we just see a single averaged particle size.
- Understand the Near Field correction factor

Overview of Project Objectives

- Understand current Acoustic Backscatter (AB) performance of UVP for characterisation of nuclear suspension in slurry pipe-flows.
- Investigate Machine Learning (ML) methods to improve UVP particle aggregate size and concentration measurements.
- Investigate the effect of large molecular weight polymers on the AB performance of UVP.
- Compare/ combine FBRM measurements to/ with UVP-DUO and ML system.
- Understand influence of discrete size fractions, as well as varying discrete size fraction mixes, and how ML is affected.
- Optimise system to give real-time results for real-time flocculation.

TRANSCEND

Transformative Science and Engineering for Nuclear Decommissioning

Thank you

Email: pmjha@leeds.ac.uk

Development of sustainable substitutes for pulverised fly ash in cement & concrete

Andrea Kozlowski, Dept of Civil & Environmental Engineering
Supervisors: Joanna Renshaw & Kate Dobson
Industrial Supervisor: Frank Taylor, LLWR

University of Strathclyde Engineering

Introduction

- Clinker substitutes
  - Reduce CO_2 emissions
  - Improve mechanical properties
  - Reduce costs
- Common substitute: Pulverised Fly Ash (PFA)
  - Coal combustion residue
  - Used in Ordinary Portland cement (OPC) to encapsulate LLW

UK phase-out coal-fired power stations in 2025[1]
local PFA supply diminishes → dependence international suppliers

[1] Department of Energy & Climate Change (18.05.2015) https://www.gov.uk/government/news/government-announces-plans-to-close-coal-power-stations-by-2025 [Accessed: 13.05/2021]

LLWR

- Facility disposal of solid LLW
- Cementation of waste for final storage
- Functions of cement
    - Limits contact ground water & waste
    - Reduce radiation
    - Improve stability of package
    - Promote stability

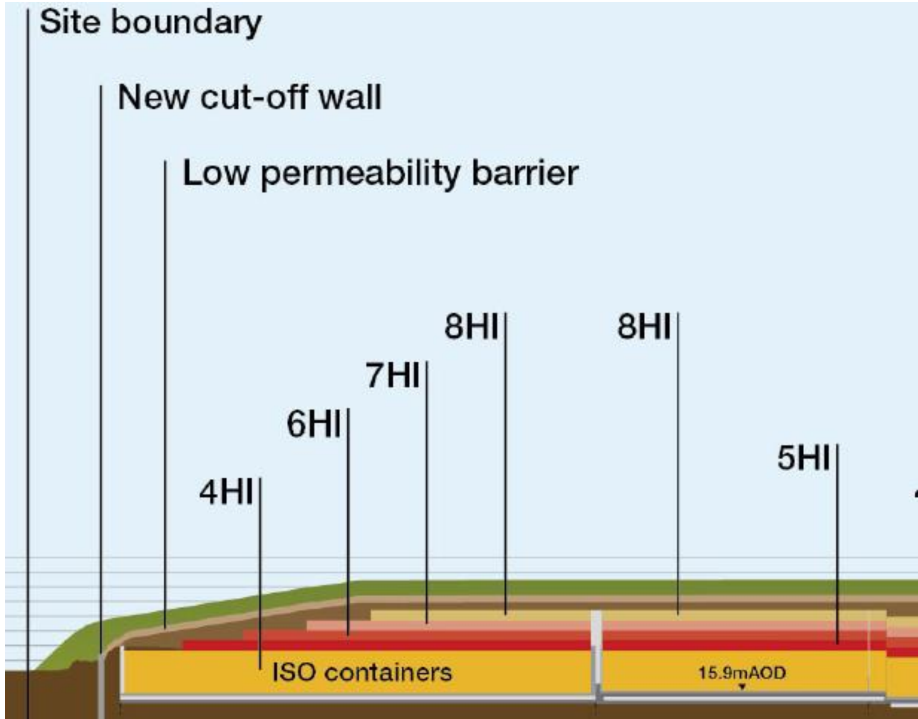

Pictures: LLW Repository Ltd. (2011): LLWR/ESC/R(11)10034 (both)

PFA & Alternatives

PFA improves workability & reduces porosity of OPC concrete

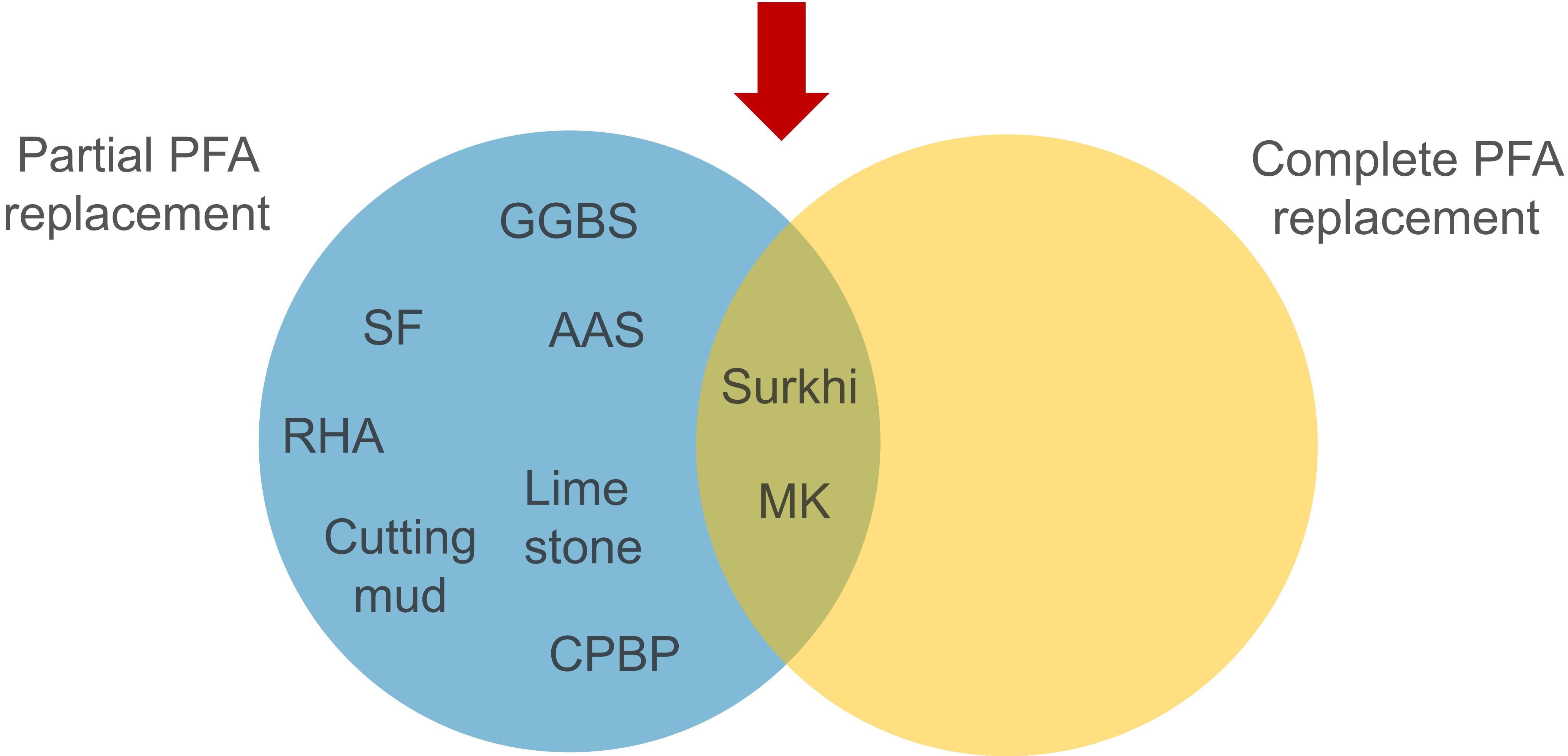

PhD Project

AIM

- Investigate alternatives for PFA
  - Sustainable
  - Meeting performance standards
- Characterise alternatives' physical, chemical, mechanical properties
- Investigation interaction with radioactive material

ACTIVITIES

- In-situ XCT testing of substitutes & reference OPC samples
- SEM on pre- & post-testing samples
- Classify porosity, phases, density of substitute-concrete samples

COLLABORATION

LLW Repository Ltd

PhD Timeline

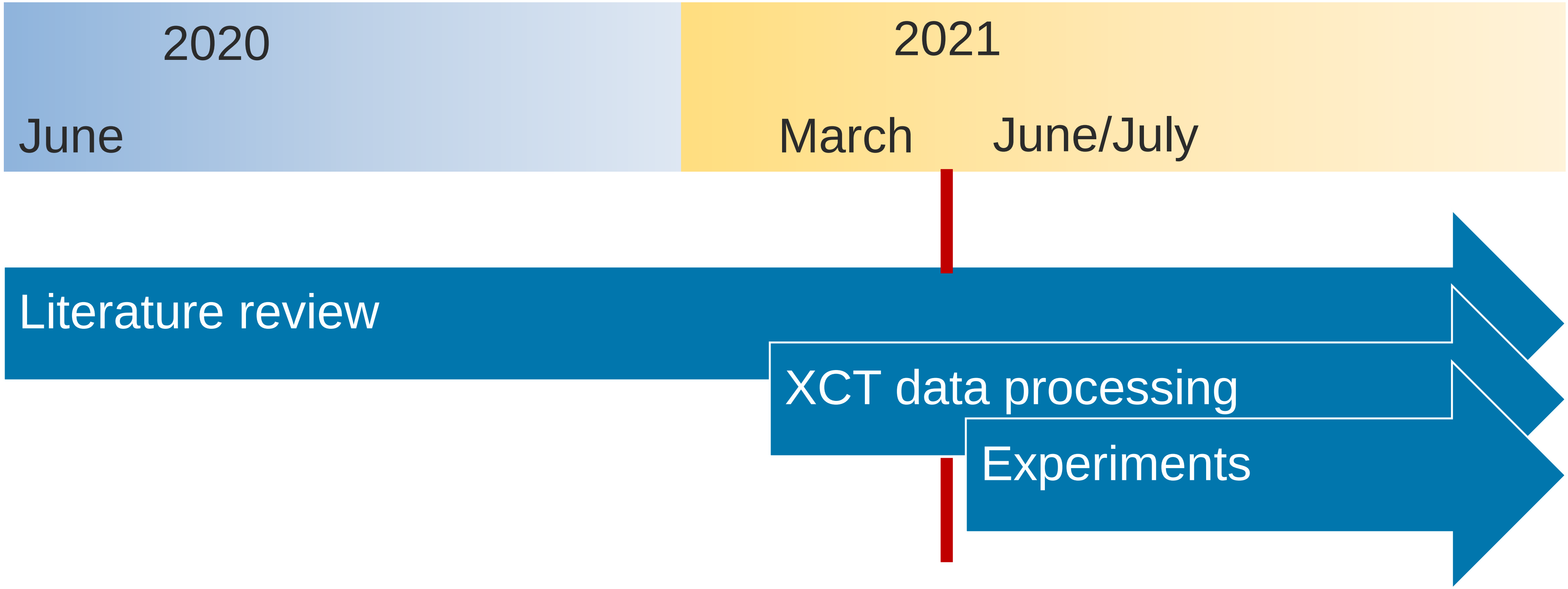

Future Work

Examination samples (different formulations & substitutes)

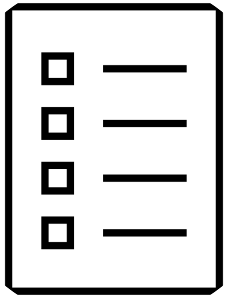

Characterisation physical, chemical, mechanical properties

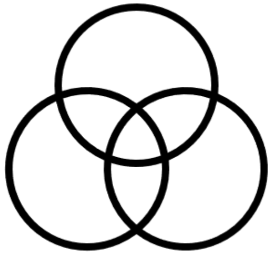

Understand impact of PFA alternatives on cement properties & performance

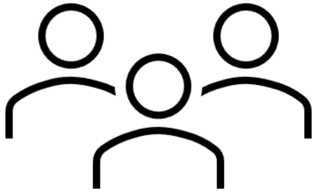

Collaboration with LLWR, advancing performance criteria of PFA substituted cement

Contact me
andrea.kozlowski@strath.ac.uk

School of Chemical and Process Engineering
FACULTY OF ENGINEERING

UNIVERSITY OF LEEDS

Simulation of behavioural modification effects in particle-laden flows through polymer additives

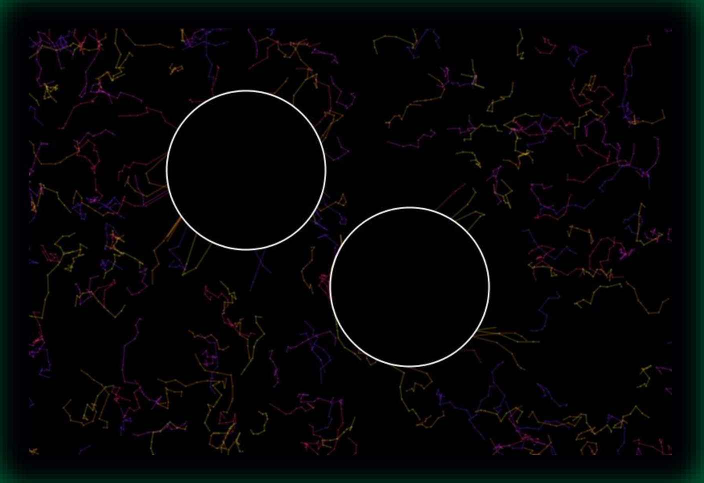

Lee Mortimer (PDRA)

Supervisor: Prof. Mike Fairweather

14th May 2021

TRANSCEND

EPSRC
Engineering and Physical Sciences Research Council

Background

- At Sellafield Ltd, waste suspension sludge flows transport solid-liquid mixtures of radioactive legacy material from ponds, silos and tanks to other interim locations where they can be safely stored.

- Such retrievals are currently underway during POCO operations in plants such as the Pile Fuel Storage Pond, the First Generation Magnox Storage Pond and a number of associated packaging, export and encapsulation plants, and settling, decant and storage tanks.

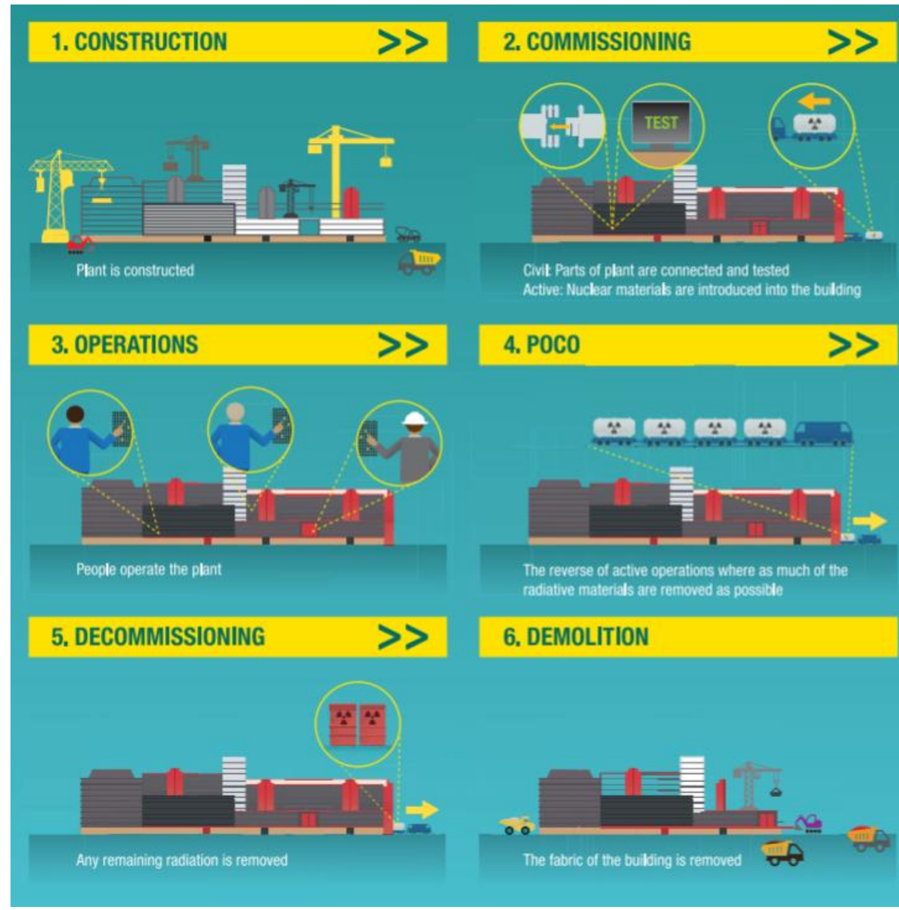

Sellafield magazine – Issue 02, 2015.

Motivation

Pile fuel storage pool at Sellafield - IAEA Nuclear Energy Series No. NW-T-2.6 - Decommissioning of Pools in Nuclear Facilities, IAEA.

- However, at present these processes are executed sub-optimally and carried out with caution due to the complex nature of the wastes and a lack of understanding of their flow behaviour.

- In practice, the bulk transportive behaviour of interest associated with these activities is sensitive to the material properties and flow conditions. This sensitivity is capable of being exploited, however, and the modification of such quantities to obtain a desired outcome is referred to as **behavioural modification**.

Motivation

- In developing such techniques, solutions can be generated to discourage or encourage waste particle agglomeration within these transport flows, ultimately controlling the extent of long-term particle migration and interaction events.

Motivation

- That said, to develop beneficial behavioural modification techniques the system response to deviations in key parameters must be known. It is extremely difficult, if not impossible, to probe the effects of such variations experimentally.

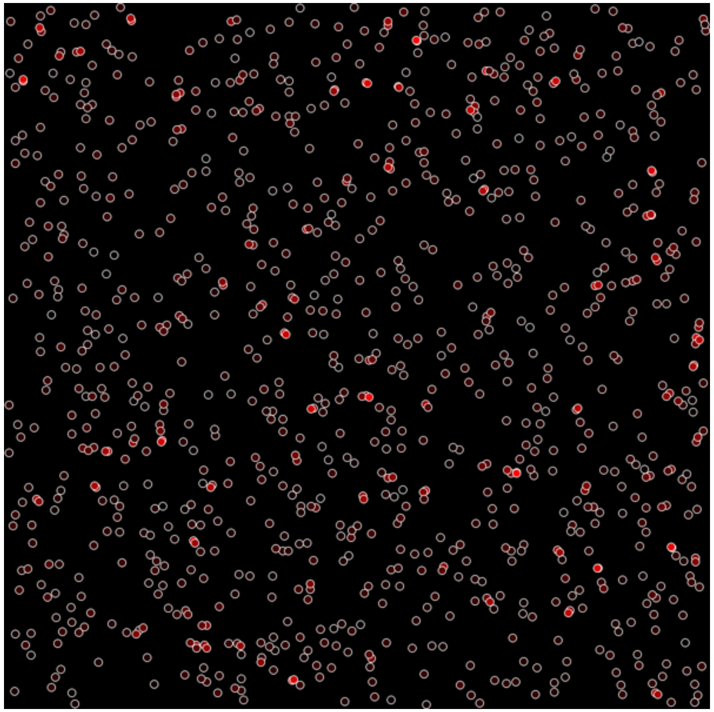

LOW HAMAKER CONSTANT

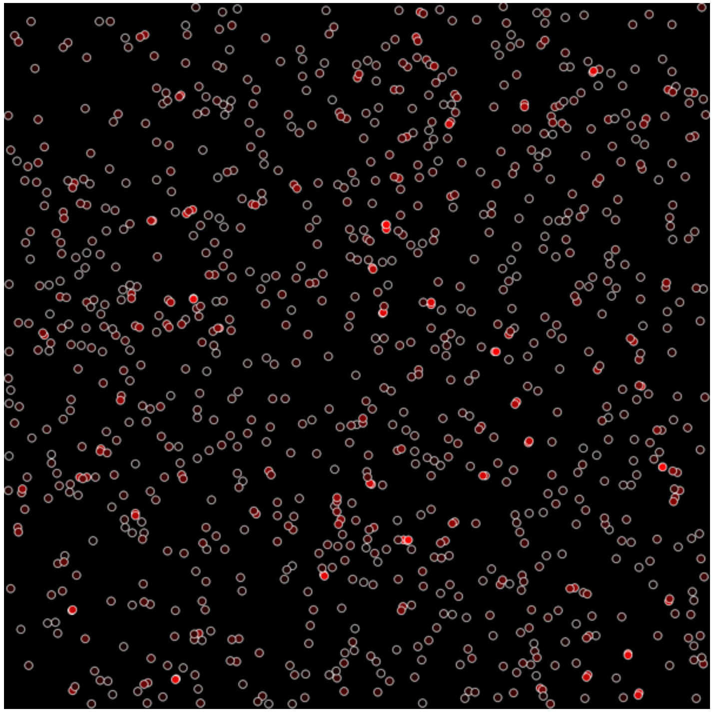

HIGH HAMAKER CONSTANT

- Computer simulations provide a means to overcome this difficulty by providing the capability to specify and explore the impact of changes to a set of precise system parameters.
- Let's exploit this and determine what happens when we add low concentrations of polymer additives to the system.

Methodology

- The accuracy and reliability of such calculations is based upon both the order of the discretisation techniques used for each phase, as well as the fidelity of the models used to predict the wide array of interactions between the phases.

CONTINUOUS PHASE

Direct numerical simulation (DNS)

PARTICULATE PHASE

Lagrangian particle tracking (LPT)

POLYMER PHASE

Finitely extensible nonlinear elastic model (FENE)

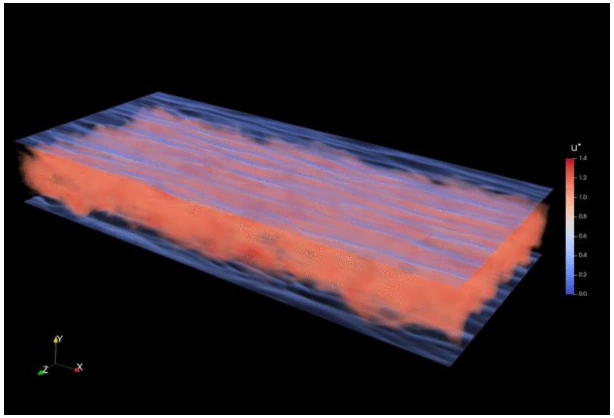

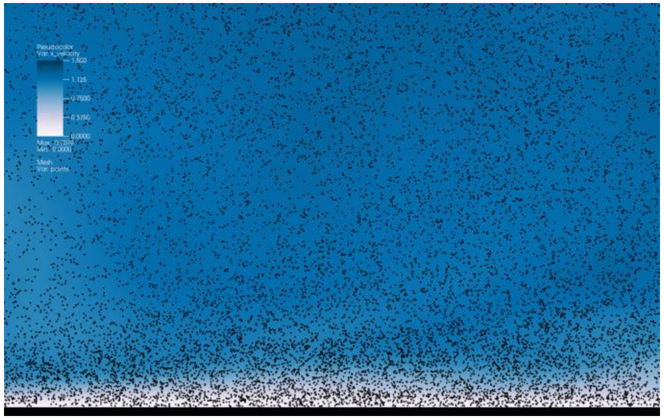

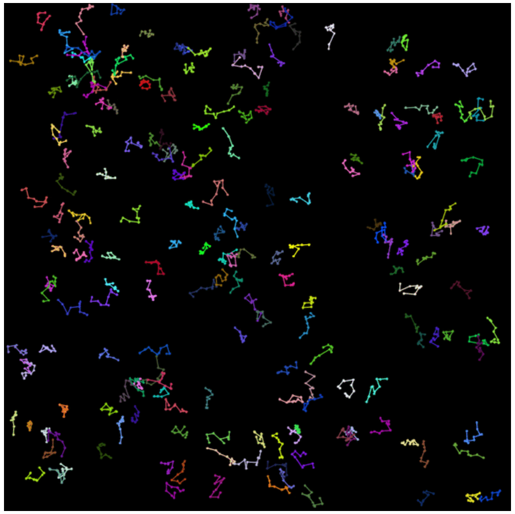

- Focus on coupling the three methods together to obtain a solver capable of predicting particle-polymer interaction.

FENE Model Recap

- FENE (finitely extensible nonlinear elastic) chain model represents the polymer as a sequence of beads connected by nonlinear springs.
- Springs used to model individual Kuhn chains, which would otherwise entail molecular dynamics simulation.

$$\underbrace{\zeta\left[\boldsymbol{v}_0^* + \boldsymbol{\kappa}^*\cdot\boldsymbol{r}_i^* - \frac{\mathrm{d}\boldsymbol{r}_i^*}{\mathrm{d}t^*}\right]}_{\text{Fluid drag}} + \overbrace{(\boldsymbol{F}_i^* - \boldsymbol{F}_{i-1}^*)}^{\text{Non-linear spring force}} + \underbrace{\sqrt{2k_\mathrm{B}T\zeta}\,\frac{\mathrm{d}\boldsymbol{W}_i^*}{\mathrm{d}t^*}}_{\text{Brownian}} = 0$$

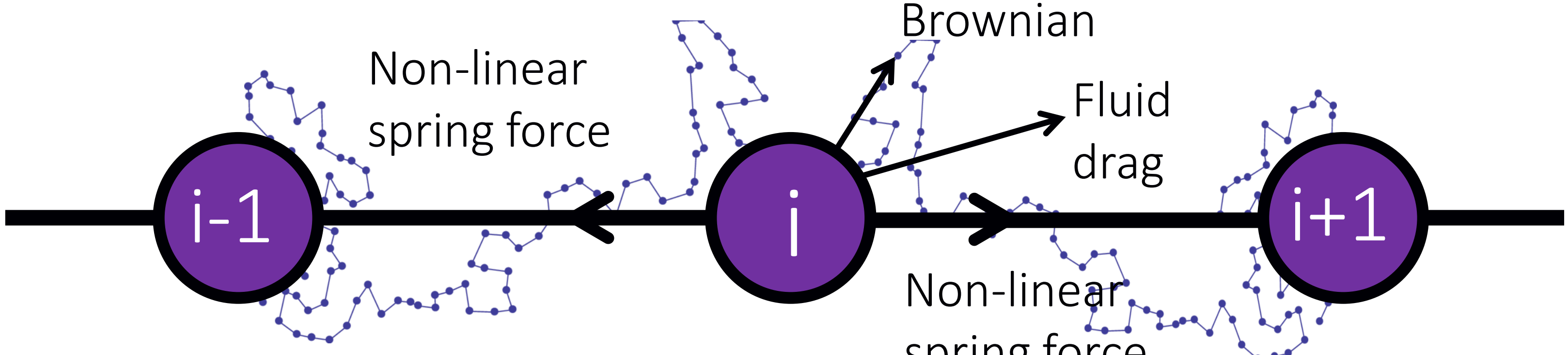

- Additional stress τ_{POL} in Navier-Stokes equations is obtained by calculating the conformation tensor C_{ij} which relates to local stretching behaviour of polymers.

Polymer-particle interaction

- During polymer phase calculation, beads which collide with the surface of a particle are considered fixed to that surface point for all subsequent calculations.

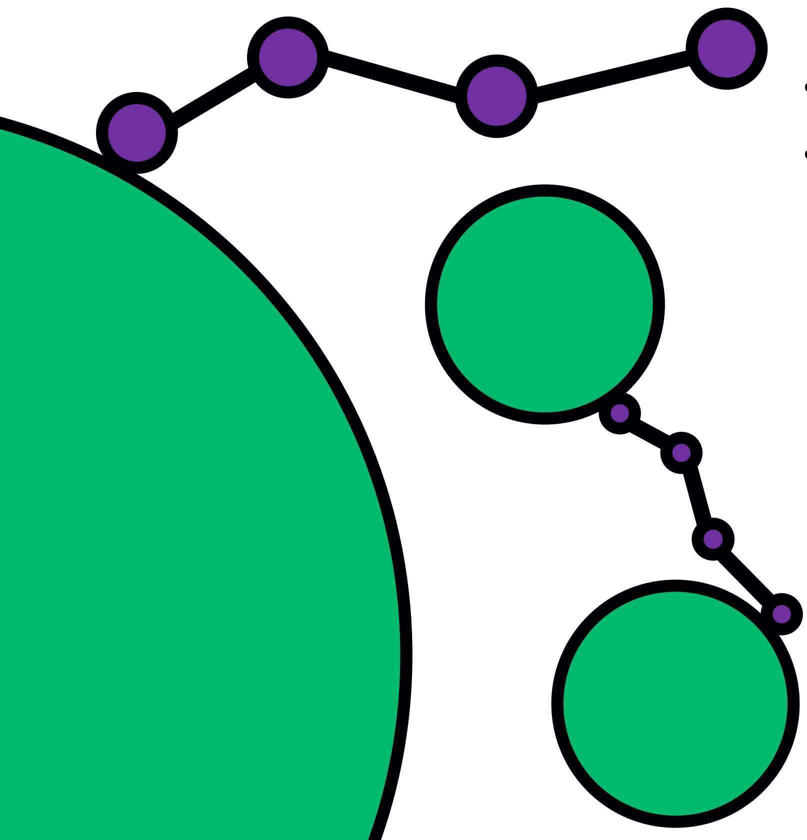

- Beads further down the chain are free to move, with bonds between the beads limited in angle.
- Beads feedback spring forces to the particle.
- Upon collisions with further particles, the polymer chain forms a bridge. To save computation time, all forces are now switched off on the polymer save the spring forces, since these are dominant.

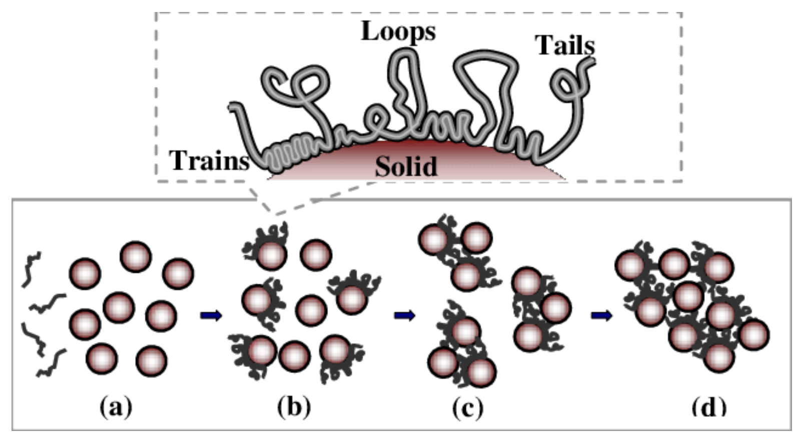

Simulation parameters and project aims

- Investigate polymer-particle interaction in fully developed turbulent flows.
- Determine the location and mechanisms by which polymers adsorb onto particles.
- Quantify the extent of polymer-bridging based agglomeration within the channel.

Parameter	**$St^+ \approx 0.1$**	**$St^+ \approx 92$**
Particle diameter, d_p^*	0.005	0.005
Number of particles, N_P	300,000	300,000
Stokes number, St_τ	0.113	91.845
Density ratio, ρ_P^*	2.5	2041
Volume fraction, Θ_P	10^{-4}	10^{-4}
Simulation timestep, Δt^*	0.005	0.005

Parameter	**Value**
Effective persistence length, λ_P	$0.082\ \mu m$
Temperature of fluid, T_F	$296\ K$
Rouse relaxation time, $\tau_{1,R}$	$0.16s$
Beads per polymer, N_B	10
Viscosity ratio, β	0.95

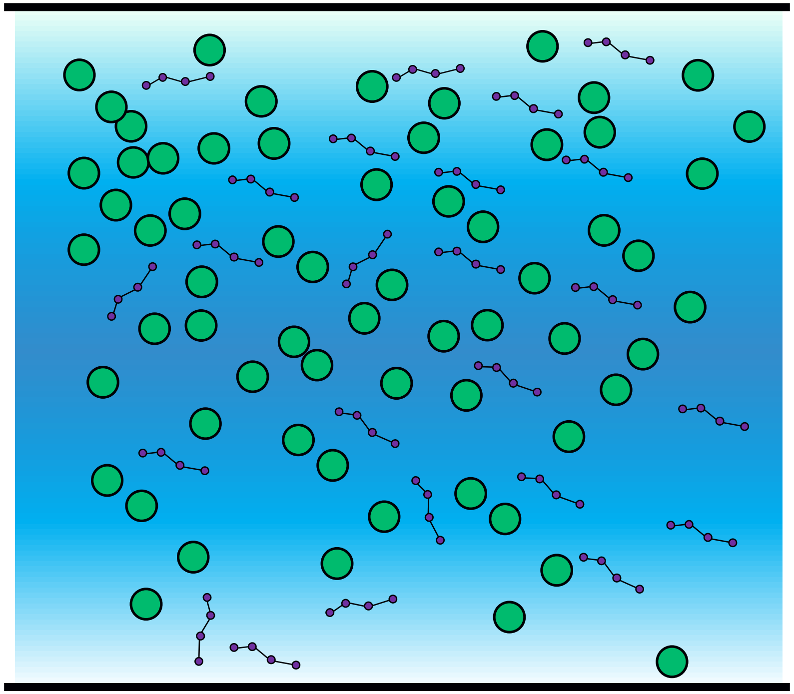

Simulation results

Initial drag reduction

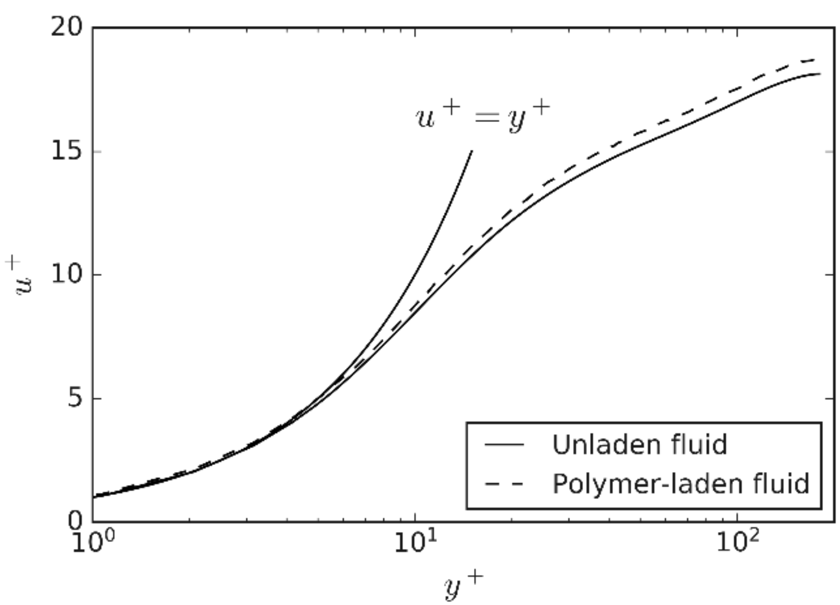

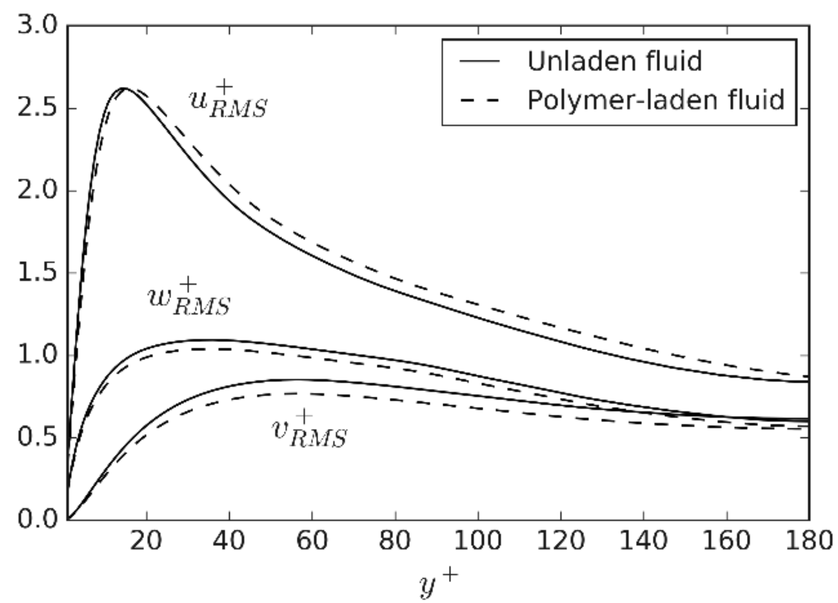

- Simulation performed with no particles initially to allow effects of drag reduction to settle.

Simulation results

Polymer conformation

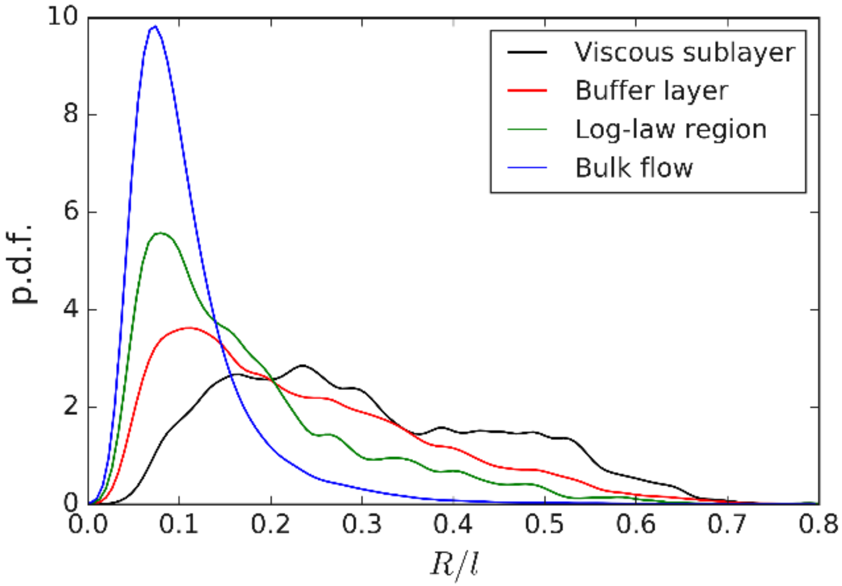

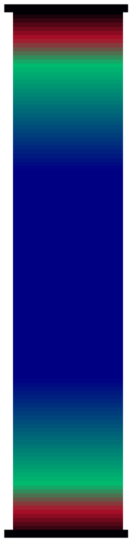

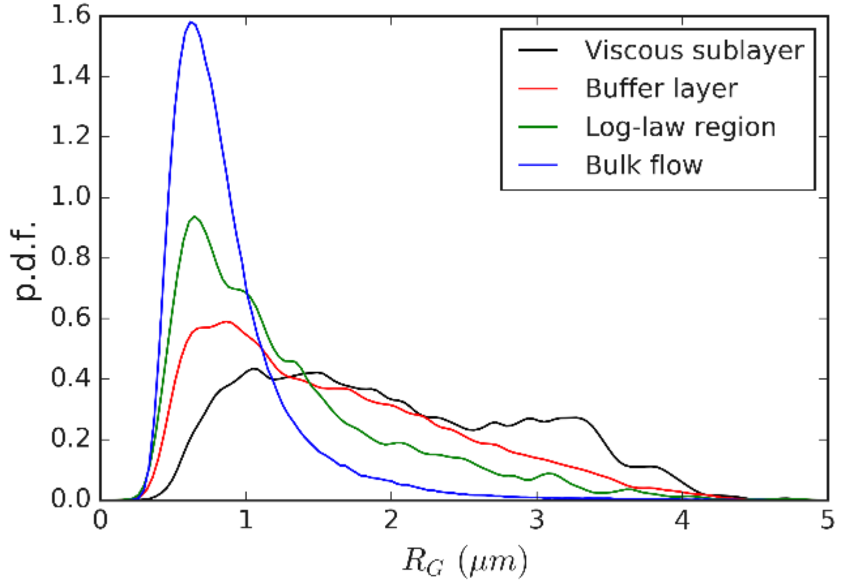

- Polymers in near-wall regions tend to be more stretched, and have increased radii of gyration.

Simulation results

Particle statistics

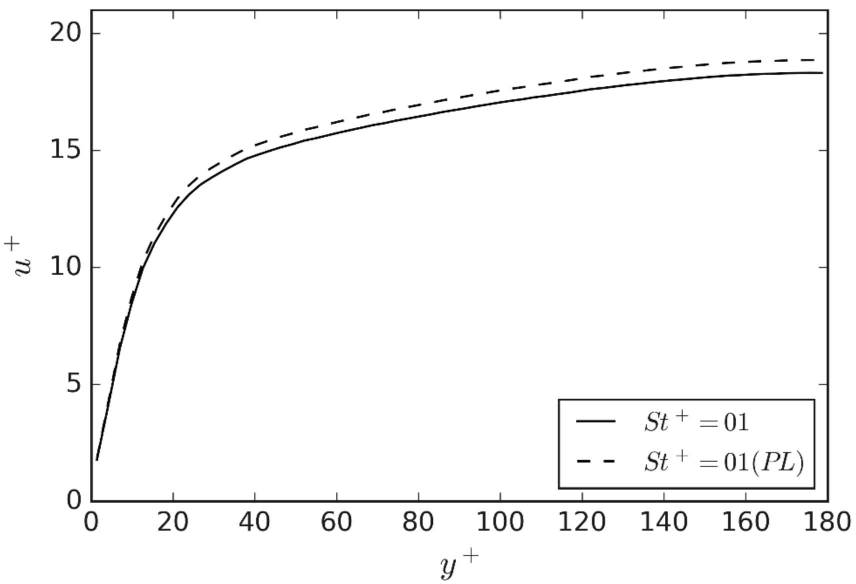

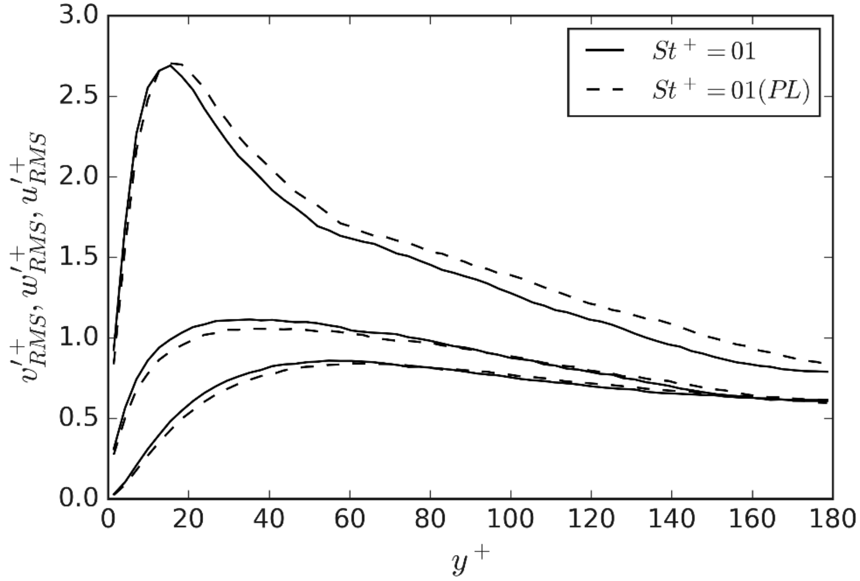

- Addition of polymers causes particle to move faster in the bulk.
- Turbulent motion of particulate phase is reoriented in the streamwise direction.

School of Chemical and Process Engineering
FACULTY OF ENGINEERING

UNIVERSITY OF LEEDS

Simulation results

Particle-polymer interaction statistics ($t^* = 10$)

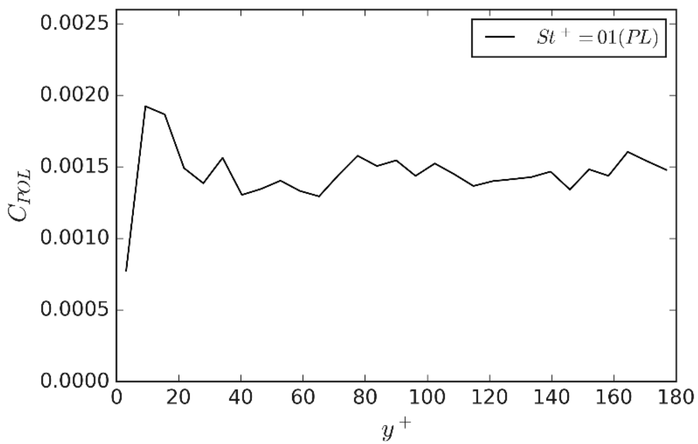

Each point represents an agglomerate (2+ particles)

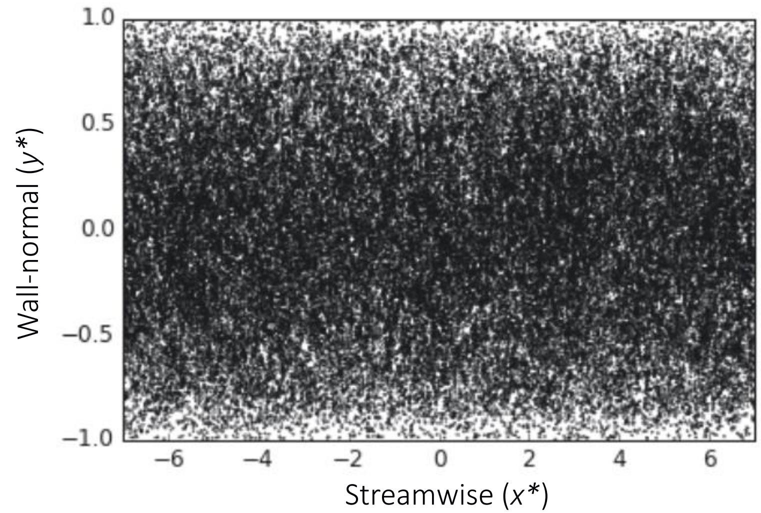

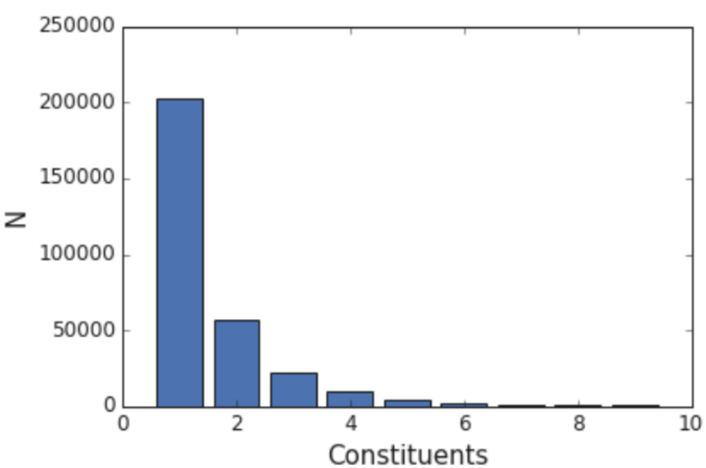

- Polymer-particle collisions fairly uniform. Slight increase in wall region.
- Even for low t* = 10, significant agglomeration events have occurred
- Agglomerates (2+ particles) mainly forming within centre of channel in the bulk.

Conclusions & Further work

- Polymer-laden particulate systems have been investigated for flows resembling calcite particles transported in water.
- Drag reduction has been observed, which increases the mean streamwise velocity of the flow for a set pressure gradient forcing.
- This has an indirect impact on the particulate phase dynamics since their carrier fluid dynamics are altered.
- The polymers also have a direct impact on the particles via hydrophobic interaction, leading to significant agglomeration within the bulk.

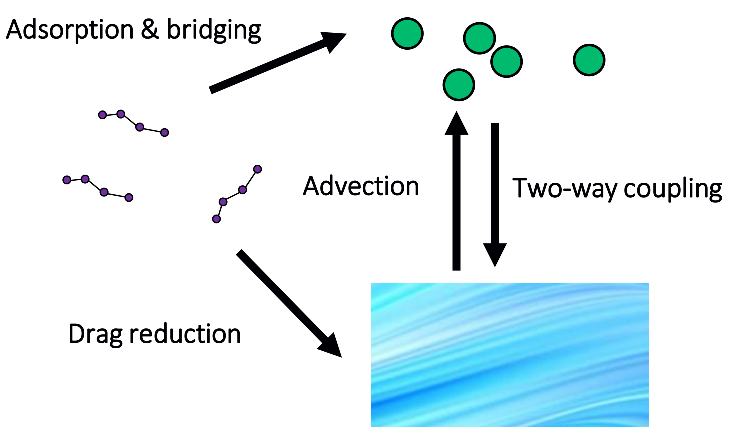

- Electrostatic interaction also responsible for polymer-particle interaction which adds further complexity to the model.
- What are the effects of variation of polymer parameters, temperature etc. ?
- Can we obtain methods further down the line to instigate breakup for agglomerated structures?

Acknowledgements

This work is supported by a UK Engineering and Physical Sciences Research Council grant at the University of Leeds from the TRANSCEND (Transformative Science and Engineering for Nuclear Decommissioning) project.

EPSRC
Engineering and Physical Sciences
Research Council

TRANSCEND

Thank you for your attention!

TRANSCEND

Transformative Science and Engineering for Nuclear Decommissioning

New materials and methods for decontamination of effluent

Antony Nearchou, University of Birmingham

14/05/21

TRANSCEND Theme Meeting

Energy

For a Low Carbon Future

Waste Management

- ^{235}U fission produces fission products such as Ba, Kr, Sr, Cs, I and Xe, with atomic masses distributed around 95 and 135.

- **^{137}Cs** and **^{90}Sr** have half-lives of ca. 30 years and produce most of the medium-lived radioactivity in spent fuel. Require removal from liquid waste.

- The radionuclides can be immobilised in a solid. Reduces waste volume as well as risk of environmental leaching.

- Current removal methods make use of **ion exchange** with **zeolite** materials. This is a facile, inexpensive, selective, consistent and high-capacity approach.

Spent fuel cooling pond at Sellafield. Source: Sellafield Ltd.

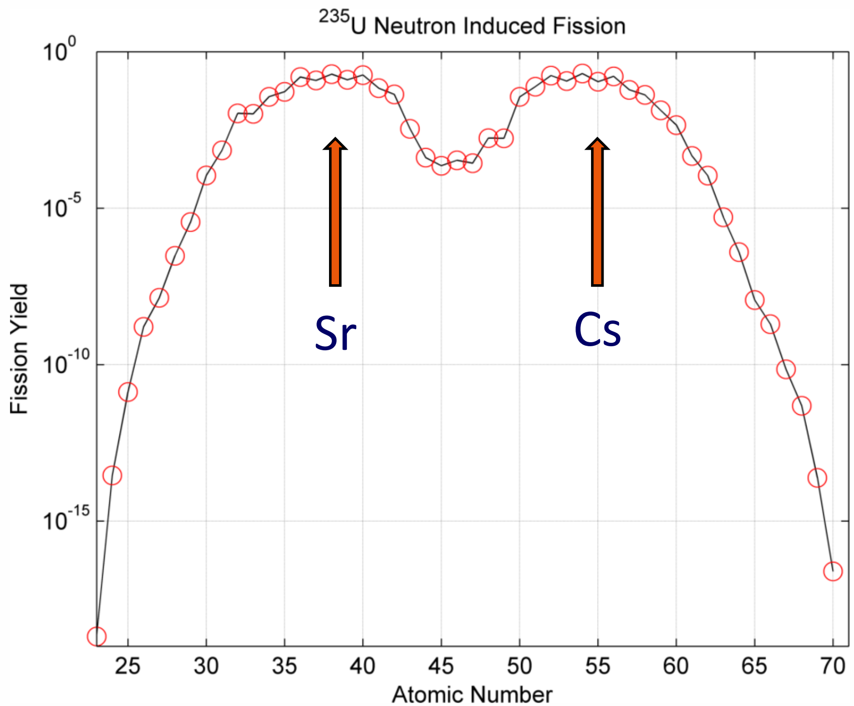

Zeolites and Ion Exchange

Zeolite Clino: $Na_6[Al_6Si_{30}O_{72}](H_2O)_9$

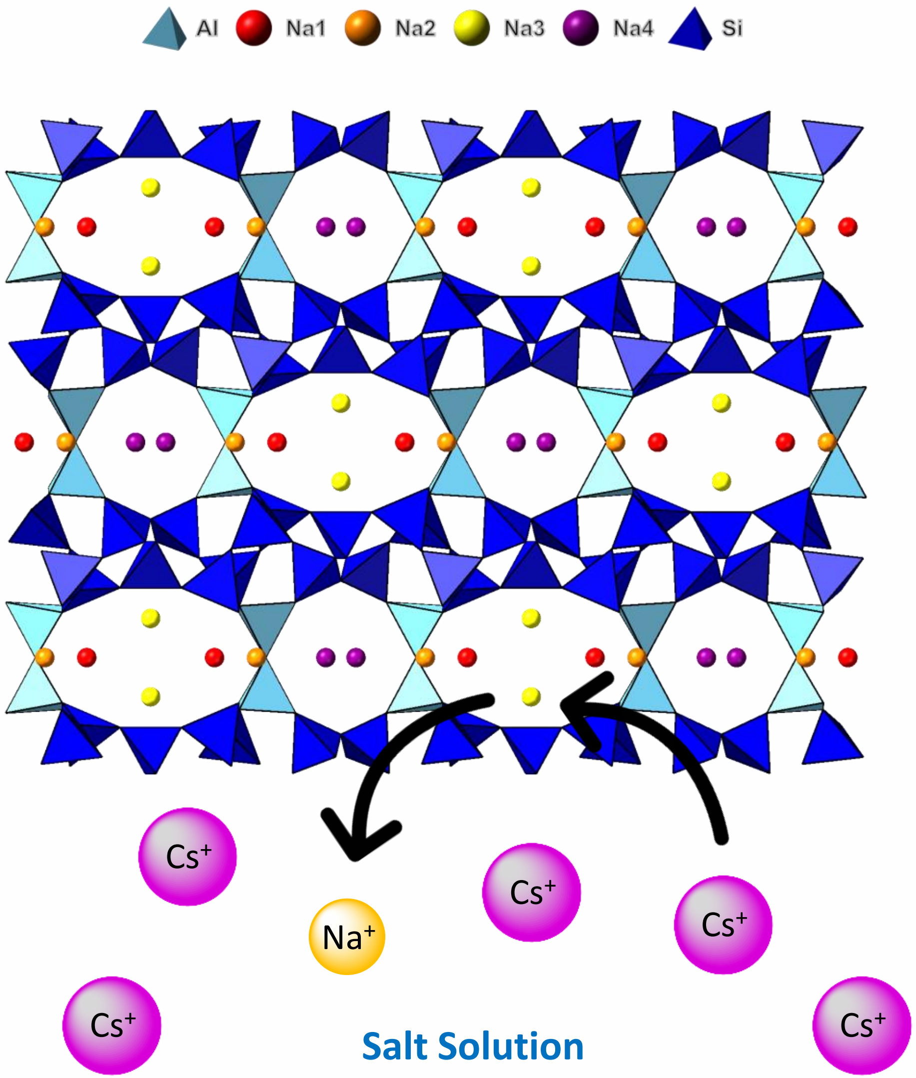

What are Zeolites?

- Crystalline, microporous (< 2nm) aluminosilicates.
- 3D network of connected SiO_4 and AlO_4 tetrahedra.
- Negatively charged framework, balanced by extra-framework cations.

Ion Exchange

- Interchange between the zeolite cations and the cations in a salt solution – i.e. Cs^+ and Sr^{2+}.
- Mud Hills clinoptilolite (clino) is used on the SIXEP plant at Sellafield.
- Clino has the best performance of natural zeolites.[1] Pore diameter is 3.5-3.9 Å, similar to hydrated Cs^+.

[1] L.L. Ames, *Am. Miner.*, 1962, **47**, 1310-1326

Zeolites and Ion Exchange

Zeolite Clino: $Na_6[Al_6Si_{30}O_{72}](H_2O)_9$

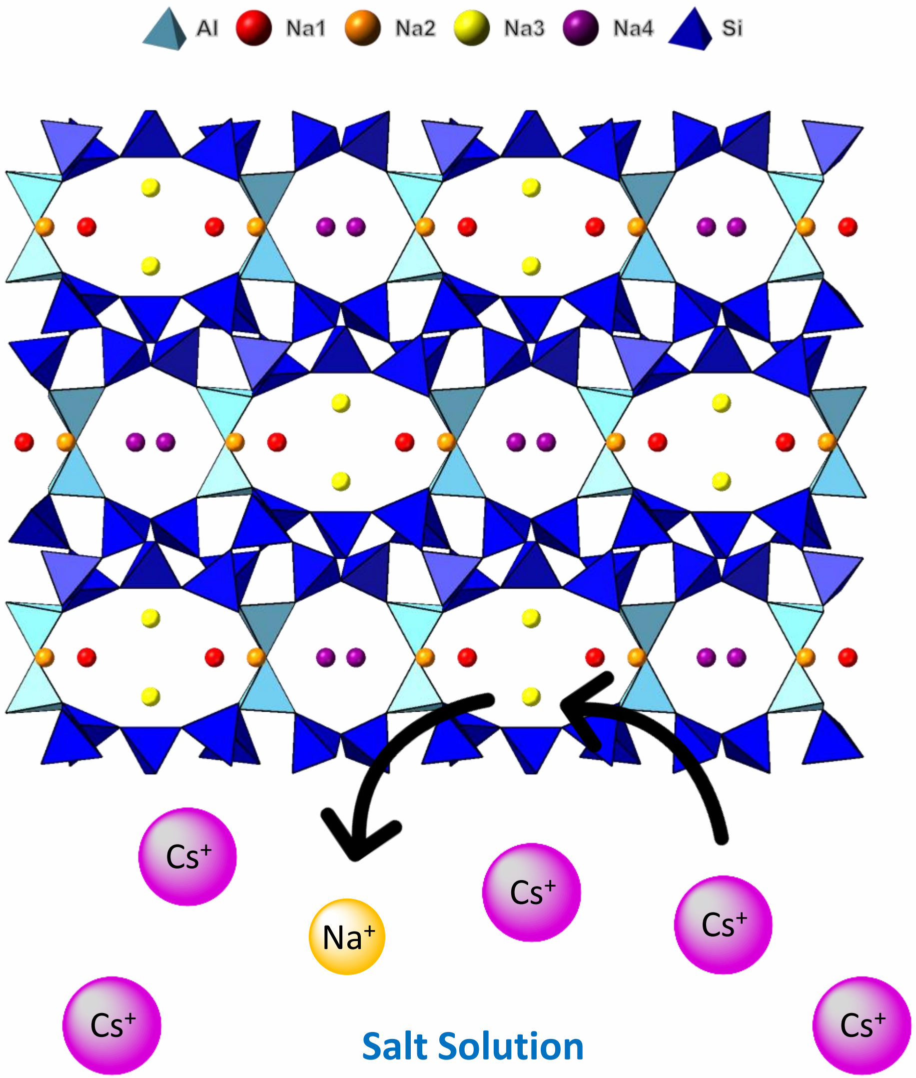

The Problem

- Clino is a finite natural resource – successor materials needed.
- Considerations needed for a successor:
  - Selectivity against excess competing cations i.e. Na^+, K^+, Ca^{2+}, Mg^{2+} etc.
  - **Cs^+ vs K^+ selectivity** – similar hydrated radii.
  - Performance at different pH.
  - Means of deployment.
  - Retention of immobilised cations.
  - Potential waste forms for geological disposal.

Transformative Science and Engineering for Nuclear Decommissioning

New Material: Umbites

$$K_2MSi_3O_9 \cdot H_2O$$

Where M = Zr, Ti, Sn, Ge

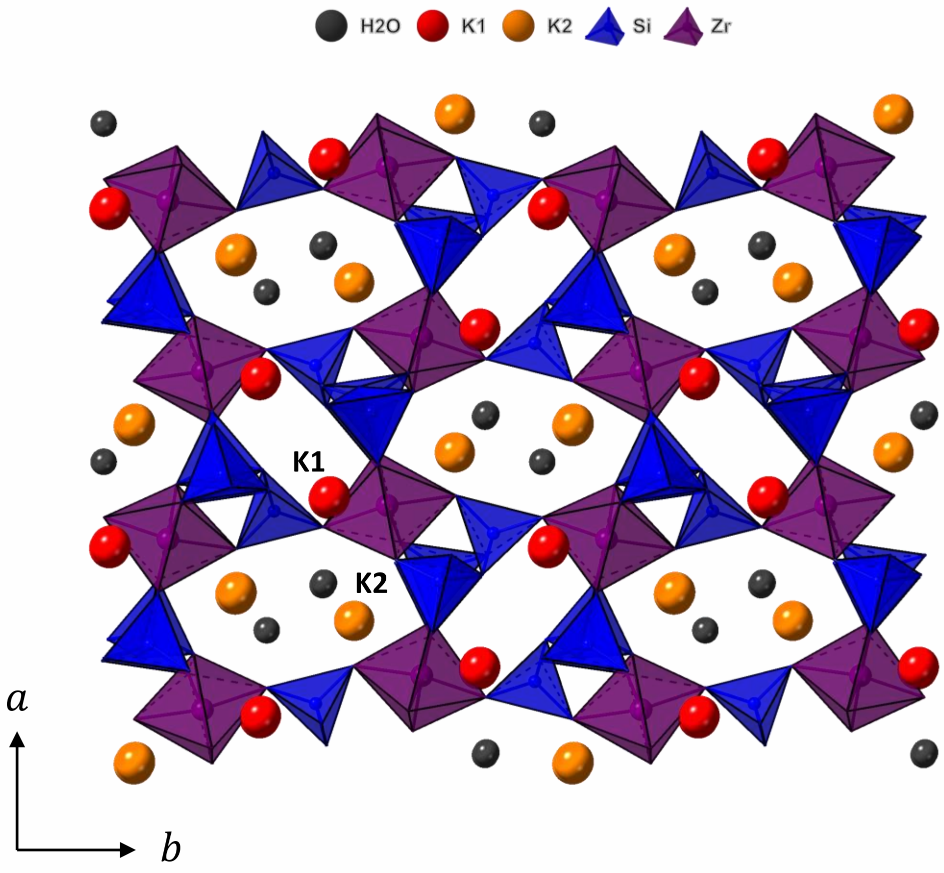

- 3.1-4.1 Å pore diameters, similar to clino.
- Previous work in the group with Sn-umbites.
- Doping the octahedral M(4+) site with a M(5+) metal improves the Cs^+ and Sr^{2+} **cation affinity**.[1]
- Doping enhances cation diffusion through the framework.

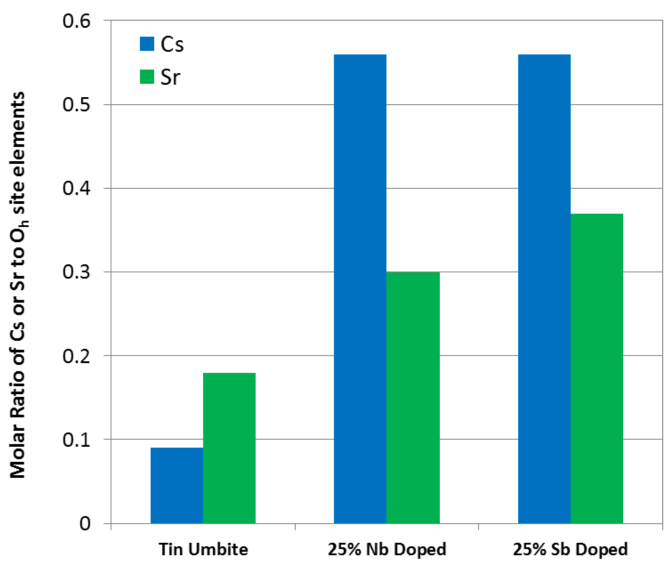

The Sn^{4+} site is 25% doped with Nb^{5+} or Sb^{5+}.

Vast increase in Cs^+ and Sr^{2+} uptake from bulk ion exchanges.

[1] Unpublished work by Tzu-Yu Chen, Dan Parsons and Ryan George University of Birmingham

New Material: Umbites

$$K_2MSi_3O_9 \cdot H_2O$$

Where M = Zr, Ti, Sn, Ge

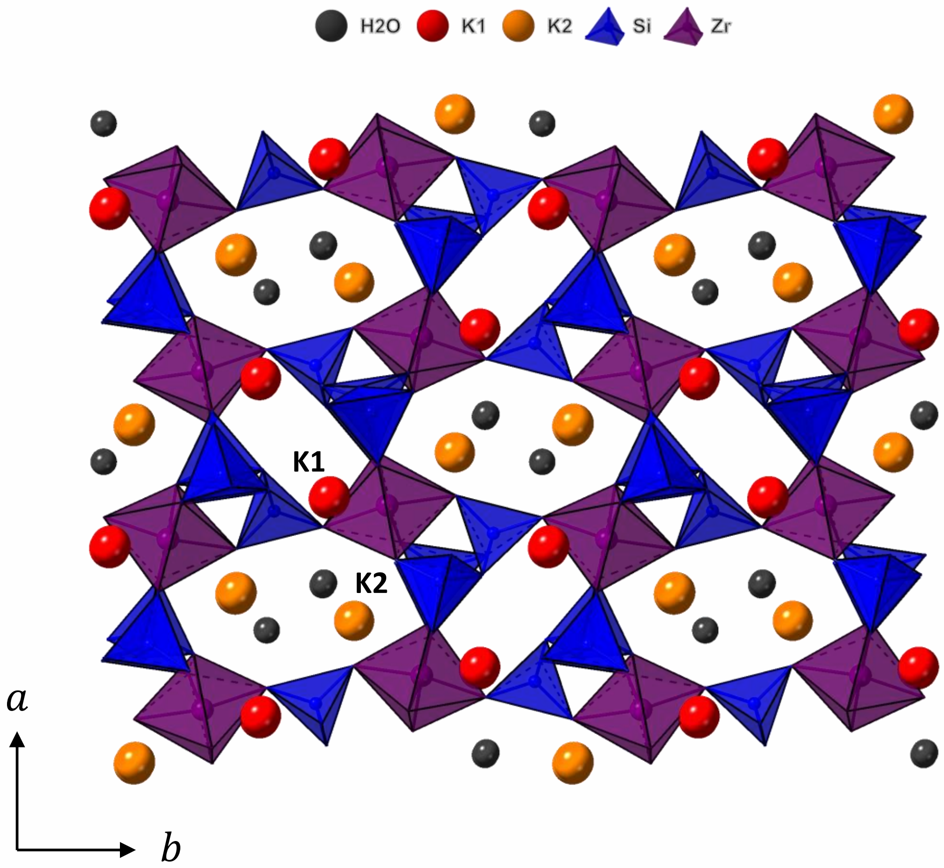

Current Research

- Synthesis optimisation of the doped Sn-umbite.
- Further ion exchange performance assessment
  - Against competitor cations (Cs^+ vs K^+).
  - Varying pH conditions.
  - Kinetics.
  - Simulant solutions.
  - Active testing.
- Production of beads, pellets or monoliths. Deployment in an ion exchange bed or column.

Optimising Synthesis

25% Sb-doped Sn-umbite
Typical synthesis 200°C 24hrs hydrothermal (a)

Explored varying temperature and time.
Use of seeding to reduce nucleation time.

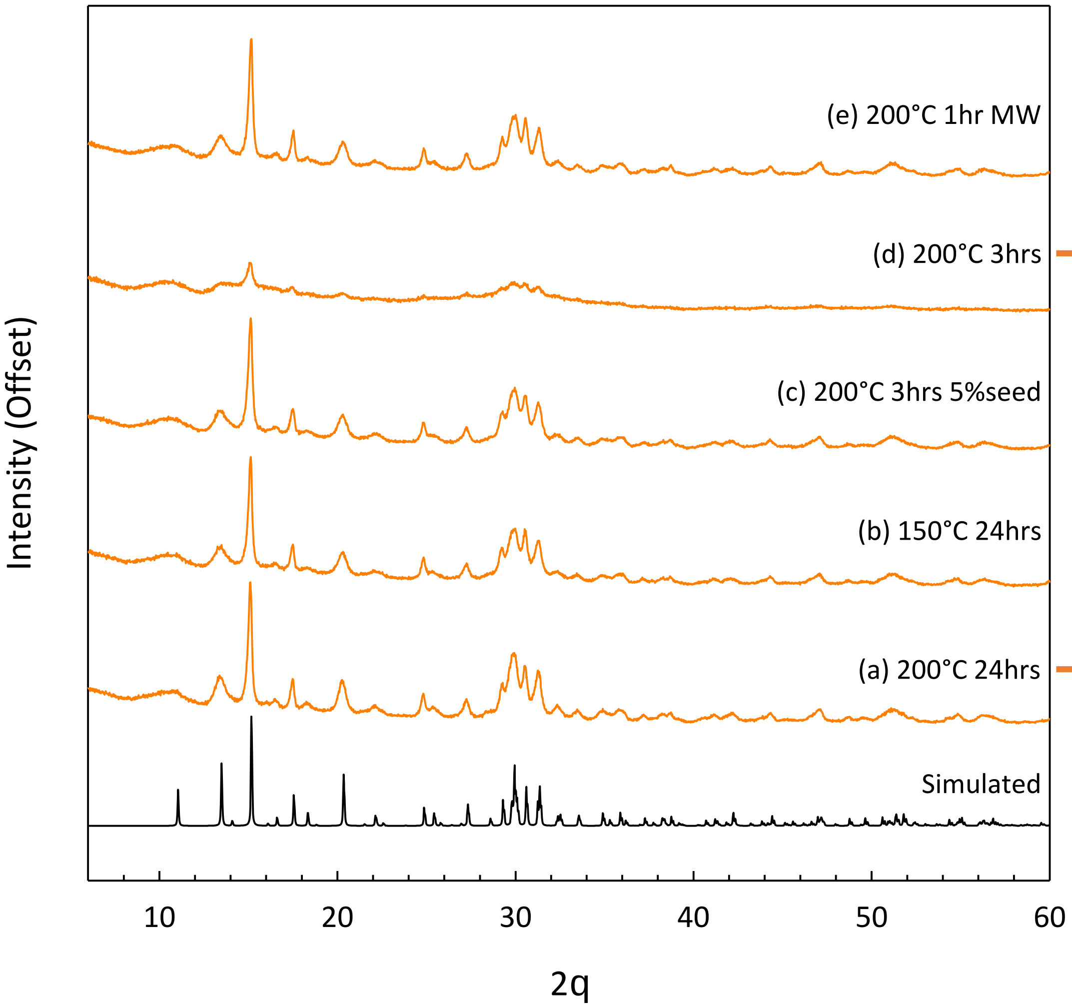

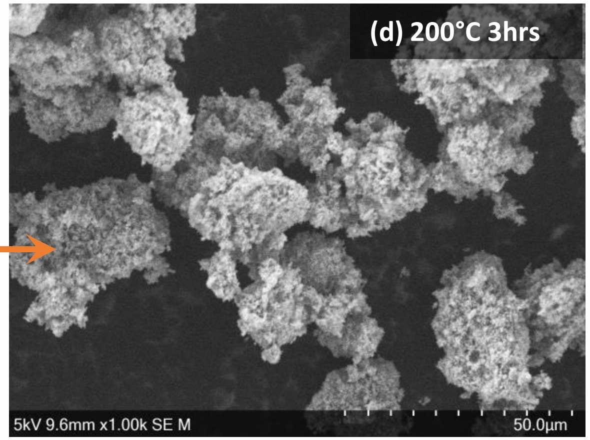

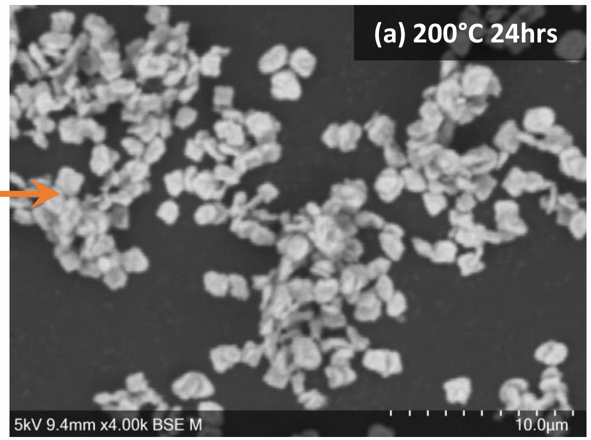

- Minimum temperature of 150˚C needed.
- **200˚C**
  - ≥ 5 hrs
  - ≥ 3 hrs with 5% seeding
- **150˚C**
  - ≥ 24 hrs
  - ≥ 16 hrs with 5% seeding
- **200˚C Microwave**
  - ≥ 1 hr
  - Exploring reduce time/temp

Ion Exchange – Cs vs K

Synthesis	Sample	Av. Particle Length /µm
(a) 200°C 24hrs	Umbite	1.65 (0.23)
(b) 150°C 24hrs	Umbite	1.09 (0.15)
(c) 200°C 3hrs 5%seed	Umbite	1.50 (0.31)
(d) 200°C 3hrs	Poorly crystalline umbite	-

Exchange with 30 mg exchanger in 15 ml solution.
Cs 10 ppm, K 0, 10 and 50 ppm – varying pH.

- Crystalline sample show consistent Cs removal with K – slight drop off at basic pH.
- Poorly crystalline sample (d) shows sharp drop off with K in acid.
- Consider: important role of H^+ in ion exchange.

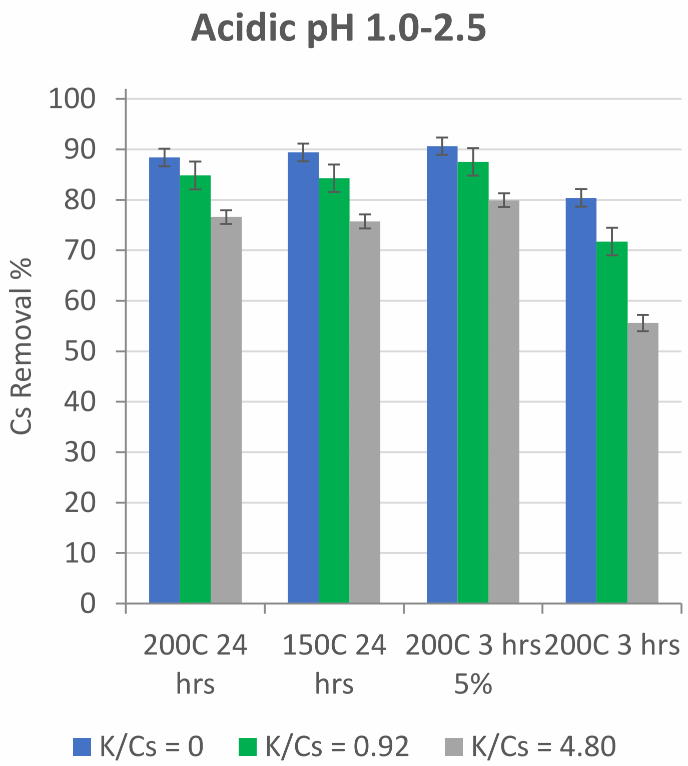

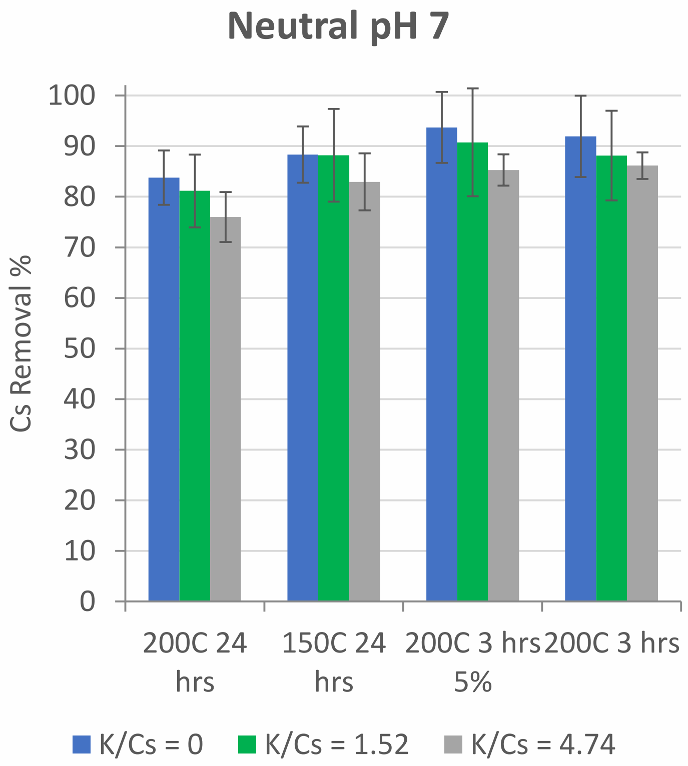

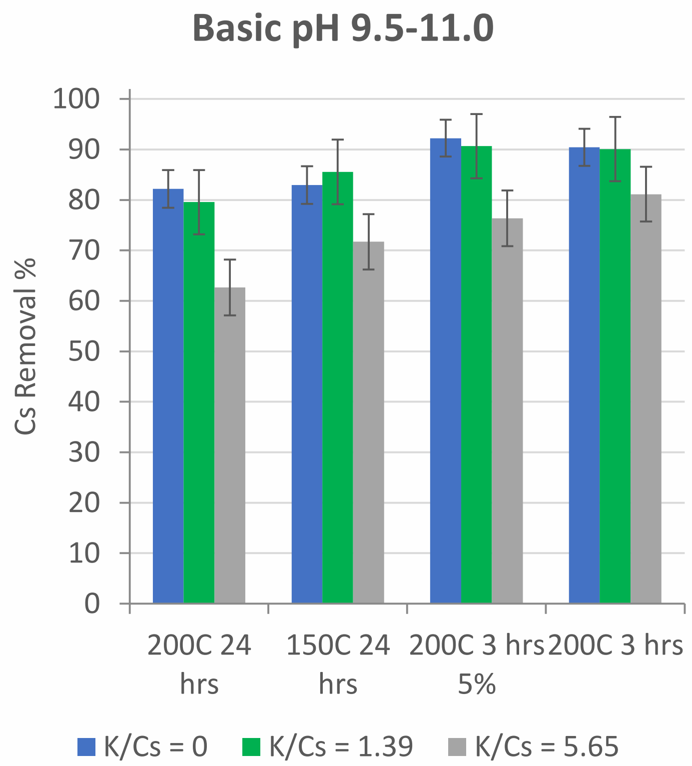

Ion Exchange – Cs, Sr vs M

Synthesis	Sample	Av. Particle Length /µm
(a) 200°C 24hrs	Umbite	1.65 (0.23)
(b) 150°C 24hrs	Umbite	1.09 (0.15)
(c) 200°C 3hrs 5%seed	Umbite	1.50 (0.31)
(d) 200°C 3hrs	Poorly crystalline umbite	-

Ion Exchange with 30 mg exchanger in 15 ml solution. Acidic pH <2.5.

Solutions tested:

- **Sr 10 ppm, K 0, 10 and 50 ppm**
- **Cs and M 50 ppm.** Where M is Na, K, Mg, Ca and Sr.
- **Sr and M 50 ppm.** Where M is Na, K, Mg, Ca and Cs.

Sr 10 ppm, K 0, 10 and 50 ppm

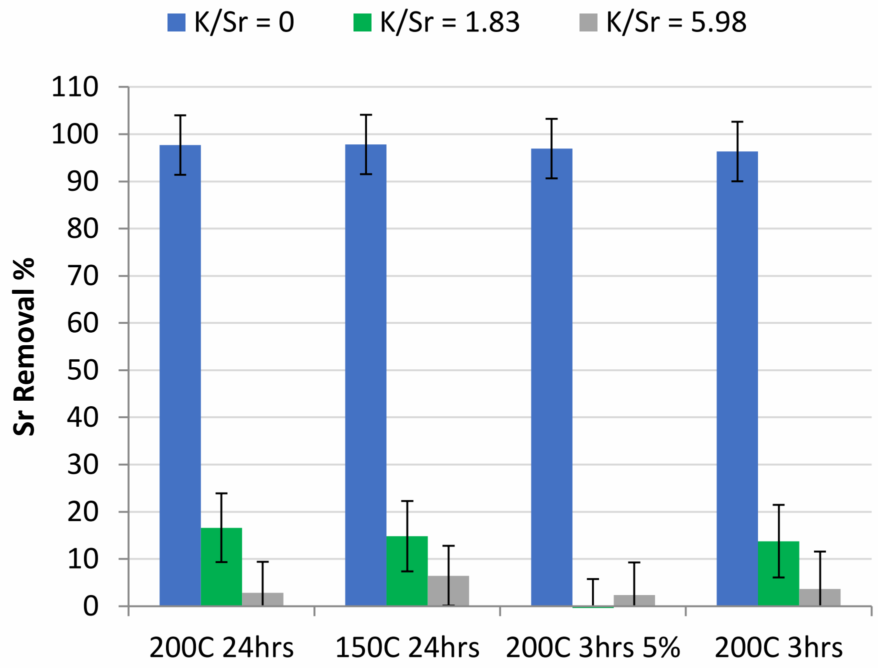

Cs or Sr 10 ppm, M 50 ppm

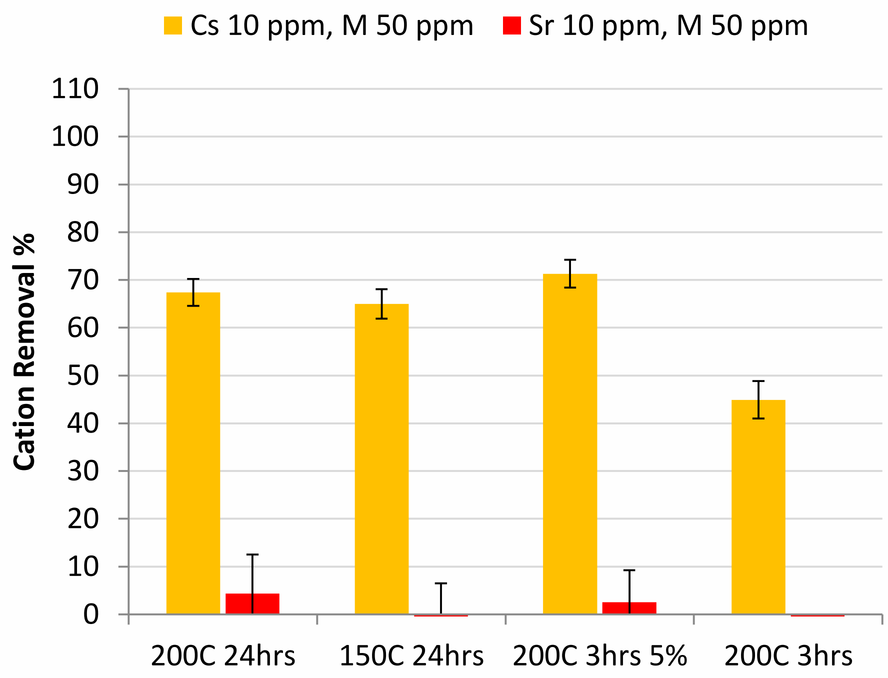

Kinetics of Ion Exchange

- Exchanger: Umbite – 200 ˚C 24 hrs
- Solution: Cs 10 ppm
- 30 mg exchanger in 15 ml solution
- Batch procedure
- Equilibrium achieved within 5 minutes

<u>Compared to Clino:</u>

- Previous work has shown that clino reaches equilibrium at around 6 hours.[1, 2]
- This is for natural and pre-treated clino
- Cs concentration: 5, 300 and 1500 ppm

First 10 minutes of exchange

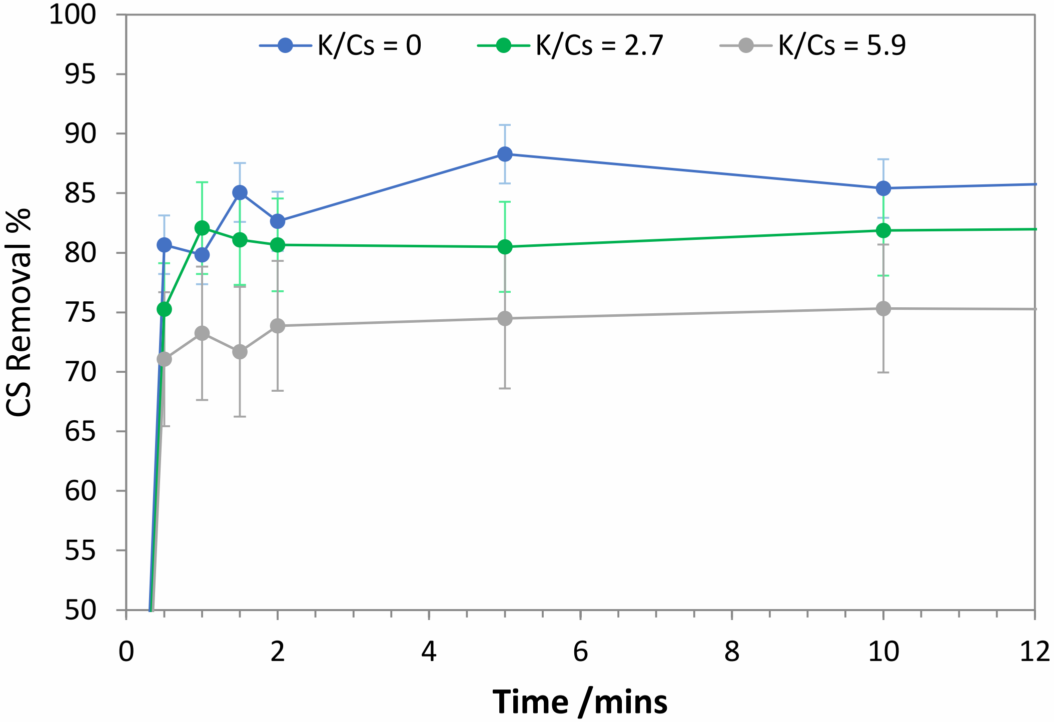

Exchange over 24 hours (logarithmic)

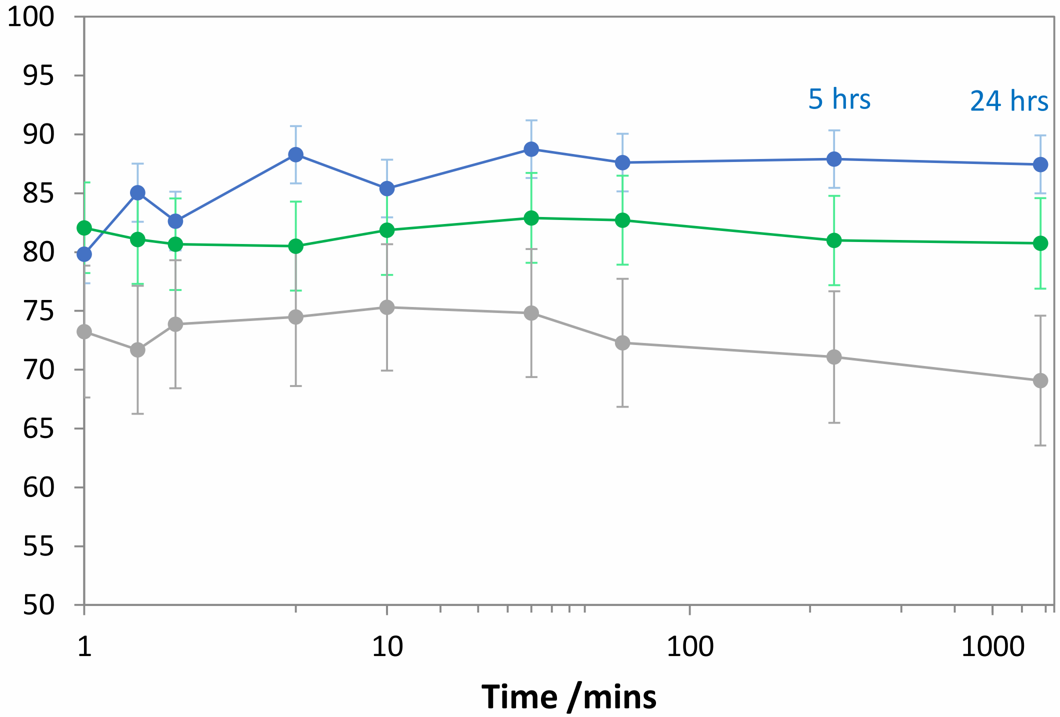

[1] M.Y. Prajitno *et al.*, *J. Environ. Chem. Eng.*, 2019, **8**, 102991
[2] I. Smičiklas et al., *Appl. Clay Sci.*, 2007, **35**, 139-144

Pellet Production

- Production of **monoliths/pellets** which can be put used in an exchange be.

- Pellet paste composition:
  - Umbite
  - Temporary binder (PVA solution)
  - Permanent binder (SiO_2, ZrO_2, TiO_2)

- Fired to calcine the material and remove the PVA - produces mesopores.

- Test pellet stability under caustic conditions.
- Test pellet structural integrity.

- Early tests show that the pellets **maintain ion exchange** properties of the powders. Further testing needed.

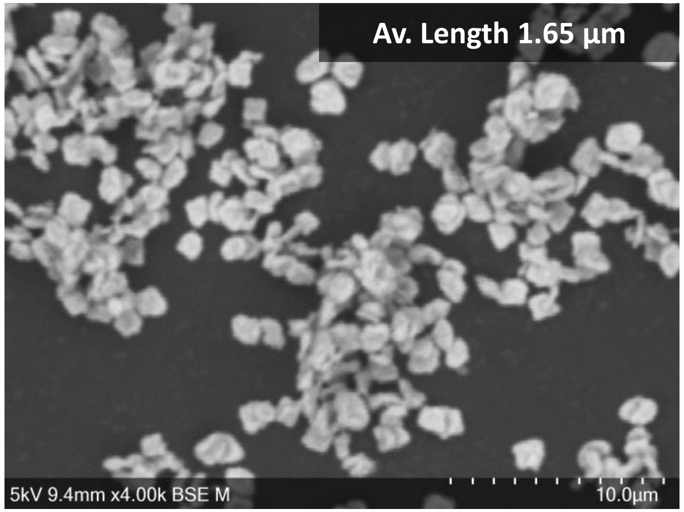

Fired Umbite Pellet ~2 mm diameter

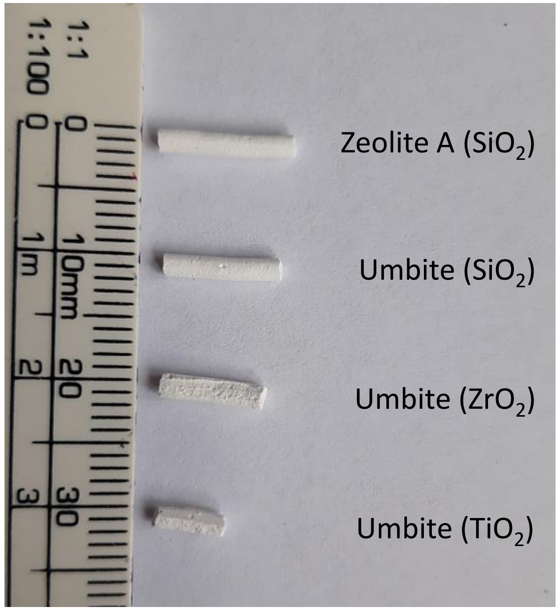

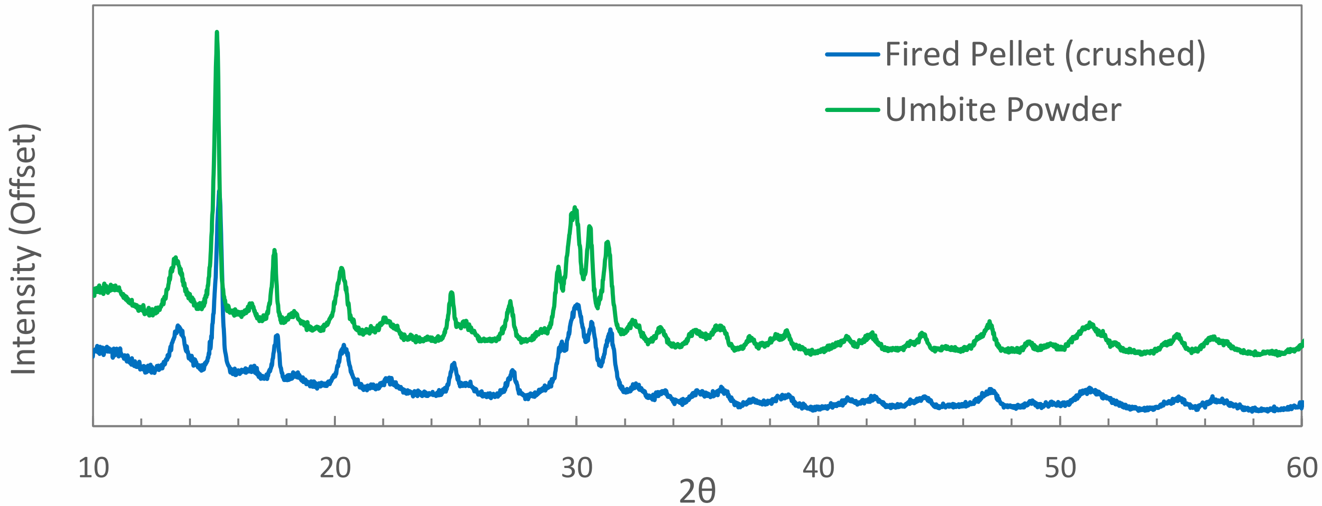

Summary and Future Work

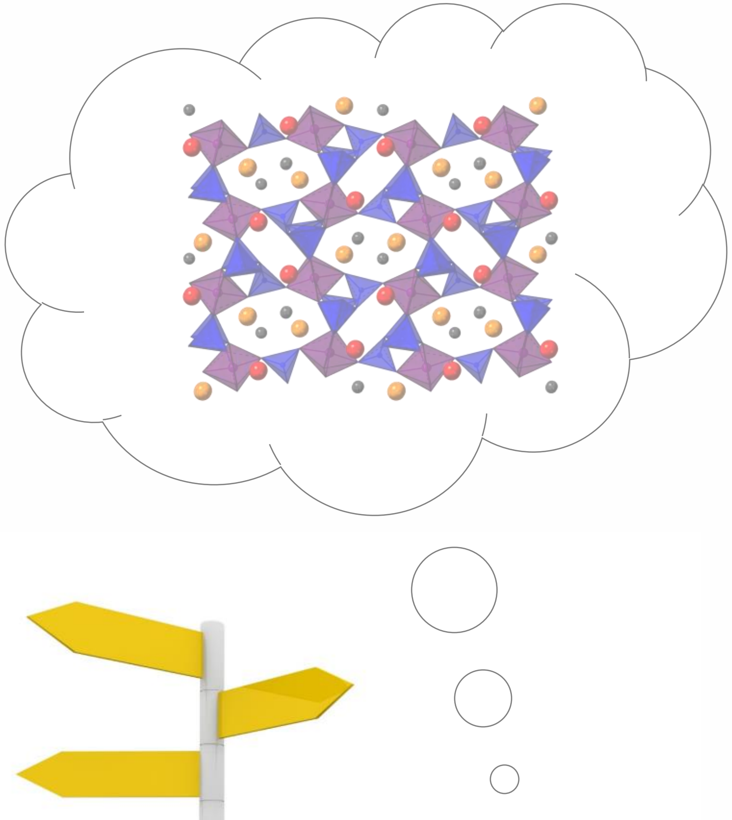

Achievements

- Optimised synthesis of umbites.
- Sustained Cs^{+} removal in the presence of competing cations and in different pH media.
- Sr^{2+} removal is high, but significantly impeded by competitors.
- Cs^{+} uptake is rapid *ca.* 30 seconds.
- Umbites can be prepared into pellets for deployment.

Ongoing and Future Work

- Ion exchange with simulant effluents and active testing.
- Optimising pellet production, to ensure pellets and chemically and mechanically stable.
- Further ion exchange testing of pellets.
- Effect of pretreatment of the umbites on ion exchange.
- Waste forms and leach testing.
- **Investigating other new materials of interest.**

Acknowledgements

Birmingham: Tzu-Yu Chen, Dan Parsons, Ryan George, James Reed, Phoebe Allan, Joe Hriljac.

ICP-MS: Norman Day, Chris Stark.

EPSRC Pioneering research and skills

NATIONAL NUCLEAR LABORATORY

TRANSCEND

UNIVERSITY OF BIRMINGHAM

Research Councils UK Energy For a Low Carbon Future

Transformative Science and Engineering for Nuclear Decommissioning

Thank you

Email: A.Nearchou@bham.ac.uk

Generation and Transport of Radiolytic Hydrogen in Hydroxide Sludges

Mel O'Leary, DCF, The University of Manchester

NDA Transcend Conference

Introduction

Experimental Setup

Transport Measurements

Bubbles

Conclusions

Mel O'Leary Email: mel.oleary@manchester.ac.uk

Sellafield Ltd

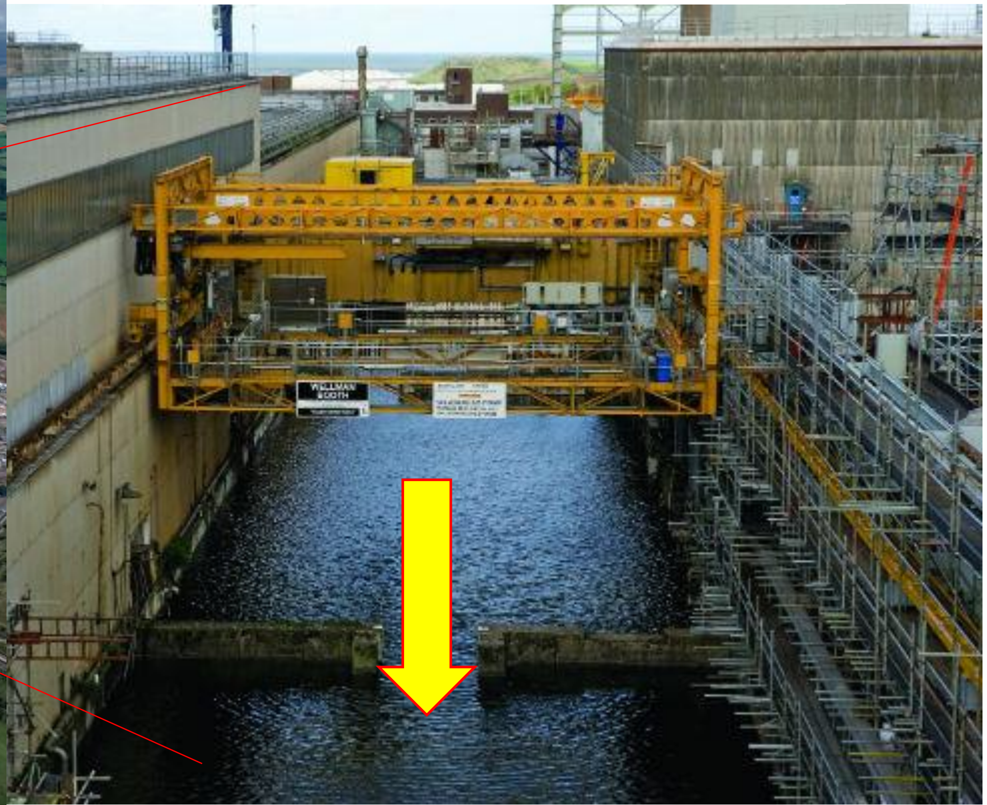

Mel O'Leary Email: mel.oleary@manchester.ac.uk

Introduction

Experimental Setup

Transport Measurements

Bubbles

Conclusions

Experimental Overview

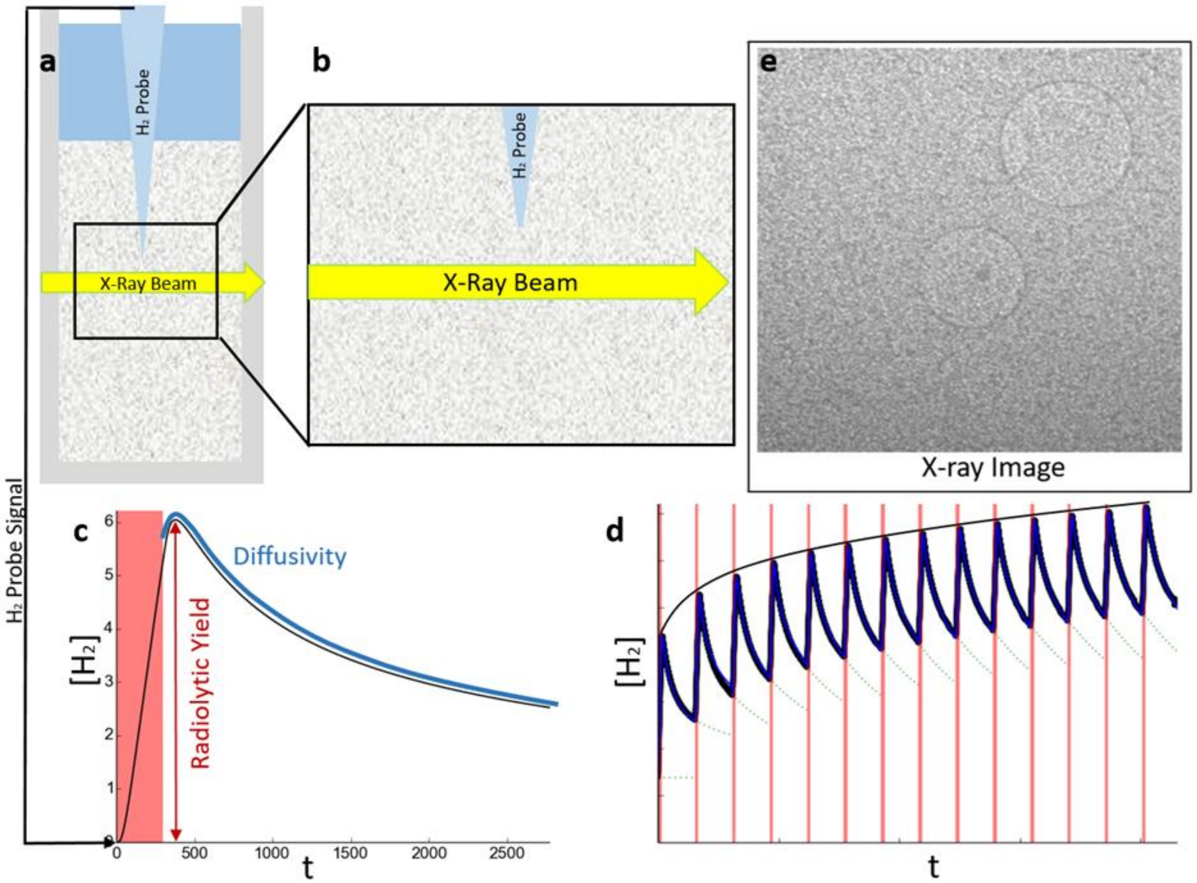

Mel O'Leary Email: mel.oleary@manchester.ac.uk

X-rays

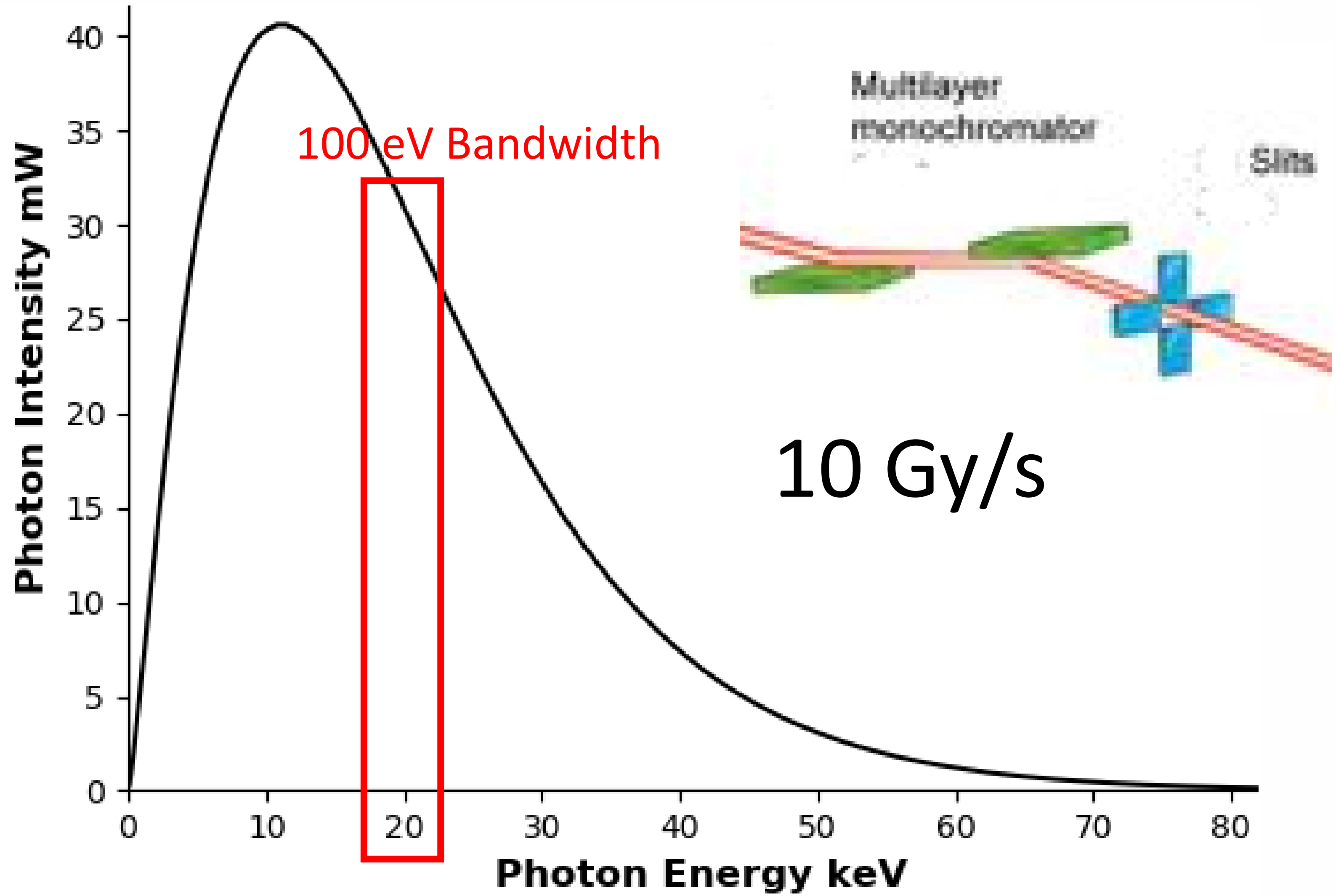

10 Gy/s

Mel O'Leary Email: mel.oleary@manchester.ac.uk

Samples

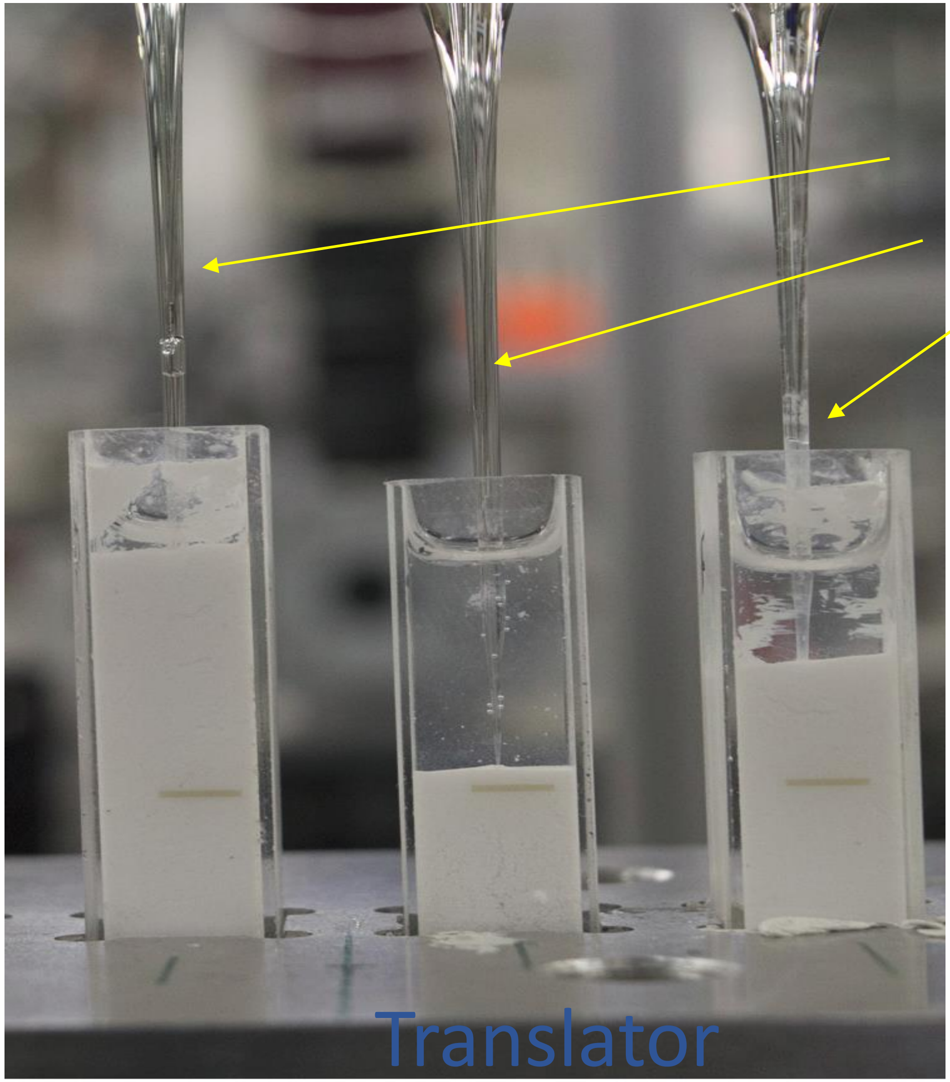

Probes

12 samples in parallel

Mel O'Leary Email: mel.oleary@manchester.ac.uk

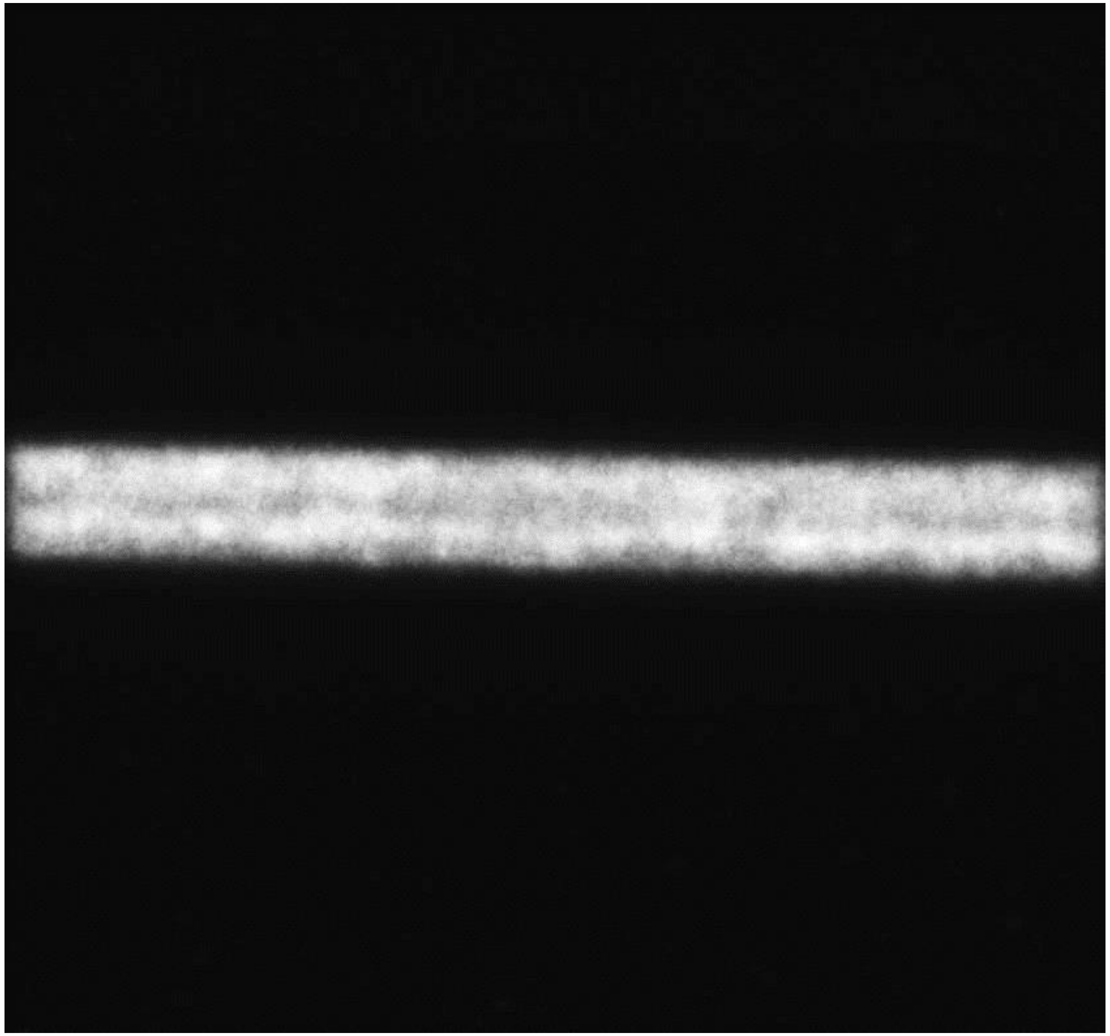

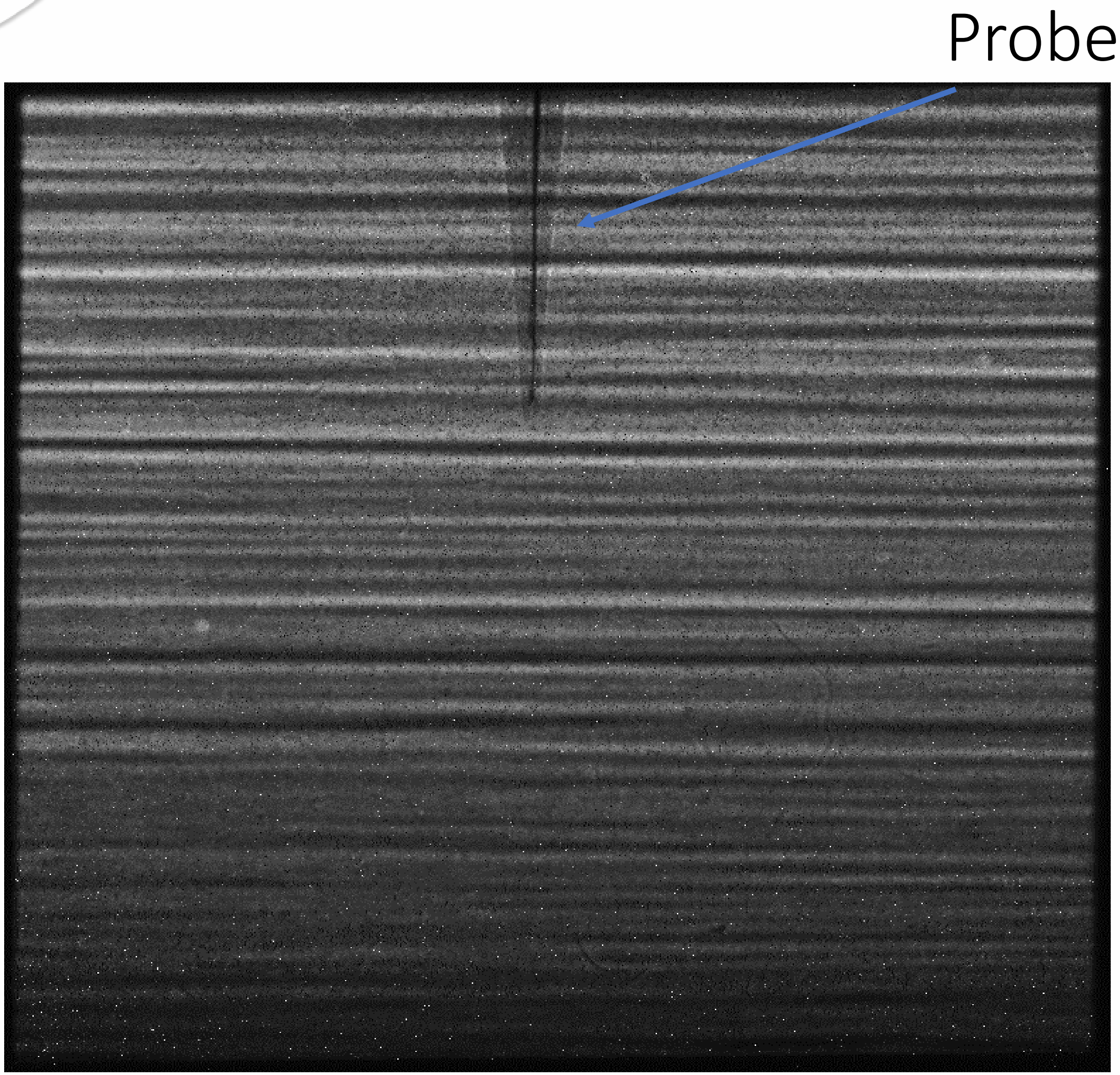

Mel O'Leary Email: mel.oleary@manchester.ac.uk

Dosimetry

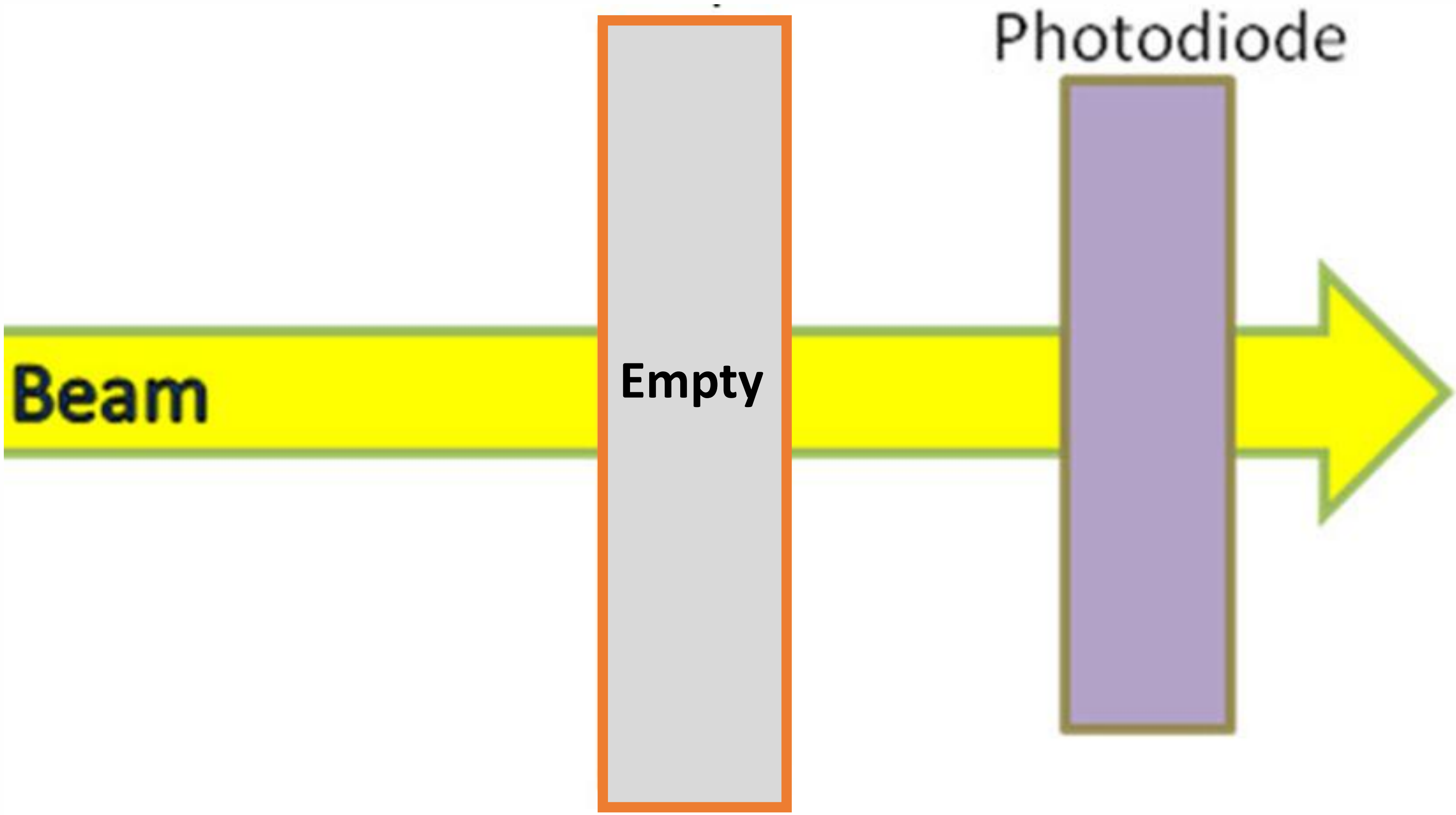

Introduction

Experimental Setup

Transport Measurements

Bubbles

Conclusions

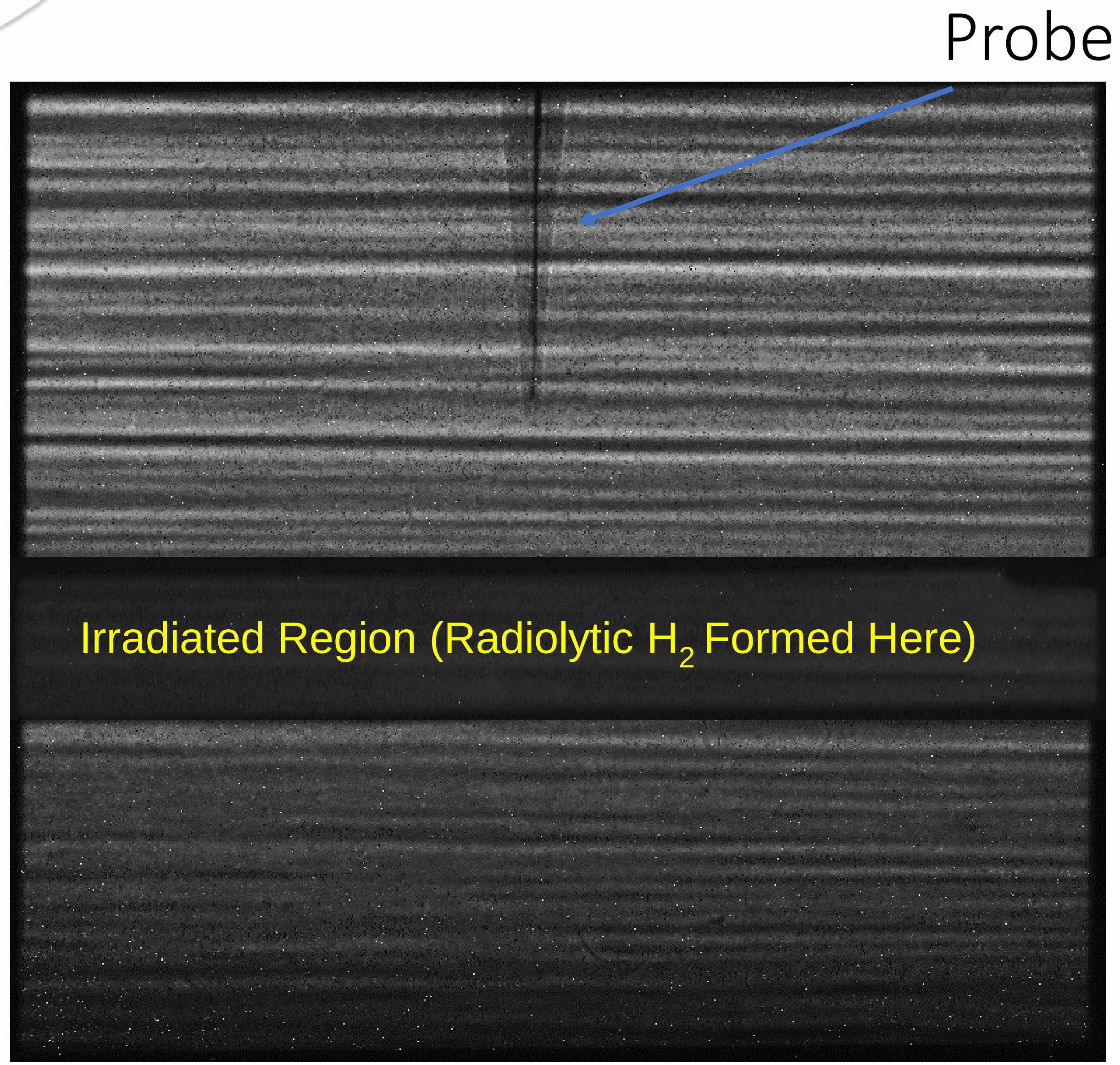

Mel O'Leary Email: mel.oleary@manchester.ac.uk

1D Diffusion

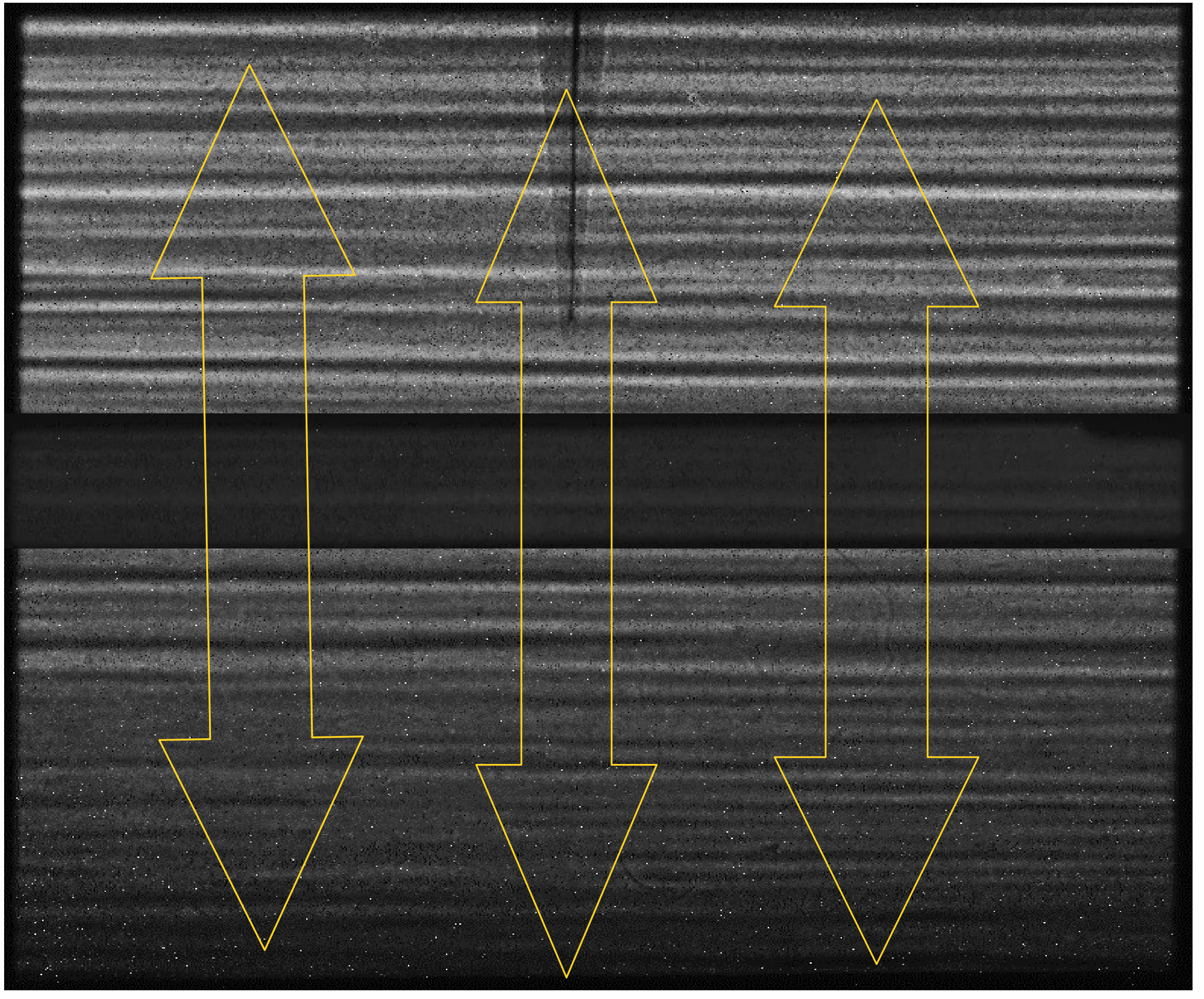

Mel O'Leary Email: mel.oleary@manchester.ac.uk

Diffusion Coefficients

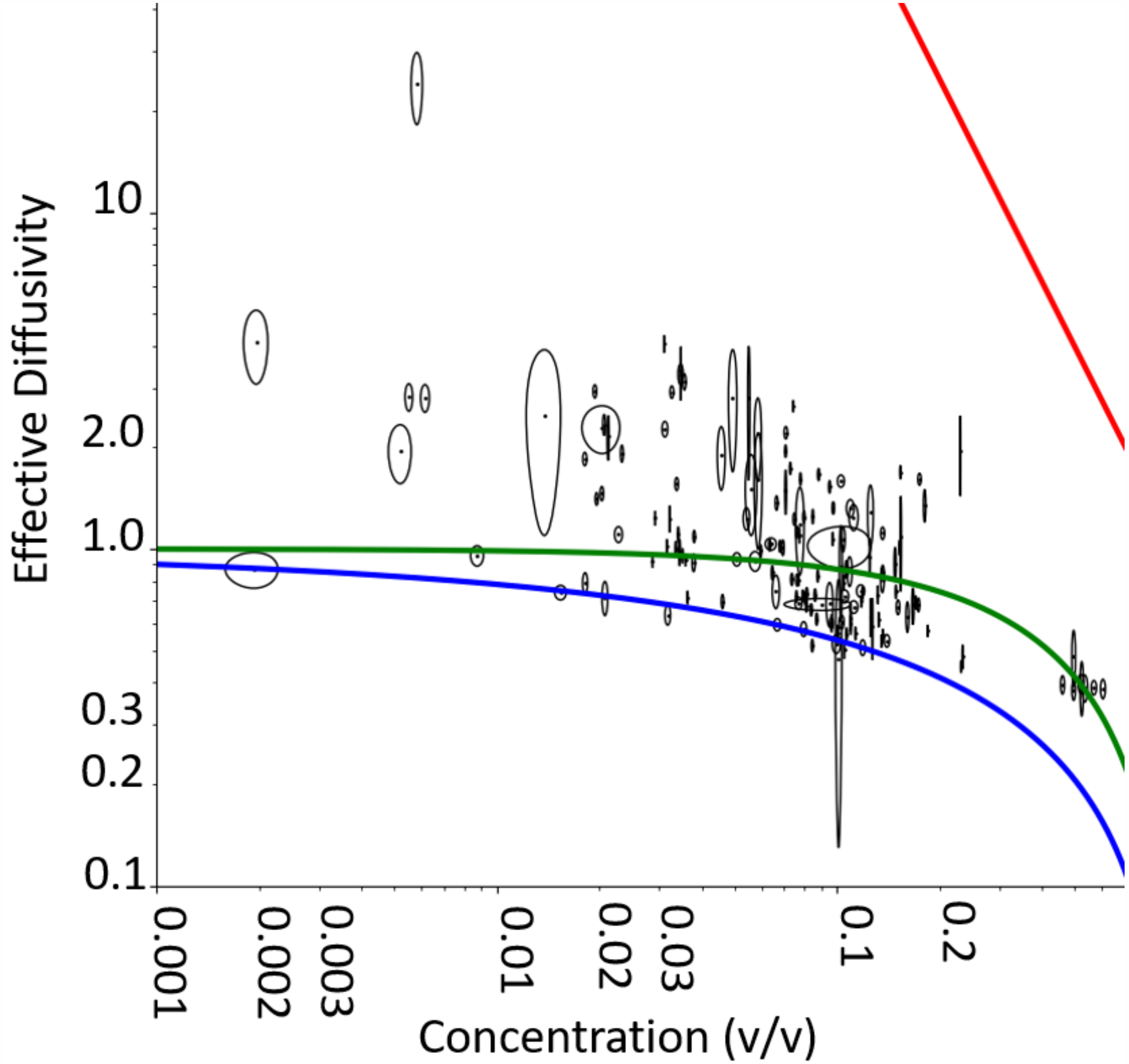

Mel O'Leary Email: mel.oleary@manchester.ac.uk

Radiolytic Yield

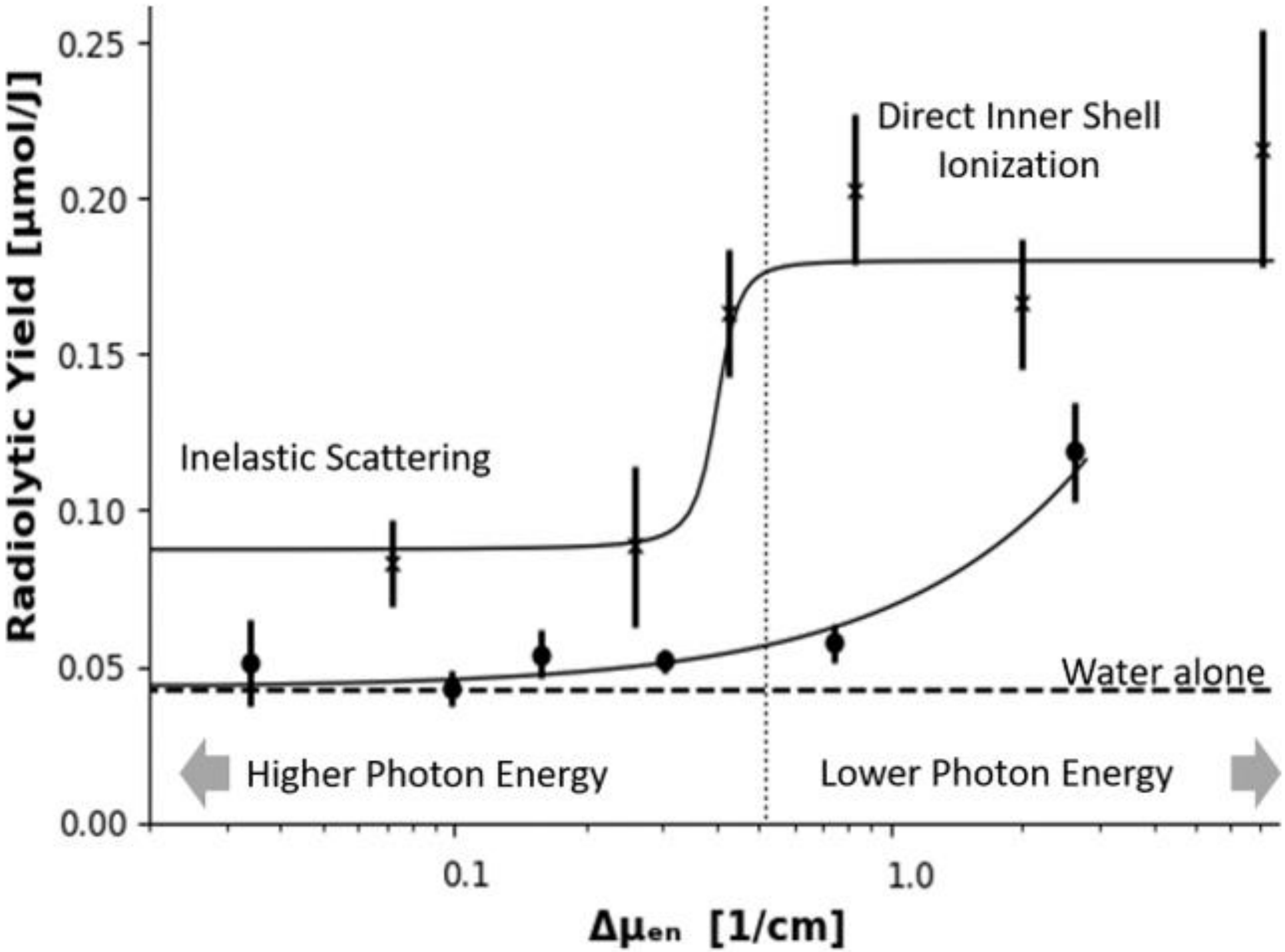

Mel O'Leary Email: mel.oleary@manchester.ac.uk

Bubbles

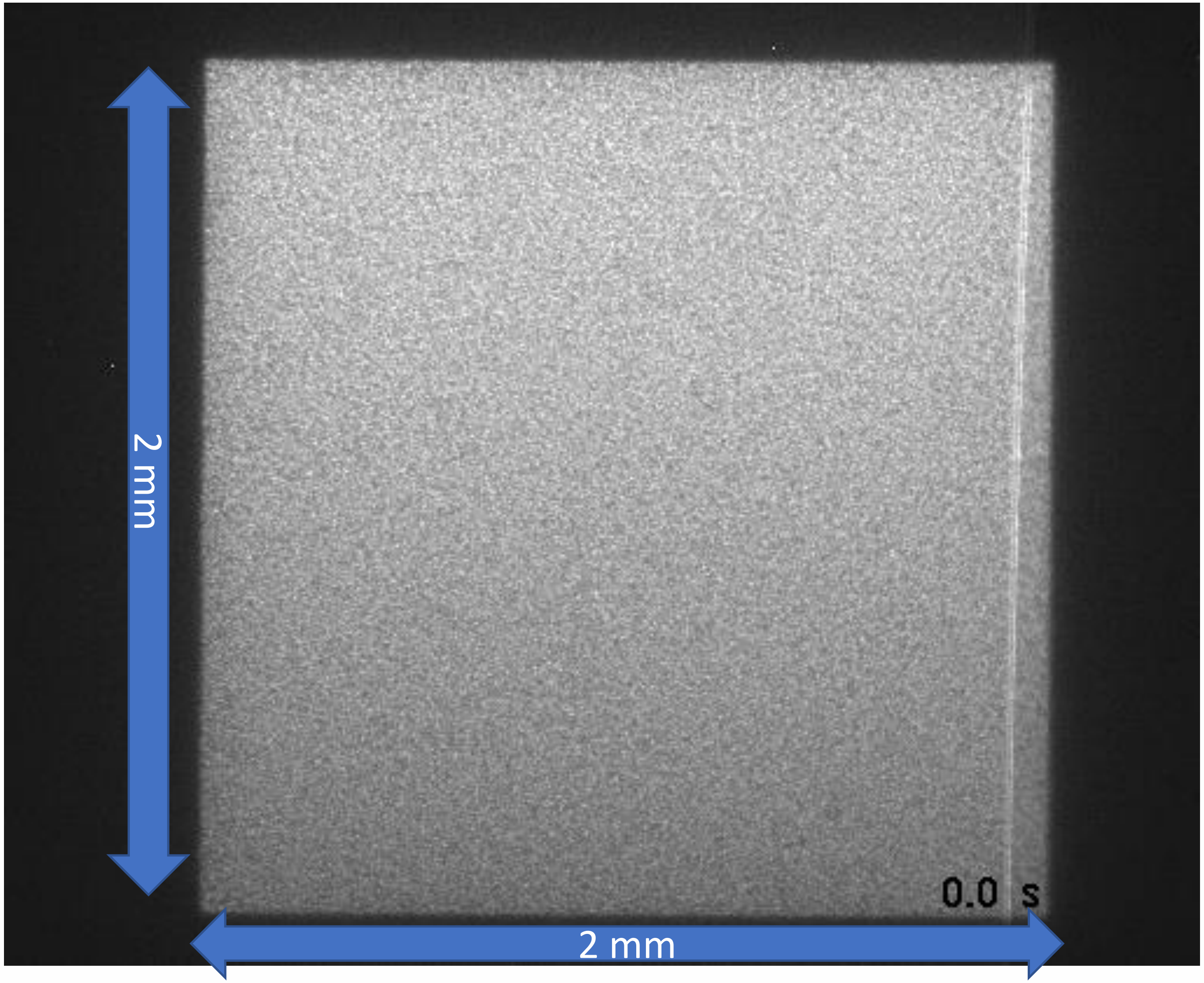

Mel O'Leary Email: mel.oleary@manchester.ac.uk

Bubble Growth

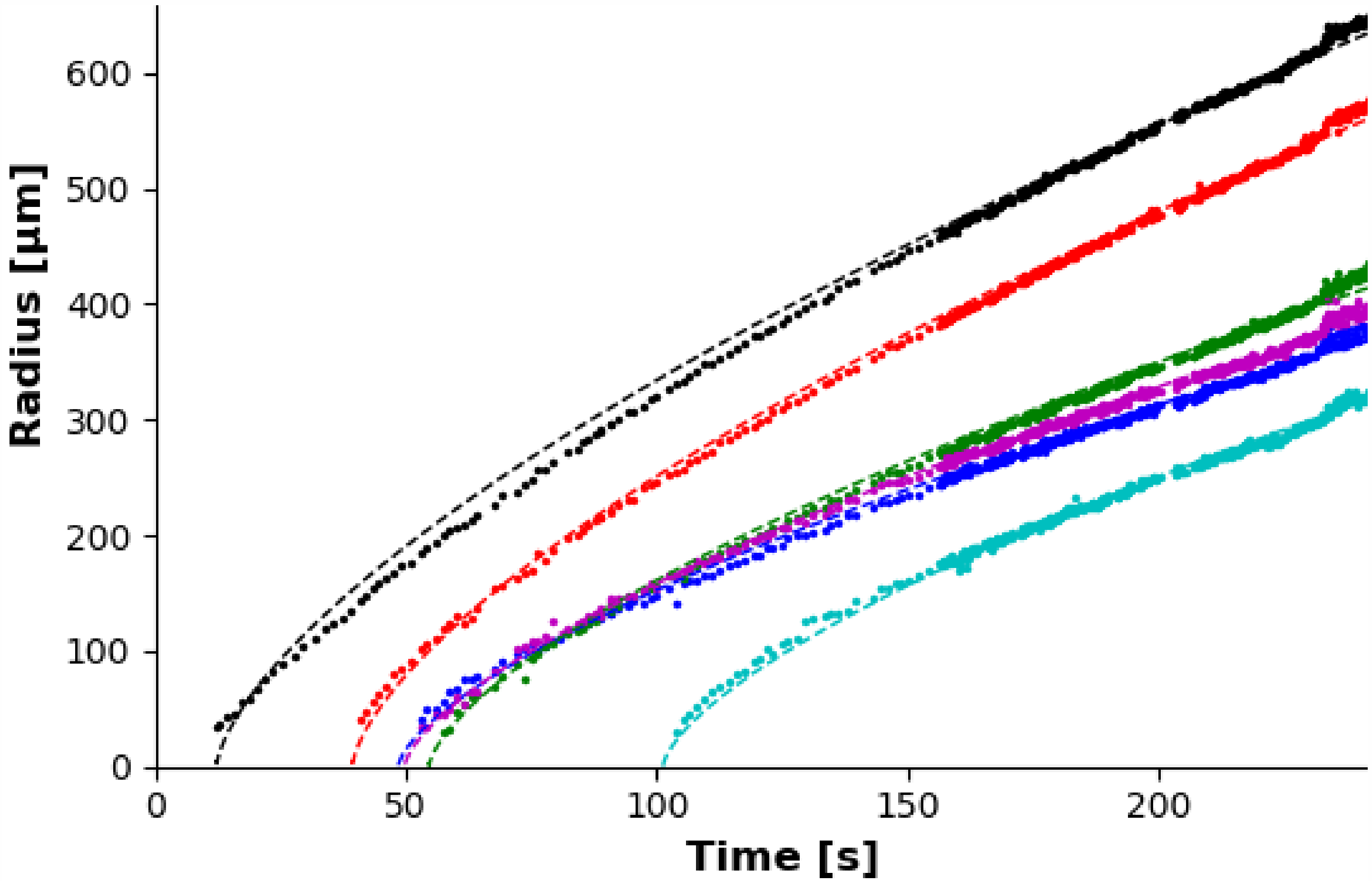

Mel O'Leary Email: mel.oleary@manchester.ac.uk

Introduction
Experimental Setup
Transport Measurements
Bubbles
Conclusions

Mel O'Leary Email: mel.oleary@manchester.ac.uk

Transformative Science and Engineering for Nuclear Decommissioning

Ongoing Work

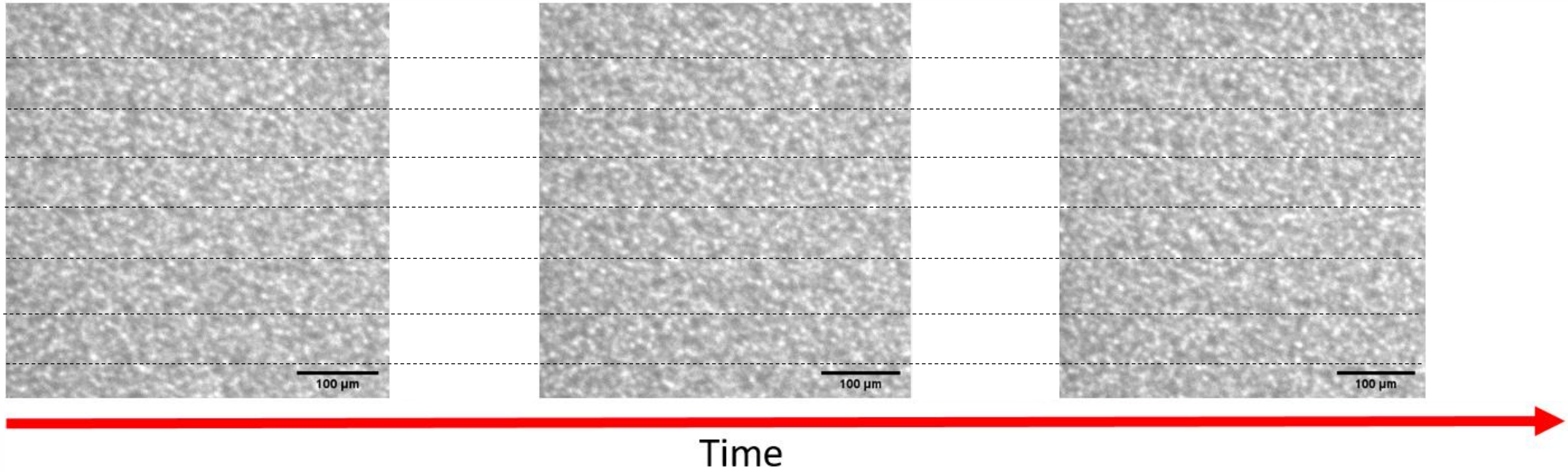

Mel O'Leary Email: mel.oleary@manchester.ac.uk

Thank you

Mel O'Leary
Email: mel.oleary@manchester.ac.uk

Ongoing Work

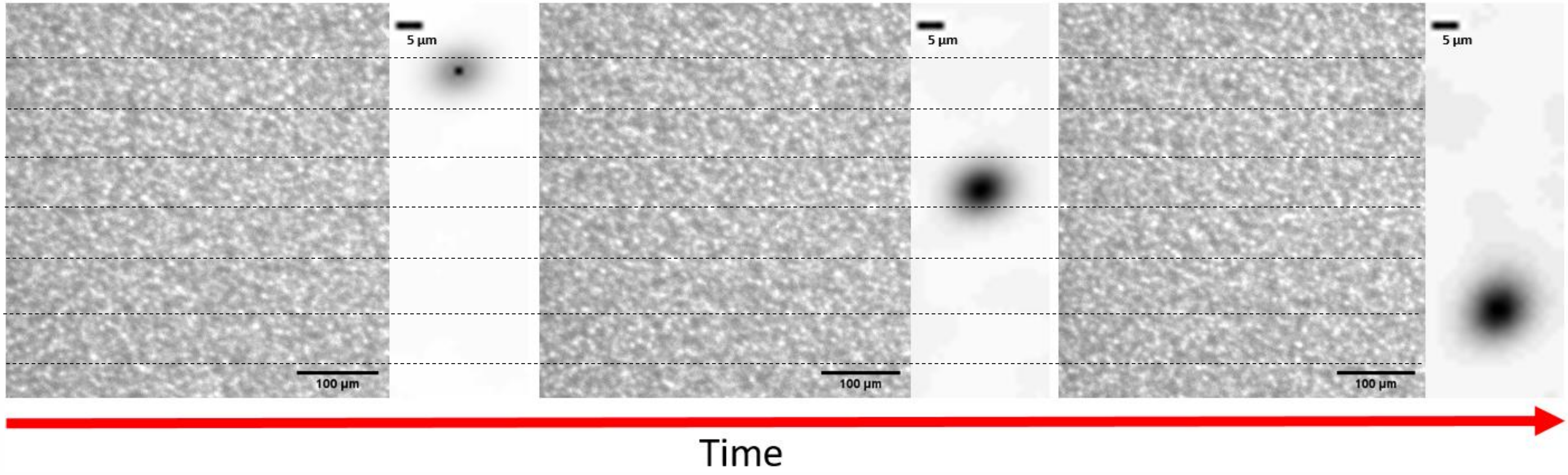

Mel O'Leary Email: mel.oleary@manchester.ac.uk

Irradiation

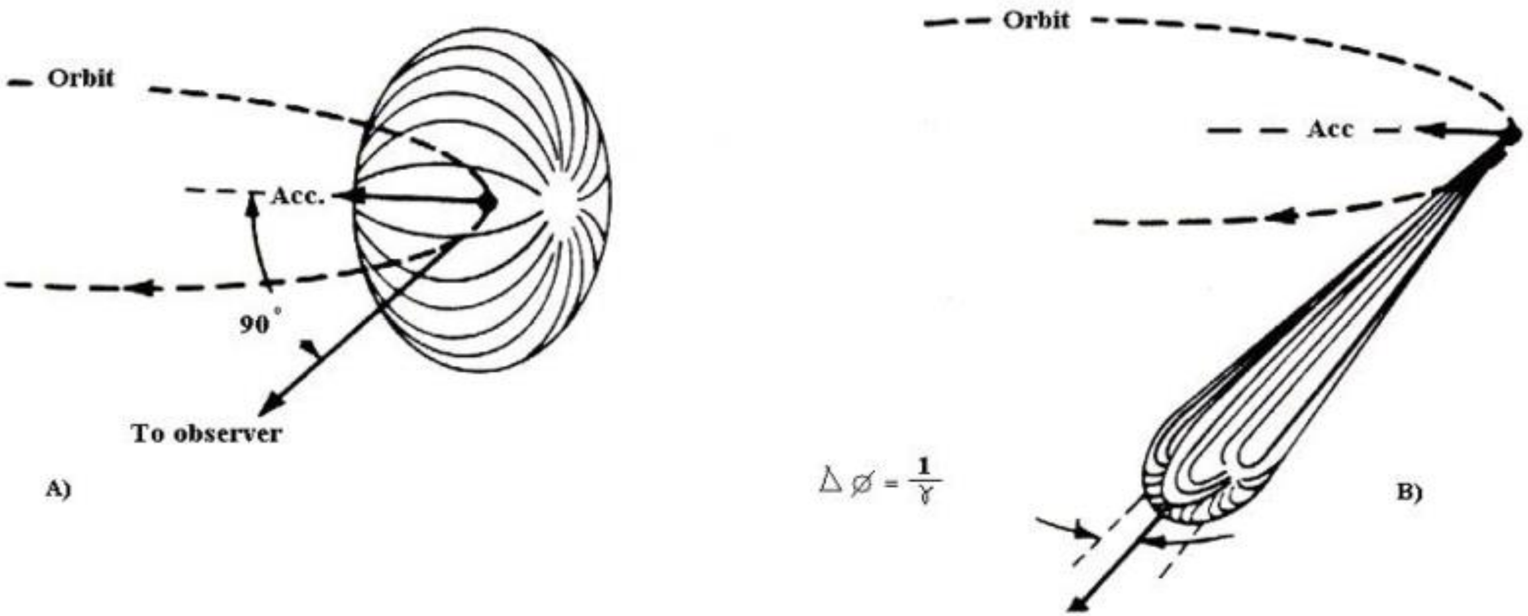

Highly collimated intense beam

Mel O'Leary Email: mel.oleary@manchester.ac.uk

Parameters from Fit

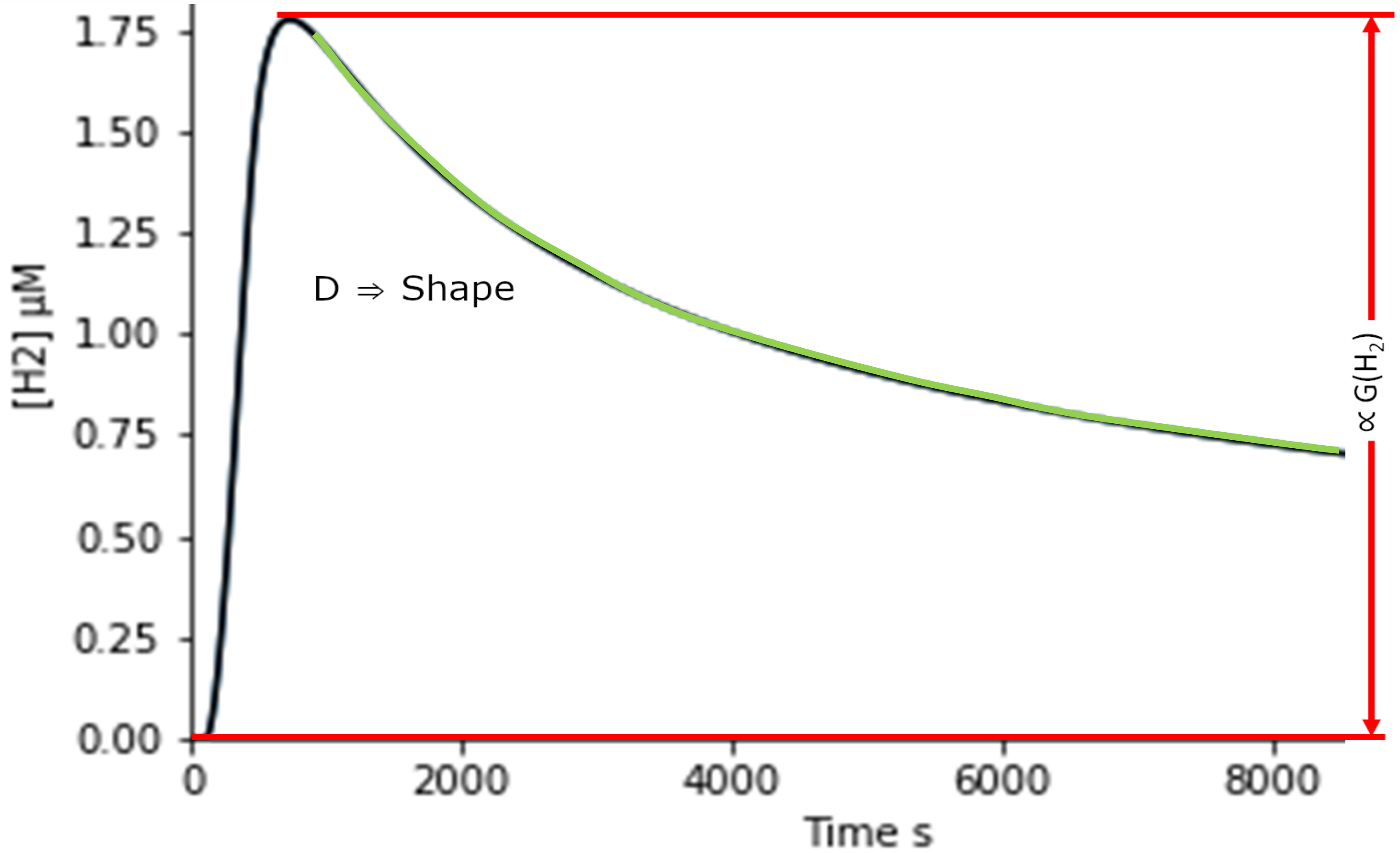

Mel O'Leary Email: mel.oleary@manchester.ac.uk

Irradiation

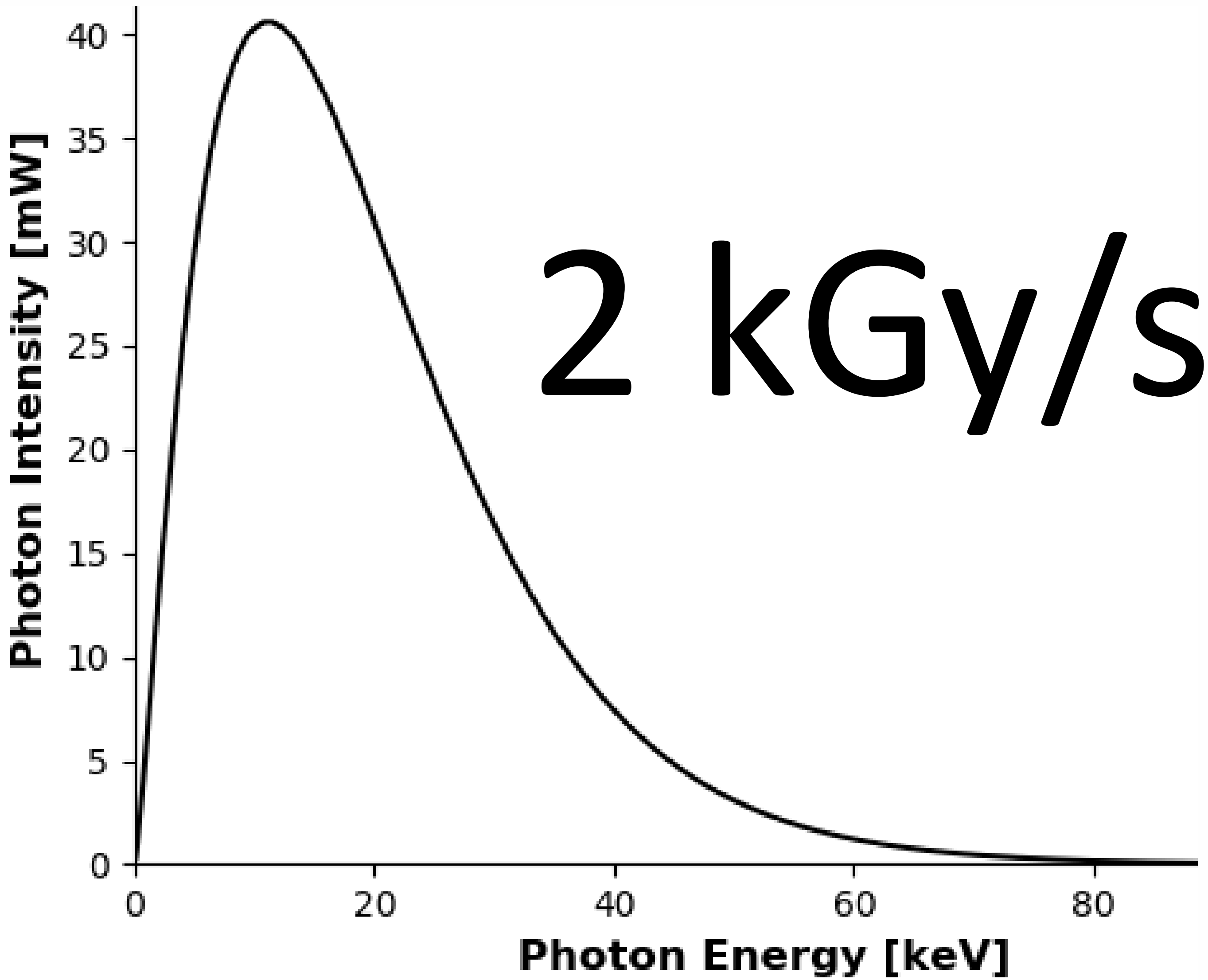

2 kGy/s

Mel O'Leary Email: mel.oleary@manchester.ac.uk

Bubbles

Irradiation

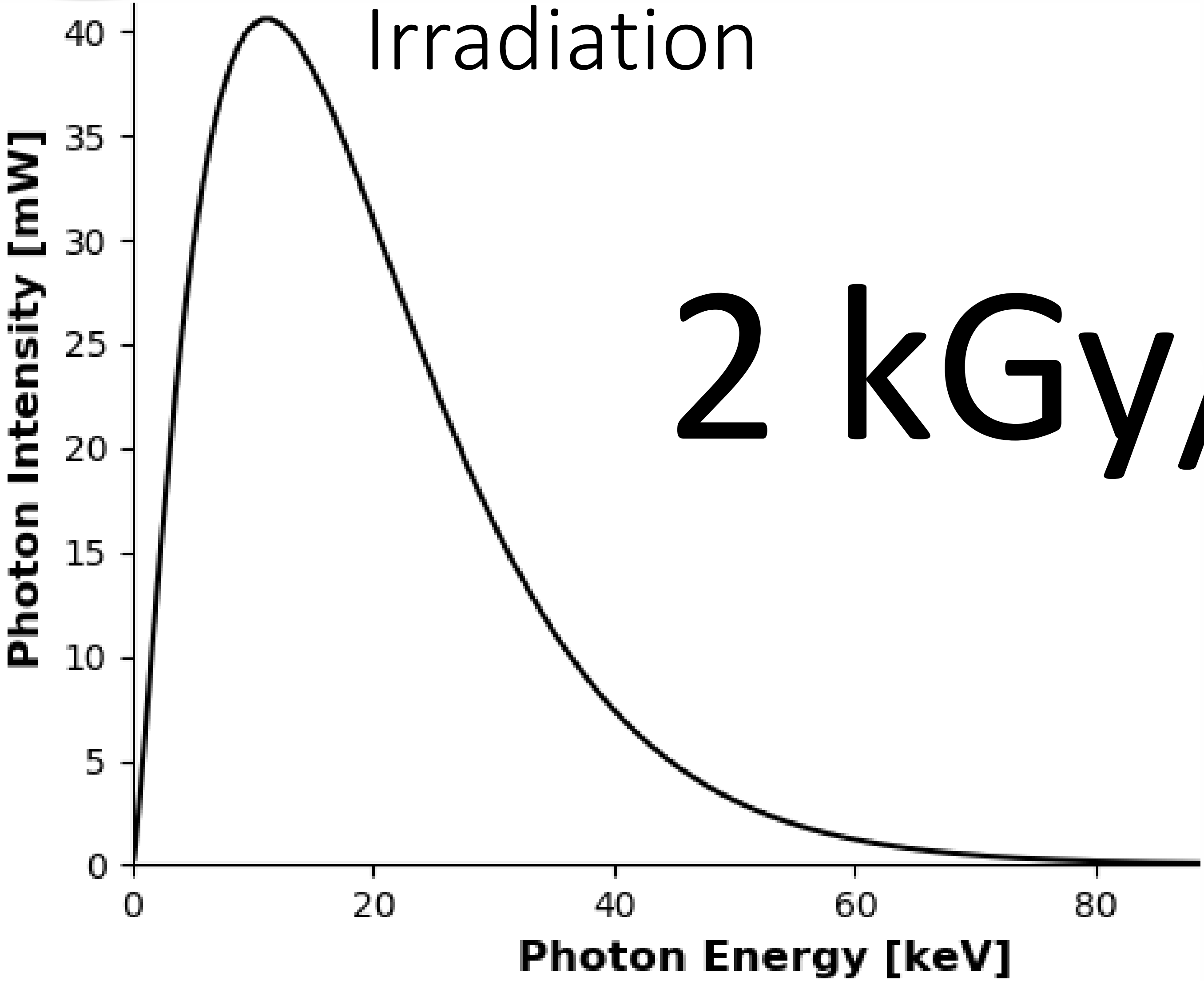

2 kGy/s

Mel O'Leary Email: mel.oleary@manchester.ac.uk

Dosimetry

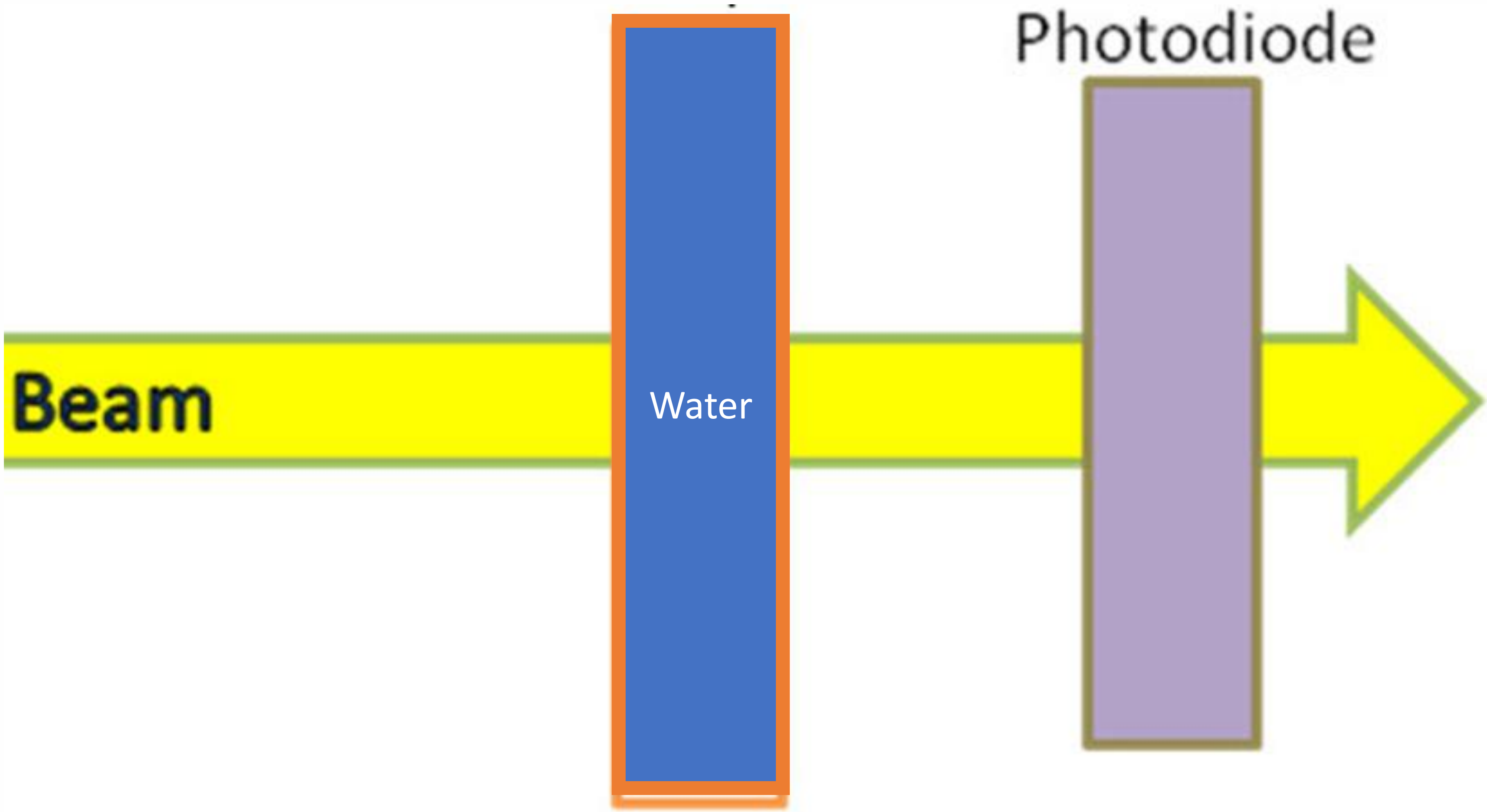

Dosimetry

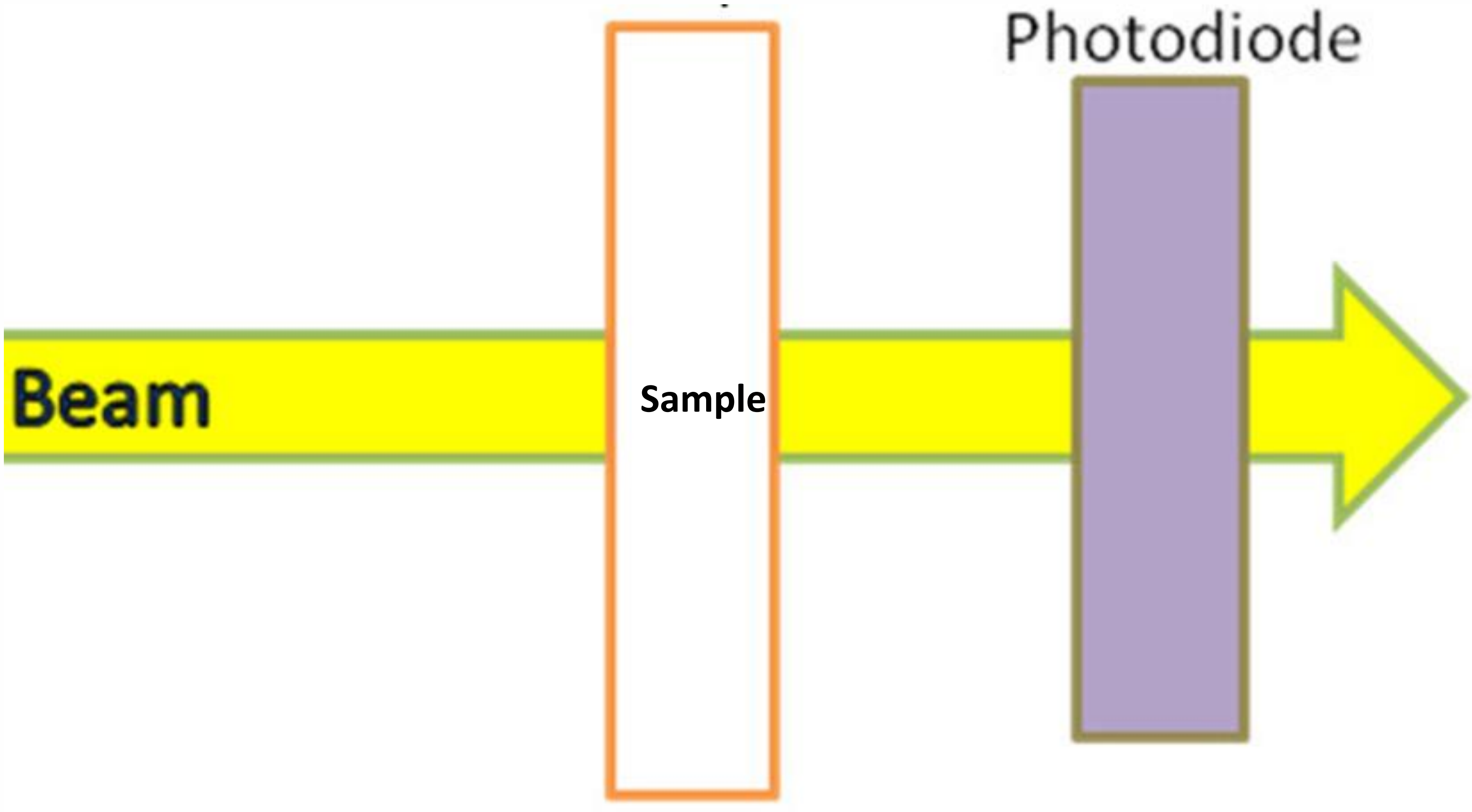

Diffusion

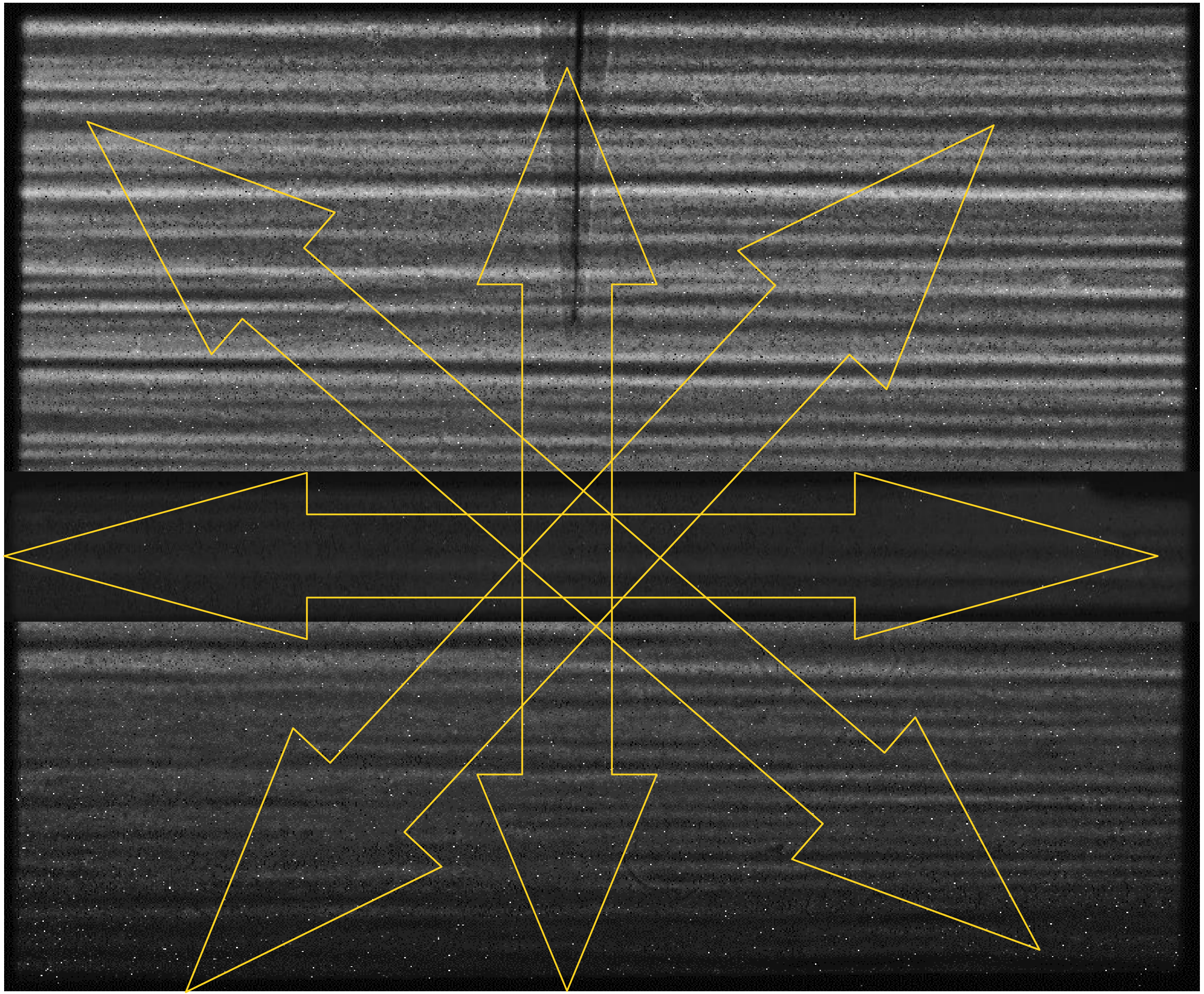

Mel O'Leary Email: mel.oleary@manchester.ac.uk

Fit to Data

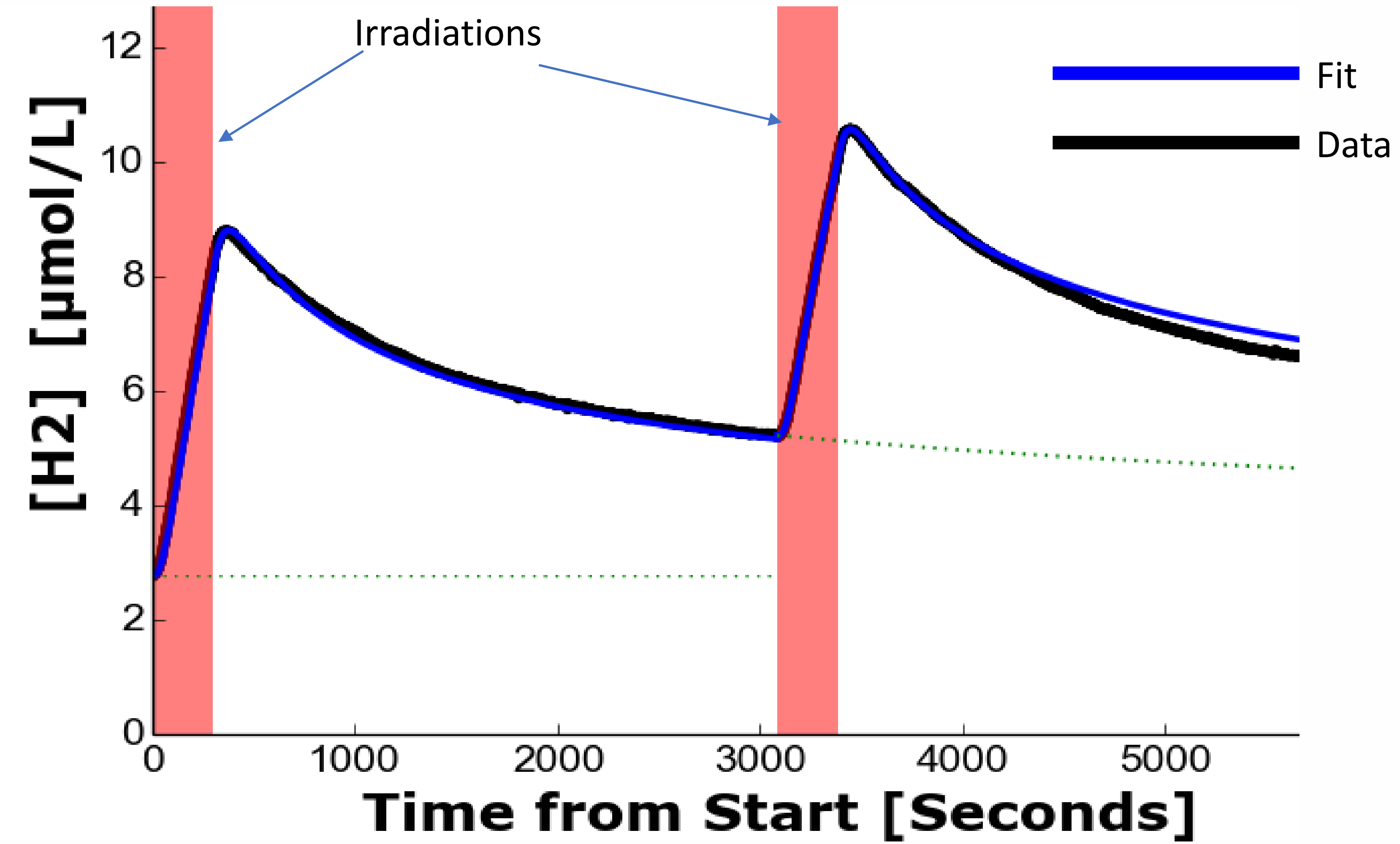

Mel O'Leary Email: mel.oleary@manchester.ac.uk

Transformative Science and Engineering for Nuclear Decommissioning

Scoping studies of ion exchange materials

James Reed, University of Birmingham

Theme Meeting 14/5/2021

Current work: 2nd year PhD student, Hriljac/ Allan group

- 3 ½ years supported by Sellafield Ltd.
- Acknowledgements to Tom Carey and Simon Kellet.
- Aim: to improve ion-exchange characteristics of naturally sourced zeolites by chemical treatments.
- Includes desilication and dealumination of the zeolite framework and phase transformations to improve uptake.

Sellafield Ltd

NATIONAL NUCLEAR LABORATORY

Why caesium and strontium?

- Cs-137 and Sr-90 are key targets in removal from nuclear waste streams worldwide.
- At the Sellafield site, SIXEP treats 100s m^3 per day.
- Currently uses a clinoptilolite sourced from Mud Hills in California.
- Supply limited, new materials must be sourced.

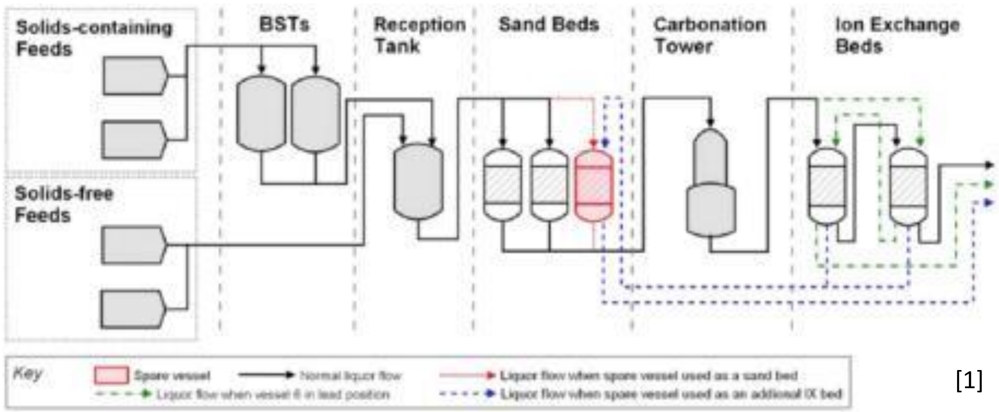

[1]

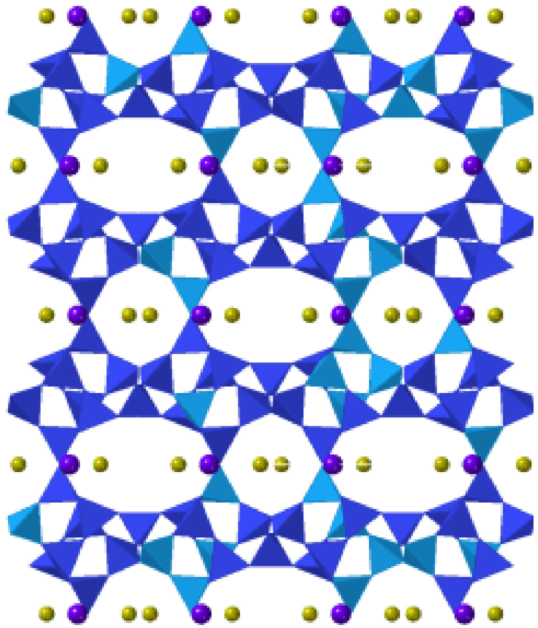

Zeolites

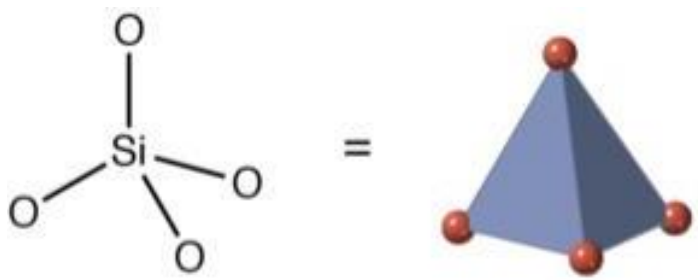

(Or Al)

FAU

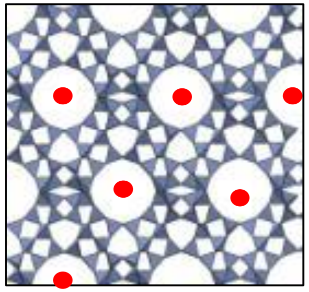

CHA

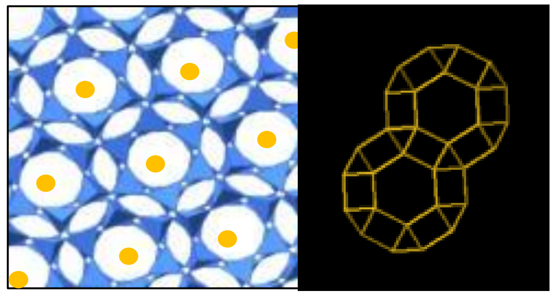

- Al tetrahedra carry negative charge.
- Cations balance this charge by sitting in spaces/ pores within the framework.
- These ions are free to move and can therefore take part in ion-exchange processes.

Si/Al ratio

Low Al content: low capacity
Used in catalysis

High Al content: high cation capacity

Used in ion-exchange

Zeolite Synthesis

Silica source + Alumina source $\xrightarrow[\text{SDA, } OH^-]{\text{Hydrothermal}}$ Many zeolite structures


[2]

$\xrightarrow[\text{Alkaline conditions}]{\text{High pressure}}$ Natural zeolites

- Cheap
- Inpure

Interzeolite Transformations

- Uses a zeolite framework as a starting material to form a different structure

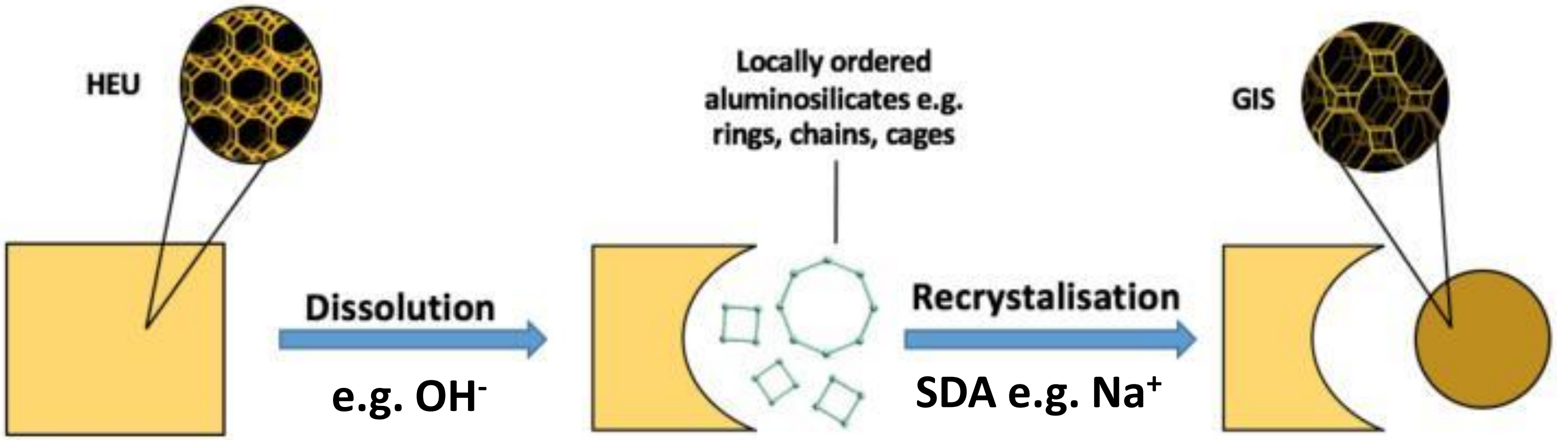

- Changes selectivity
- Increases purity
- Can add value to ‘low value’ materials

MH-CLINO (HEU)

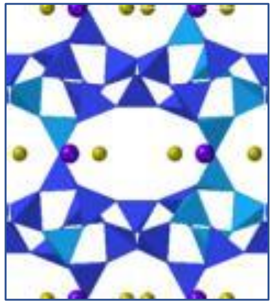

Cs: 88 % uptake
Sr: 67 % uptake

Z-CLINO (HEU)

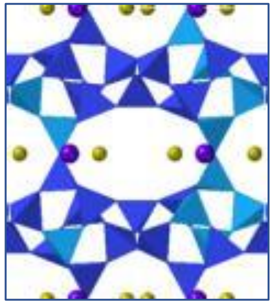

Cs: 87 % uptake
Sr: 43 % uptake

I-MORD (MOR)

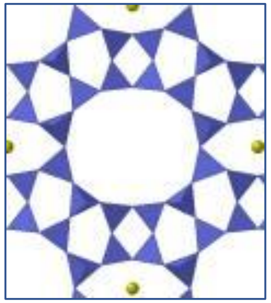

Cs: 97 % uptake
Sr: 27 % uptake

N-CLINO (HEU)

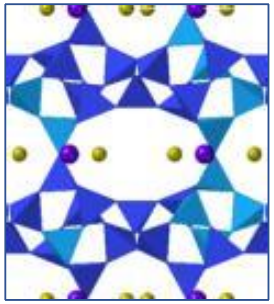

Cs: 84 % uptake
Sr: 70 % uptake

S-CLINO (HEU)

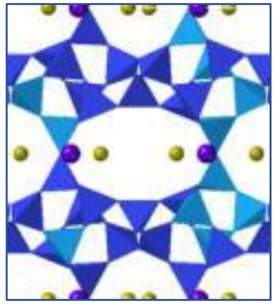

Cs: 80 % uptake
Sr: 78 % uptake

- Caesium uptake good to excellent in all systems.
- Strontium uptake poorer, especially in mordenite.
- Improvement in strontium uptake required.

Z-CLINO (HEU)

Cs: 87 %
Sr: 43 %

0.3-0.5 M NaOH, 100°C, 24 h

PP bottle

Zeolite-P (GIS)

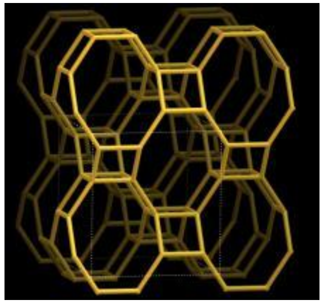

Cs: 13-51 %
Sr: 85-89 %

8 ring channels along [100] and [010]

Tetragonal unit cell
$a = b =$ 9.80 Å, $c =$ 10.16 Å
FD = 16.4 T/1000 Å^3

N-CLINO (HEU)

Cs: 84 %
Sr: 70 %

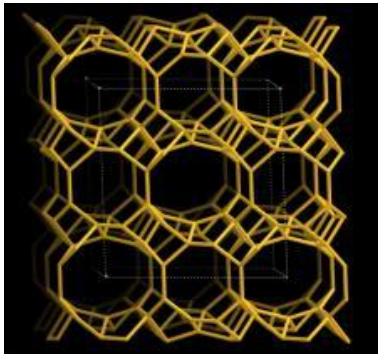

S-CLINO (HEU)

Cs: 80 %
Sr: 78 %

10 and 8 ring channels along [001]

Monoclinic unit cell
$a =$ 17.52 Å, $b =$ 17.04 Å, $c =$ 7.40 Å
FD = 17.5 T/1000 Å^3

MH-CLINO (HEU)

Cs: 88 %
Sr: 68 %

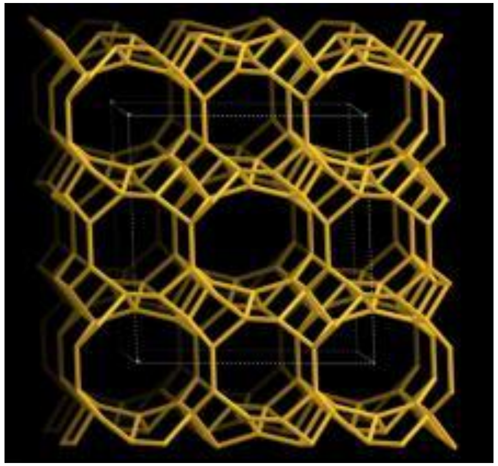

10 and 8 ring channels along [001]

Monoclinic unit cell
a = 17.52 Å , *b* = 17.04 Å , *c* = 7.40 Å
FD = 17.5 T/1000 Å^3

0.5 M NaOH, 100°C, 24 h

PP bottle

Chabazite (CHA)

Cs: 45 %
Sr: 98 %

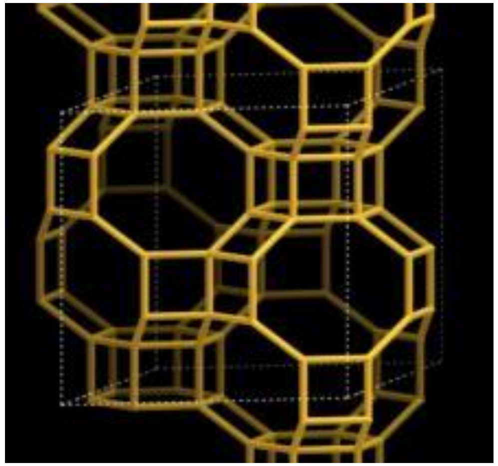

8 ring channels along [100] and [010]
6 ring channels along [001]

Trigonal unit cell
a = *b* = 13.68 Å , *c* = 14.77 Å
FD = 15.1 T/1000 Å^3

$$\text{I-MORD (MOR)} \xrightarrow[\text{PP bottle}]{0.70\ \text{M NaOH},\ 100^{\circ}\text{C},\ 24\ \text{h}} \text{Zeolite-P (GIS)}$$

I-MORD (MOR)

Cs: 97 %
Sr: 27 %

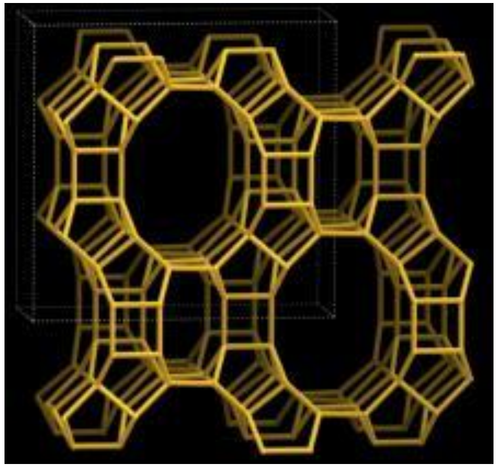

12 and 8 ring channels along [001]

Orthombic unit cell
a = 18.26, *b* = 20.53 Å , *c* = 7.54 Å
FD = 17.0 T/1000 Å^3

Zeolite-P (GIS)

Cs: 38 %
Sr: 91 %

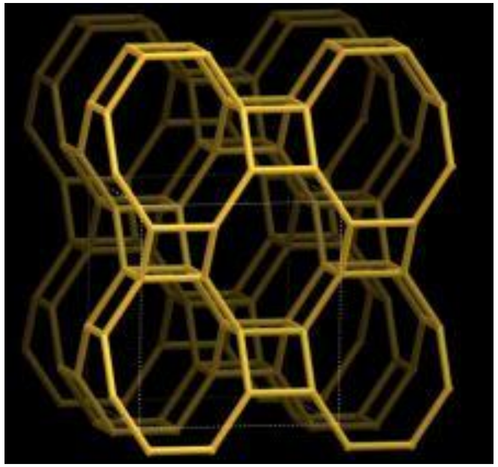

8 ring channels along [100] and [010]

Tetragonal unit cell
a = *b* = 9.80 Å , *c* = 10.16 Å
FD = 16.4 T/1000 Å^3

Partial transformations

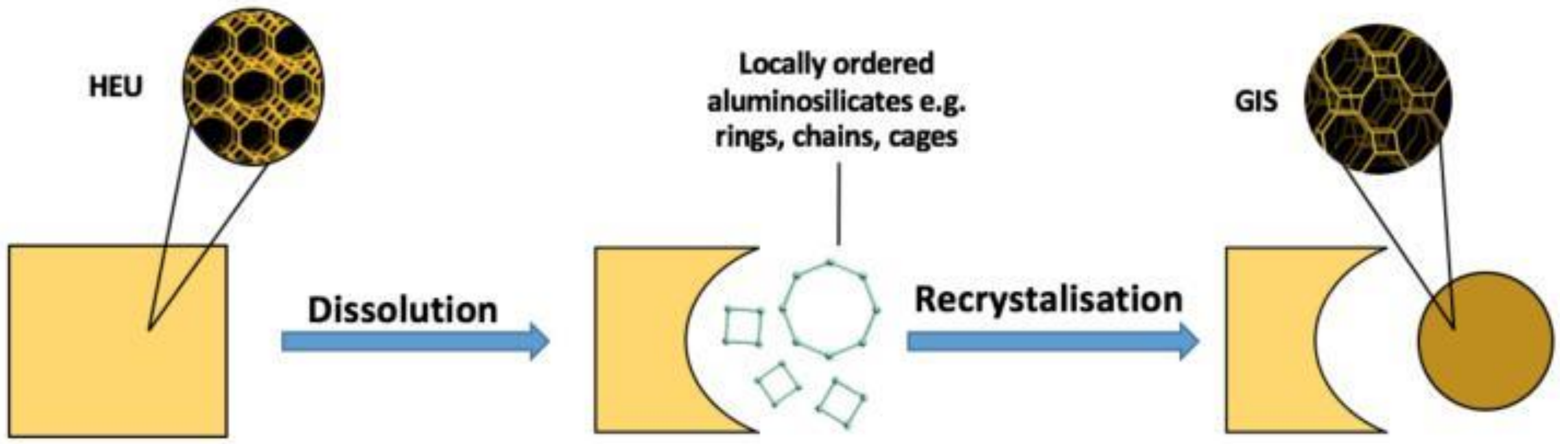

- Would this retain some selectivity from the parent zeolite?
- If so, this could lead to valuable selectivity profiles.
- Concern over physical stability of parent zeolite.

MH-CLINO (HEU) Cs: 88 % Sr: 67 %	0.4 M NaOH →	**HEU/CHA** Cs: 70 % Sr: 98 %
Z-CLINO (HEU) Cs: 88 % Sr: 67 %	0.3 M NaOH →	**HEU/GIS** Cs: 85 % Sr: 80 %
I-MORD (MOR) Cs: 97 % Sr: 27 %	0.45 M NaOH →	**MOR/GIS** Cs: 87 % Sr: 80 %
N-CLINO (HEU) Cs: 84 % Sr: 70 %	0.30 M NaOH →	**HEU/GIS** Cs: 84 % Sr: 78 %
S-CLINO (HEU) Cs: 80 % Sr: 78 %	0.30 M NaOH →	**HEU/GIS** Cs: 74 % Sr: 88 %

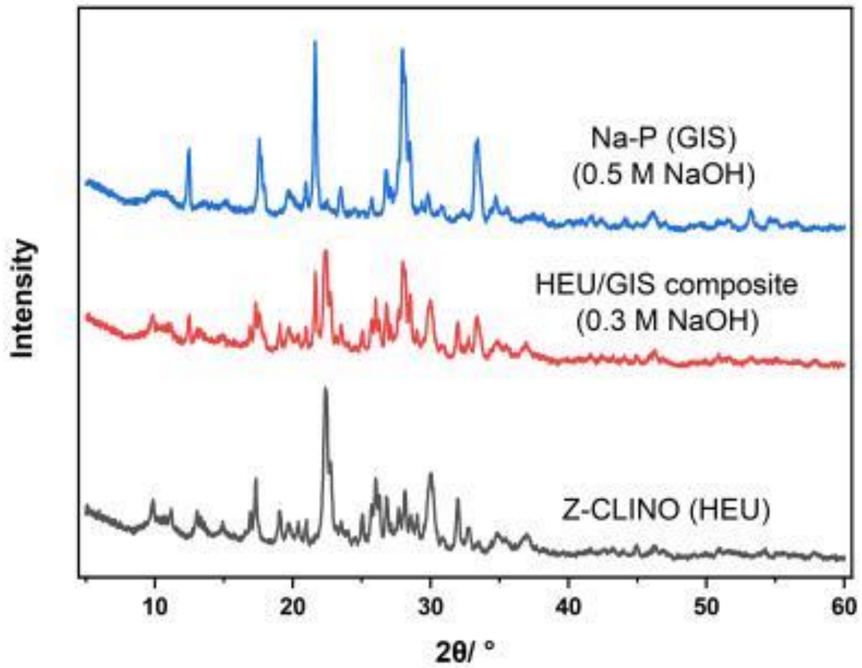

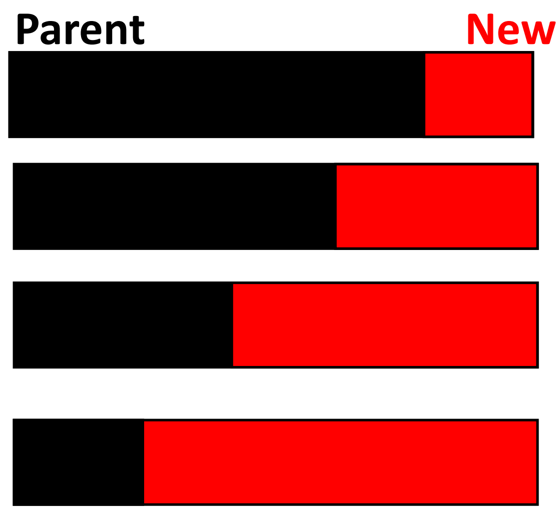

Generating a series of composites

- Series of composites generated by varying [NaOH].
- Weight fractions of each phase obtained through Rietveld refinement of powder diffraction data.
- Potential to 'tune' material for a given waste stream.

For Z-CLINO:

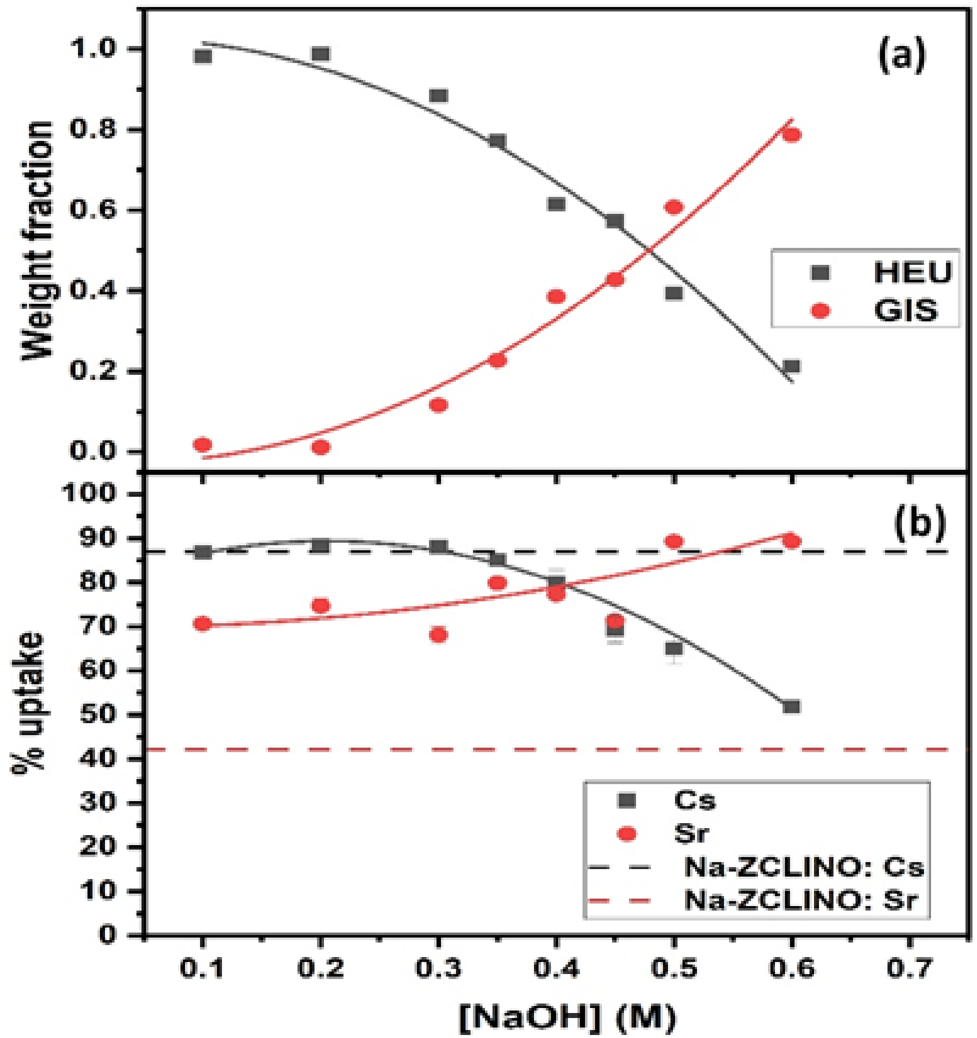

Zeoclere clinoptilolite

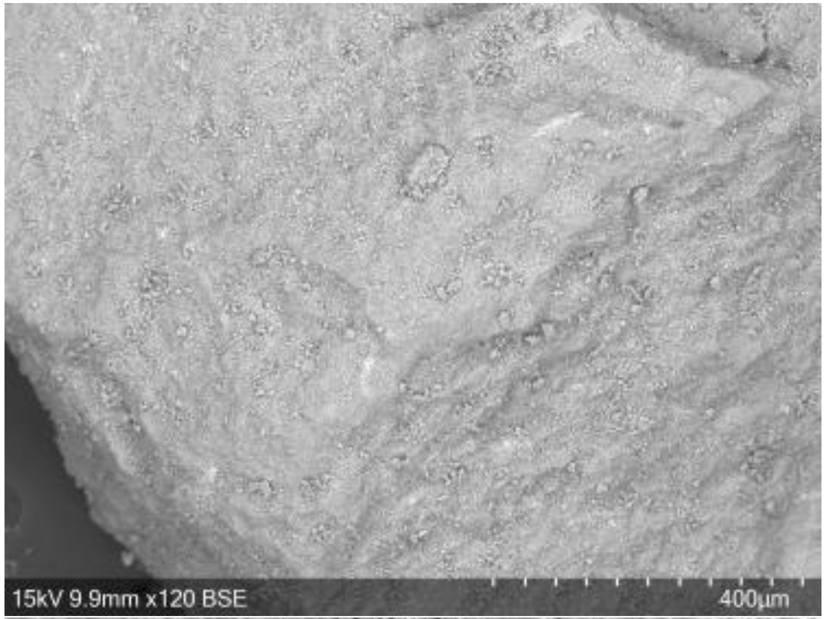

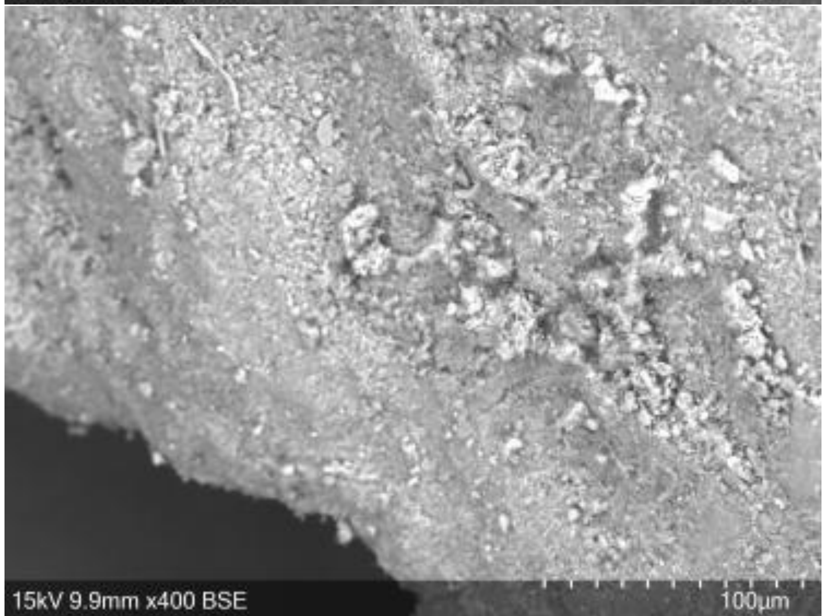

Mud Hills clinoptilolite

HEU/GIS composite (from Zeoclere)

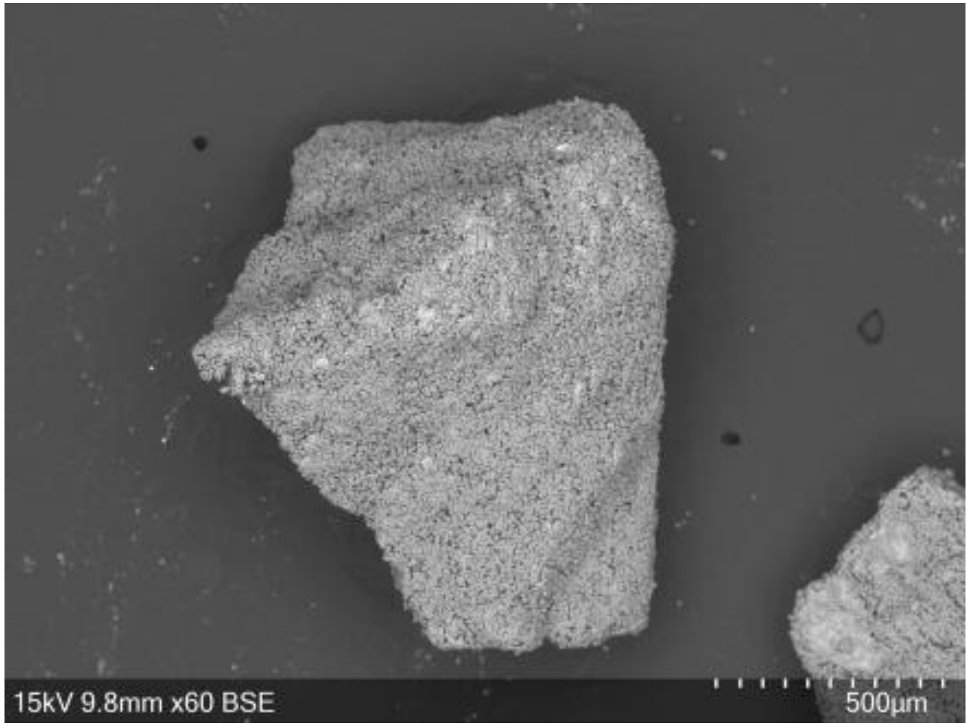

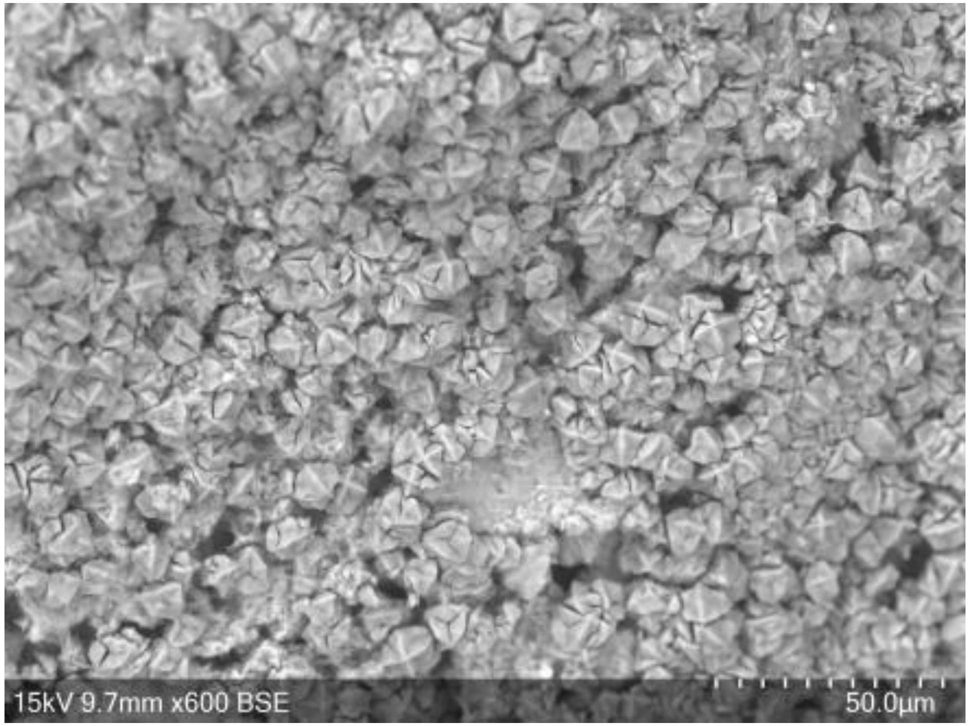

CHA (from Mud Hills clinoptilolite)

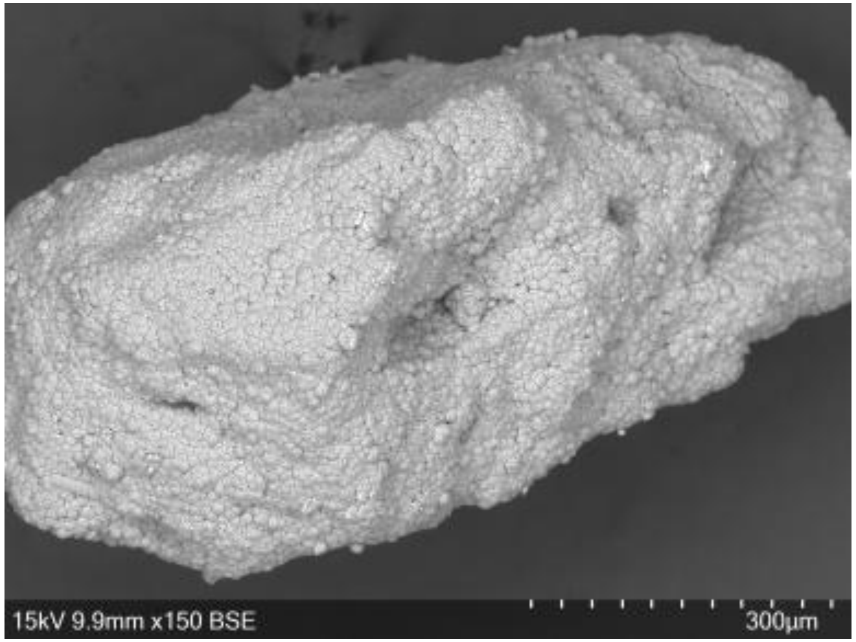

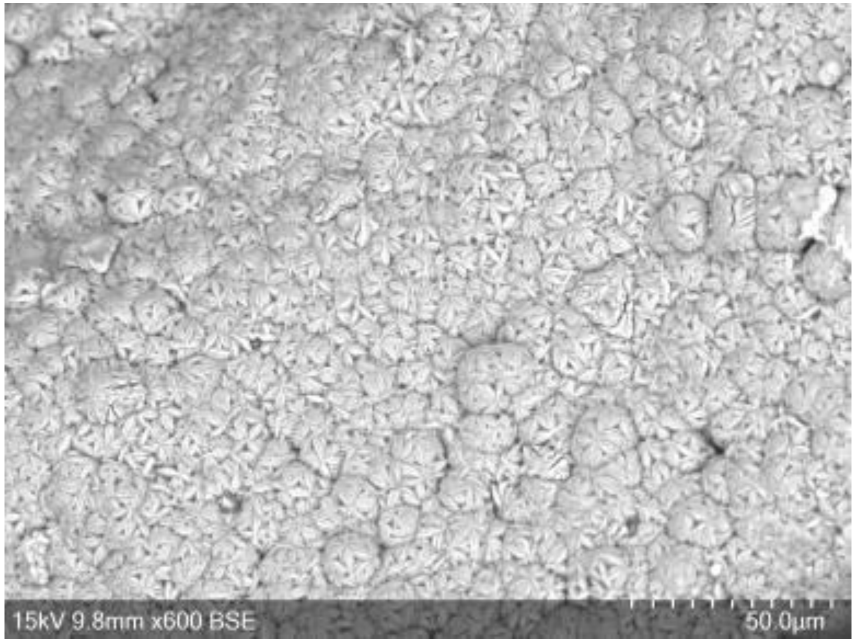

HEU/CHA composite (from Mud Hills)

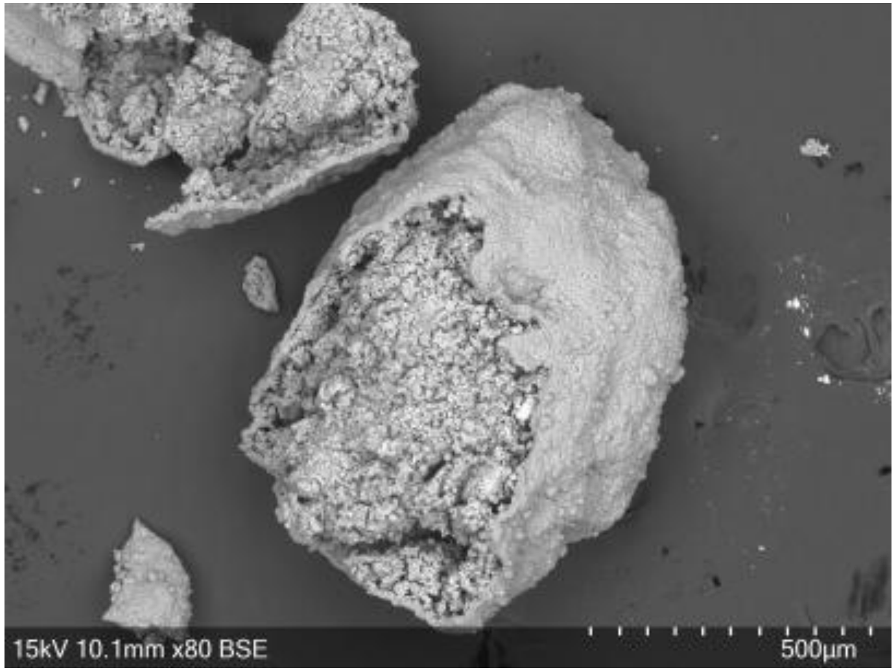

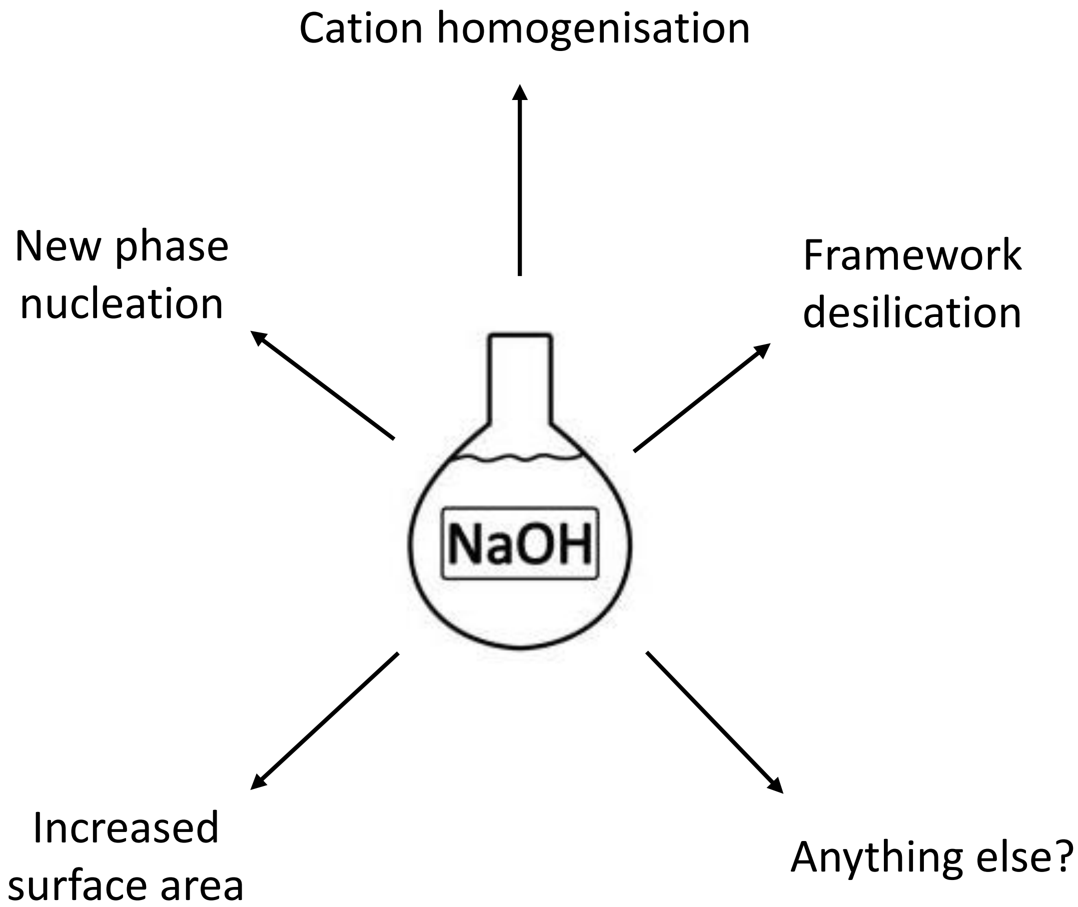

Future work:

- Collect ion-exchange data for all composite series
- New ‘mock’ waste streams
- Active testing

References

[1] A. Dyer, J. Hriljac, N. Evans, I. Stokes, P. Rand, S. Kellet, R. Harjula, T. Moller, Z. Maher, R. Heatlie-Branson, J. Austin, S. Williamson-Owens, M. Higgins-Bos, K. Smith, L. O'Brien, N. Smith and N. Bryan, Journal of Radioanalytical and Nuclear Chemistry, 2018, 318, 2473-2491.

[2] https://theconversation.com/why-cant-we-predict-when-a-volcano-will-erupt-53898

[3] Images taken from Google earth

TRANSCEND

Transformative Science and Engineering for Nuclear Decommissioning

Thank you

jlr552@student.bham.ac.uk

Transformative Science and Engineering for Nuclear Decommissioning

A Monte Carlo Study of Nanoparticles Relevant to Nuclear Waste

Ella Schaefer, UoM

Integrated Waste Management – Theme 1

14.5.21

ella.schaefer@postgrad.manchester.ac.uk

For a Low Carbon Future

Background

What type of NPs?

Nuclear – light metal hydroxides/oxides

(e.g. Al_2O_3 and $Mg(OH)_2$)

Why Oxides/Hydroxide NPs?

- **Present in waste storage ponds**
- **From corrosion of the cladding on nuclear fuel rods in the nuclear waste storage ponds in Sellafield**

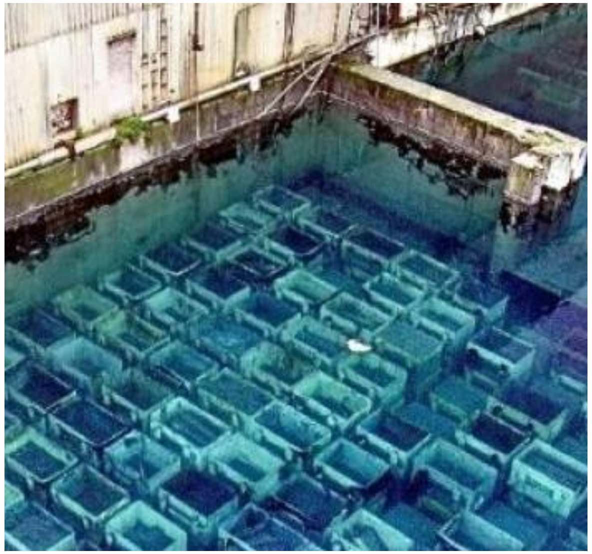

Figure 1 – a) Photograph of a legacy pond at *Sellafield* and b) Close up of a legacy pond at *Sellafield* showing cloudy water containing particulates

Background

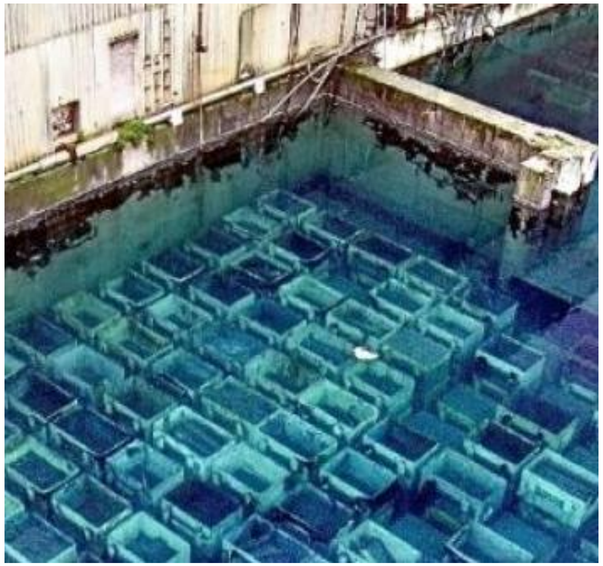

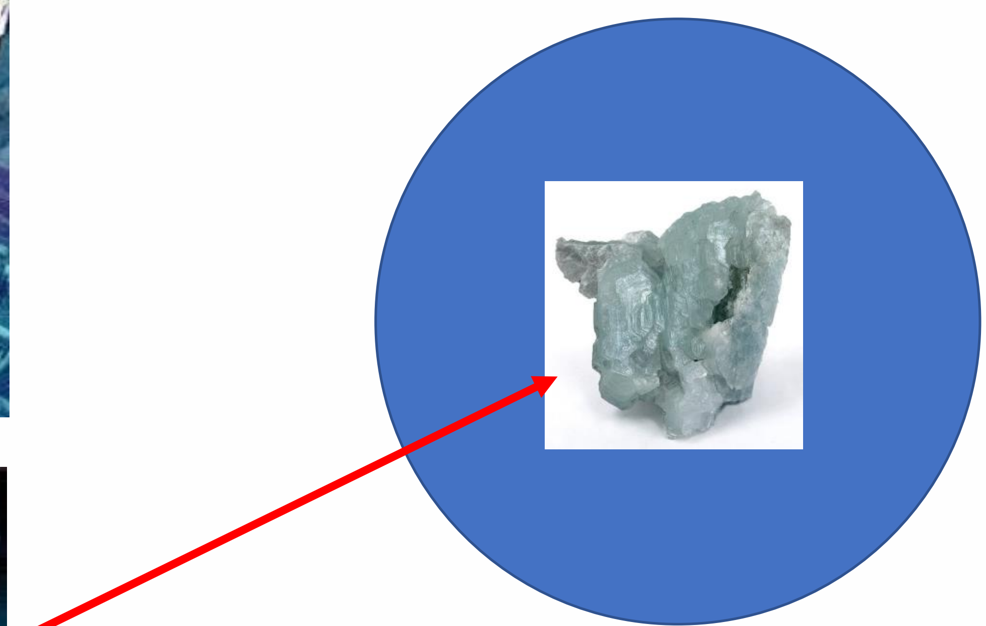

Figure 1 – a) Photograph of a legacy pond at *Sellafield* and b) Close up of a legacy pond at *Sellafield* showing cloudy water containing particulates
Figure 2 – Schematic showing an image of brucite compound inside ‘water’

Background

Why Nanoparticles (NPs)?

- Irradiated NPs produce chemical changes in the surrounding media
- Including •OH, low E e^-s and H_2
- In healthcare •OH and low E e^-s are used in radiotherapy
- H_2 formation is relevant to nuclear safety cases – **Fukushima** (tsunami caused 3 H_2 explosions) and **Chernobyl** (reaction with H_2 contributed to the roof blowing off reactor 4)

A Simplified View of an Irradiated NP

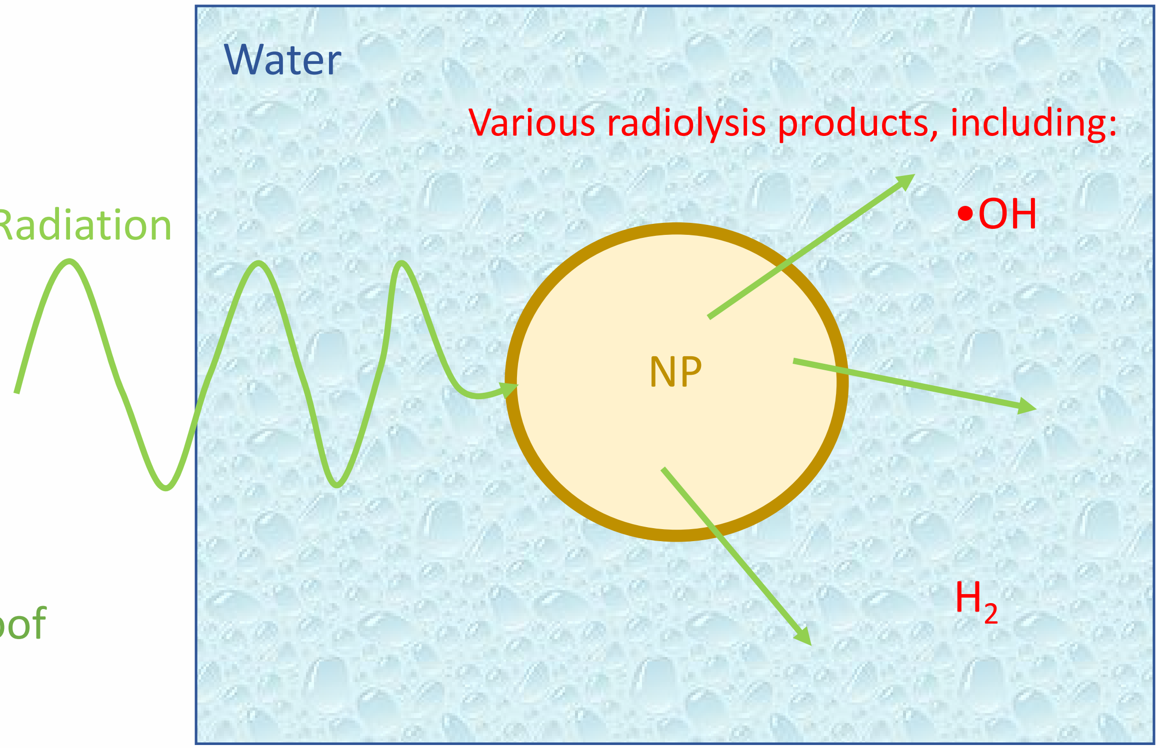

Figure 3 – Diagram showing the irradiation of a NP resulting in various radiolytic species, noting two of interest; the hydroxyl radical and gaseous molecular hydrogen.

Radiation Interaction with NP

A few important processes that occur when a NP is irradiated:

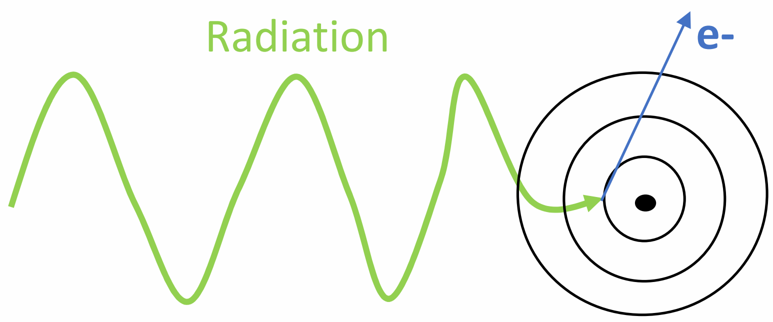

- **Photoelectric effect** – absorption of a photon resulting in the emission of an e^-

Figure 4 – Schematic demonstrating the *photoelectric effect*

Radiation Interaction with NP

A few important processes that occur when a NP is irradiated:

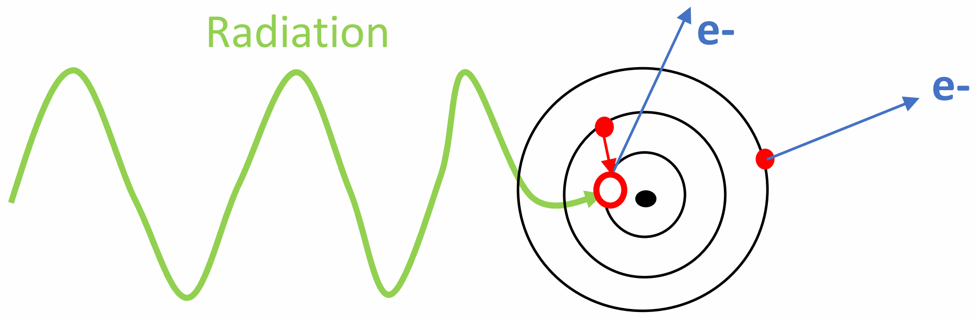

- **Photoelectric effect** – absorption of a photon resulting in the emission of an e^-

  (This includes the ***Auger effect* –** core e^- is ejecting leaving a hole in the core shell to maintain stability a valence e^- will move into the vacancy causing a second e^- to be ejected

Figure 5 – Schematic demonstrating the *Auger effect*

Radiation Interaction with NP

A few important processes that occur when a NP is irradiated:

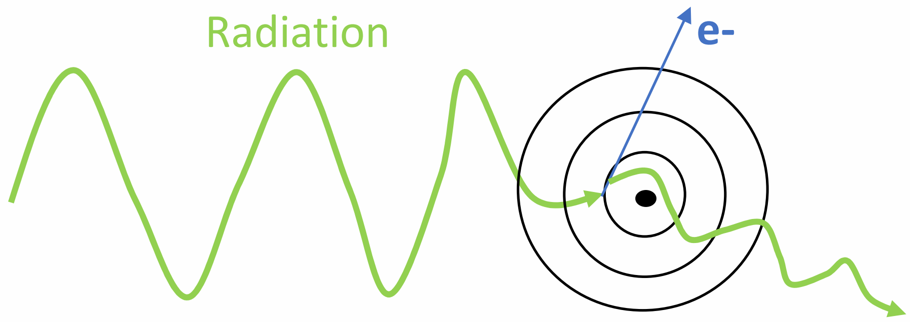

- **Photoelectric effect** – absorption of a photon resulting in the emission of an e^-

  (This includes the ***Auger effect* –** core e^- is ejecting leaving a hole in the core shell to maintain stability a valence e^- will move into the vacancy causing a second e^- to be ejected

- **Compton effect** - a photon is scattered by a charged particle, typically an e^-, which is then ejected with the difference of the photon energy being transferred to this recoil electron

Figure 6 – Schematic demonstrating the *Compton effect*

Radiation Interaction with NP

A few important processes that occur when a NP is irradiated:

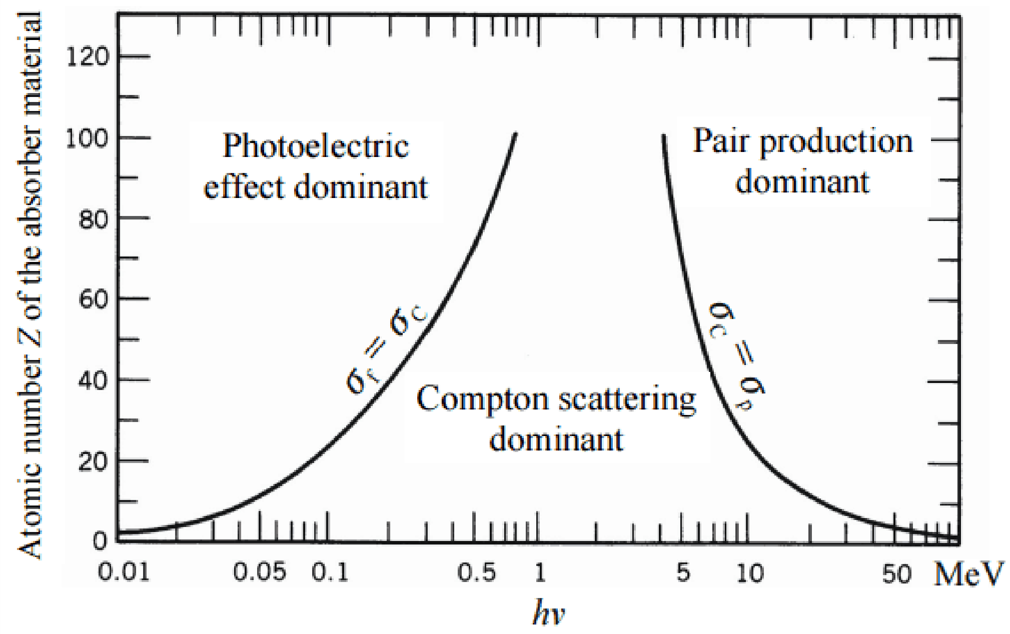

- **Photoelectric effect** – absorption of a photon resulting in the emission of an e$^-$

  (This includes the ***Auger effect –*** core e$^-$ is ejecting leaving a hole in the core shell to maintain stability a valence e$^-$ will move into the vacancy causing a second e$^-$ to be ejected

- **Compton effect** - a photon is scattered by a charged particle, typically an e$^-$, which is then ejected with the difference of the photon energy being transferred to this recoil electron

Figure 7 – Dominance regions for the three absorption processes

Method

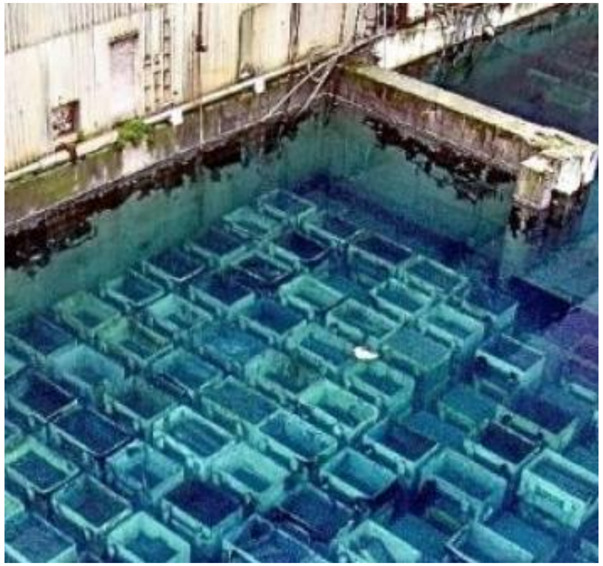

Figure 1 – a) Photograph of a legacy pond at *Sellafield* and b) Close up of a legacy pond at *Sellafield* showing cloudy water containing particulates
Figure 2 – Schematic showing an image of brucite compound inside ‘water’

Method

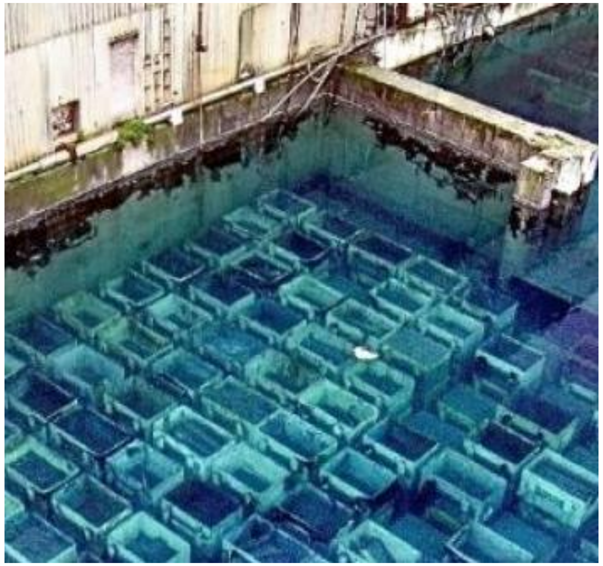

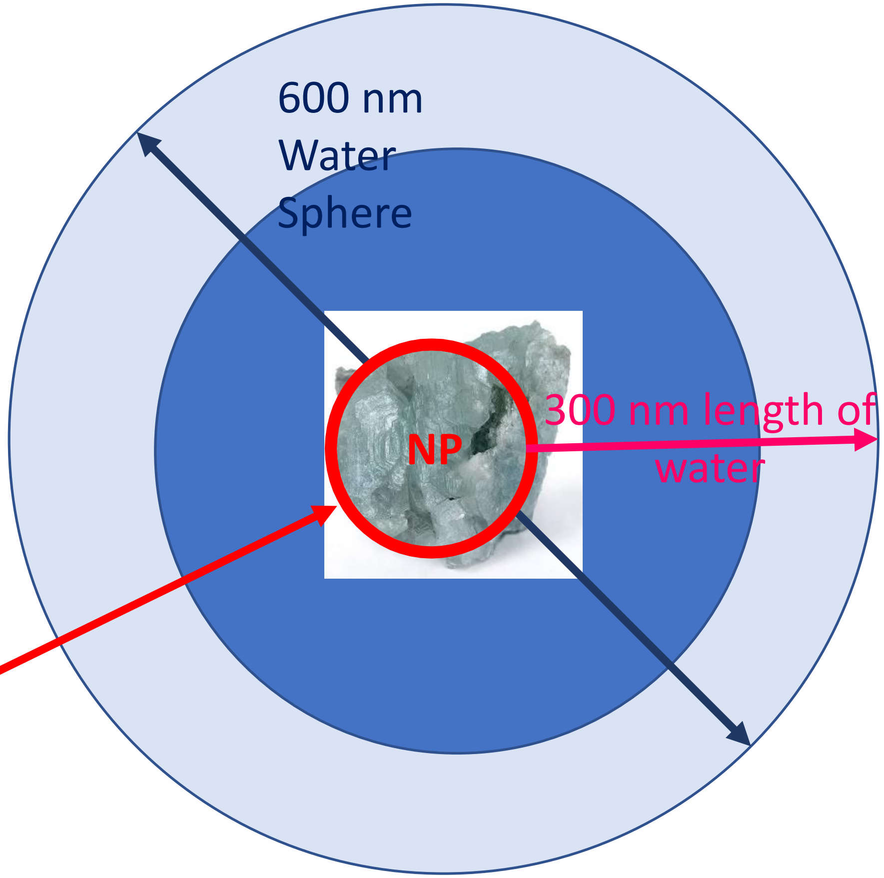

Radial Dose Distribution –
Dose is measured in 1nm sections from the NP surface to the edge of the water sphere

Figure 8 – Visualisation of the method

Radial Dose Distributions (RDDs)

- 20 – 60 keV relates to specific measurements that can be performed at the Synchrotron
- Although E in ponds is much greater, after ~60 keV the underlying physics is the same, MeV can be calculated but require much longer times/computational power
- At lower E dose is higher for a longer range
- Al_2O_3 deposits greater dose than $Mg(OH)_2$

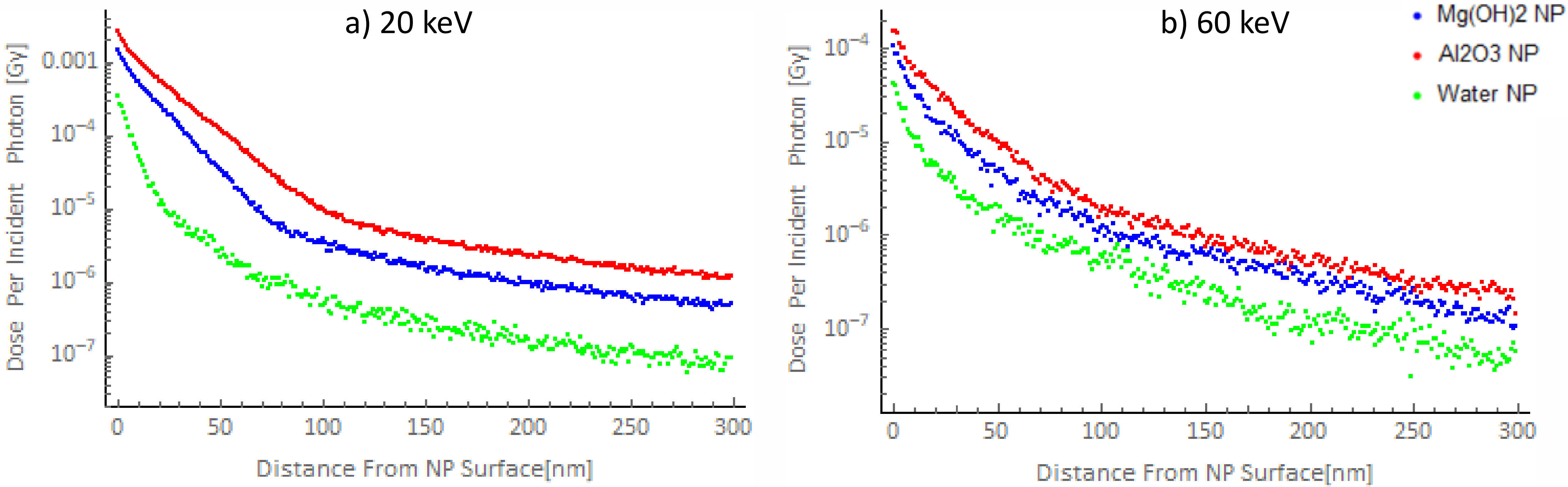

Figure 9 – Graphs showing the radial dose distributions per incident photon for Al_2O_3, $Mg(OH)_2$ and water NPs irradiated by a) 20 and b) 60 keV

Transformative Science and Engineering for Nuclear Decommissioning

RDDs as Ratios

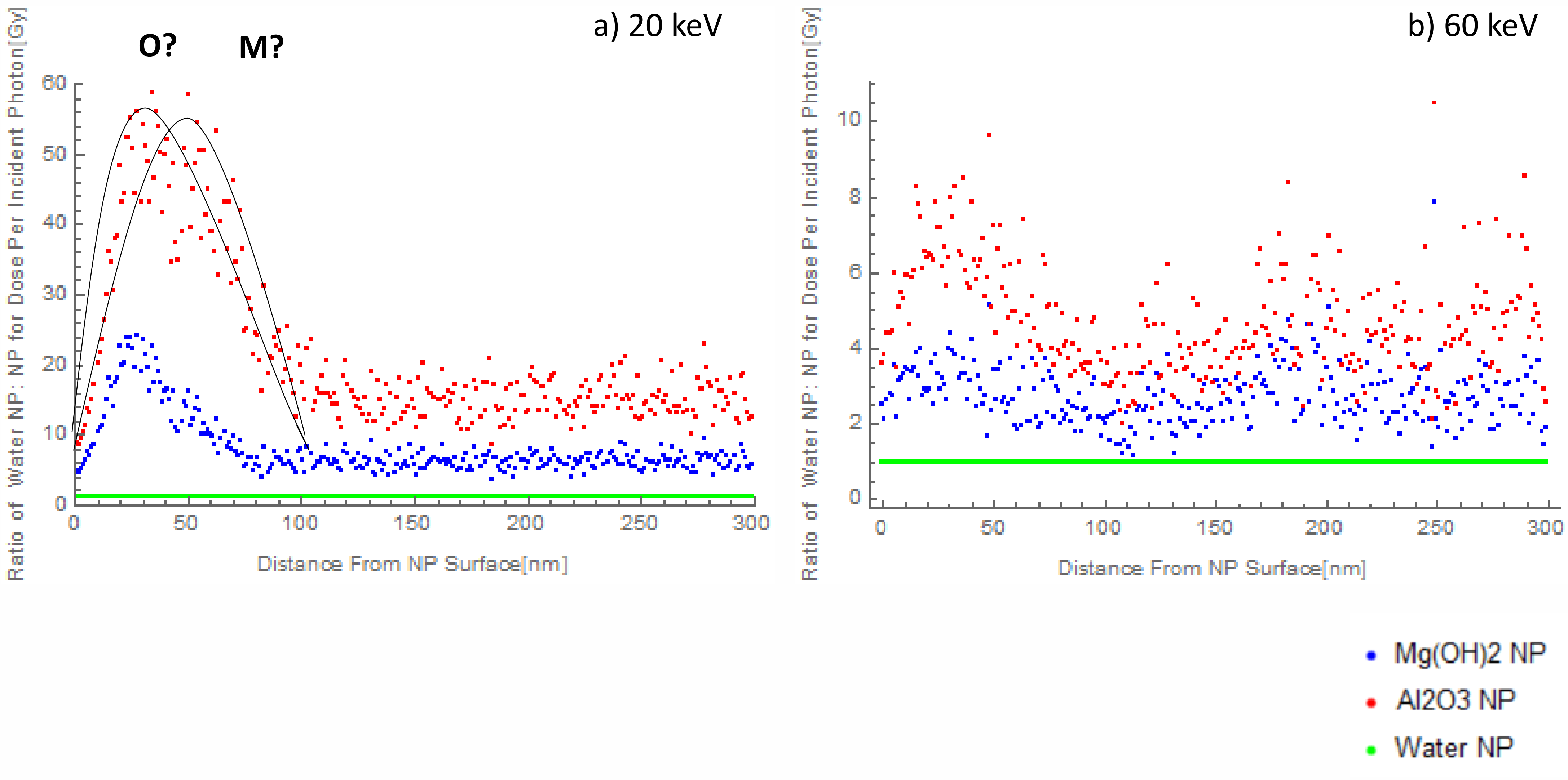

Figure 10 – Graphs showing the radial dose distributions per incident photon for Al_2O_3 and $Mg(OH)_2$ NPs as ratios to Water NPs irradiated by a) 20 and b) 60 keV

Al_2O_3 Scorer

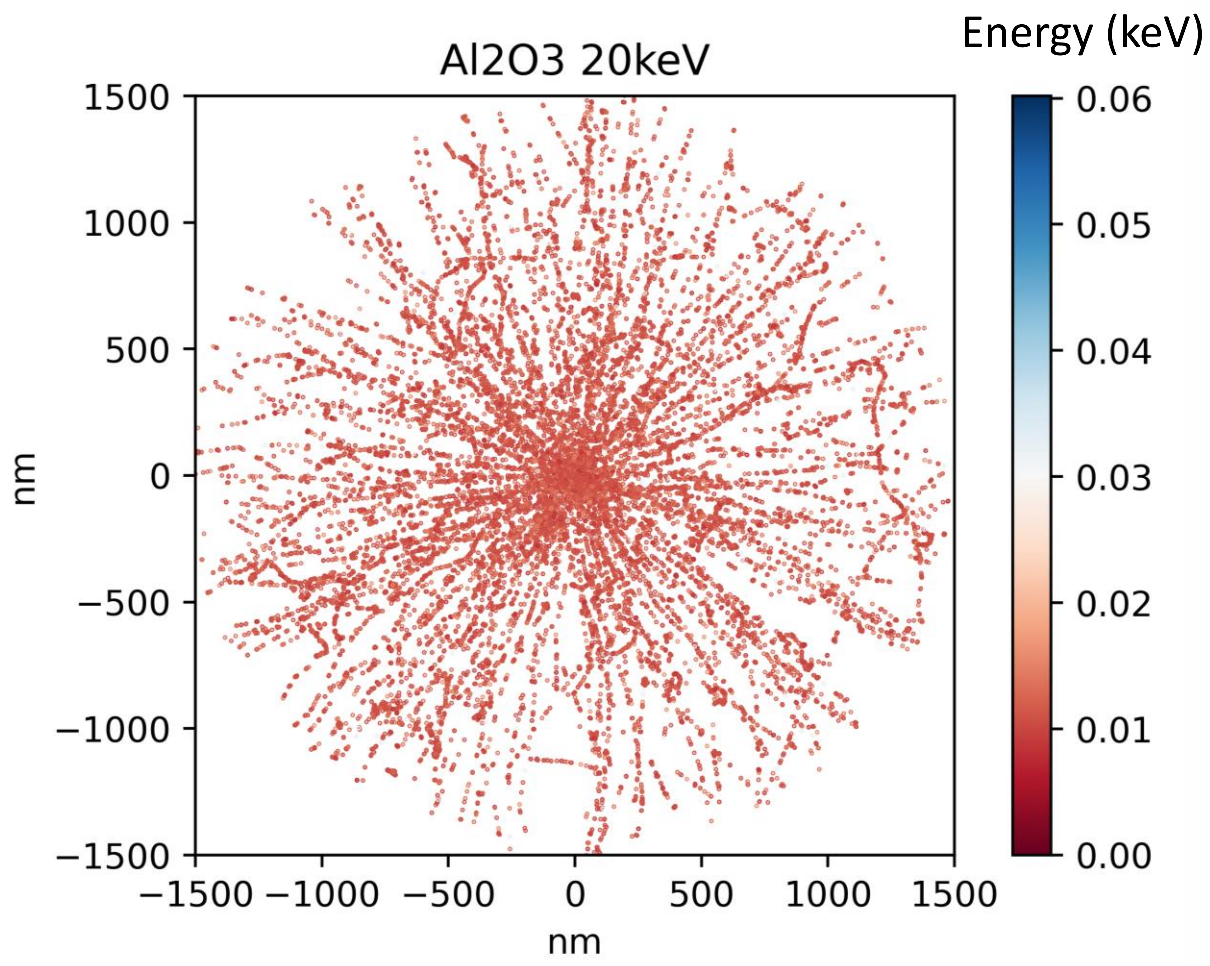

- Simulation was further developed to detect when an ionisation or excitation occurs
- When an ionisation/excitation occurs the process, position and energy of the generated e^- is recorded

Figure 11 – Figure showing the ionisations and excitations occurring in a 1500nm world following the irradiation of an Al_2O_3 NP by photons of 20 keV

Al_2O_3 Scorer

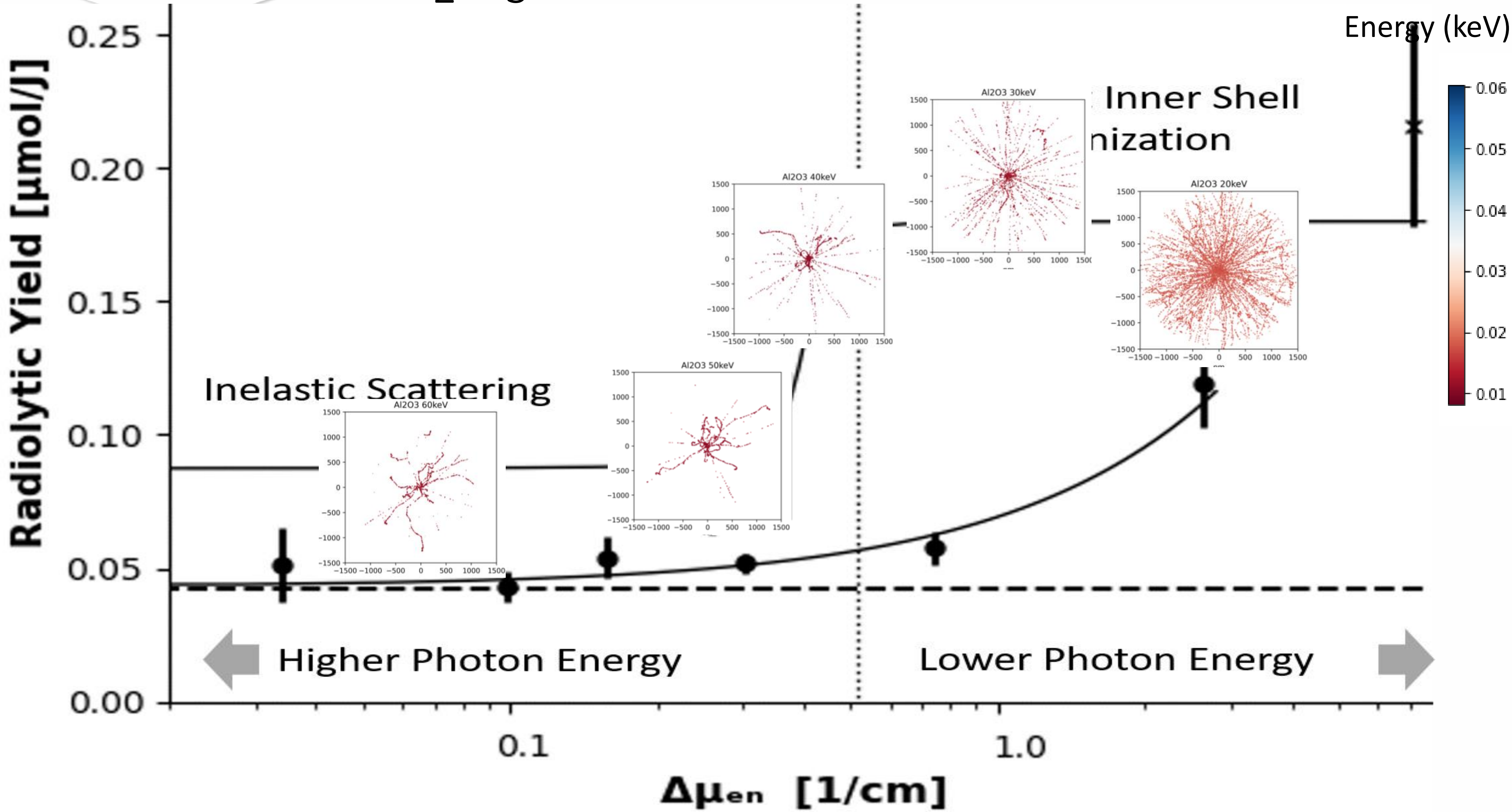

Figure 12 – Plot of the measured radiolytic hydrogen yields against the difference between energy absorption coefficients of the particulate phase and the aqueous phase [M. O'leary] overlayed with figures showing the ionisations and excitations occurring in a 1500nm world following the irradiation of an Al_2O_3 NP by photons of energies a) 20, b) 30, c) 40, d) 50 and e) 60 keV

$Mg(OH)_2$ Scorer

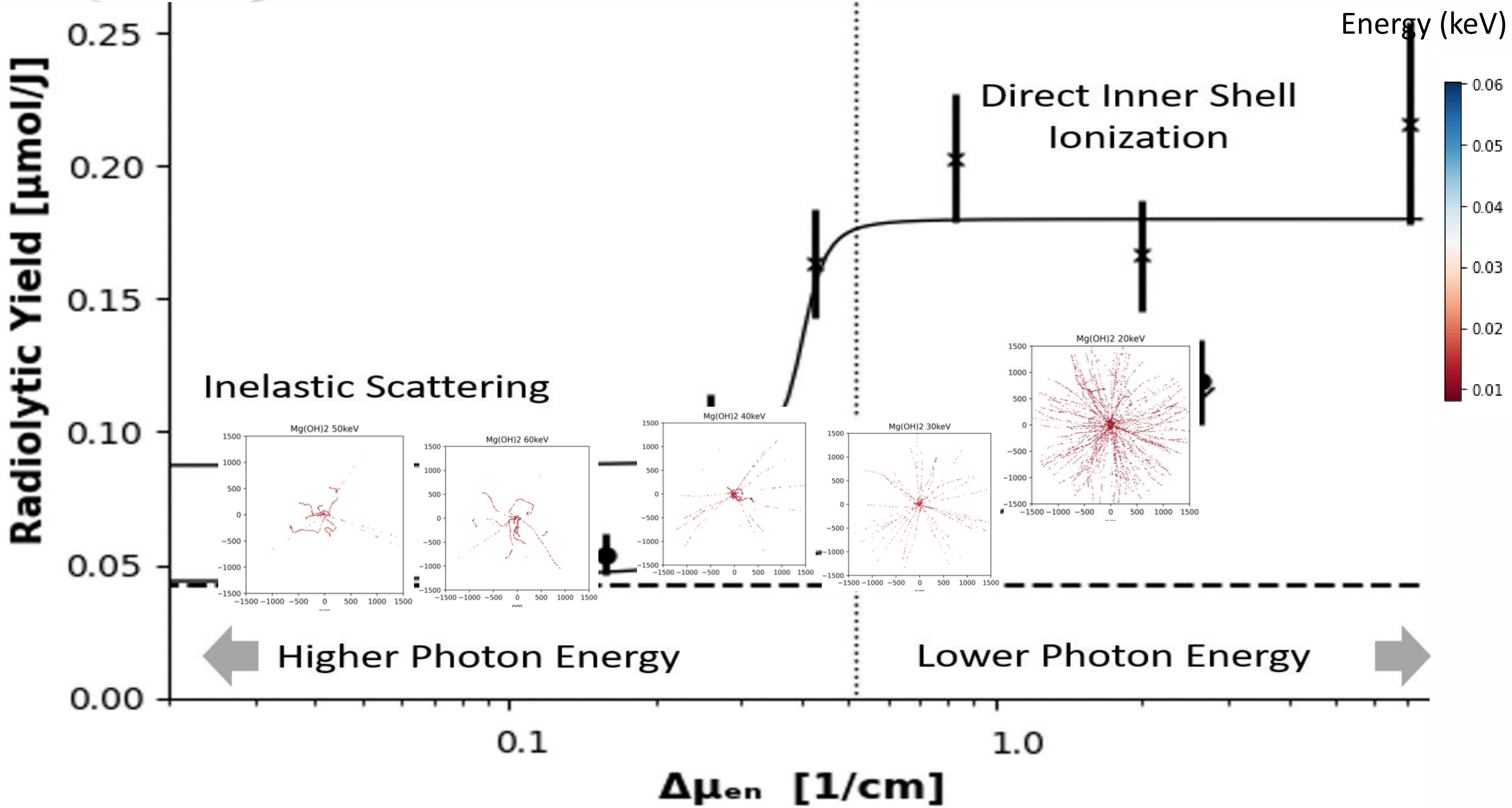

Figure 13– Plot of the measured radiolytic hydrogen yields against the difference between energy absorption coefficients of the particul ate phase and the aqueous phase [M. O'leary] overlayed with figures showing the ionisations and excitations occurring in a 1500nm world following the irradiation of an $Mg(OH)_2$ NP by photons of energies a) 20, b) 30, c) 40, d) 50 and e) 60 keV

Discussion

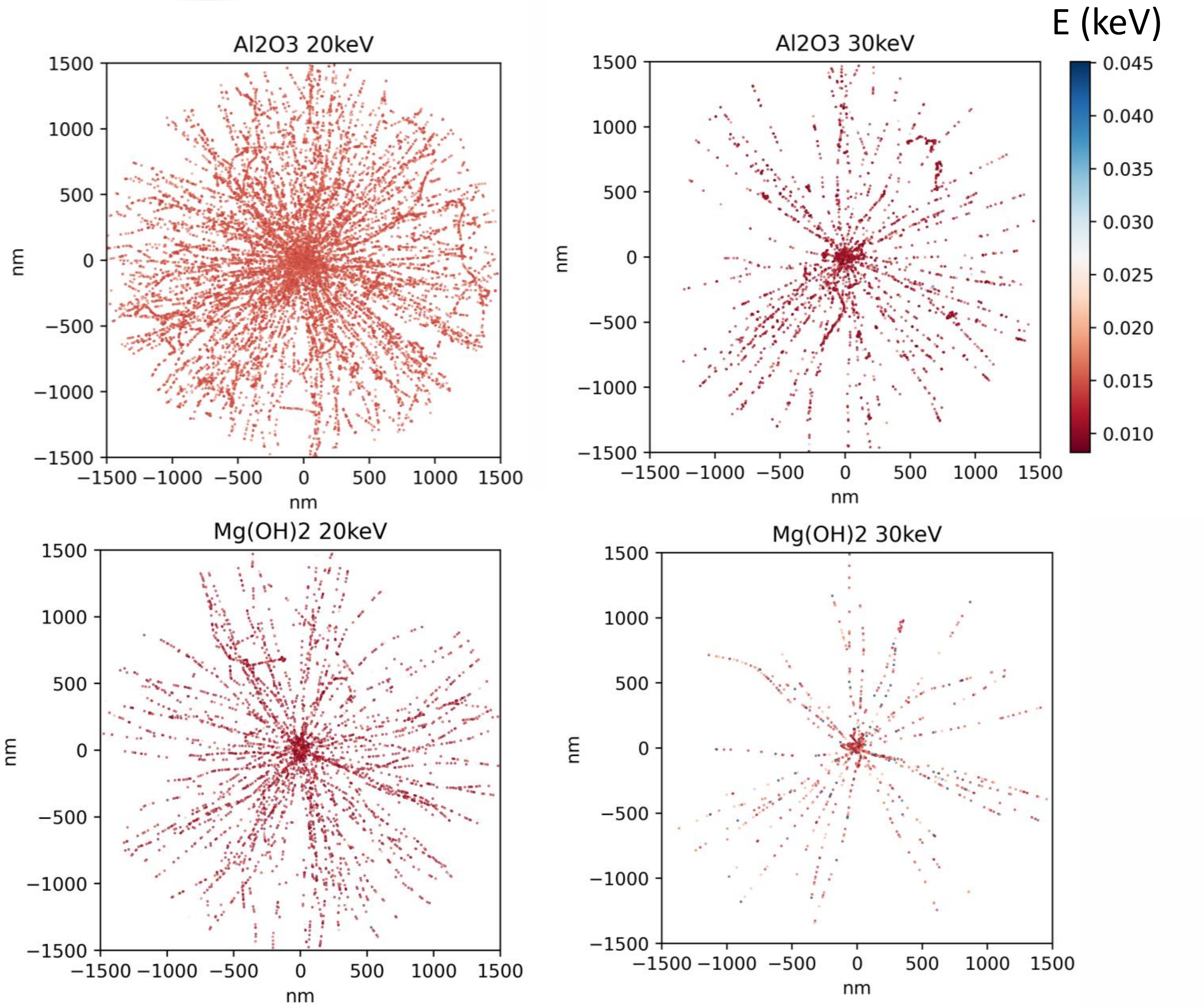

- Difference in colour shows the difference in E
- Much greater activity and E in Al_2O_3
- Especially noticeable at 20 and 30 keV – which is where the switch from Compton to photoelectric processes occur
- Likely due to Auger cascade

Figure 14 – Figures showing the ionisations and excitations occurring in a 1500nm world following the irradiation of an Al_2O_3 NP by a) 20 and b) 30 keV and a $Mg(OH)_2$ NP by c) 20, and d) 30 keV

TRANSCEND

Transformative Science and Engineering for Nuclear Decommissioning

MANCHESTER 1824

The University of Manchester

NATIONAL NUCLEAR LABORATORY

Thank you

Ella Schaefer
ella.schaefer@postgrad.manchester.ac.uk

TRANSCEND

Transformative Science and Engineering for Nuclear Decommissioning

Imperial College London

Nanotechnology for effluent treatment and radionuclide assay

Dr. Gurpreet Singh

Imperial College London

Supervisors: Prof. Luc Vandeperre & Prof. Mary Ryan

02/12/2020
TRANSCEND Project

Energy
For a Low Carbon Future

Previous Works

- Fortner's group (ref 1) had reported since 2015 about magnetic nanoparticles of mixed Mn/Fe oxide nanocrystals covered with a bilayered oleyl phosphate to adsorb/exchange uranyl ions in solution.
- Adsorption Capacity reported to be 1667 mg/g of mixed oxide nanocrystals.
- In 2018 Imperial's PhD student (Ref 2) further enhanced the work by using pure magnetite coated with oleic acid (12nm in size).

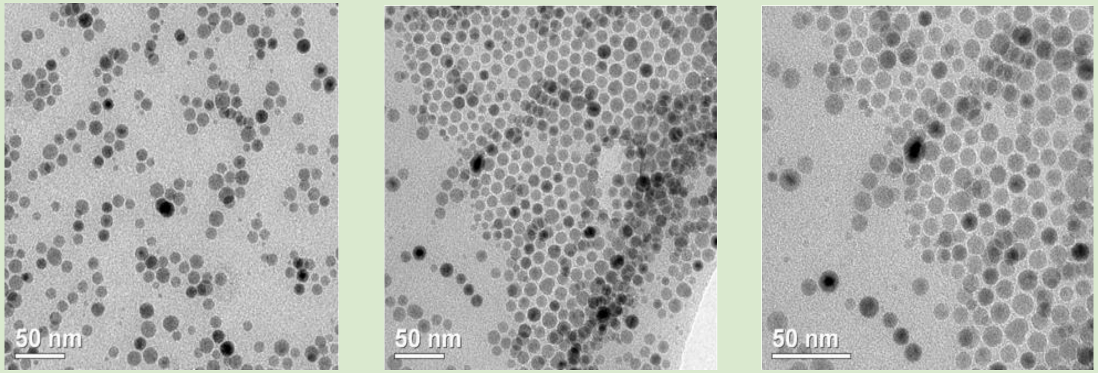

- The nanoparticles were further functionalised with phosphate groups to sequester uranium.
- The reported uptake capacity of Uranyl ions at neutral pH 7 was 1700 mg/g of Fe in 200ppm U(VI) nitrate solution
- This is the highest ever to be reported in the literature

Proposed developments

The TRANSCEND project is aimed at the following:

1. To understand the mechanism of adsorption
2. To extend the application at acidic pH
3. To target other radionuclides with new functionalised coatings
4. To investigate magnetic steering of nanoparticles for repairing cracks in concrete

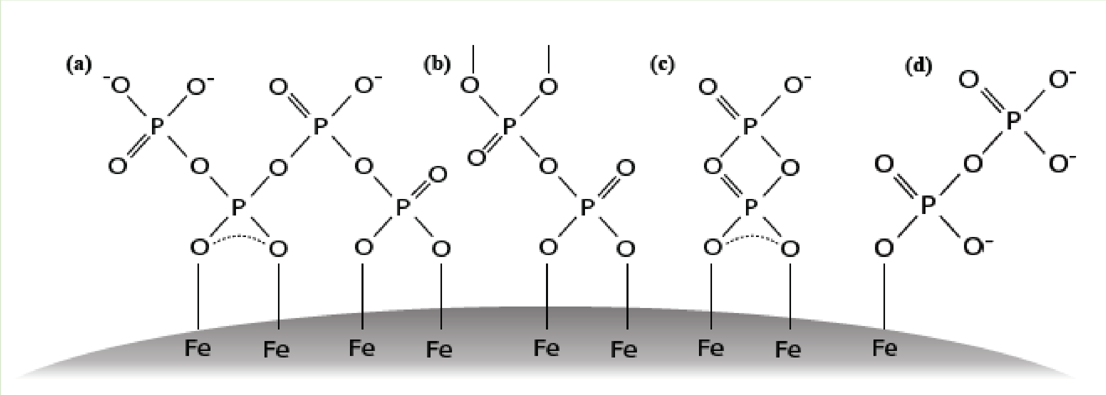

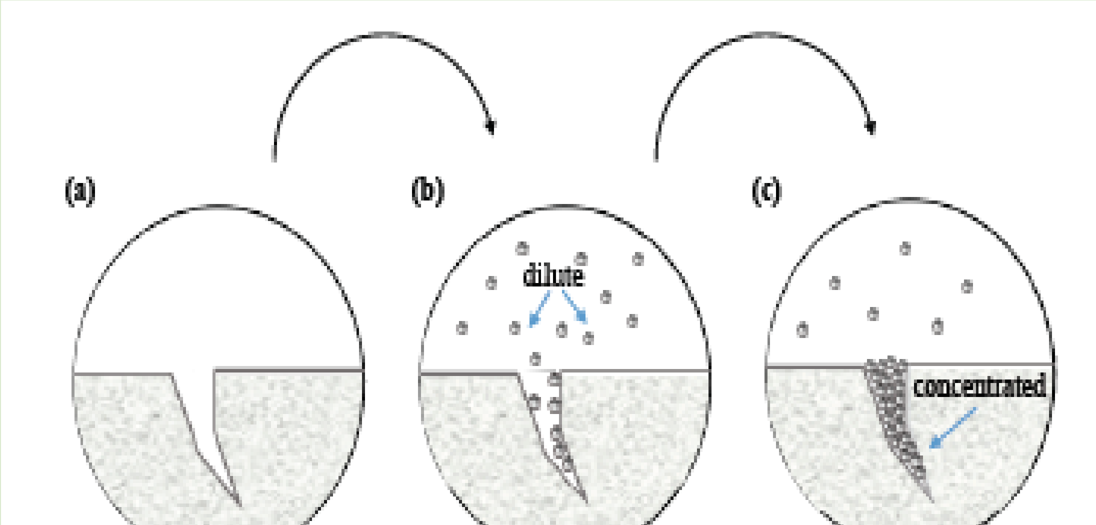

Current Work

- Previous works utilized thermal decomposition method – Tedious, Costly & utilizes higher temperatures of 320°C.
- The current work was improvised to test cheaper, quicker & lower working temperatures.
- Co-precipitation & microemulsion techniques were explored
- Various schemes were explored: 2 Finalised to take forward

<u>Scheme 1</u>

Fe(2+) & Fe(3+) salts → Magnetite (<25nm) aggregated → Coating with Oleic acid/ Na-Ol

Co-precipitated

Conditions: 30 min, 70°C, no inert atm

Phosphate ligands ← Phase-exchange & coating of silica

<u>Scheme 2</u>

Fe(2+) & Fe(3+) salts → Magnetite (<25nm) aggregated → Coating with silica (Stober's)

Co-precipitated

Conditions: 30 min, 70°C, no inert atm

Incorporating Phosphate Ligands

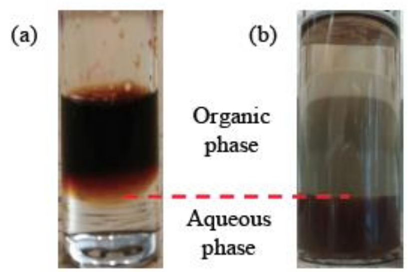

Scheme – 1 Structures

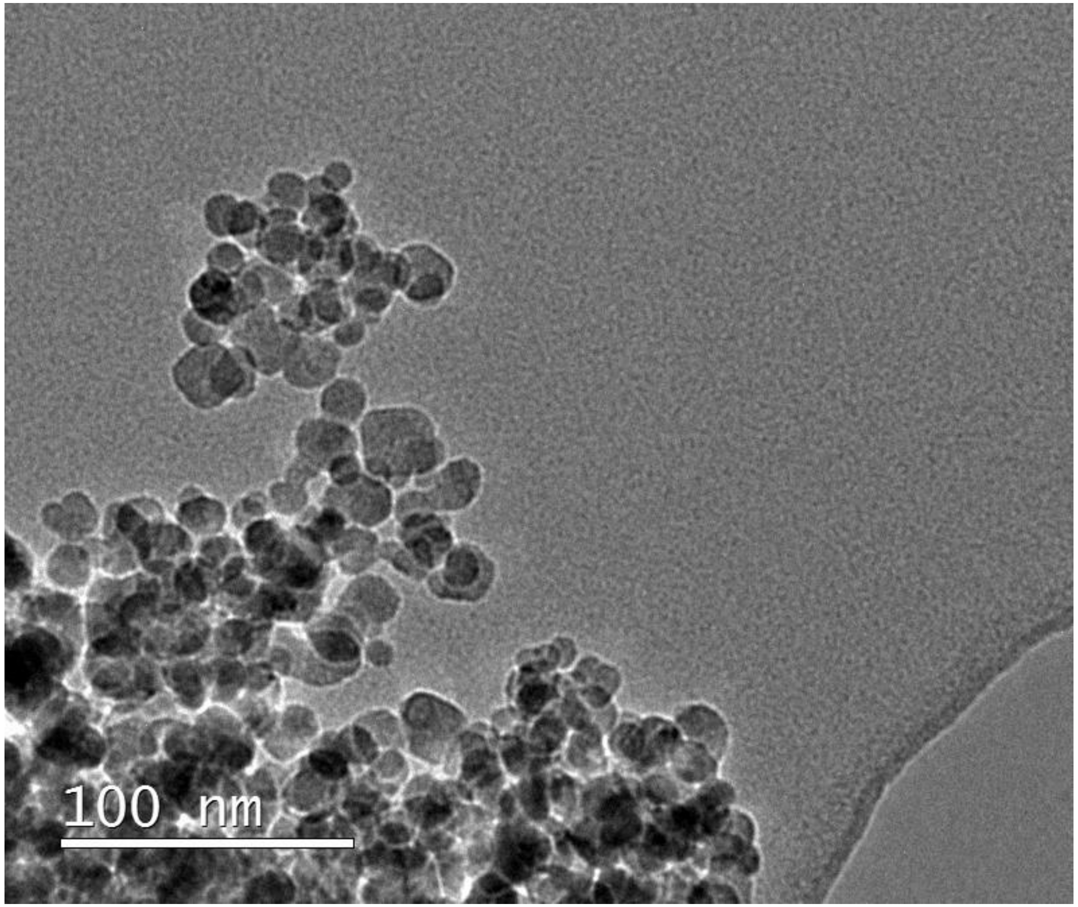

Magnetite coated with Oleic Acid

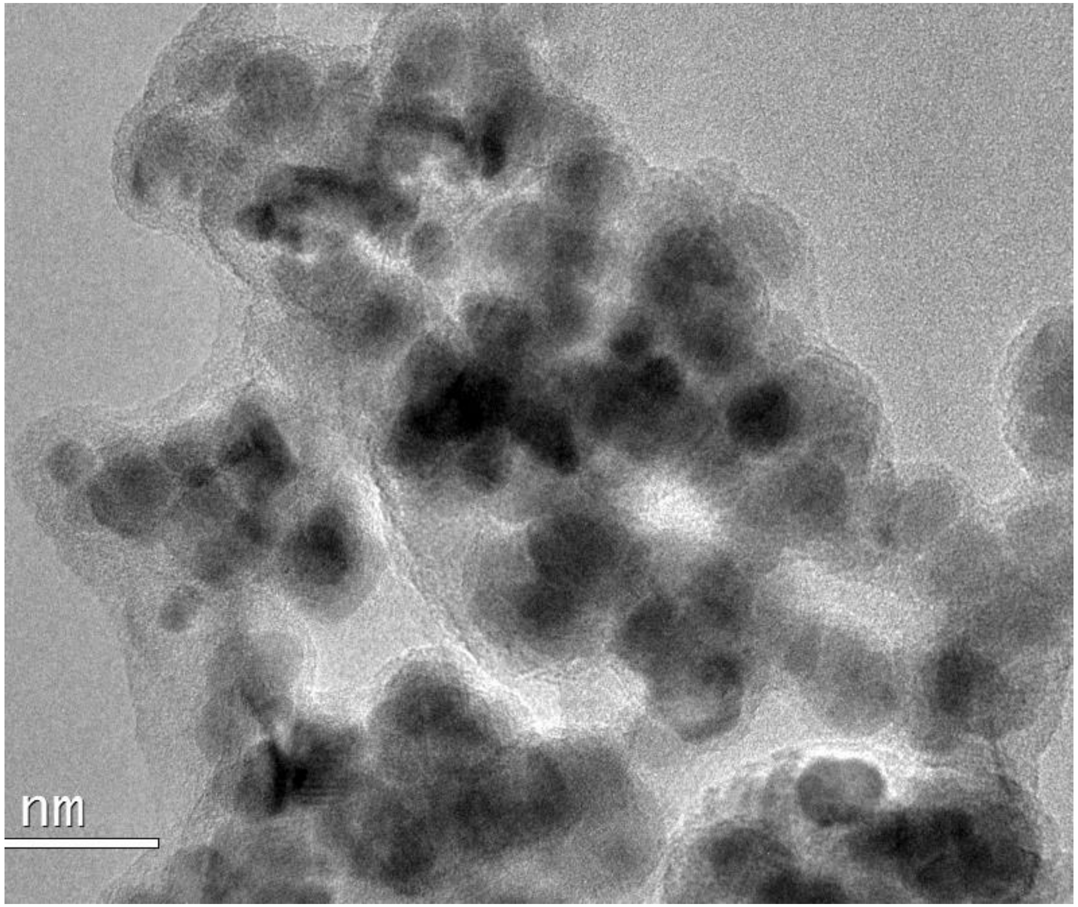

Phase-exchanged & coated with silica

Scheme - 2

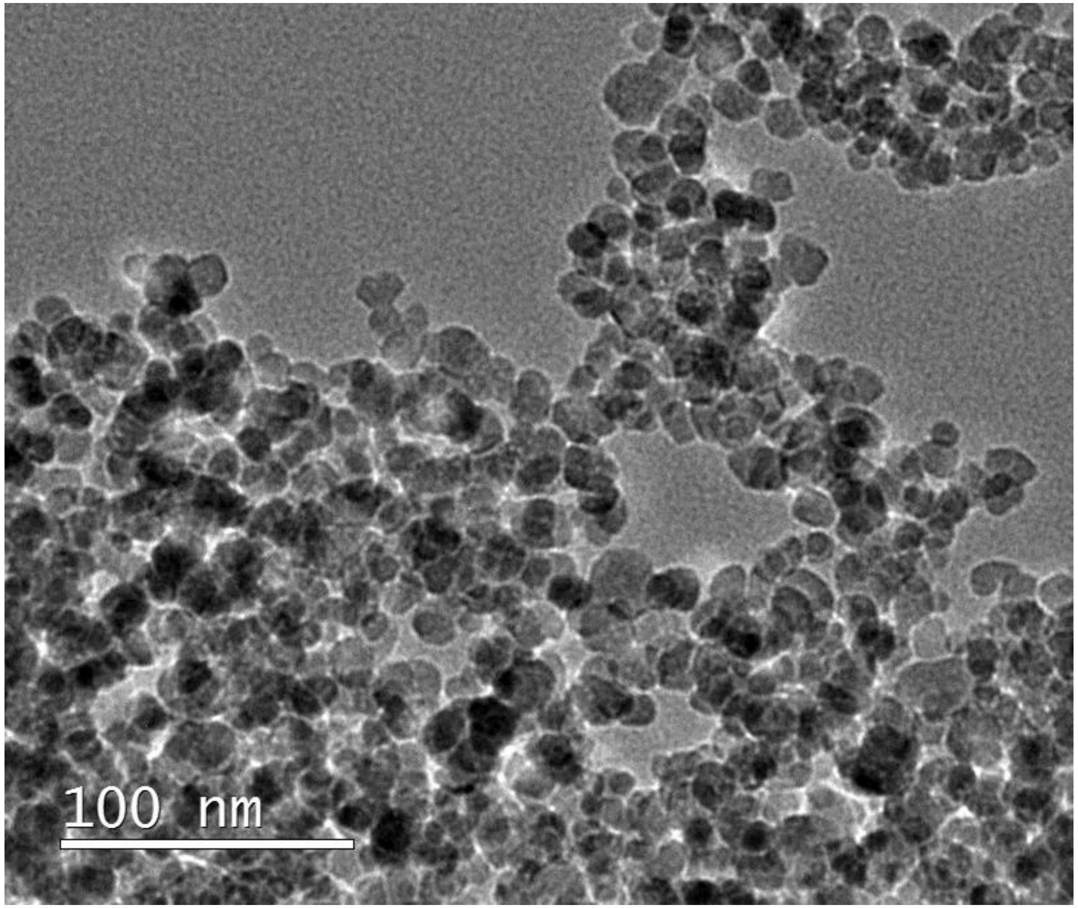

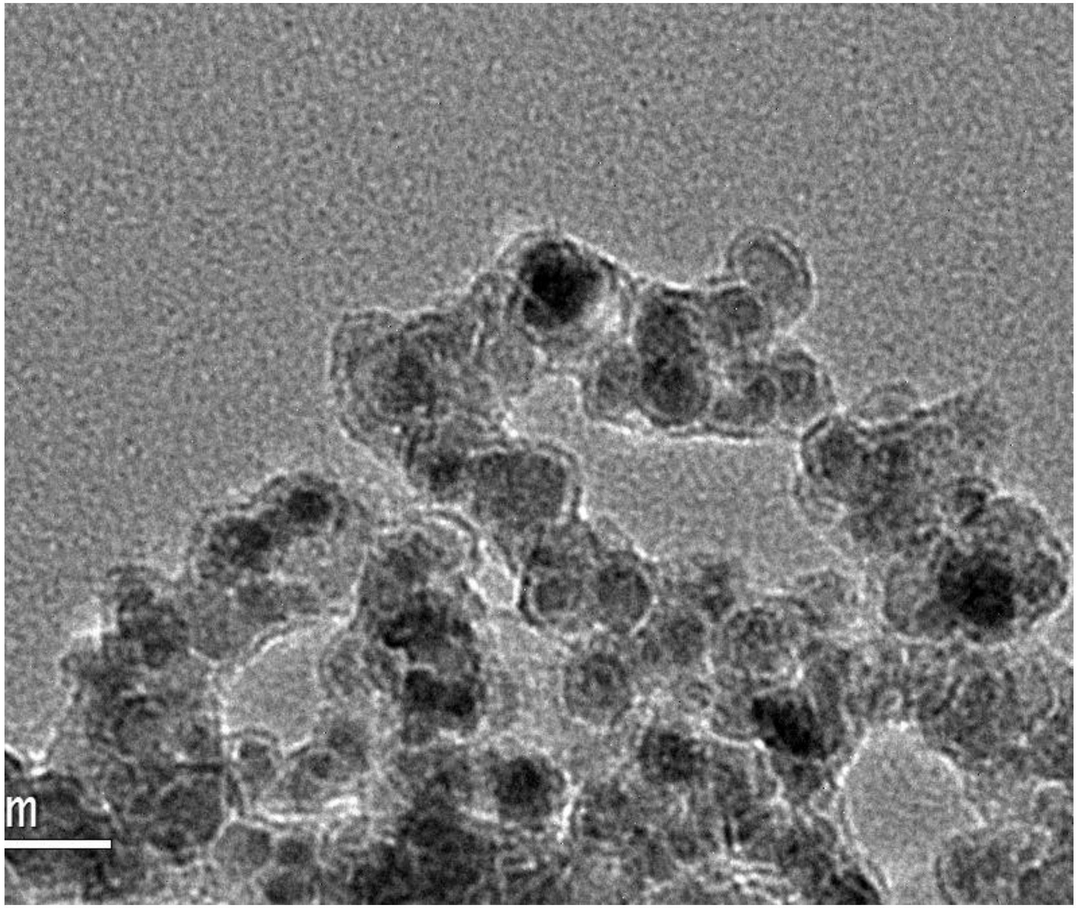

Uncoated Magnetite in water

Coated magnetite with silica

Future Works

- To optimise the processes & achieve maximum mono-dispersity
- To thoroughly characterise w.r.t to surface energy, magnetisation values & pore size of silica coating
- To collaborate for active Uranium studies
- To deduce the mechanism of action
- Perform the cost-benefit analysis

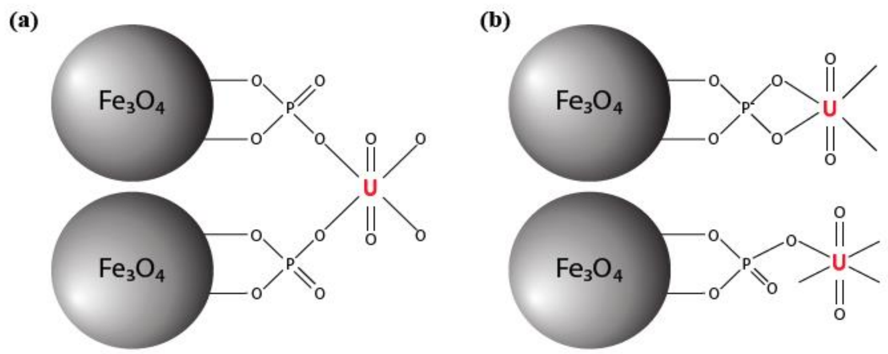

Transformative Science and Engineering for Nuclear Decommissioning

REFERENCES

1. Wenlu Li, John T. Mayo, Denise N. Benoit, Lyndsay D. Troyer, Zuzanna A. Lewicka, Brandon J. La↵erty, Je↵rey G. Catalano, Seung Soo Lee, Vicki L. Colvin, and John D. Fortner. Engineered superparamagnetic iron oxide nanoparticles for ultra-enhanced uranium separation and sensing. J. Mater. Chem. A, 4(39):15022–15029, 2016.

2. Calì, E. & Qi, Jiahui & Preedy, O. & Chen, S. & Boldrin, D. & Branford, Will & Vandeperre, L. & Ryan, M.. (2018). Functionalised magnetic nanoparticles for uranium adsorption with ultra-high capacity and selectivity. Journal of Materials Chemistry A. 6. 10.1039/C7TA09240G.

Thank you

Email: gsuri@ic.ac.uk

TRANSCEND

Transformative Science and Engineering for Nuclear Decommissioning

Off-Gas Emissions From Vitrification of Nuclear Waste

Alex Stone, Sheffield Hallam University

With special thanks to: P. A. Bingham, D. McKendrick, S. Morgan, A. Holloway, A. Nabok

Transcend Theme Meeting 2020

12/05/2020
Transcend Theme
Meeting 2020

Energy
For a Low Carbon Future

The Problem

- The UK has 133,000 m^3 of radioactive waste in storage and an estimated 4,420,000 m^3 arising in the future[1]
- A majority of this waste is from (or will arise from) site decommissioning and legacy (eg. Sellafield, Magnox)
- Vitrification has been considered as a waste treatment technique for ILW as is already in use for HLW. This involves the heating of waste to high temperatures up to 1400°C which may volatilise some of the components of the waste[2]

1. NDA. (2020). *The 2019 Inventory*. NDA Department for Business, Energy and Industrial Strategy. https://ukinventory.nda.gov.uk/the-2019-inventory/2019-uk-data/
2. Caurant, D. (2009). *Glasses, glass-ceramics and ceramics for immobilization of highly radioactive nuclear wastes*. Nova Science Publishers, Inc.

Waste Survey

- ILW can be particularly problematic because it encompasses a wide range of materials
- High volume wastes of ILW classification:
  - Some Plutonium Contaminated Material (PCM)
  - SIXEP Sand/Clinoptilolite ion exchange material
  - Magnox Sludge

The Project

Develop technologies for real time emission monitoring

Establish techniques for reduction of emissions from melts

Create an off-gas system for measuring emissions and trial previous steps

Scale up and apply to industrial size vitrification tanks

Gaseous Components of interest

- Radionuclides (^{137}Cs, ^{129}I, ^{36}Cl, ^{99}Tc, ^{106}Ru, Pu)
  - Toxic to humans and the environment
  - Can accumulate in wildlife
  - Potential for contaminating groundwater
  - Non-active analogues can be used
- Organics (Dioxins, Furans, VOCs)
  - Toxic to humans
  - Accelerates ozone decay
  - Produced from PVC and Wood decomposition
- CO, NOx, SO_2, O_2, H_2O

Experimental Procedure

- Gas is extracted from the furnace at a constant flowrate bubbling through solutions usually of dilute nitric acid or sodium hydroxide.
- Analysis of the solutions by ICP-MS and the flowrate gives a known average concentration of gas.

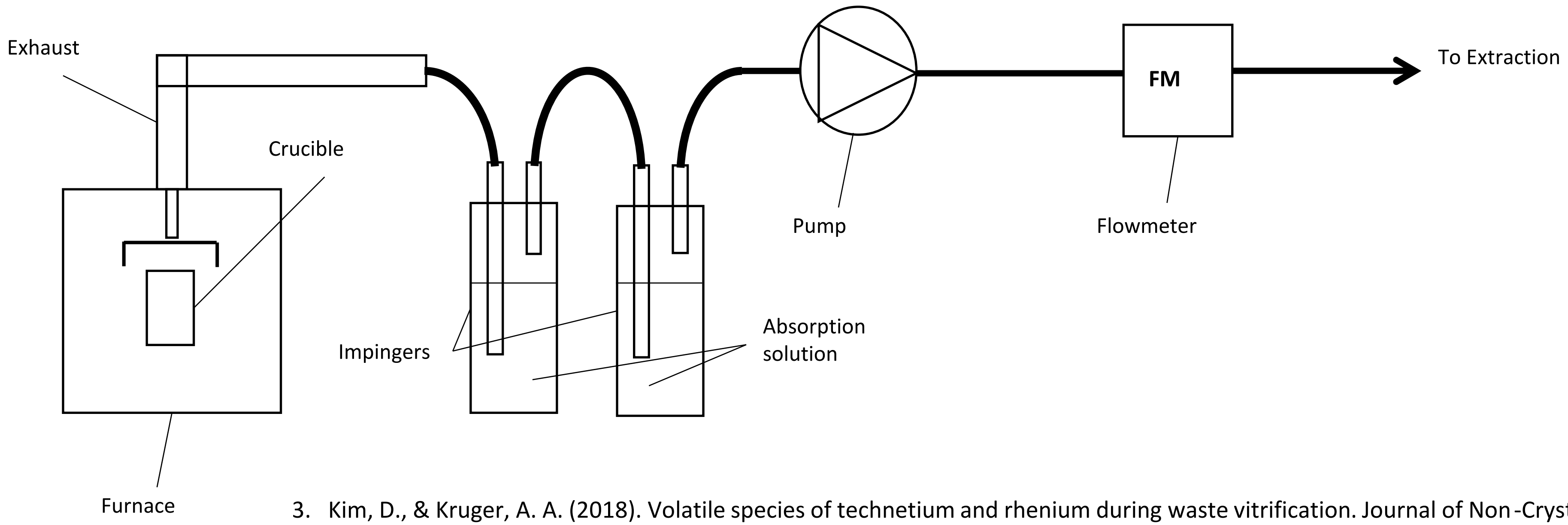

3. Kim, D., & Kruger, A. A. (2018). Volatile species of technetium and rhenium during waste vitrification. Journal of Non-Crystalline Solids, 481(October 2017), 41–50. https://doi.org/10.1016/j.jnoncrysol.2017.10.013

Experimental Procedure

Borosilicate

Magnesium Aluminosilicate

Mixture Windscale

SIXEP Sludge

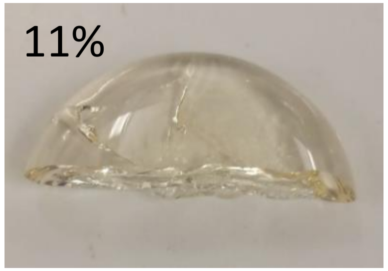

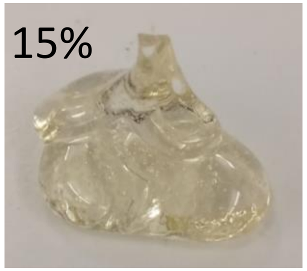

Clinoptilolite/Sand Mixture

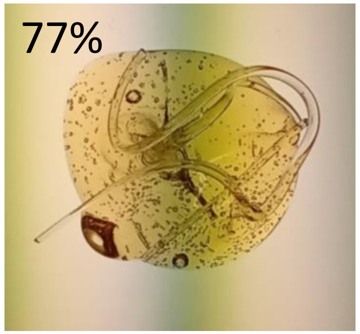

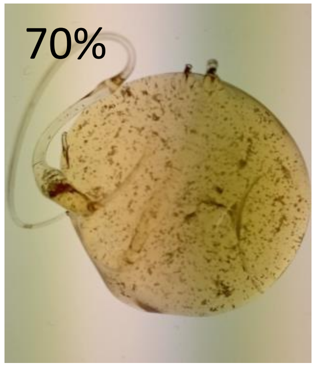

Waste Loading is indicated in the top left of the image and was selected to maximise WL for each glass.

4. Cassingham, N. J., Corkhill, C. L., Stennett, M. C., Hand, R. J., & Hyatt, N. C. (2016). Alteration layer formation of Ca- and Zn-oxide bearing alkali borosilicate glasses for immobilisation of UK high level waste: A vapour hydration study. Journal of Nuclear Materials, 479, 639–646. https://doi.org/10.1016/j.jnucmat.2016.06.009

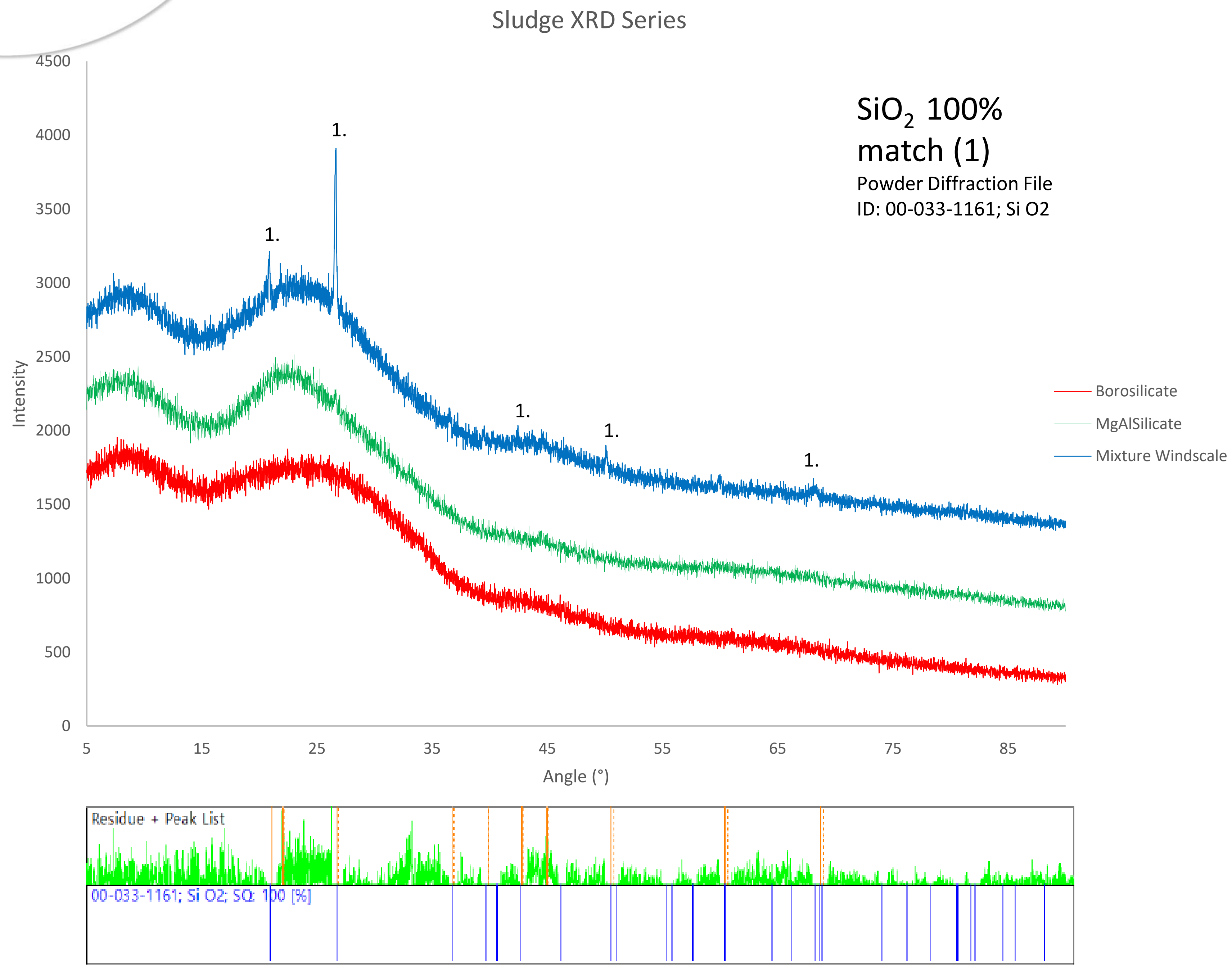
Sludge XRD Series
Intensity
Angle (°)
0
500
1000
1500
2000
2500
3000
3500
4000
4500
5
15
25
35
45
55
65
75
85
1.
1.
1.
1.
1.
SiO2 100%
match (1)
Powder Diffraction File
ID: 00-033-1161; Si O2
Borosilicate
MgAlSilicate
Mixture Windscale
Residue + Peak List
00-033-1161; Si O2; SQ: 100 [%]

Chloride Volatilisation

	0wt% Chloride MW Glass (Blank) (ppm)			1wt% Chloride MW Glass (ppm)			2wt% Chloride MW Glass (ppm)		
	Cl	B	Na	Cl	B	Na	Cl	B	Na
Impinger Set 1 ($0.7M\ HNO_3$)	7	1	5	87	3	2	115	-	-
Impinger Set 2 (0.1M NaOH)	1	0	N/A	20	1	N/A	65	3	N/A
Tube Washes	5	0	2	144	11	107	312	-	-
Post Solution Filter	0	0	0	0	0	0	0	0	0
Total	14	1	7	251	15	109	492	-	-

TRANSCEND

Conclusion and Future Work

- Initial waste glass trials complete with:
  - Simulant contaminated SIXEP sand/clinoptilolite
  - SIXEP sludge
- Good waste loading shown in a number of samples
- Collaboration with real time system developers
- Off Gas system experiments begun
- Future waste/glass modifications to reduce emissions and melting times/temperature

References

1. NDA. (2020). *The 2019 Inventory*. NDA Department for Business, Energy and Industrial Strategy. https://ukinventory.nda.gov.uk/the-2019-inventory/2019-uk-data/
2. Caurant, D. (2009). *Glasses, glass-ceramics and ceramics for immobilization of highly radioactive nuclear wastes*. Nova Science Publishers, Inc.
3. Kim, D., & Kruger, A. A. (2018). Volatile species of technetium and rhenium during waste vitrification. Journal of Non-Crystalline Solids, 481(October 2017), 41–50. https://doi.org/10.1016/j.jnoncrysol.2017.10.013
4. Cassingham, N. J., Corkhill, C. L., Stennett, M. C., Hand, R. J., & Hyatt, N. C. (2016). Alteration layer formation of Ca- and Zn-oxide bearing alkali borosilicate glasses for immobilisation of UK high level waste: A vapour hydration study. Journal of Nuclear Materials, 479, 639–646. https://doi.org/10.1016/j.jnucmat.2016.06.009

TRANSCEND

Transformative Science and Engineering for Nuclear Decommissioning

Thank you

alex.h.stone@student.shu.ac.uk

TRANSCEND

Transformative Science and Engineering for Nuclear Decommissioning

Simulation of behavioural modification effects in suspension waste pipe flow

Bisrat Wolde, University of Leeds

TRANSCEND Virtual Conference Meeting

14th of May 2021
Virtual Conference

Energy
For a Low Carbon Future

A brief overview of my project:

- Modelling and simulating for Understanding Pond and Silo Sludge Behaviour
- In the decontamination of legacy ponds and silos, the provision of a predictive capability to understand how sludges will behave is crucial to successful retrieval and completion of post operational clean out (POCO) operations
- Develop and validate multiphase direct numerical simulation in a horizontal pipe of radius R, axial length 25R in turbulent flows at Re_{τ}= 360 and 720 based on diameter
- Both polydispersed and irregular shaped particles will be tracked
- Apply behavioural modification effects to the fluid and solid particle properties to promote the desired outcome

- Supervisors: Professor Michael Fairweather

  Dr Lee Mortimer

Governing Equations:

The Navier Stokes equation can be expressed as follows for constant density:

$$\nabla . u^* = 0$$

$$\frac{\partial u^*}{\partial t^*} + (u^* . \nabla) u^* = -\nabla p^* + \frac{1}{Re_b} \nabla . \tau^* + f_i \, ,$$

Here, $u^*(x^*, t^*)$is the fluid velocity vector, non-dimensionalised using the bulk velocity, $\mathrm{u_b}$,

the position vector, x^* and time, t^* non-dimensionalized as $x^* = \frac{x}{D}$ and $t^* = \frac{t}{D/\mathrm{u_b}}$ respectively,

p^* is the non-dimensionalised pressure term for high-velocity flow, $p^* = \frac{p}{\rho \mathrm{u_b}^2}$,

The bulk Reynolds number Re_b is already a non-dimensional and defined as $\mathrm{u_b D}/\nu$, where, D is the pipe diameter, ν is the kinematic viscosity and $\mathrm{u_b}$ is the mean bulk velocity,

τ^* is the non-dimensionalized stress tensor, $\tau^* = \nabla u^* + \nabla u^{*T}$ and f_i is arbitrary forcing terms used in multiphase flows

A solution for the unknow $p, u, v \; and \; w$ is sought using continuity equation, $\nabla . \boldsymbol{u} = 0$ and boundary conditions

Methods:

To solve the descriptive equations numerically a computational fluid dynamics solver Nek5000 used. This solver is based on spectral element method (SEM) – that is a high order weighted residual technique

Nek5000 is favourable for:

- ✓High spectral accuracy
- ✓Very little numerical dispersion and dissipation
- ✓High parallelisation

The high-level computational algorithm is:

- To integrate the Navier Stokes equations, split the controlled volume into small cells (meshing)
- Numerically integrate the Navier-Stokes equations throughout the cells
- Solve numerical equations for u, v, w and p in combination with boundary conditions
- Save the solutions for post processing

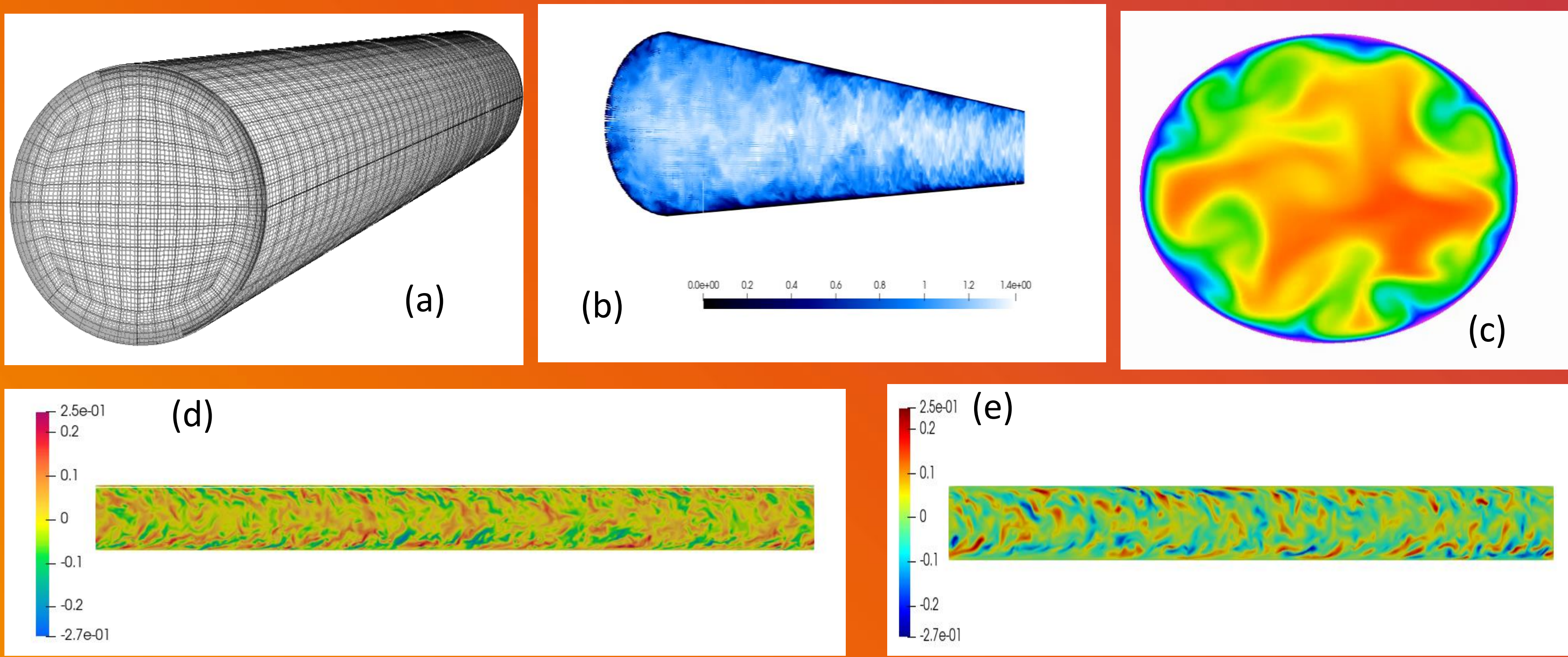

Computational mesh and pseudo-colour visualisation of the instantaneous velocity:

Panels: (a) is the computational mesh with Gauss–Lobatto–Legendre quadrature points (N = 7) for both simulations at Re_τ = 360 and 720, (b) instantaneous streamwise velocity normalized by bulk velocity, U_b , (d) and (e) are the instantaneous radial velocities for Re_τ = 360 and 720 respectively, (c) is the flows at a different timestep

Fluid results:

$$Re_\tau = 720$$

(a) The mean axial velocity profiles DNS validation at $Re_\tau = 720$. u_z^* __ solid lines are present DNS contrasted with, – – dashed lines are El Khoury's DNS, ○ open circle markers are Den Toonder experiment at $Re_\tau \approx 630$, + cross markers are Singh's DNS. **(b)** – log scale.

(c) Inner scaled statistical profiles root mean square of fluctuating velocities of DNS at $Re_\tau = 720$. The axial z_{rms}^*, radial r_{rms}^*, azimuthal θ_{rms}^*, and Reynolds shear stress $< u_z \ u_r >^*$ as a function of $(1-r)^*$ compared against the following DNS and experimental datasets. __ Solid lines are present DNS result, – – dashed lines are El Khoury's DNS, ○, open circle markers are Den Toonder experiment at $Re_\tau \approx 630$ and + cross markers are Singh DNS at $Re_\tau \approx 640$. **(d)** log scale.

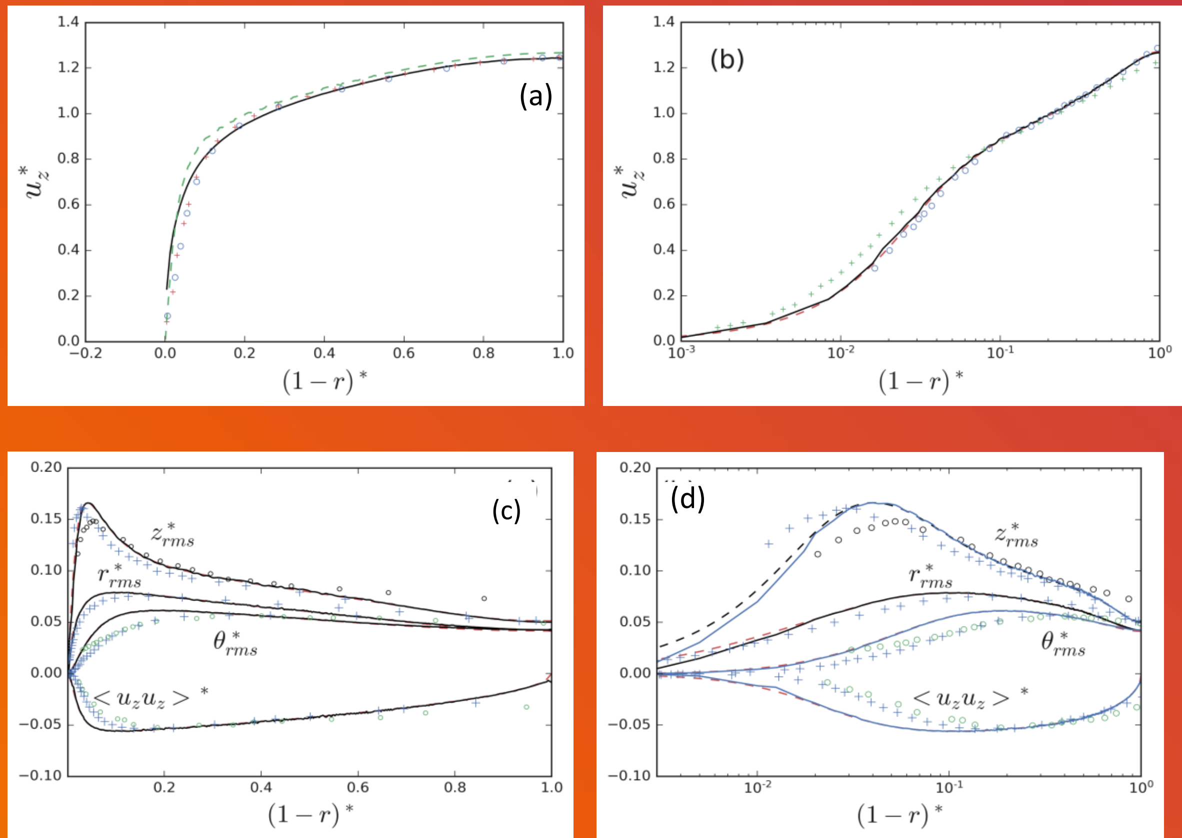

Fluid flow results:

$$\mathbf{Re}_\tau = \mathbf{277}$$

(a) Validation of mean axial velocity profiles at $Re_\tau = 277$. u_z^*, stream wise direction, __ solid lines are present DNS contrasted with +, cross markers Vreman's dataset. (c) is the statistical root mean square velocity fluctuation profiles validation at $Re_\tau = 277$. The axial z_{rms}^*, radial r_{rms}^*, azimuthal θ_{rms}^*, and Reynolds shear stress $< u_z \ u_r >^*$ as a function of $(1-r)^*$ compared against the Vreman's DNS result. __ solid lines are present DNS result, +, cross markers are Vreman DNS. b and d are log scales.

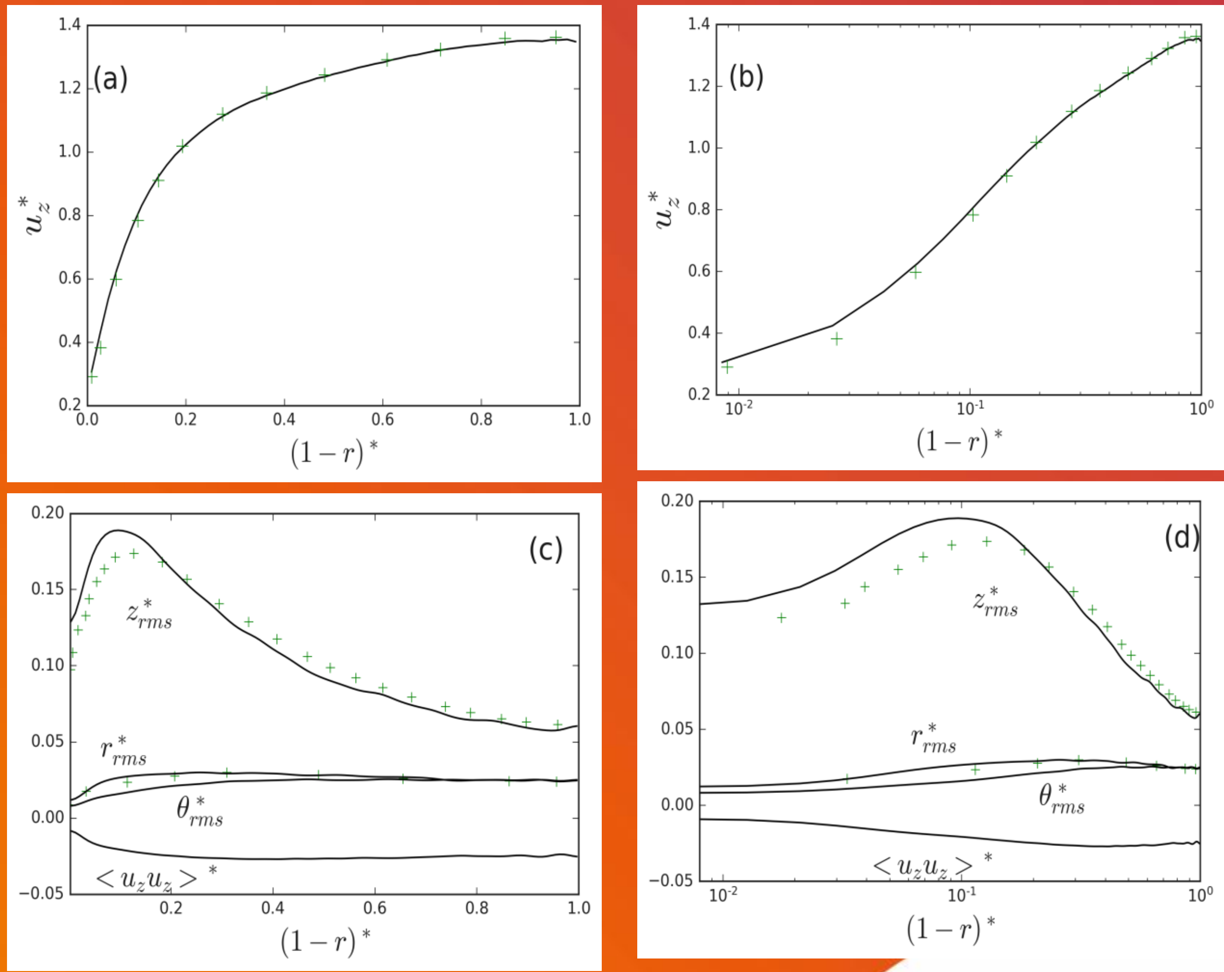

A Lagrangian particle tracker has been developed to model large quantities of dispersed solids and to investigate the bulk behaviour of high concentration dispersions:

- The particles are injected at random position within the fully developed fluid flow domain
- Assigned the fluid velocity at that location
- Particle collision with the pipe wall considered to be elastic
- A fourth order Runge-Kutta method implemented to solve the particle equation of motion for each particle at every time-step
- Statistical data gathered for analysis after letting a few response times to adjust to the surrounding fluid

The non-dimensional particle equations of motion is given by:

$$u_p^* = \frac{\partial x_p^*}{\partial t^*}$$

$$\frac{\partial u_p^*}{\partial t^*} = \frac{3C_D|\boldsymbol{u_s^*}|}{\boldsymbol{4d_p^*}\,\rho_p^*}\boldsymbol{u_s^*} + \boldsymbol{g} * (\boldsymbol{1} - \rho_p^*) + \frac{3\,C_L}{4\rho_p^*}(\boldsymbol{u_s^*}\,\boldsymbol{x}\,\boldsymbol{\omega_f^*}) + \frac{\mathrm{D}'\boldsymbol{u_f^*}}{2\rho_p^*\,\boldsymbol{Dt*}} + \frac{\mathrm{D}\boldsymbol{u_f^*}}{\rho_p^*\,\boldsymbol{Dt*}}$$

Drag Gravity Lift Virtual Mass Pressure Gradient

Multiphase results:

$$Re_\tau = 277$$

(a) LPT validation of inner scaled statistical particle mean velocity profiles of a DNS at $Re_\tau = 277$, (c) statistical particle profiles, root mean square of velocity fluctuations of a DNS at $Re_\tau = 277$ for axial z^*_{rms}, radial r^*_{rms}, azimuthal θ^*_{rms} and Reynolds shear stress $< u_z \; u_r >^*$ shown. — solid lines are current work, and + markers are Vreman at $Re_\tau = 277$ DNS, and (b) and (d) are log scale.

Parameters	$St^+ \cong 78$
Particle diameter, $d_p [\mu m]$	60
Particle diameter, d^*_p	$3.0E^{-03}$
Axial length	25R
Number of particles, N_p	$29.4E^{+03}$
Shear stokes number, St_τ	78
Density ratio, ρ^*_p	$2.058E^{+03}$
Volume fraction, ϕ	$4.24E^{-05}$
Particle and fluid timestep, Δt^*	$1.0E^{-03}$

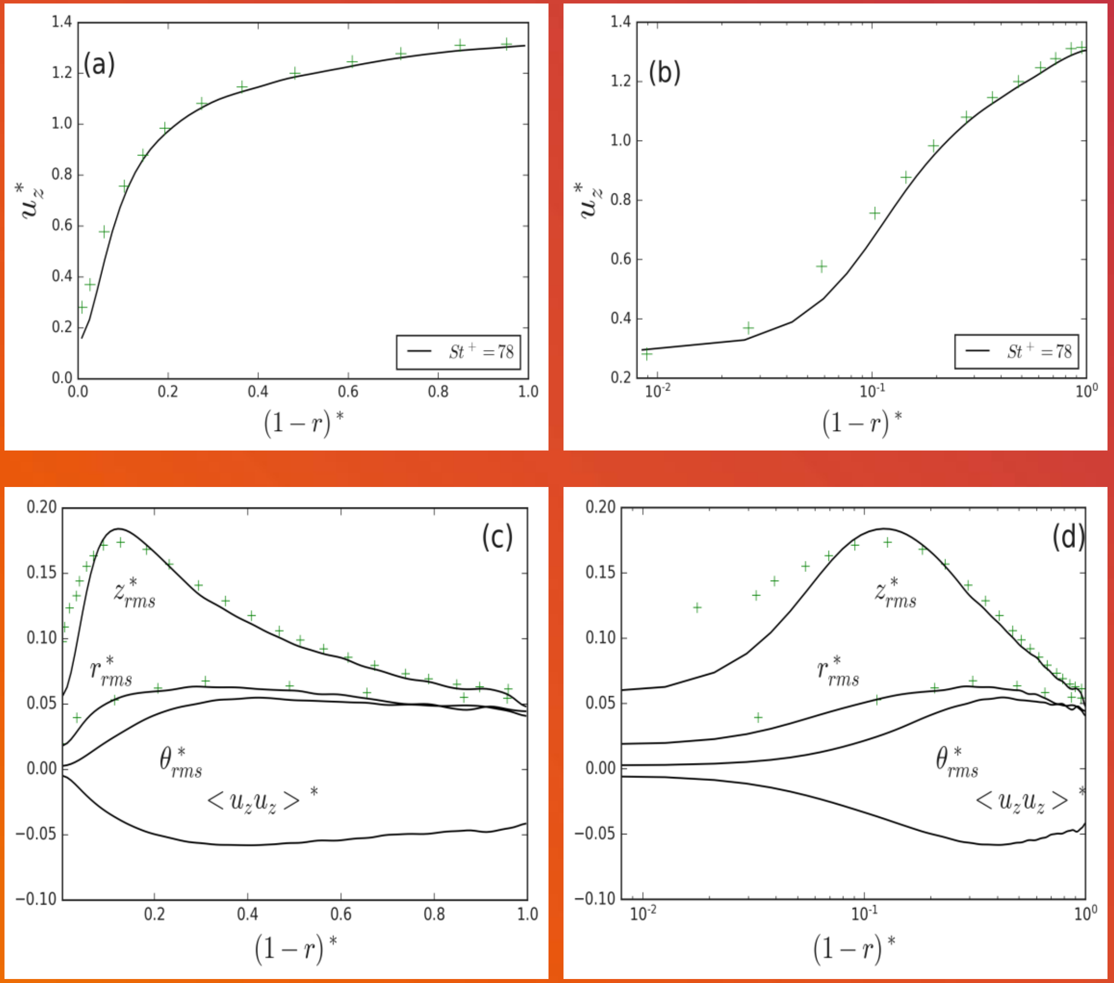

Multiphase results:
$$Re_\tau = 277$$

Probability density function for the particle Reynolds number in viscous, buffer, log-law and bulk flow regions of the pipe at $St^+ = 78$.

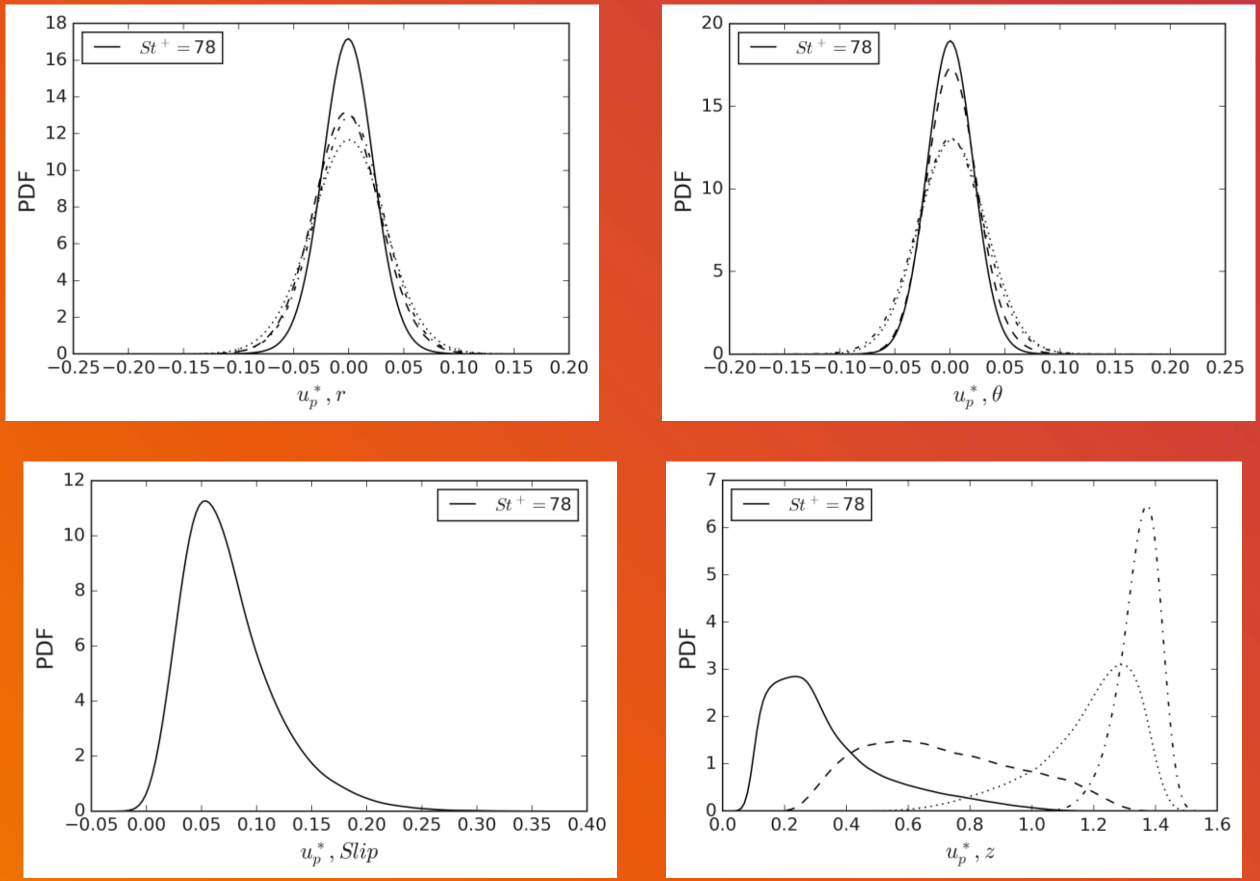

Top left is the radial and right is azimuthal. Lower left is the slip velocity and on the right is axial. Solid line: viscous sublayer; dashed: buffer layer; dotted: log-law region; dot- dashed: bulk flow

Dimensional analysis:

$V_c = f(d, D, \phi, (\rho_s - \rho_f)g, \rho_f, \mu)$

Where,
$\mu = [ML^{-1}T^{-1}]$ – Dynamic viscosity
g $= [LT^{-2}]$ Acceleration due to gravity
$V_c = [LT^{-1}]$ critical velocity
d = [L] particle diameter
D = [L] pipe diameter
$Q_s = [L^3T^{-1}]$ solid-phase volumetric flow rate
$Q_f = [L^3T^{-1}]$ solid-phase volumetric flow rate
$\rho_s = [ML^{-3}]$ Density of solid phase
$\rho_f = [ML^{-3}]$ Density of fluid phase

Side note: - $\phi = \frac{Q_s}{Q_s+Q_l} = [M^0L^0T^0] = [1]\ and\ s = \frac{\rho_s}{\rho_f}[M^0L^0T^0] = [1]$

To develop a functional relationship the above equation set to:

$$\frac{V_c}{\sqrt{gd(s-1)}} = i_0\left(\frac{d}{D}\right)^{i_1} \phi^{i_2} (1-\phi)^{i_3} \left(\frac{\mu}{d\rho_f\sqrt{gd(s-1)}}\right)^{i_4}$$

$i_0 - i_4$ values determined by regression using experimental data.

The following model derived using linear regressor is:

$$\frac{V_c}{\sqrt{gd(s-1)}} = 1.85\left(\frac{d}{D}\right)^{-0.18} \phi^{0.154} (1-\phi)^{0.16} \left(\frac{\mu}{d\rho_f\sqrt{gd(s-1)}}\right)^{0.09} \quad \text{(Eq 1)}$$

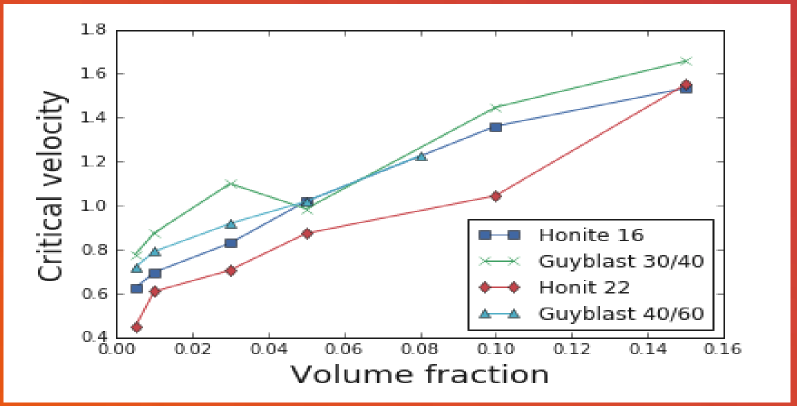

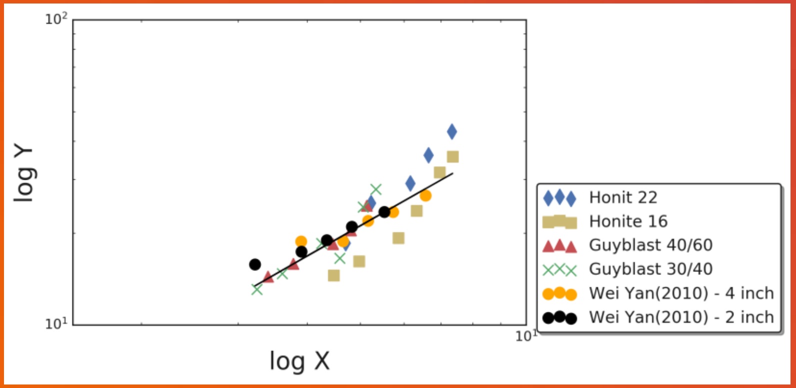

Experimental deposition data were also plotted against the same empirical correlation (equation 1.) Deposition based dataset plotted against the same empirical correlation.

Dimensional analysis:

To test Rice's (2013) contention that one can evaluate deposition velocity from resuspension or deposition. Experimental deposition data were also plotted against the same empirical correlation (equation 1.)

Pakzonka et al. (1981) investigated using three different pipe diameters, D = 50.8mm, 103mm and 202mm and Al-Lababidi et al. (2012) used D =103mm. Sinclair and Graf dataset also plotted.

The model derived using linear regressor is:

$$\frac{V_c}{\sqrt{gd(s-1)}} = 1.85\left(\frac{d}{D}\right)^{-0.18} \phi^{0.154} (1-\phi)^{0.16} \left(\frac{\mu}{d\rho_f\sqrt{gd(s-1)}}\right)^{0.09} \qquad \text{(Eq 1)}$$

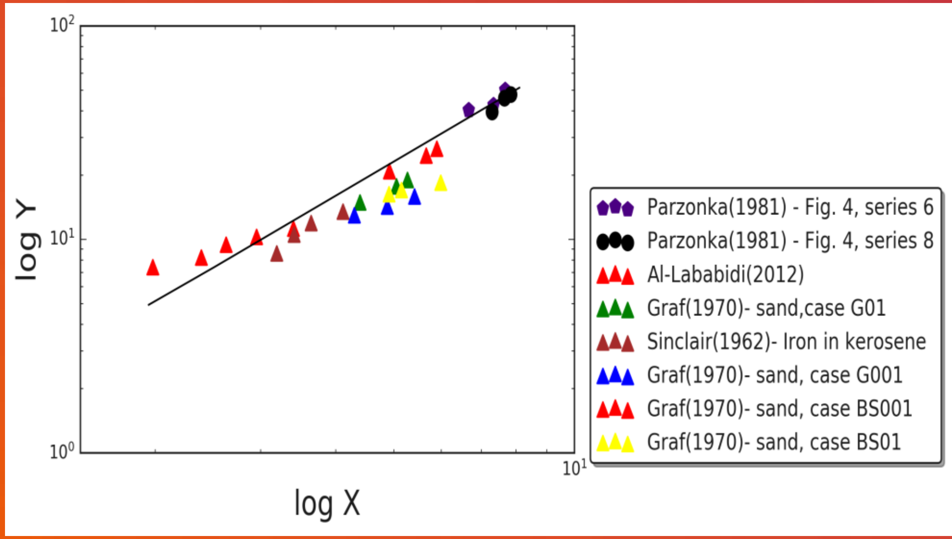

Deposition based dataset plotted against the same empirical correlation

Deposition based predictions

Particle distribution in the vertical direction computed as follows:

$$D^*_{y(t)} = \left(\sum_{i=1}^{n_t} \frac{(y^*_{i(t)} - y^*_{m(t)})^2}{n_t} \right)^{1/2}$$

(eq 2)

Where, $D^*_{y(t)}$, Dispersion function, $y^*_{i(t)}$ is the particle displacement in vertical direction and $y^*_{m(t)}$ is the mean value. The particle mean displacement and dispersion function equation 2 used to analyse if a deposition is occurring.

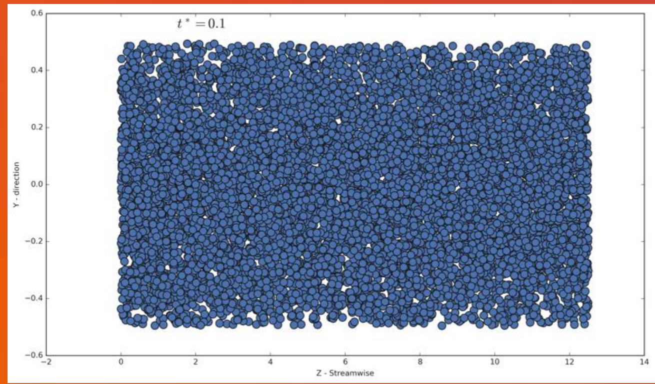

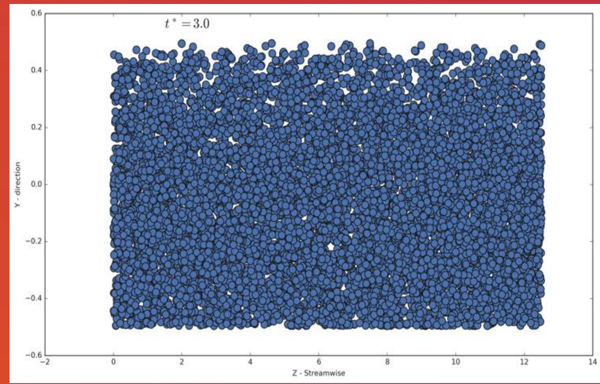

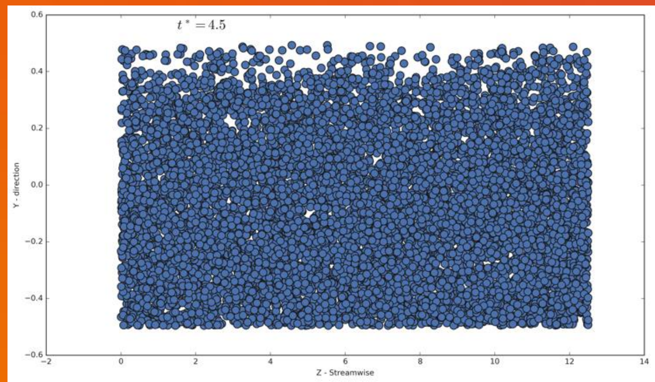

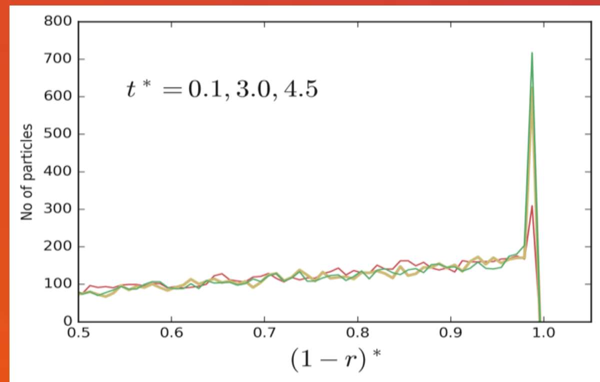

Particle concentration at t* = 0.1 (red), 3.0(yellow) and 4.5(green)

Transformative Science and Engineering for Nuclear Decommissioning

Four-way coupling results:

The four way coupling which takes into account Collisions between particles and particle fluid Dynamics.

The mean axial velocity profiles at $Re_\tau = 720$. u_z^*, stream wise direction, __ solid lines are 1-way coupling and – are four-way coupling. (c) is the statistical root mean square velocity fluctuation profiles validation at $Re_\tau = 720$. The axial z_{rms}^*, radial r_{rms}^*, azimuthal θ_{rms}^*, and Reynolds shear stress $< u_z \ u_r >^*$ as a function of $(1-r)^*$. (b) and (d) are log scale.

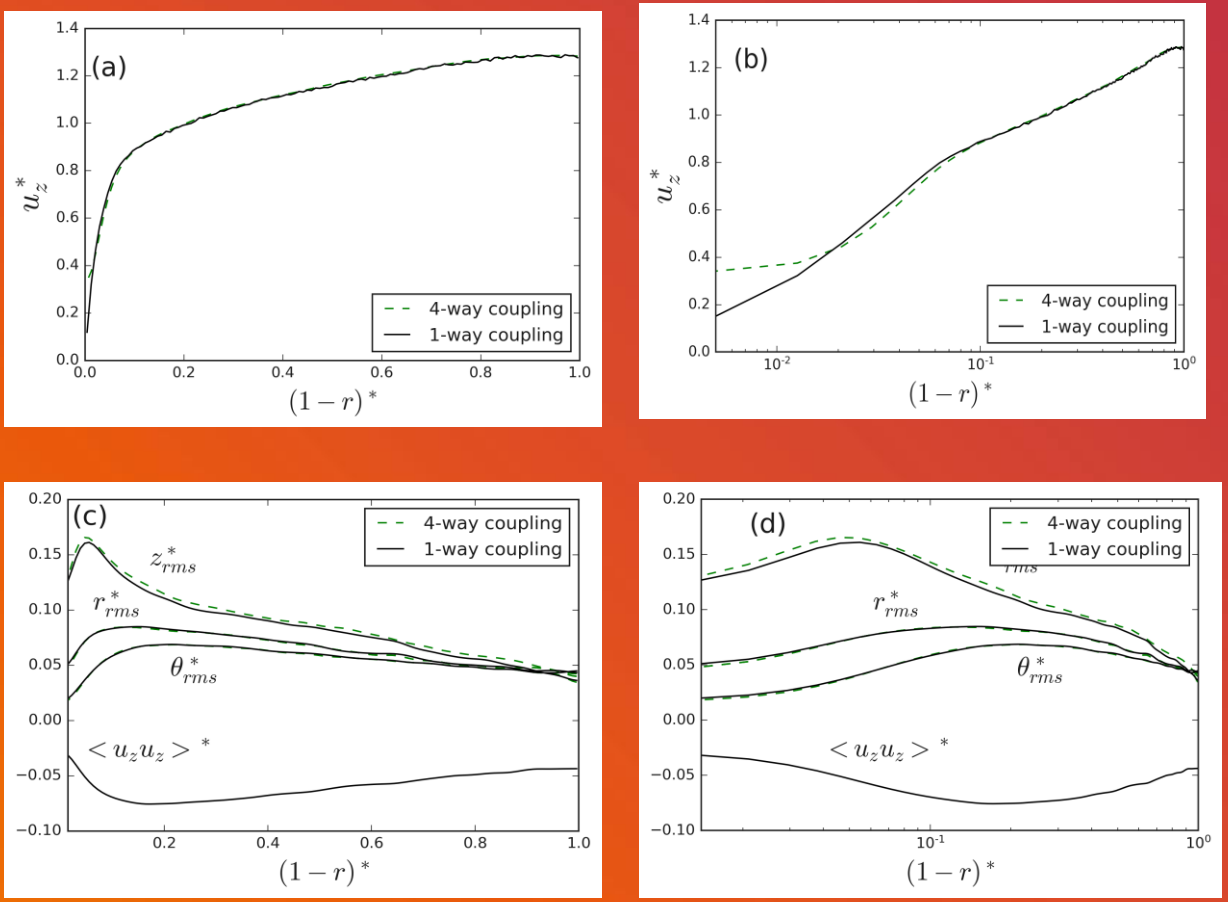

Parameters	1 way coupling	4-way coupling
Volume fraction	0.001	0.001
Number of particles	150,000	150,000
Stokes	1.951	1.951
Diameter of particle	100 μm	100 μm
Pipe diameter	0.02m	0.02m
Density ratio	2.71	2.71

Energy
For a Low Carbon Future

Planned work:

- Implement four-way coupling with agglomeration
  - DLVO theory will be applied
- Modelling and understanding pond and silo sludge behaviour
- Apply behavioural modification effects to the fluid and solid particle properties to promote the desired outcome such as reducing particle agglomeration, and hence, the likely deposition of particles during processing
- The behavioural modification effects to be studied includes changes in:

❖ Temperature

❖ Ionic strength

❖ Polymers and pH of the liquid phase

Any questions?

Transformative Science and Engineering for Nuclear Decommissioning

Thank you

pmbw@leeds.ac.uk

TRANSCEND

Transformative Science and Engineering for Nuclear Decommissioning

Radiation effects on nuclear waste forms:

How does the degree of crystallinity in a glass-ceramic affect radiation tolerance?

Tamás Zagyva – The University of Manchester, Dalton Cumbrian Facility

Theme 1 Integrated Waste Management

14th May 2021
Online

MANCHESTER 1824
The University of Manchester
Dalton Nuclear Institute

NATIONAL NUCLEAR LABORATORY

Energy
For a Low Carbon Future

Introduction

Highly active liquor (HAL)

Vitrification (1050 °C)

waste oxide

+

glass frit

Solid glass wasteform

Introduction

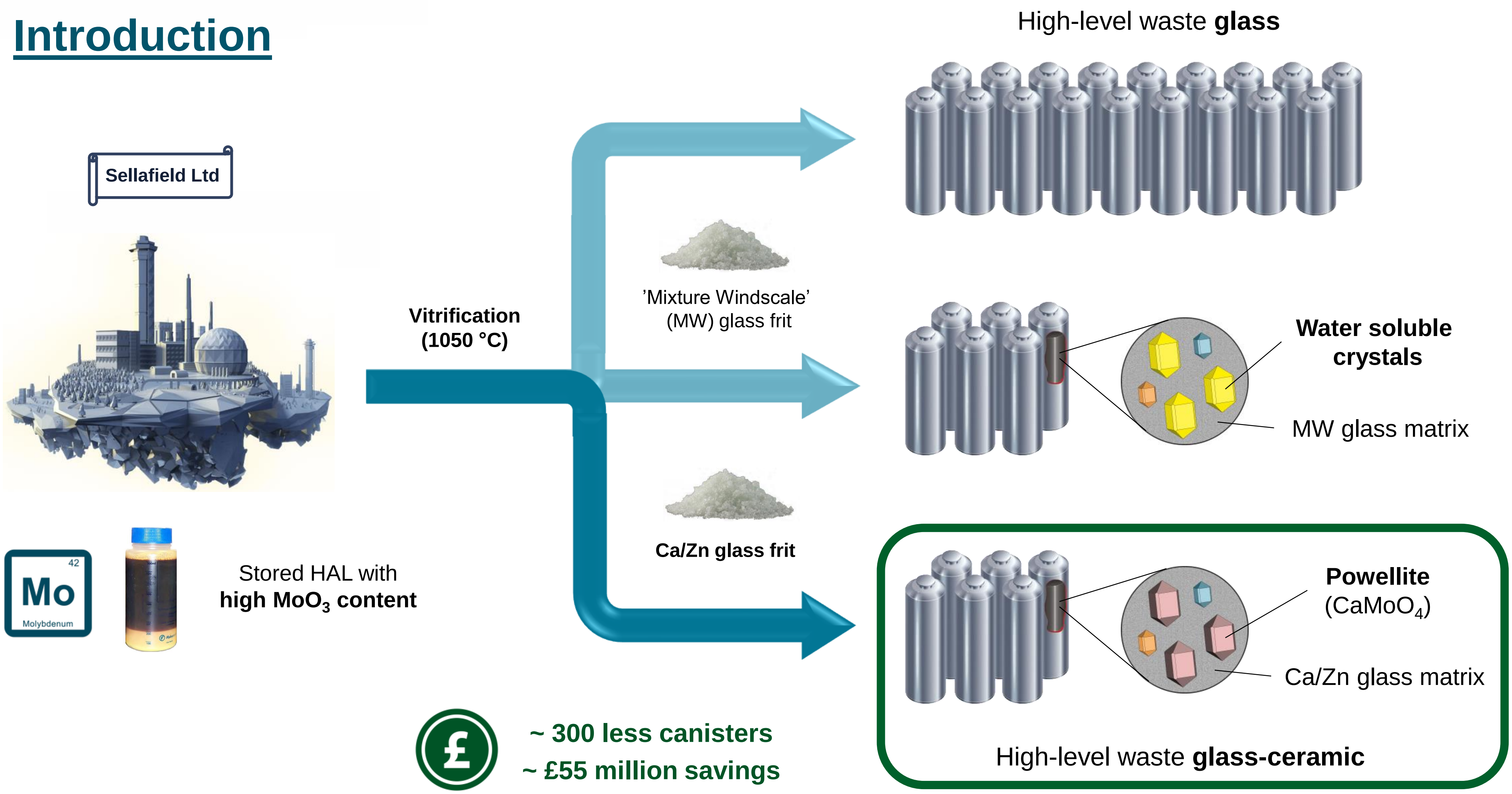

[1] Paterson et al. 2017

Radiation effects on HLW glass-ceramics

1. Glass-ceramic

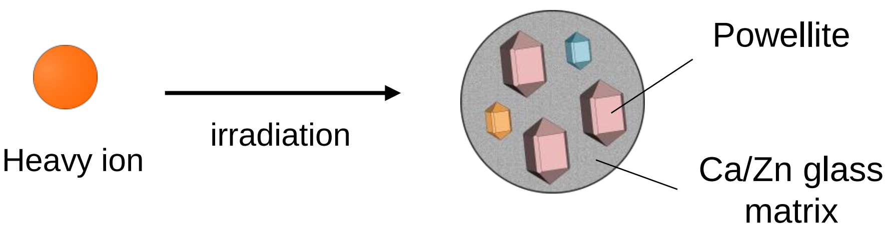

Vitrification Test Rig (VTR) samples:

cracking
ion migration
change in crystallinity

2. Glass

Analytical techniques:

- XAS
- EPR
- UV-Vis

microstructural changes

Crystal formation in VTR samples

– powellite
– zircon
– ceria-zirconia
– zincochromite
– ruthenium oxide
– barium molybdate

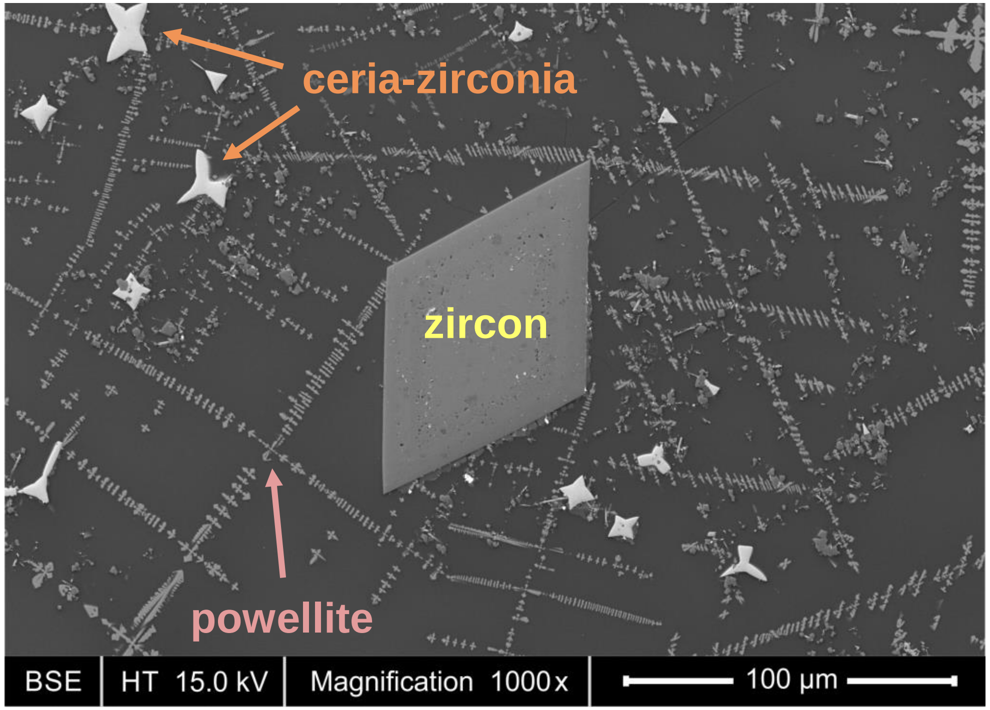

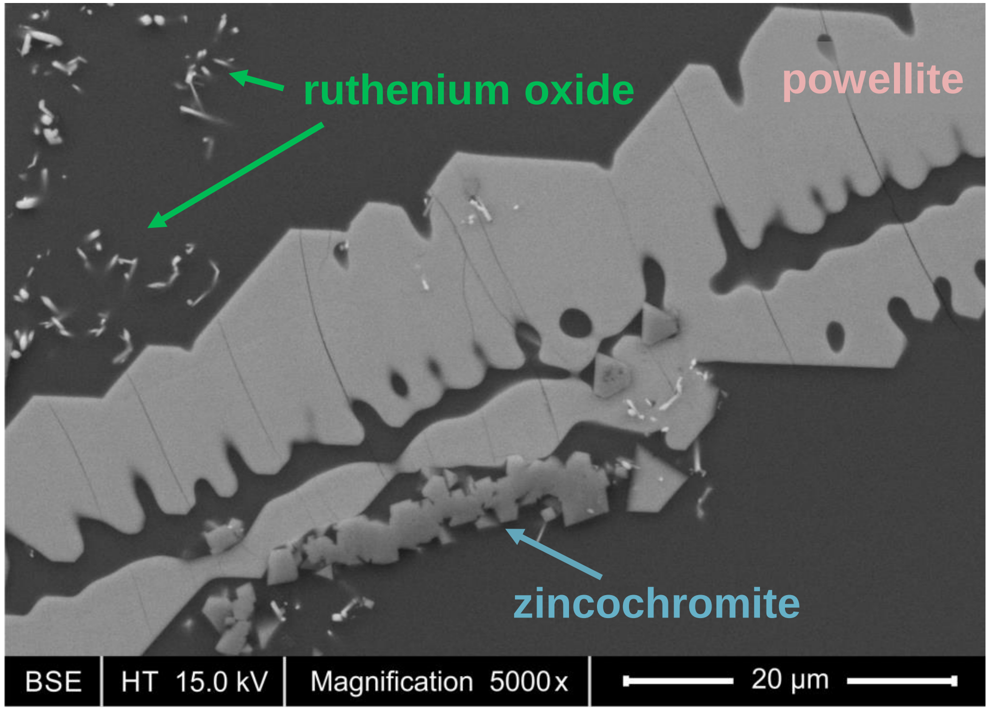

Crystal formation in VTR samples

– powellite
– zircon
– ceria-zirconia
– zincochromite
– ruthenium oxide
– barium molybdate

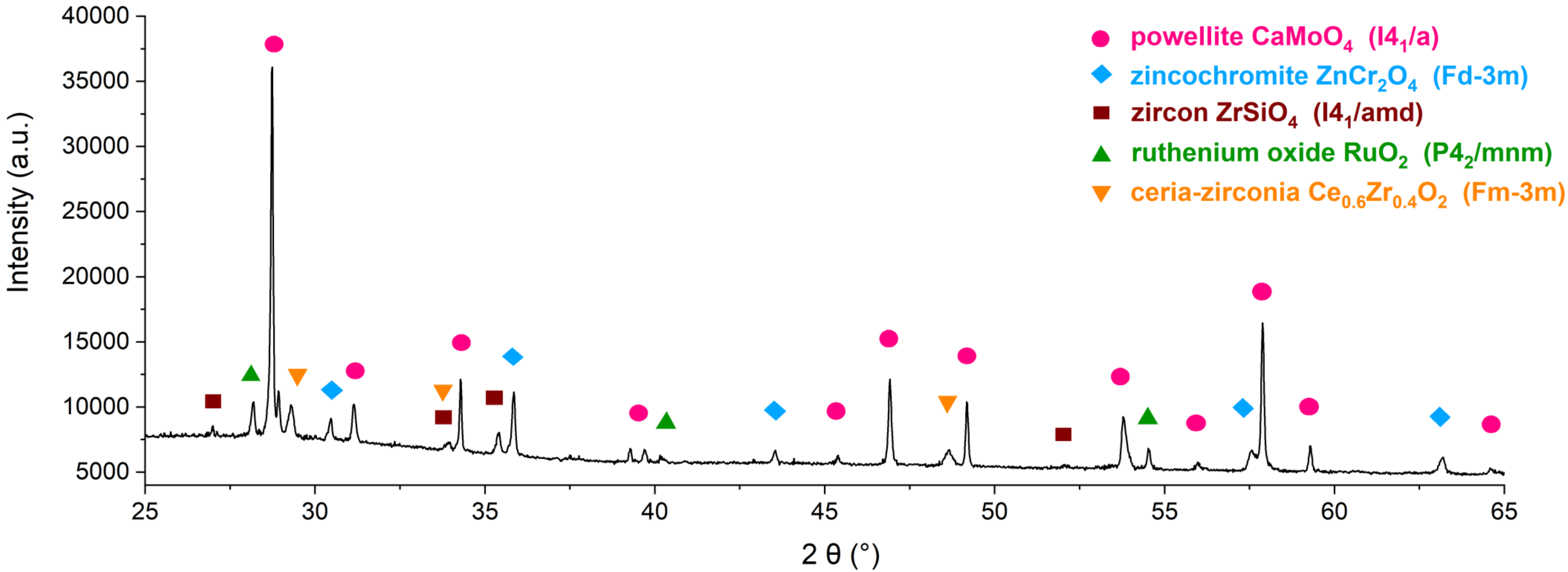

Powellite formation

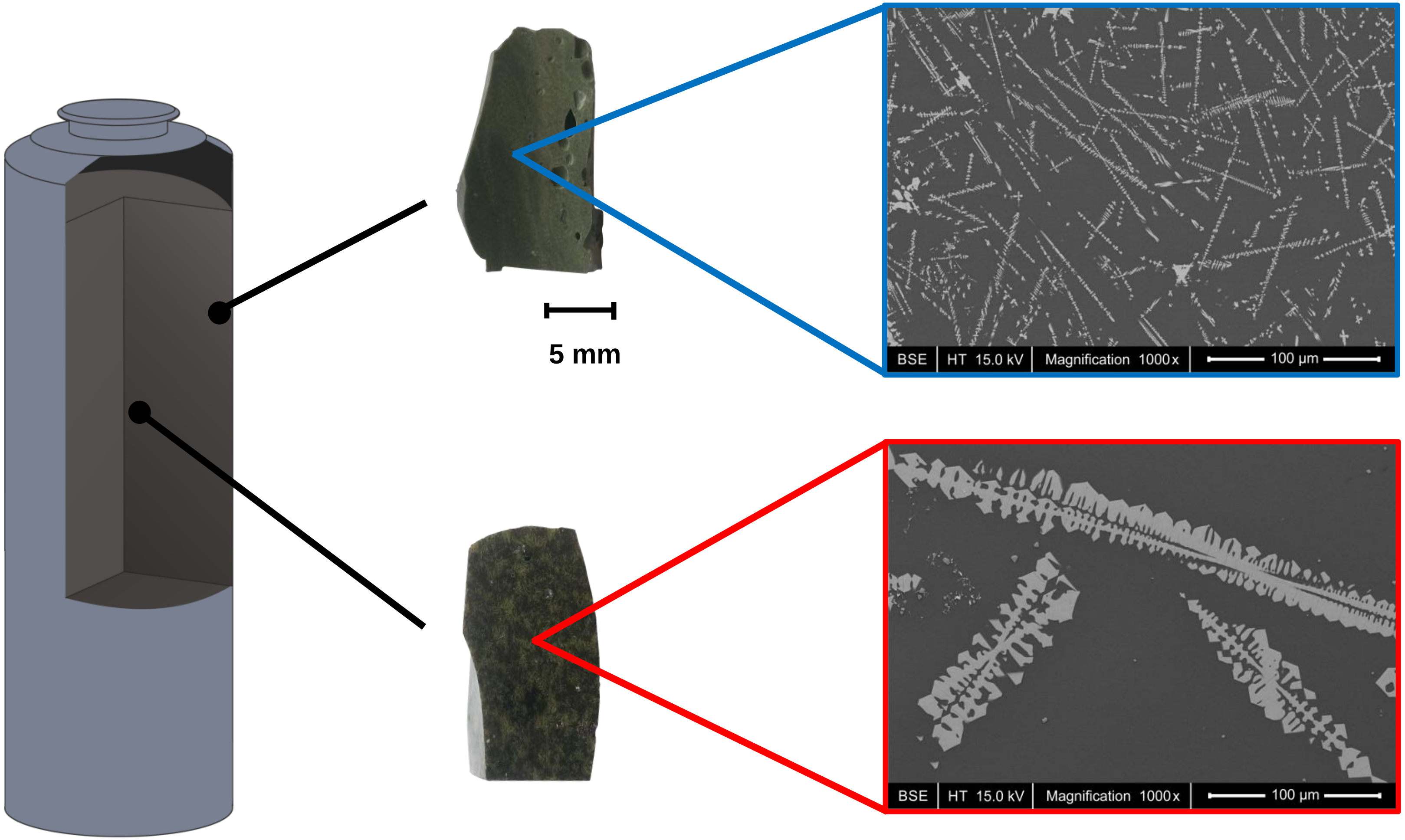

Fast cooling rate

Slow cooling rate

Cracking in VTR samples

- – horisontal cracking inside large powellite crystals
- – cracking of glass around large zircon crystals

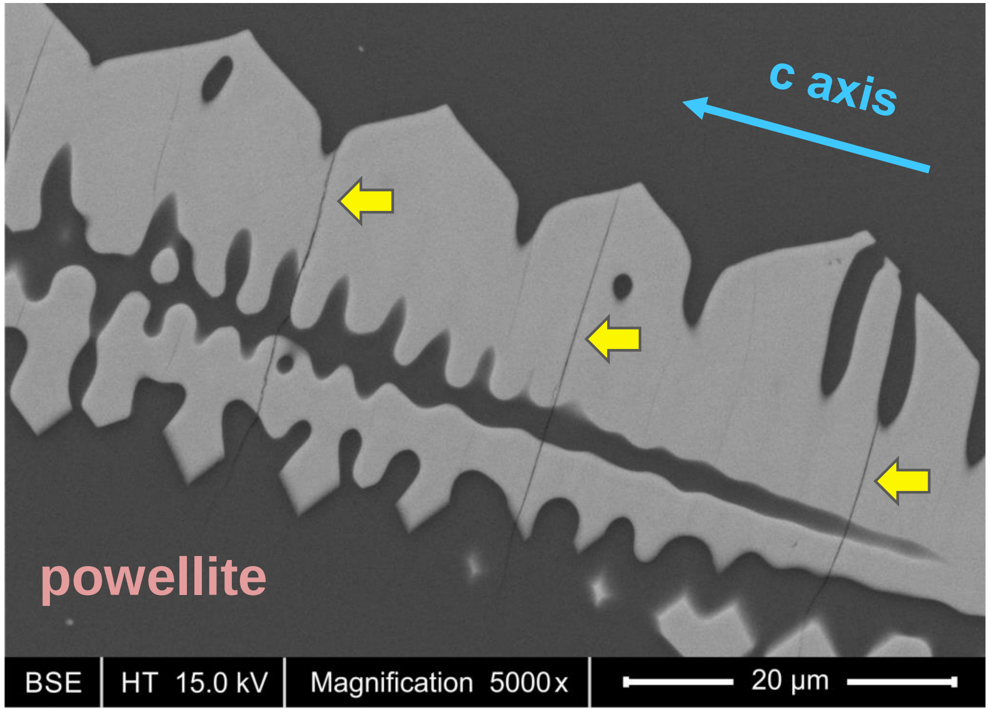

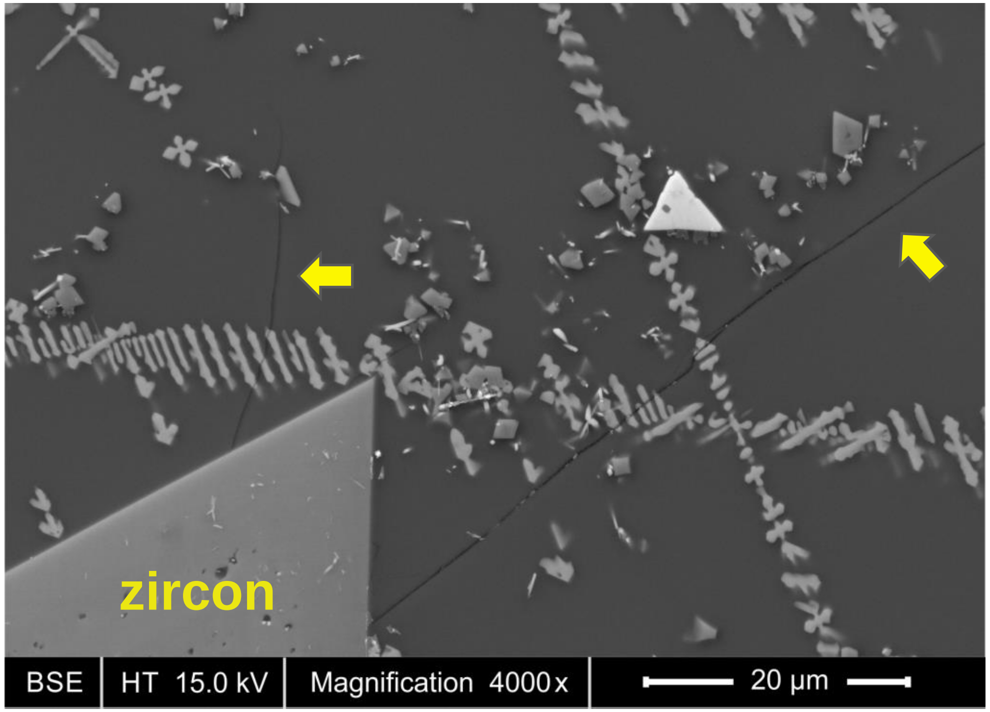

TEC $(\times 10^{-6}/°C)$: $\alpha_a = 13.5$ $\alpha_c = 22.8$ [2] $\alpha_a = 3.4$ $\alpha_c = 5.6$ [3]

[2] Bayer at al. 1971; [3] Achary et al. 2006

Transformative Science and Engineering for Nuclear Decommissioning

<u>Ni irradiation experiment</u> → change in crystallinity, cracking (?)

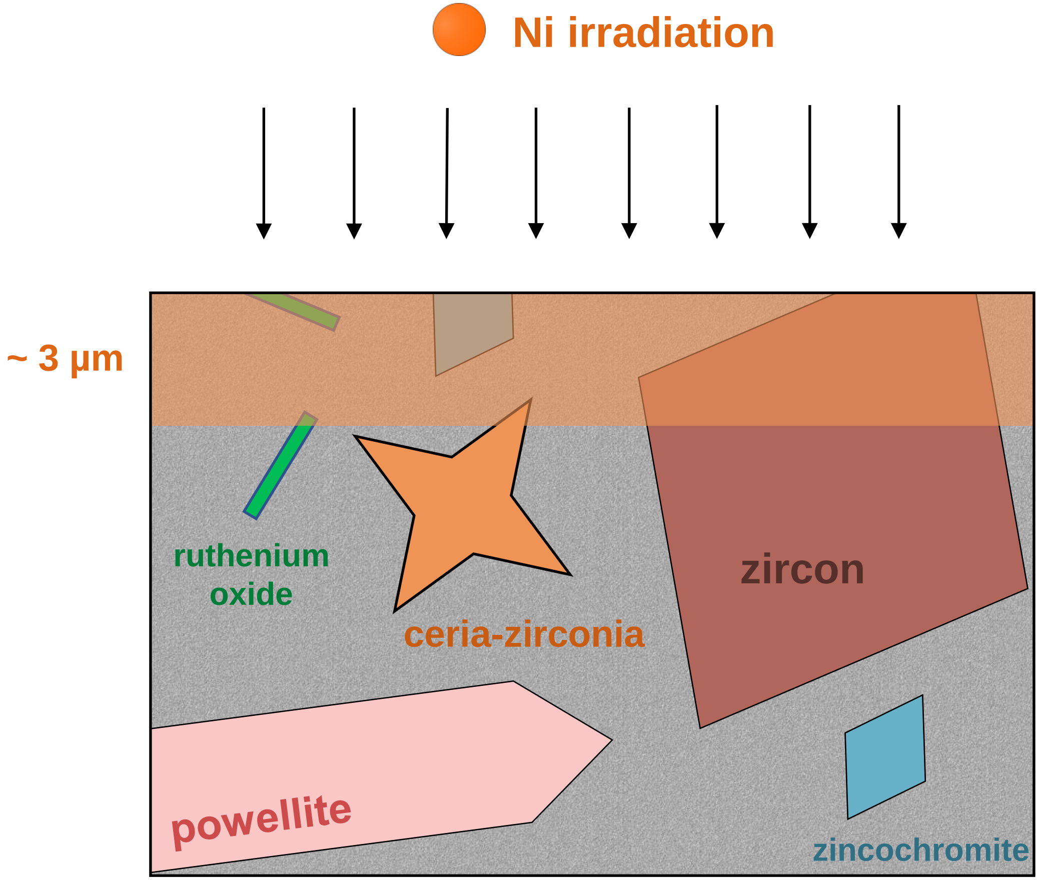

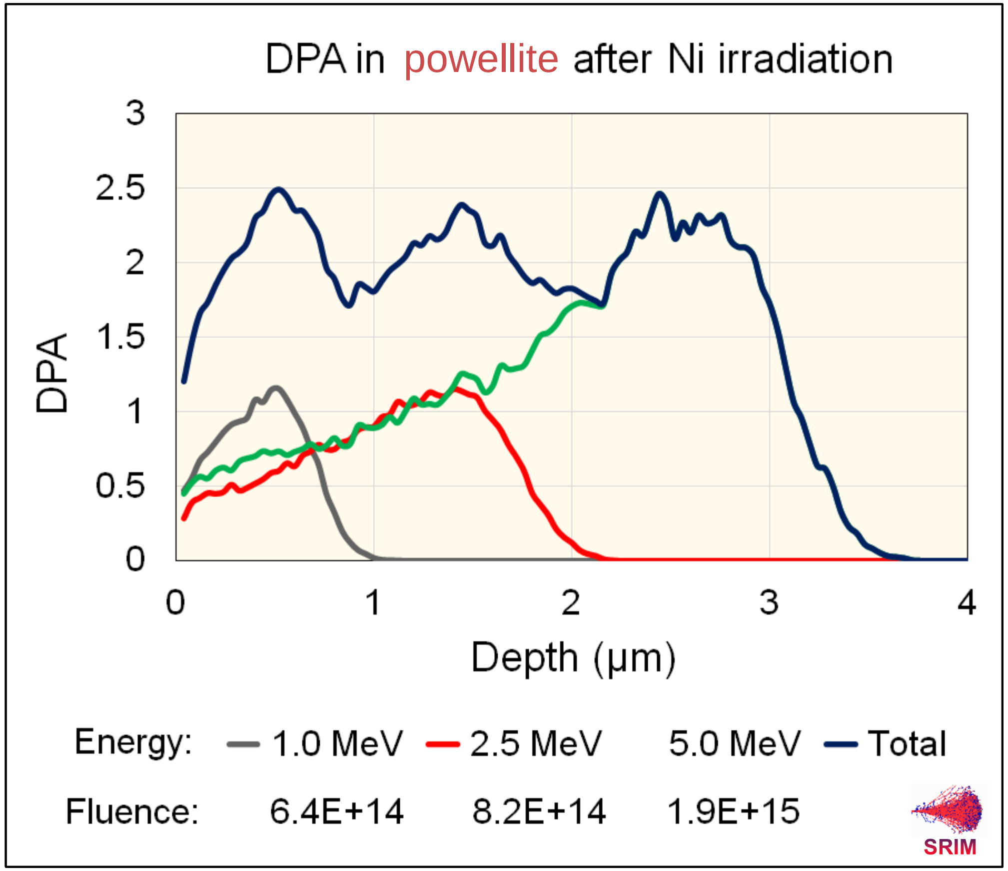

<u>Expectations:</u>

substantial change for zircon [4], no (or minimal) change for powellite [5]

[4] Nasdala et al. 2018; [5] Wang 2013

TRANSCEND

Transformative Science and Engineering for Nuclear Decommissioning

Radiation tolerance of crystals (SEM before & after irradiation)

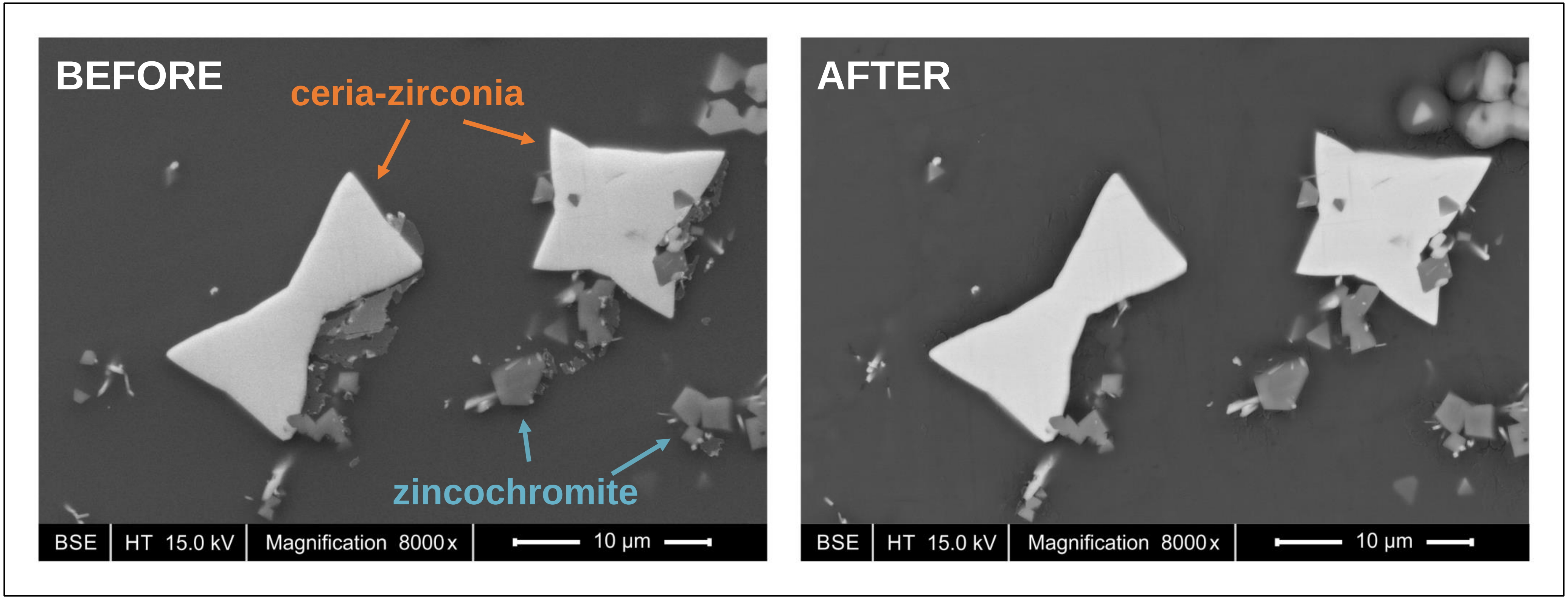

Radiation tolerant crystals: ceria-zirconia, zincochromite, ruthenium oxide

Radiation tolerance of crystals (SEM before & after irradiation)

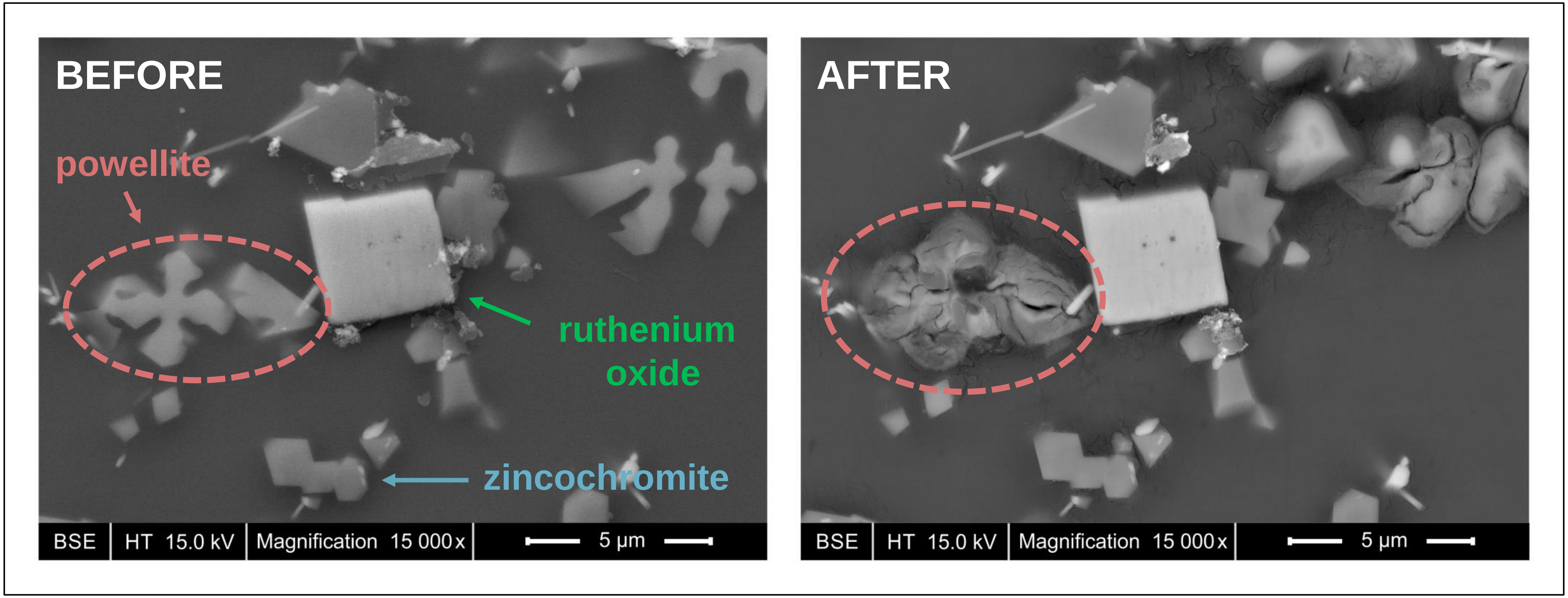

Radiation tolerant crystals: ceria-zirconia, zincochromite, ruthenium oxide

Substantial swelling of powellite crystal

Radiation tolerance of crystals (SEM before & after irradiation)

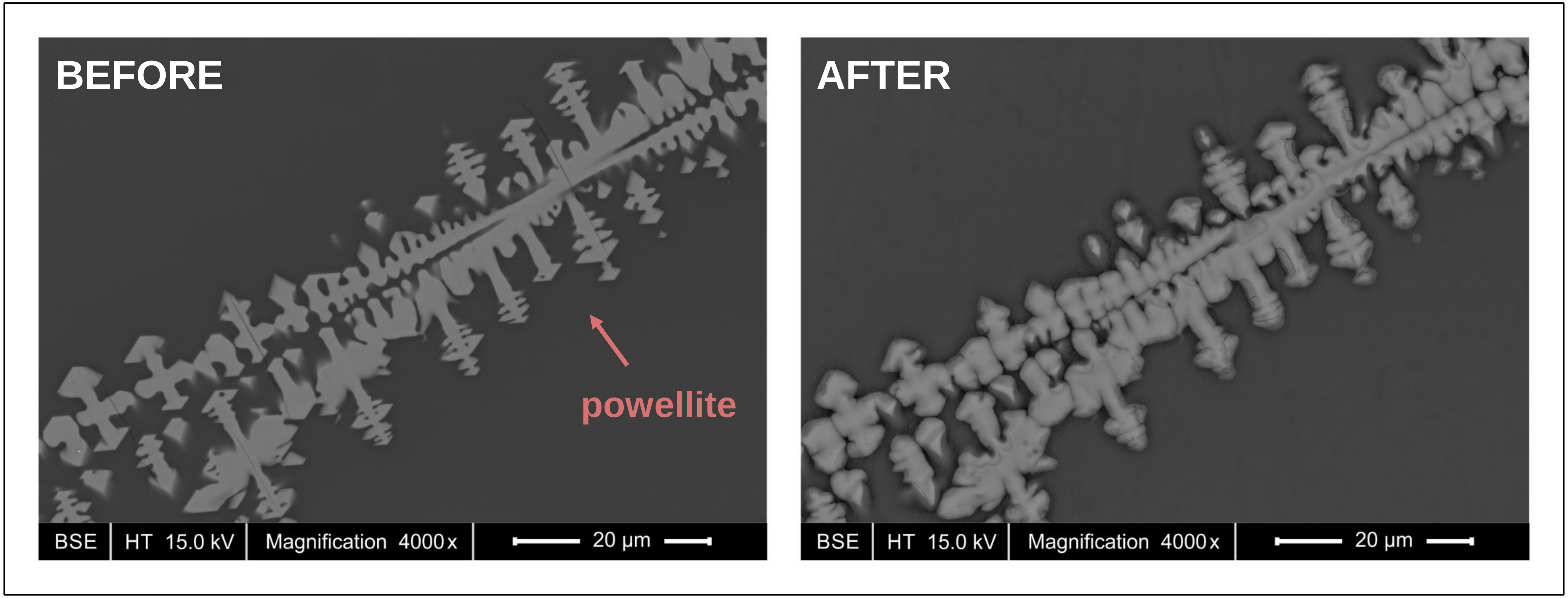

Substantial swelling of powellite crystal (bigger than the expected 5%)

Radiation tolerance of crystals (SEM before & after irradiation)

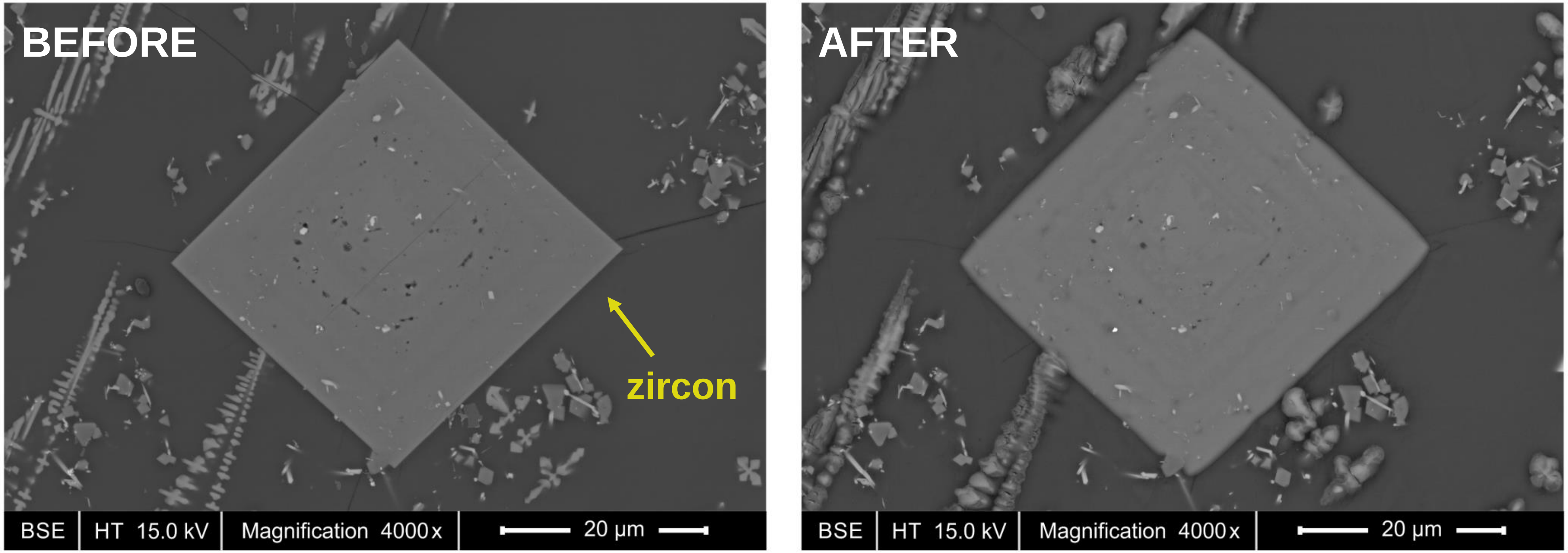

Substantial swelling of zircon crystal (as expected), crystal zones still visible

Radiation tolerance of crystals (SEM before & after irradiation)

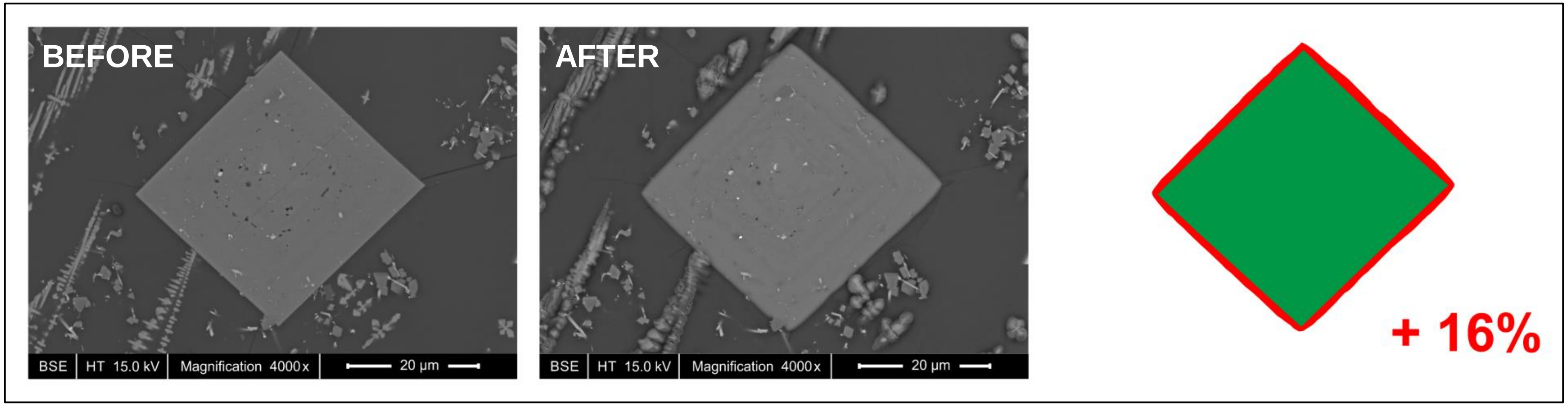

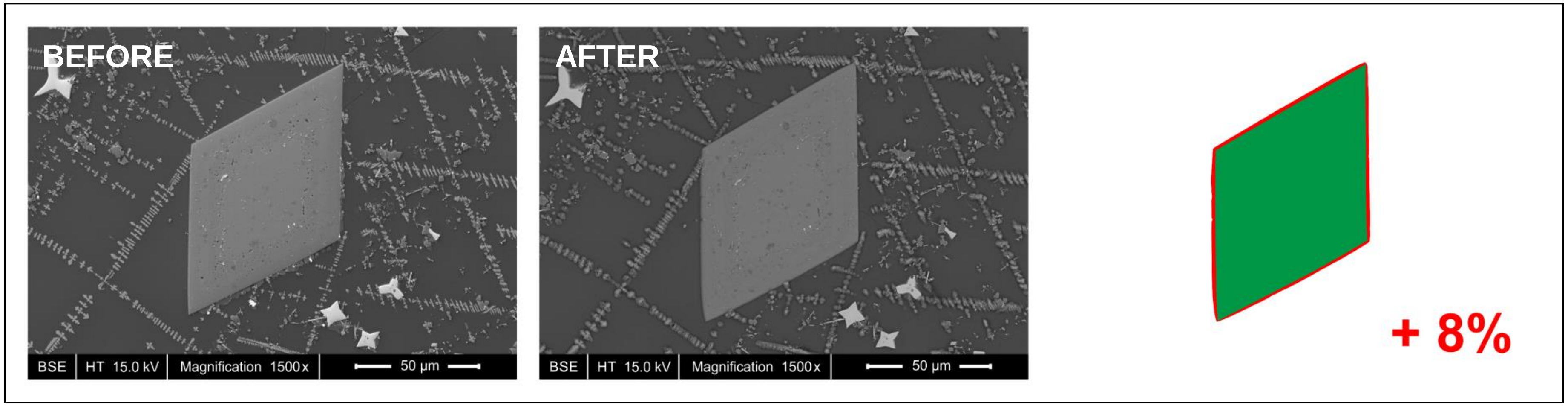

Substantial swelling of zircon crystal (as expected), crystal zones still visible

Cracking (SEM before & after irradiation)

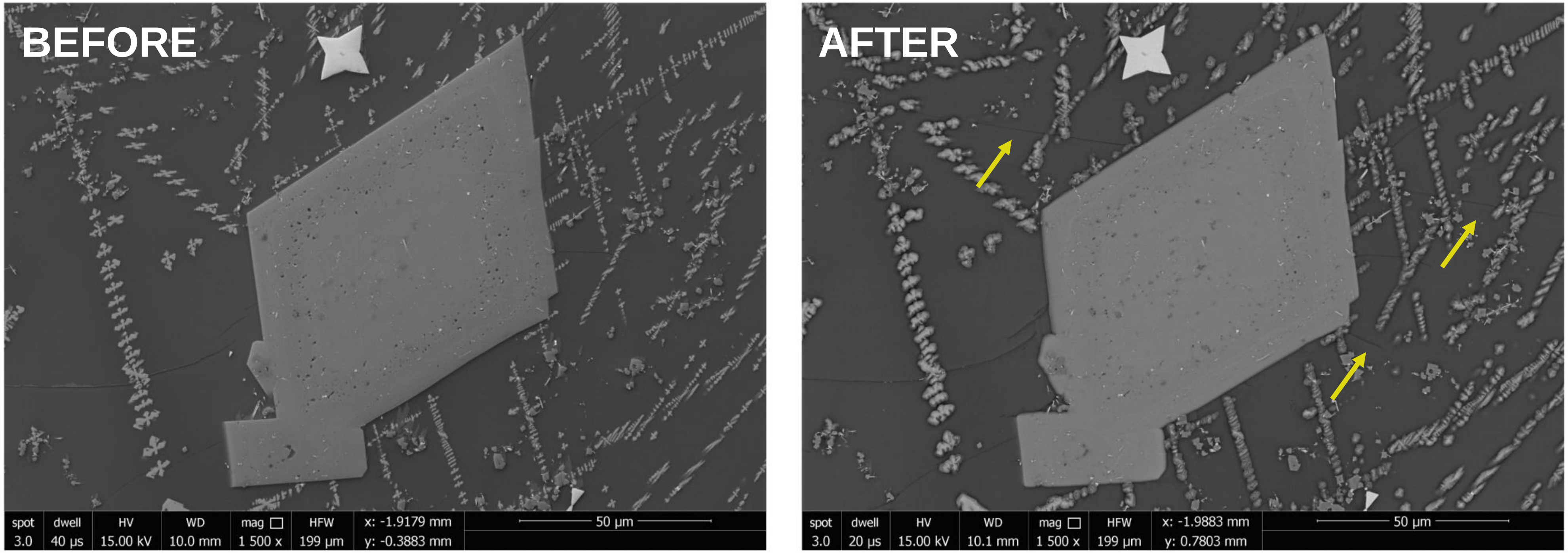

Formation of new cracks and crack widening around zircon.

Cracking (SEM before & after irradiation)

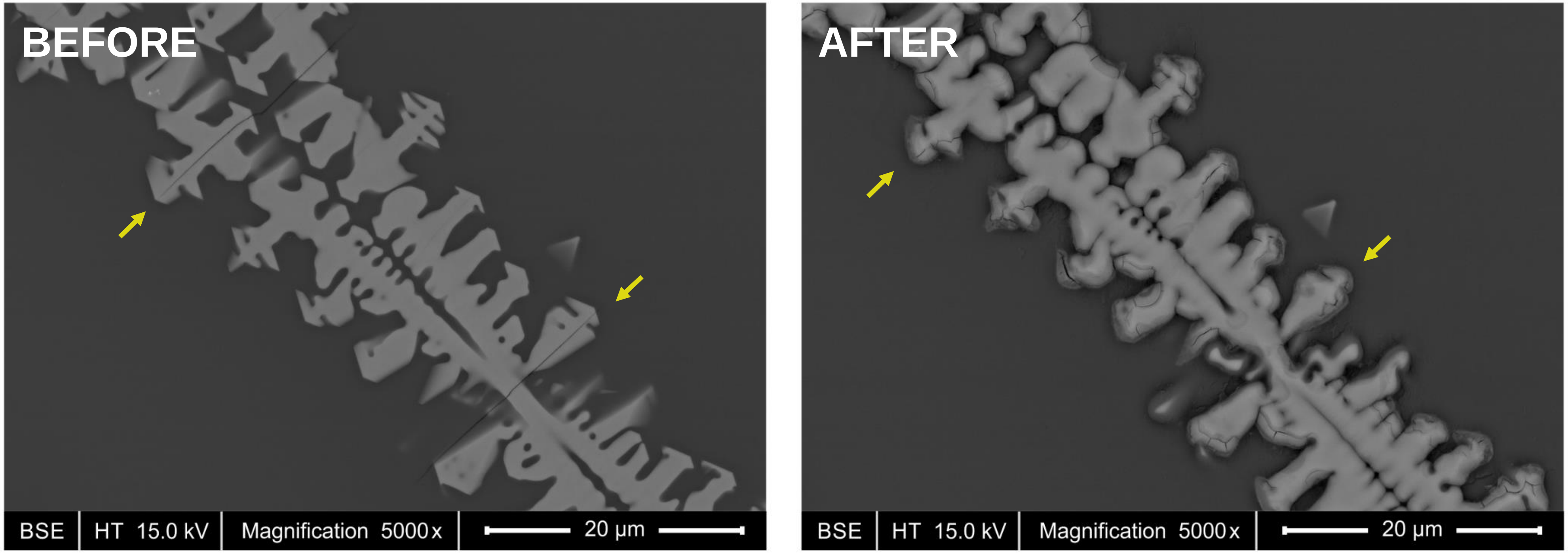

Crack healing inside the crystal and formation of microcracks around powellite.

SEM results summary (before and after Ni irradiation)

Radiation tolerance of crystals:

- Radiation tolerant: ceria-zirconia, zincochromite, ruthenium oxide
- Substantial change was observed: **zircon, powellite**

Cracking:

- Crack healing inside **zircon** and **powellite** crystals
- Formation of new cracks around **zircon** (and **powellite**)
- No crack propagation

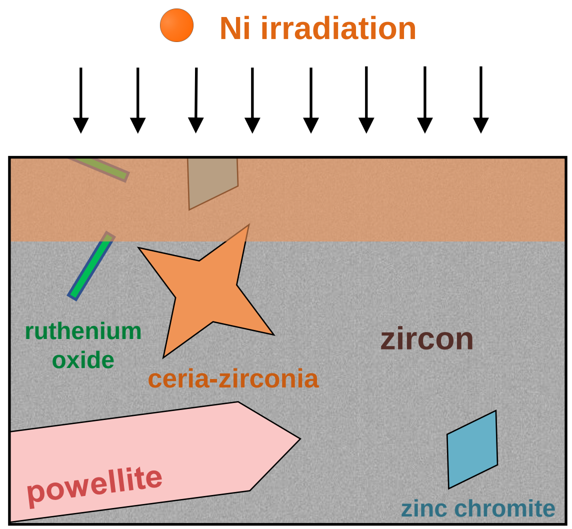

EBSD (before Ni irradiation)

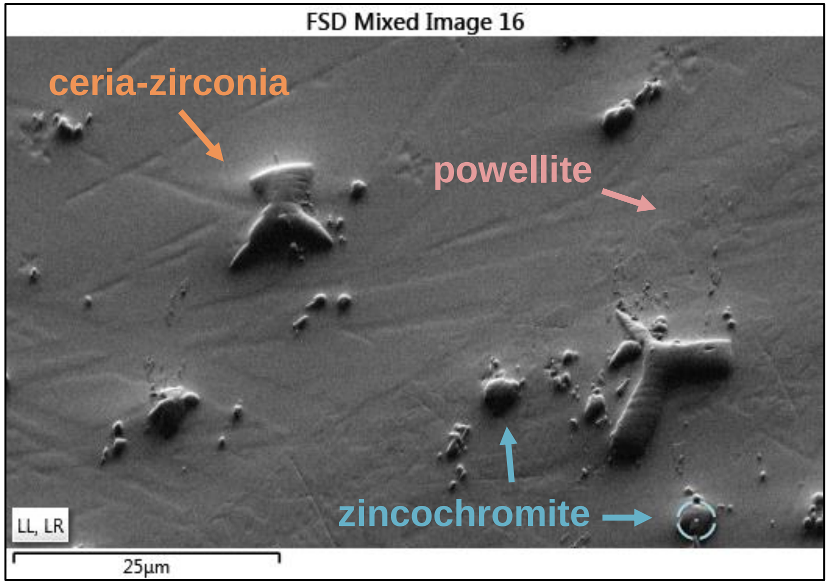

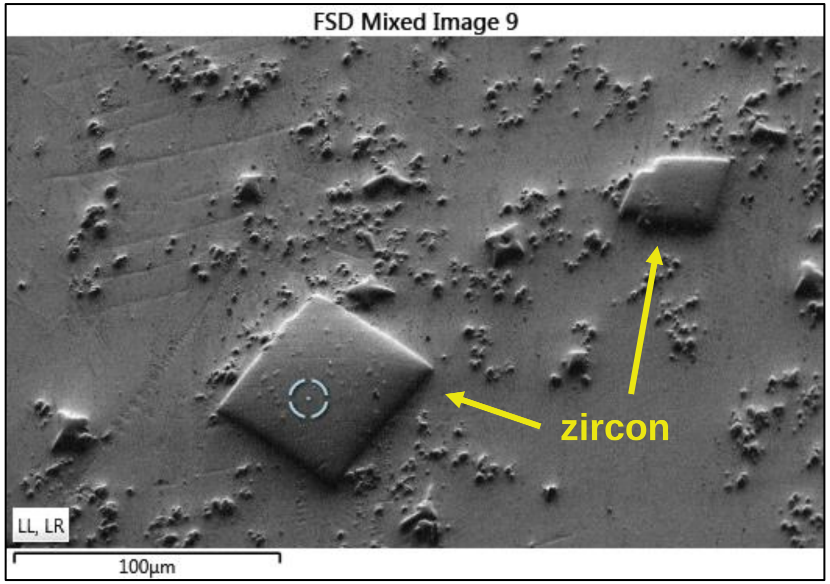

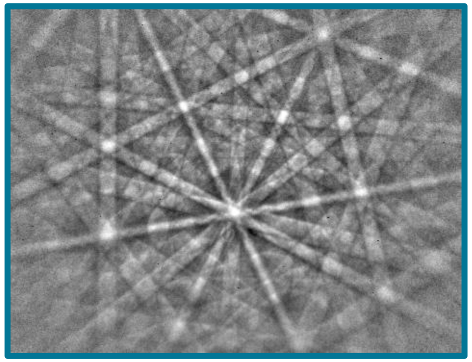
powellite

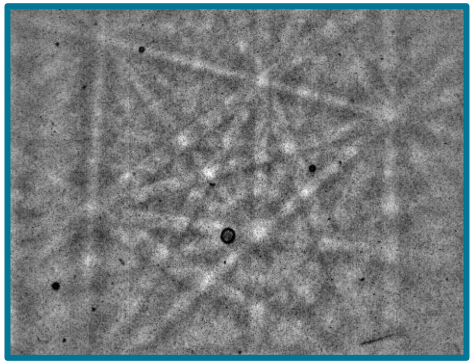
zircon

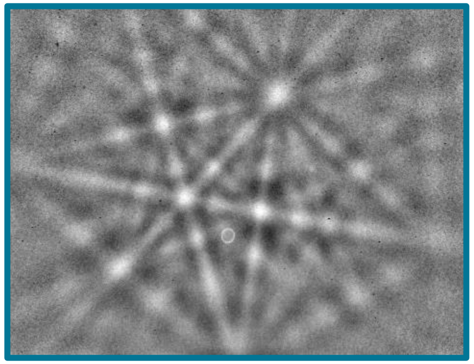
ceria-zirconia

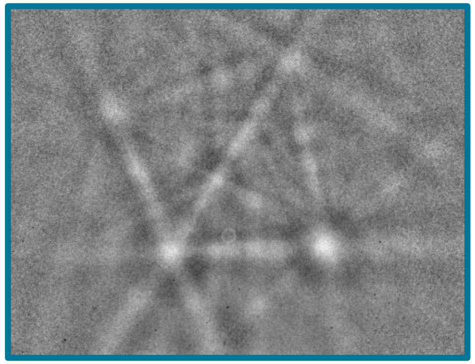
zincochromite

Raman (before and after Ni irradiation)

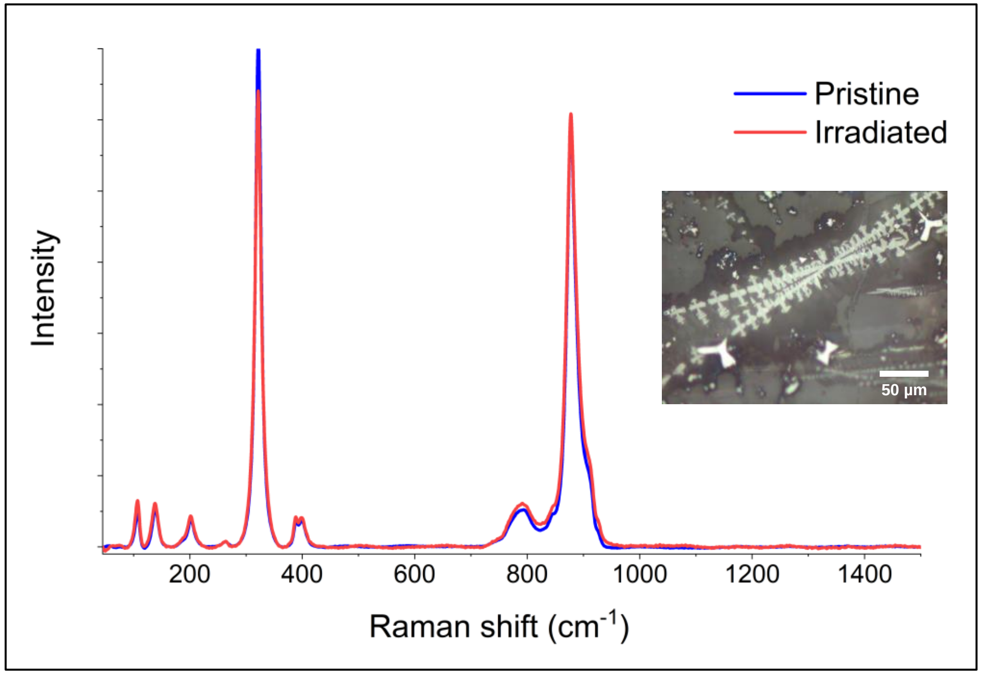

powellite

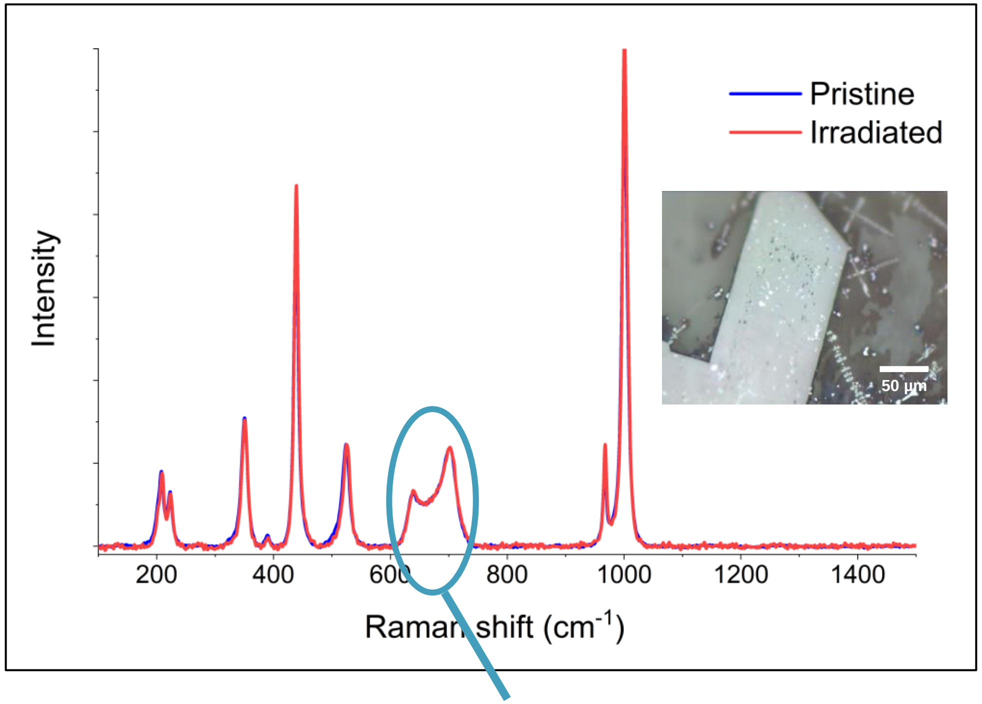

zircon with zincochromite inclusions

Results (so far): no change was observed for **powellite**, **zircon**, and **zincochromite.**

Either the crystals were extremely radiation tolerant, or the Raman penetration depth was deeper than 3 µm.

Radiation effects on HLW glass-ceramics

1. Glass-ceramic

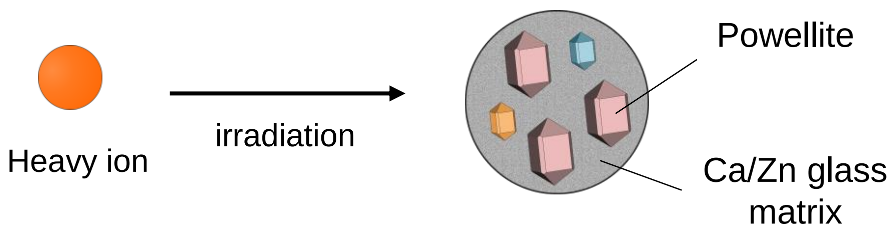

Vitrification Test Rig (VTR) samples:

cracking
ion migration
change in crystallinity

Plans for the near future

- **Raman and EBSD for amorphisation**
- **EPMA for ion migration**
- **GIXRD for amorphisation or/and determining swelling rate / strain**

Radiation effects on HLW glass-ceramics

1. Glass-ceramic

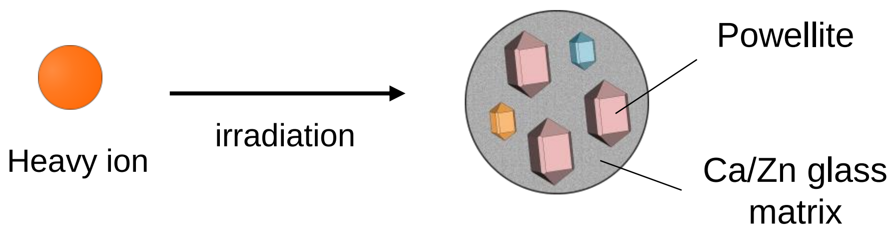

Vitrification Test Rig (VTR) samples:

cracking
ion migration
change in crystallinity

2. Glass

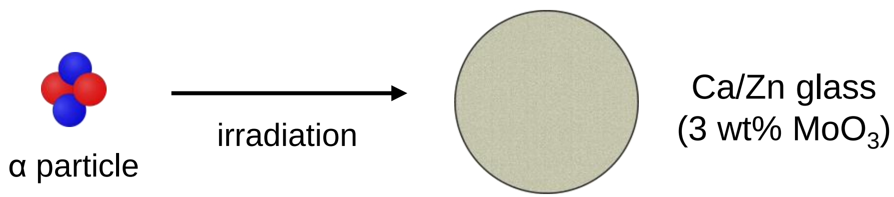

Analytical techniques:

- **XAS**
- **EPR**
- **UV-Vis**

microstructural changes

References

Articles:

[1] Paterson et al. “Novel glass formulations for post-operational clean out of highly active storage tanks” 2017.

[2] Bayer at al. ”Thermal expansion of ABO4- compounds with zircon and scheelite structures” 1971.

[3] Achary et al. “High temperature crystal chemistry and thermal expansion of synthetic powellite ($CaMoO_4$): A high temperature X-ray diffraction (HT XRD) study” 2006.

[4] Nasdala et al. “Irradiation effects in monazite–(Ce) and zircon: Raman and photoluminescence study of Au-irradiated FIB foils.” 2018.

[5] Wang “Chemical Fractionation in Molybdenum-rich Borosilicate Glass-ceramic and Behavior of Powellite Single Crystal under Irradiation” 2013.

Images:

Radioactive Waste Management https://www.gov.uk/guidance/why-underground#the-science-files

FAVPNG https://favpng.com/

Thank you for the help!

Brian O'Driscoll
Robert Harrison
Laura Leay

Tracey Taylor
Mike Harrison

NATIONAL NUCLEAR LABORATORY

Paul Bingham
Prince Rautiyal
Györgyi Glodán
Chetna Tyagi
Samir de Moraes Shubeita
Carl Andrews

Special thanks for the support from National Nuclear Laboratory.

NATIONAL NUCLEAR LABORATORY

Thank you

Contact Details
tamas.zagyva@postgrad.manchester.ac.uk

TRANSCEND

Transformative Science and Engineering for Nuclear Decommissioning

Characterisation of Thermal Treatment Products

Daniel Parkes, University of Sheffield

TRANSCEND May 2021

The University Of Sheffield.

May 2021
Virtual

Energy
For a Low Carbon Future

Project Drivers

Waste Type	Current Disposal Technique	✓ ✗	Improvement
HLW (High Level Waste)	Vitrification in borosilicate glass	✓	-
ILW (Intermediate Level Waste)	Compaction and encapsulation in cement	Compaction issues, volume increase and metal reactivity. ✗	Decay storage, thermal treatment, improved encapsulation and decontamination, focus on boundary waste and reclassification to LLW.
LLW (Low Level Waste)	Compaction, incineration and metal decontamination	✓	-

- The purpose of this project is to characterise a range of thermally treated products representative of potential UK ILW waste streams, including an assessment of the radionuclide (surrogate) distribution and durability
- ILW wide range of compositions – one solution does not fit all
- Plasma – simulants of UK Plutonium Contaminated Material (PCM)
- Geomelt – examples from Hanford and Fukushima

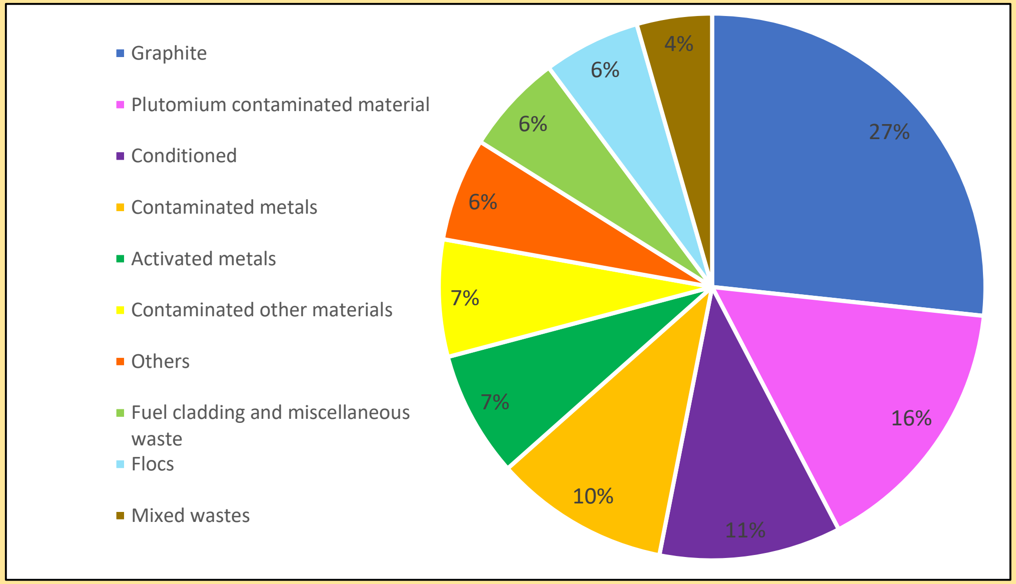

PCM – Trials at Valingar - Process

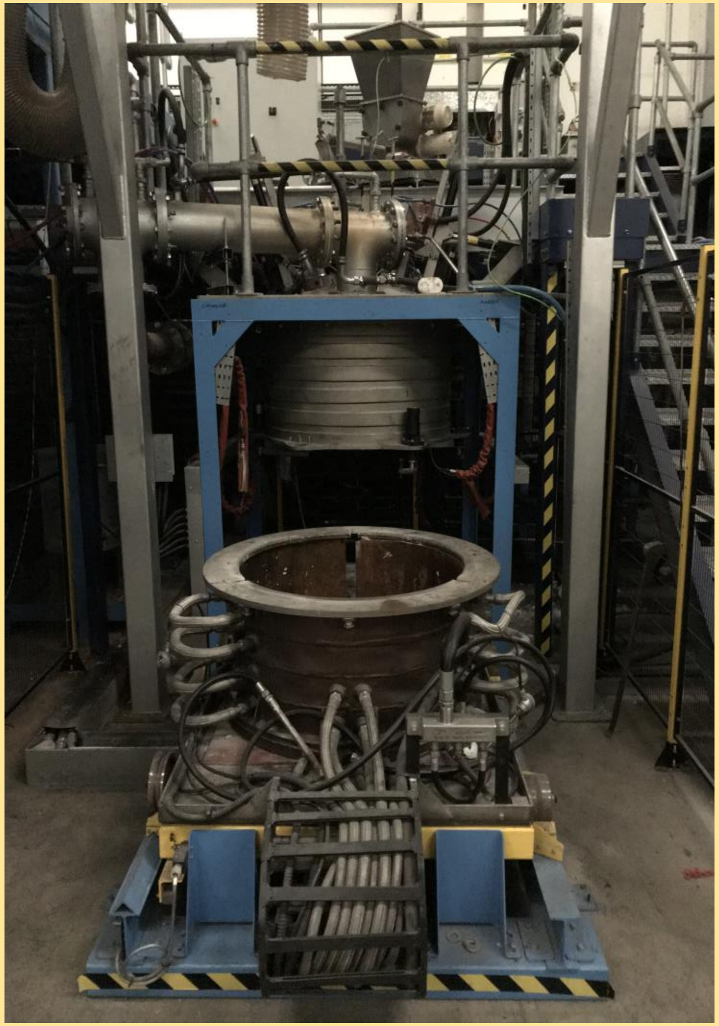

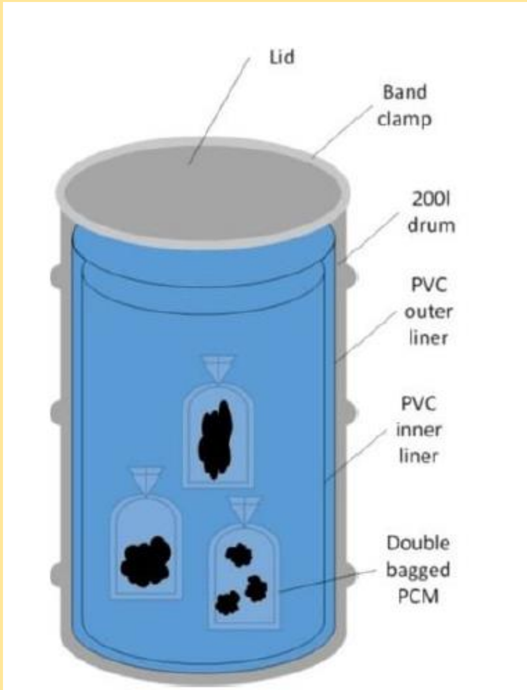

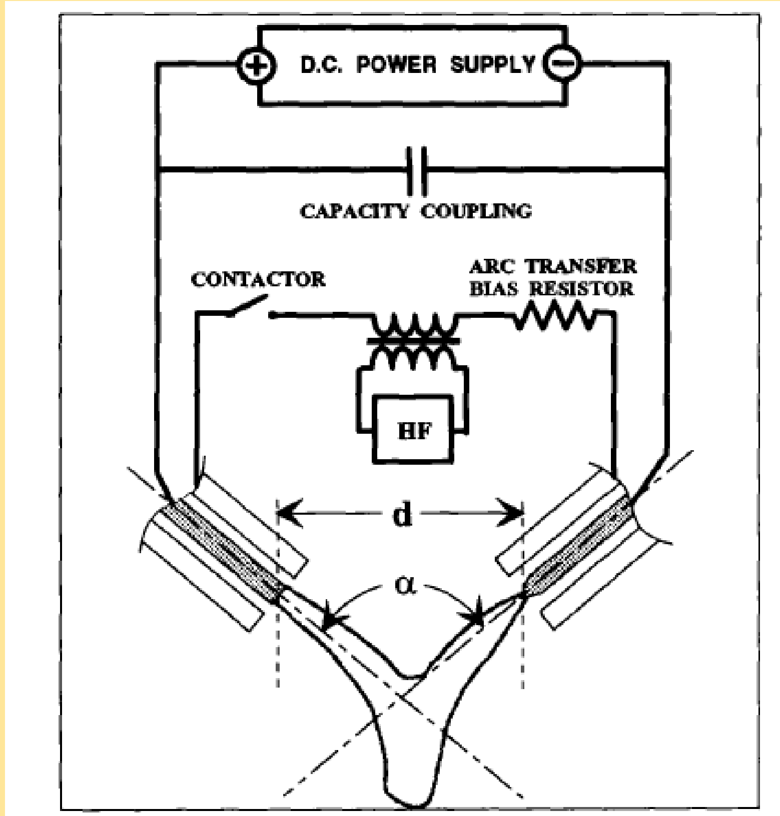

- Valingar (now Tetronics) carried inactive trials for Sellafield on simulant PCM waste
- Plasma vitrification at Sellafield
- Plasma is advantageous as it is high temperature so can cope with the range of PCM waste removing the need for prior drum screening
- Vitrified using 52% Si, 32% Ca, 16% Al glass frit

PCM – Trials at Valingar - Process

Drum S Material	Actual Weight [kg]
Drum & Lid	17.36
PVC Liner	1.86
Hand Tools & Ancillary Equipment	20.16
Rubber Hose	1.78
Wellingtons	1.86
PVC Suit + Double Bags	7.24
Paper	0.126
Scaffolding Board	1.88
Lab Glassware	0.56
Floor Sweepings	0.54
Vermiculite + Water	0.25
Strippable Coating (Decongelsure)	0.322
Polybottles	0.266
Alumina Furnace Bricks	0.568
Electric Cable (2.5mm)	0.551
Rubber Gloves	0.25
Total	55.57

Drum T Material (High Organic Wood)	Actual Weight [kg]
Drum & Lid	17.4
PVC Liner	1.52
Steel Drum Liner	8.84
Scaffolding Boards	29.4
Total	57.16

Drum U Material (High Organic PVC)	Actual Weight [kg]
Drum & Lid	17.4
PVC Liner	1.52
Steel Drum Liner	8.78
PVC Suits	12.9
Total	40.60

Drum V Material (High Inorganic)	Actual Weight [kg]
Drum & Lid	17.4
PVC Liner	1.52
Steel Drum Liner	8.74
Whitehaven Bricks	18.04
Windscale Spec Concrete	17.14
Total	62.84

Drum W Material (High Metal)	Actual Weight [kg]
Drum & Lid	17.42
PVC Liner	1.52
Steel Drum Liner	8.82
50mm MS Pipe	3.16
50mm Pipe Flanged	2.42
Galvanised Steel Sheet	1.30
Cast Iron	2.00
50mm SS Pipe	1.06
1 Beam	10.26
Steel Scaffolding Poles	9.84
Aluminium Scaffolding Poles	0.98
6mm Steel Plate	5.20
22mm Copper Pipe	0.28
Total	64.26

- 5 different drum compositions
- Represents end members of waste at Sellafield
- Unfortunately not all material available – material from Trial 1 (Drum V) and Trial 5 (Drum T)
- Mixed slag – glass – metal product
- Purple colouration from Cr-Spinels

PCM – Trials at Valingar - Samples

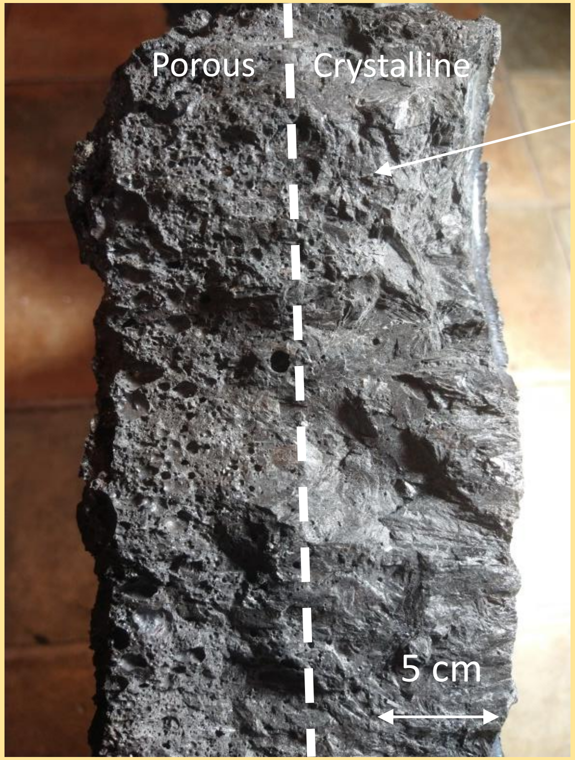

Trial 1 small slag/glass pieces attached to drum – glass: slag ratio us spatially variable.

Trial 5 small amount of slag appears to have to two textures:

1. **Crystalline** – clear crystal faces and textures visible.
2. **Porous** – clear rounded pores (holes) visible.

PCM – Trials at Valingar - Analysis

Sample	Description
PCM-V5 (Porous)	Porous material from trial 5
PCM-V5 (Crystalline)	Crystalline material from trial 5
PCM-V1 (Slag)	Slag sample from trial 5
PCM-V1 (Mixed)	Slag and glass material from trial 5
PCM-V1 (Glass)	Hand separated glass material from trial 5

- Glass Crushing - sample preperation for analysis
- Produce 3 size fractions –
  - < 75 µm - chemical, XRF and XRD
  - 75 -150 µm - PCT dissolution tests
  - 150 µm- SEM analysis and MCC-1 dissolution tests.

PCM – Trials at Valingar – Analysis - Composition

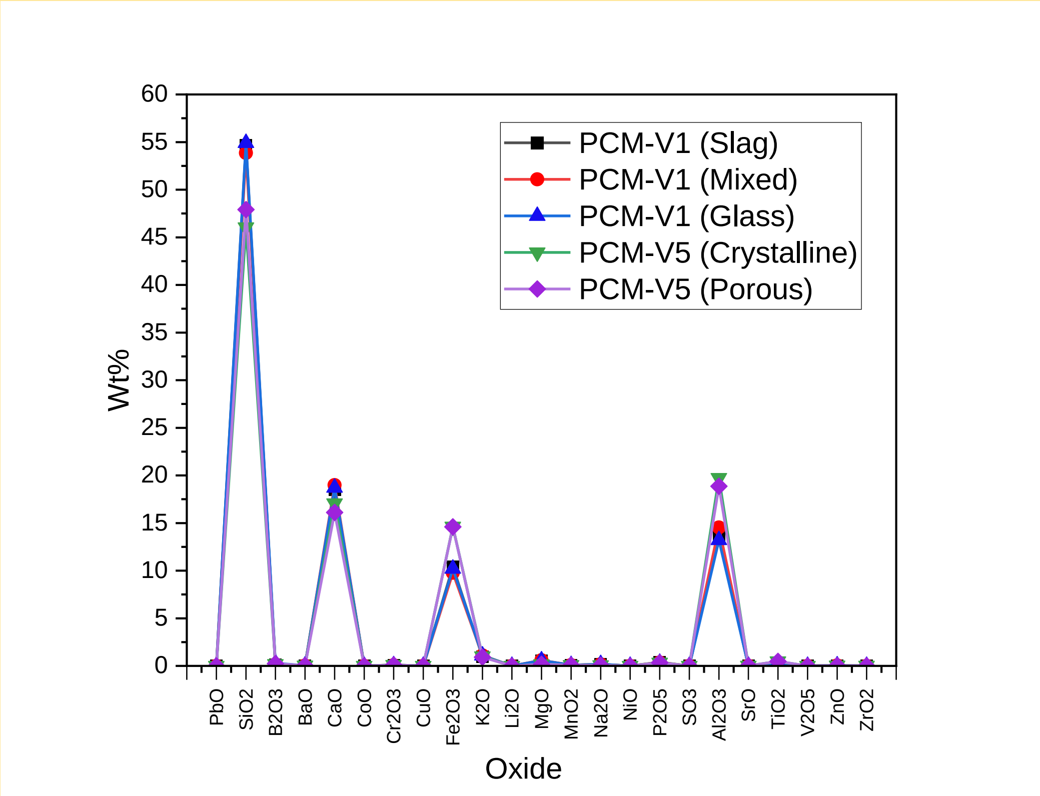

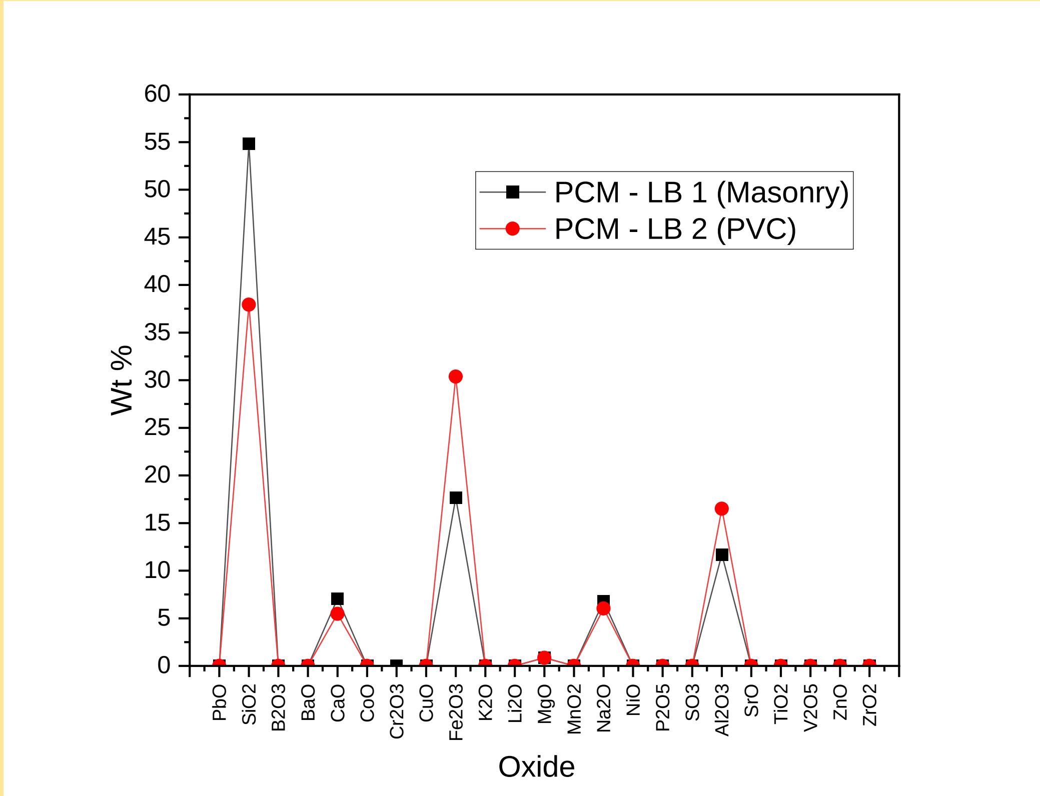

- In Valingar samples (left graph) some variation due to drum composition
- Variation in L.Boast PhD (right Graph) vs Valingar – different glass frit (Luke - 52% Si, 10% Ca, 13% Na, 1% Al and 1.5% Mg and Valingar – 52% Si, 32% Ca and 16% Al) – important for lab trials.

PCM – Trials at Valingar – Analysis – Mineral Phases

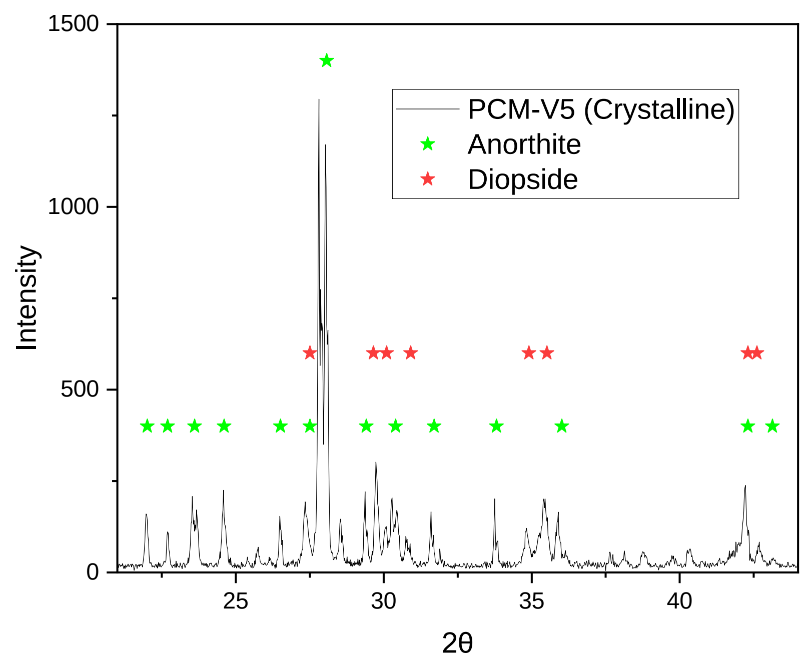

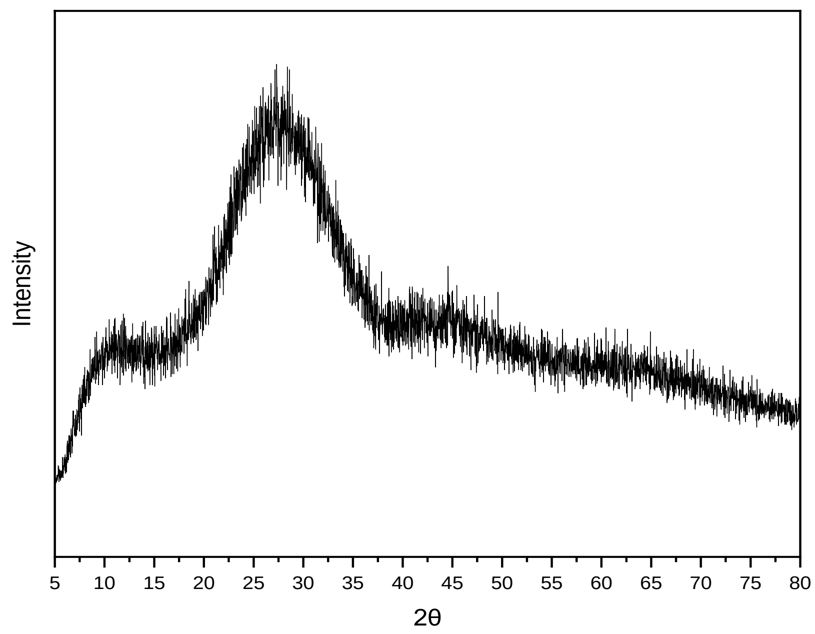

Sample	Identified Phases (Confident)	Identified Phases (Possible)
PCM-V1 (Slag)	Anorthite ($Ca_xNa_{(1-x)}Al_{(2-x)}Si_xSi_2O_8$	Iron phosphate and Aluminium Oxide
PCM-V1 (Glass)	Amorphous	Amorphous
PCM –V1 (Mixed)	Anorthite ($Ca_xNa_{(1-x)}Al_{(2-x)}Si_xSi_2O_8$	Iron phosphate and Aluminium Oxide
PCM –V5 (Porous)	Anorthite ($Ca_xNa_{(1-x)}Al_{(2-x)}Si_xSi_2O_8$	$Na_xCa_{(1-x)})FeSi_2O_8$ – diopside?
PCM – V5 (Crystalline)	Anorthite ($Ca_xNa_{(1-x)}Al_{(2-x)}Si_xSi_2O_8$	$Na_xCa_{(1-x)})FeSi_2O_8$ – diopside?

- Anorthite is common to all samples the ratio of Na:Ca and Si:Al changes between trial 1 and 5
- Possible other minor phases need more evidence from EDX to confirm due to complex pattern, peak overlap and possible solid solutions.
- Glass is amorphous in PCM-V1 (Glass).

PCM – Plans moving forward

1. Continue analysis of the PCM Valingar material including results from XRF analysis and SEM/EDX analysis which will help to better understand the structure and mineralogy of the samples.
2. Dissolution studies of the samples – based on the more detailed analysis will decide which components to carry out the tests on – PCT and MCC tests.
3. Remake the simulants in the lab on a smaller scale and include Ce as a non-active tracer for Pu – interest is in the distribution of the Ce and its level of release during dissolution.

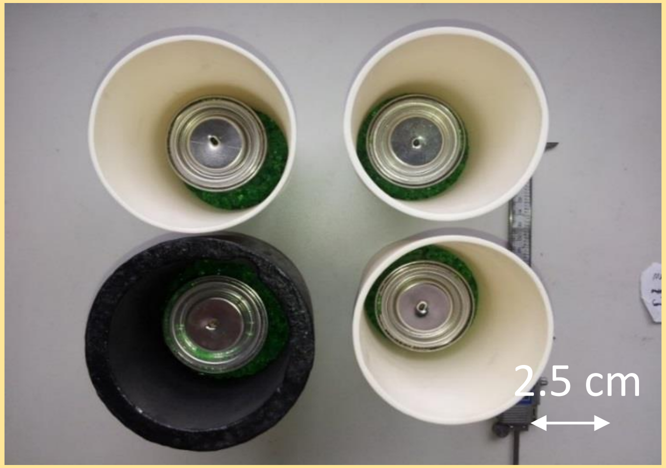

US Geomelt - Samples

- Glass vitrified using ICV of waste from both Hanford, USA and Fukishima, Japan
- Inactive trials demonstrating the technology using inactive tracers of Ce (Pu) and Ds, Re and Sr
- Plan is to complete similar studies as for PCM

Glass	Tracers of Interest	Sample Details
1	Ce	Glass produced in 2003 for the US Dept. of Energy Hanford Site
2	Cs, Re	Glass produced in 2006 for the Hanford Demonstration Bulk Vitrification System (DBVS) project.
3	Cs, Sr	Glass produced in 2020 as part of a series of feasibility trials for a range of water treatment secondary wastes arising from the Fukushima Daiichi NPP disaster.
4	Cs, Sr	Same as above, 2021 glass.

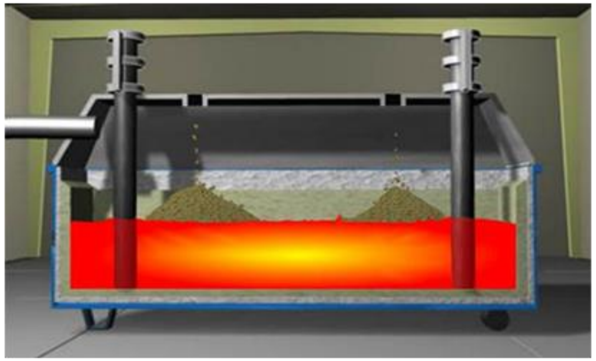

GeoMelt® In-Container Vitrification (ICV)TM

Veolia's geomelt system

Glass 2

Glass 3

Thank you!

- Dr Claire Corkhill and Dr Clare Thorpe
- MIDAS and HADES facilities, UoS
- Valingar (now Tetronics)
- Veolia
- NNL